



Received for publication: December, 27, 2020
Accepted: March, 10, 2022

Original paper

Effect of nitrogen fertilization, cropping seasons and cutting on growth and nutritive value of vetiver

**A. BEN ROMDHANE^{1,†} S. BOUKEF^{2,†} S. DHANE^{1,†} K. HARBAOUI¹,
G. TIBAOUI¹, C. KARMOUS^{3,*}**

¹Department of Crop sciences, Agricultural High School of Mateur, Route de Tabarka, 7030 Mateur, Tunisia.

²Higher Institute of Agronomic sciences of Chott-Mariem, BP 47, 4042 Chott-Mariem, Sousse, Tunisia.

³National Institute of Agronomy of Tunisia, Laboratory of Genetics and Cereal Breeding (LR14AGR01), Carthage University, Cite Mahrajène 1082 Tunis, Tunisia.

†: These authors equally contributed, joint first authors.

Abstract

Vetiver introduced as perennial grass crop in Mediterranean basin is tested for its potential fodder ability. Effects of nitrogen (N) fertilization, on growth, yield and forage quality parameters were assessed during two cropping seasons using a randomized complete block design with three replicates. Three N levels as ammonium-nitrate, were tested: 0, 30 and 60 kg N ha⁻¹. Results showed that biomass increases under maximum N rate compared to control. The improvements in fresh and dry weights were 39.61% and 257.14%, respectively. Second cutting increased DY by 14.70% compared to first cut. Forage yield increase was closely related to a rise of number of tillers by 24.7% under 60 kg N ha⁻¹. The increased tillers enhanced forage yield by 14% during cropping seasons. N produced a linear increase in crude protein under 30 and 60 kg N ha⁻¹ of 40% and 63.8%, respectively. In addition, the increase of leaf cellulose content was less impacted by N fertilization allowing vetiver to be more digestible forage. The results showed that vetiver could be grown as a forage crop in Mediterranean areas. N fertilization since a low rate of 30 kg N ha⁻¹ is sufficient to stimulate regrowth, increase biomass yield and nutritional value.

Keywords

Chrysopogon zizanioides, dry yield, fodder, crude protein, Mediterranean climate.

To cite this article: ROMDHANE AB, BOUKEF S, DHANE S, HARBAOUI K, TIBAOUI G, KARMOUS C. Effect of nitrogen fertilization, cropping seasons and cutting on growth and nutritive value of vetiver. *Rom Biotechnol Lett.* 2022; 27(2): 3331-3342 DOI: 10.25083/rbl/27.2/3331.3342

Introduction

Pasture and fodder crops are among the main world agriculture sowing species, occupying 70% of the world land agricultural area and providing 85% of ruminant protein needs [1,2]. In Tunisia, rangeland and permanent grasslands cover about 4.8 million ha and suffer from overgrazing and low productivity [3]. Forage crops are sown on approximately 321 000 ha representing only 6% of the arable agricultural area, leading to cover only 19% of the livestock needs with 715 million UF [4]. Forage deficit is the result of several limiting factors such as water shortage, rainfall irregularities and frequent droughts [5,6], as well as empirical cultivation practices especially nitrogen (N) fertilization.

In Tunisia, *Avena sativa* is the main forage specie occupying 70% of total forage area [7]. Thus, several forage species have been introduced to primarily fill the forage deficit, such as *Atriplex nummularia*, *Accacia salicina* and *Erharta calycina*. Recently, vetiver (*Chrysopogon zizanioides*) native to the tropics and subtropics [8,9] has been introduced in Tunisia as a perennial grass species. *C. zizanioides* L. belongs to the Poaceae family. The vetiver adaptability to Mediterranean conditions characterized by increasing temperature and day length significantly increased plant height [10]. In the Mediterranean areas, these range of temperature and photosynthesis conditions are obtained mainly from April to September and are considered as optimum growth period.

The genus *C. zizanioides* is characterized by its extreme hardiness and adaptability to wide pedo-climatic conditions [11,12]. Moreover, the plant is used in many countries for water conservation, land stabilization, phytoremediation, and bioethanol production [13–15]. *C. zizanioides* is characterized by high levels of crude protein, carotene, lutein and high-quality edible herbage for cattle and goats, particularly in the vegetative growth stages [16]. Fresh yield, dry yield and crude protein are considered as the main components of forage quality for the grassland species [17].

Few studies highlighted the opportunities of cropping *C. zizanioides* in rainfed conditions through the evaluation of its N fertilization and cutting responses. The present study aimed to emphasize the impact of N fertilization, cutting and cropping seasons on vetiver growth, yield and forage quality.

Materials and methods

Experimental site

A two-year field study was conducted from 2015 to 2017 at the experimental station of Agricultural Hight School of Mateur, Tunisia (37°03'15"N., 9°37'11"E., Altitude 20 m). This area is characterized by a Mediterranean sub-humid climate conditions.

The experiment was carried out on a silty-clay soil texture characterizing the exploited vetiver root depths. Prior to seeding, soil samples from each plot were taken and analyzed. The soil showed an average of 1.93% total organic carbon (TOC) and a low total organic nitrogen (TN) of 0.2%.

Cultural practices and Experimental design

The plants were obtained from 25 cm long vetiver cuttings, grown for one month in greenhouse on brown peat substrate. Vetiver field transplantation was released on July 15th, 2015 on a follow field. The experiment was arranged as Randomized Complete Block Design (RCBD) with three replications; 36 plants were placed in experimental units of 9 m² (3×3 m). The plots were constituted by four rows spaced by 0.5 m and plots spacing was 3 m. Before transplantation, a homogenization cut was released to keep plant height to 10 cm above the ground. A manual weeding was carried out during initial plant growth stages. All the plots were irrigated by sprinkling (3 bars) when evaporation was 70 mm from the surface of evaporation pan class "A". Three level N fertilization as ammonium nitrates (33.5% N) were tested: (0, 30 and 60 kg N ha⁻¹). The N treatments were spread manually after each cutting on a moist soil (20% humidity). After 21 days of plant growth, vetiver plants were cut. During each year, two cuts were applied separated by 21 days.

Measured parameters and data analysis

Plant height (H) and leaf chlorophyll content (Ch) were weekly measured on nine plants per treatment for 21 days. After three weeks of plant growth and to avoid edge effects, five plants per plot in the two middle rows were cut and weighed. The nitrate content (Nc) was determined on 20 g of fresh leaves cut into thin strips and then ground until juice is extracted, which is then analyzed with nitrat-check No₃ meter (LAQUA twin, HORIBA).

The leaves (L) and stems (S) of each plant were separated and weighed. The leaf per stem ratio (L/S) is then calculated. Leaves and stems were separately cut into 1 cm layers dried at 60°C for 48 h to calculate ratio of leaves dry matter per stems dry matter (DM_l/ DM_s). The forage yield (kg/m²) was estimated randomly using 0.5 m² quadrates on each plot.

Dried samples were used to analyze plant nutritive components. The dried matter content of the entire plant (DM_p) was obtained by keeping the fresh samples at 80°C in forced air oven till constant weight. Ashes (Ash) was determined after burning the samples in muffle furnace at 550°C for 10 h while the organic matter (OM) is then calculated from the weight loss. The crude protein (CP) was carried out by micro-kjeldhal digestion [18]. Crude cellulose (Cel) was determined using FIBERSAC procedures outlined by

Table 1. Physical and chemical properties of the experimental field soil.

Depth (cm)	pH	C (%)	SI (%)	S (%)	TOC (%)	TN (%)	CaCO ₃ T (%)	CaCO ₃ act (%)
0-30	8.3	22.5	57.3	17.3	1.9	0.2	20.1	10.1
30-60	8.4	21.6	57.3	18.3	2.08	0.21	20.9	9.8
60-90	8.5	18.5	52	16.1	1.83	0.21	19.9	10.1

C: clay, SI: silt, S: sand, TOC: total organic carbon, TN: total organic nitrogen, CaCO₃T: total limestone, CaCO₃act: active limestone

ANKOM method (AOCS procedures Ba 6a-05). Extractable ether was determined using Soxhlet (ISO 6492:1999). The calcium content of plants (Ca) was determined by SAAF method (ISO6869:2000), and the concentration of phosphorous (P) were estimated by spectrophotometric method (ISO 6491:1998).

Collected data were subjected to analysis of variance using the GLM procedure. The treatment means differences were compared using Tukey HSD test ($P < 0.05$). Pearson correlation coefficient was determined for all the measured components for two cropping seasons and two cutting under three N treatments. The stepwise analysis was released upon vetiver fresh forage yield (FY) as the most important forage yield components as dependent variable the choice of predictive variables is carried out by an automatic procedure. All statistical analysis were released using Statistica 12.0 (TIBCO Software).

Results

Impact of weather growth conditions on vetiver growth

As a perennial crop, vetiver growth started in March with a maximum during summer season characterized by increased temperature reaching a mean temperature of 27.3°C

in August. The growth is completely stopped in winter where minimum mean temperature reached 11.3°C in January. The average annual rainfall (30 years, 1984-2014) was 547 mm, of which over 70% occurred between November and March. During the two cropping seasons 2015-2016 and 2016-2017, precipitation was 17.9% and 22.12% below the thirty's year average. The maximum values of evapotranspiration were recorded during July and August, with an average of 208.1 mm and 201.7 mm, respectively (Figure 1).

Agronomic parameters

Vetiver growth

Statistical analysis showed significant effect ($P < 0.01$) of N fertilization, cropping seasons (Cs), cutting (Cut), N×Cs, and Cs×Cut interactions on vetiver growth parameters as plant height (H) and number of tillers per plant (Nt) (Table 2).

The maximum H and Nt were obtained under 60 kg N ha⁻¹ with respective increase of 31.64% and 31.64% compared to control (0 kg N ha⁻¹). H reached its maximum after two cropping seasons (113.73 cm) and in Cut1 (114.7 cm). The same trend of increase was observed for Nt after two cropping seasons reaching 36.07 tillers per plant in the second cropping season of 2016-2017. Meanwhile, maximum Nt was noted after Cut2 with an increase of 16.85% compared to Cut1 (Figure 2, A).

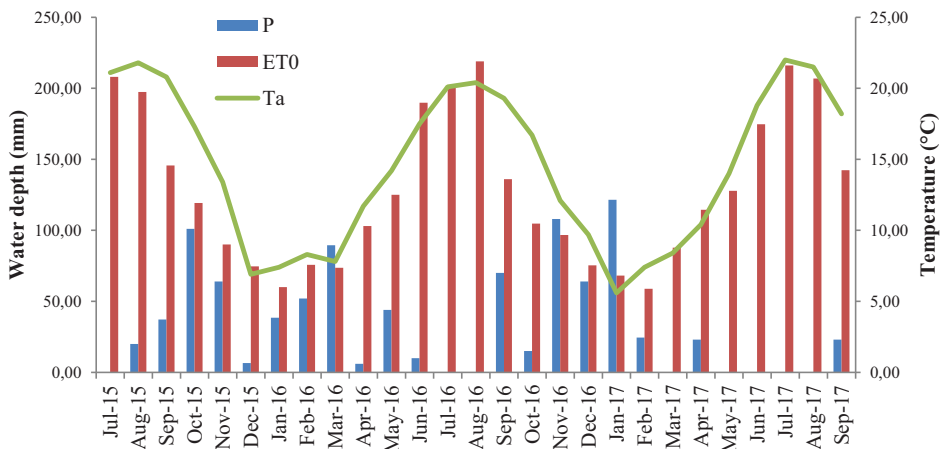


Figure 1. Precipitation (P), reference evapotranspiration (ET0) and mean air temperature (Ta) during the two cropping season assays.

Results showed a significant effect ($P < 0.01$) of N, Cs, Cut and Cs×Cut on Plant fresh weight (FW_p) (Table 3). Maximum N fertilization (60 kg N ha⁻¹) increased FW_p and DM_p respectively by 55.17% and 12.36% compared to control. FW_p increased significantly after Cut2 by 20.42% and after two years cropping by 31.85%.

Moreover, the L/S ratio was affected significantly by N, Cs and N×Cs. Maximum L/S (1.91) was observed under control conditions and was reduced since 30 kg N ha⁻¹ (Table 2).

Results showed a significant effect ($P < 0.01$) of only Cs on the ratio of leaves dry matter per stems dry matter (DM_l / DM_s). The maximum leaf growth was observed in the first cropping season of 2015-2016 with an increase of 3.98%.

Vetiver chlorophyll and nitrate content

Results showed a significant effect of N ($P < 0.01$) and Cs×Cut ($P < 0.05$) on Leaf chlorophyll content, estimated by SPAD (Ch). The maximum SPAD measured three weeks (21 days) after each cutting, was reached since 30 kg N ha⁻¹ (Table 2).

Leaf nitrate content (Nc) showed significant ($P < 0.01$) effects on the interactions N×Cs, N×Cut and Cs×Cut. The maximum Nc was reached at maximum N fertilization rate with 73.14% increase compared to control. The second cutting (Cut2) and cropping season (2016-2017) were among a respective increase of 53.9% and 57.76% compared to control. The same trend of increase was observed for Nc under Cs, Cut and N fertilization. Maximum Nc increase was observed under maximum N input in second cropping season in Cut2 (Figure 2, B).

Vetiver forage yield

The analyzed data showed that fresh forage yield (FY) was significantly ($P < 0.01$) affected by N, Cs, Cut, N×Cut, N×Cs and Cs×Cut (Table 2). N and N×Cs showed significant effects ($P < 0.01$) on dry forage yield (DY). FY and DY increased under maximum N fertilization rate respectively by 39.62% and 252.11% compared to control. The same trend was noted for Cut2 with 13.2% and 14.74% increase respectively for FY and DY, compared to Cut1. The second Cs (2016 - 2017) was higher for both vetiver forage yield as FY and DY by 53.81% and 60.71%, respectively.

Both yield components as (FY and DY) increased with rising N rates, cropping seasons and number of cutting.

Vetiver forage quality

Vetiver forage quality components were evaluated after each cutting. The results showed that cellulose content (Cel) was under the significant effects ($P < 0.01$) of N, Cs, Cut, N×Cut, N×Cs and Cs×Cut (Table 2).

Increasing N rates was associated with Cel increase reaching 14.18% in average under 60 Kg N ha⁻¹ compared

Table 2. Effects of three nitrogen rates (N), cropping seasons (Cs) and cutting (Cut) on vetiver height (Ht, cm), number of tillers per plant (Nt), fresh weight per plant (FW_p , Kg), ratio of leaves fresh weight per stem fresh weight (L/S ratio), plant dry matter content (DM_p , %), ratio of leaves dry matter per stems dry matter (DM_l/DM_s), fresh forage yield (FY, kg m⁻¹), dry forage yield (DY, kg m⁻¹), leaf chlorophyll content estimated by SPAD (Ch), leaves nitrate content (Nc, ppm), leaf cellulose content (Cel, %), extractible ether (EE, %), organic matter (OM), ashes (Ash, %), calcium (Ca, %) and crude protein (CP, %).

	H	Nt	FW	L/S ratio	DM_p	DM_l/DM_s	Ch	Nc	FY	DY	Cel	EE	OM	Ash	Ca	P	CP
Nitrogen rates (N)	0 kg N	87.65 c	24.29 c	1.16 c	12.46 c	2.71 a	31.38 b	676.79 c	2.07 c	0.14 c	25.47 c	1.89 b	84.57 a	15.43 b	0.29 c	0.287a	9.32c
	30 kg N	106.77 b	26.89 b	1.56 b	13.46 b	2.47 b	38.84 a	852.14 b	2.57 b	0.28 b	27.06 b	2.86a	82.87b	17.13 a	0.37b	0.268b	13.05b
	60 kg N	115.39 a	30.29 a	1.80 a	14 a	2.4 b	43.12 a	1171.79 a	2.89 a	0.50 a	29.68 a	2.95a	82.59 b	17.41 a	0.43a	0.249c	15.27a
Cutting (Cut)	Cut 1	114.7a	26.87b	1.42b	13.24a	2.57a	37.42a	757.63b	2.50b	0.34a	26.86b	2.63a	82.82b	17.18a	0.37a	0.280a	12.49a
	Cut 2	91.85b	31.40a	1.71a	13.58a	2.54a	38.09a	1166a	2.83a	0.39a	26.97a	2.52b	83.86a	16.14b	0.36a	0.257b	12.60a
Cropping seasons (Cs)	2015-2016	92.82b	22.20b	1.35b	13.13a	2.61a	37.2a	746.30b	2.10b	0.28b	27.04b	2.58a	82.88b	17.12a	0.37a	0.269a	12.81a
	2016-2017	113.73a	36.07a	1.78a	13.68a	2.51a	39.6a	1177.33a	3.23a	0.45a	27.78a	2.56a	83.80a	16.20b	0.36a	0.268a	12.28a

Means followed by different letters are significantly different ($P < 0.05$) according to Tukey HSD test.

to control (Table 2). This trend was more pronounced in Cut2 during second cropping season. In addition, cutting increased vetiver cellulose accumulation by 7.3% in Cut2 compared to Cut1 (Figure 2, C).

Results showed a significant effect ($P < 0.01$) of all studied factors and the interaction of N×Cut×Cs on the

ashes (Ash) (Table 2). N fertilization increased vetiver Ash content with a maximum in Cut1 during the first cropping season (2015-2016). In average, Ash increase by 12.81% under 60 kg N ha⁻¹ compared to control. The maximum increase was observed under Cut1 (6.44%) and in first Cs (5.67%).

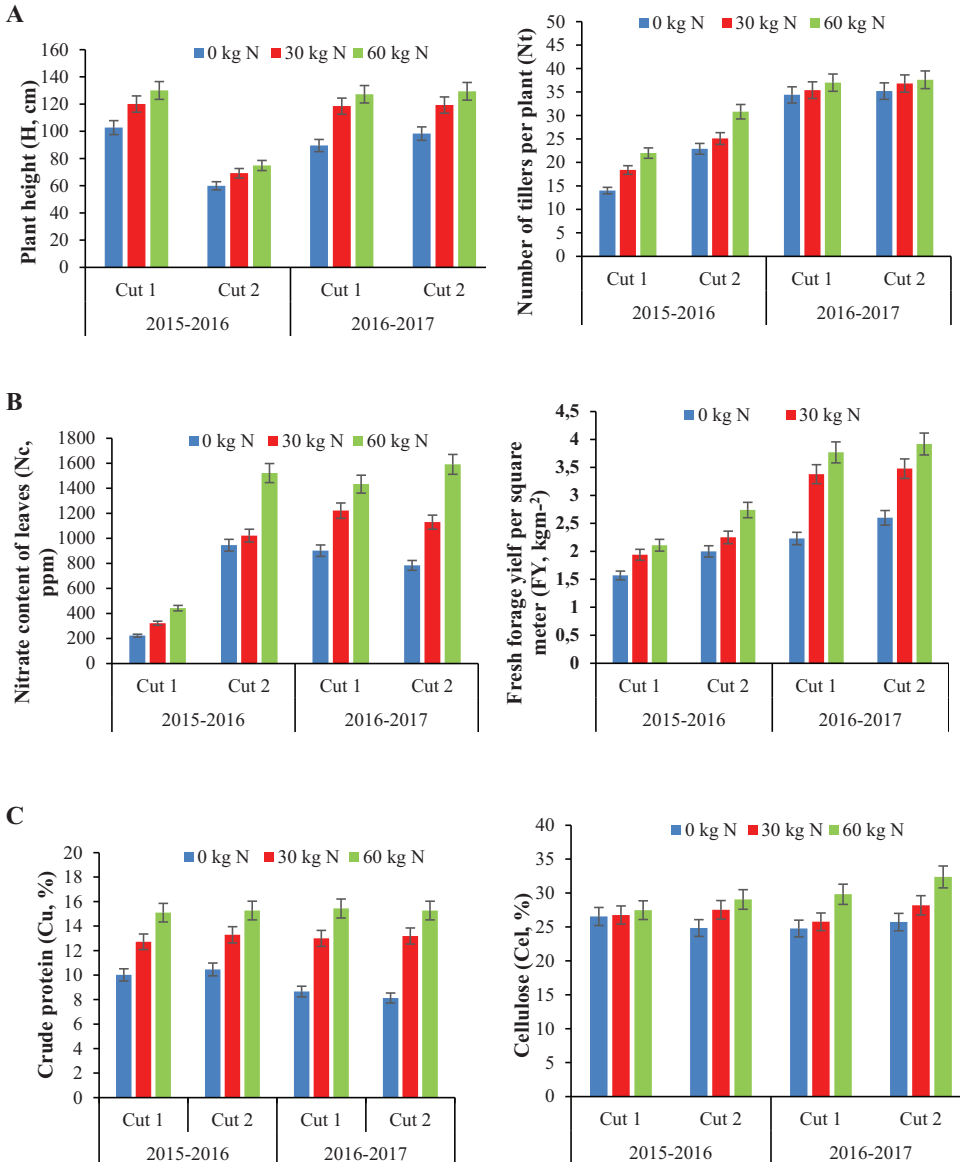


Figure 2. Variation of main morphologic (A), physiologic (B) and forage quality parameters (C) of vetiver grown during two cropping seasons (2015-2016 and 2016-2017), under three nitrogen fertilization rates (0, 30 and 60 kg N ha⁻¹) and two cuttings (MW1 and MW2). A: plant height (H) and number of tillers per plant (Nt). B: Nitrate Content of leaves (Nc) and Fresh forage yield (FY); C: Crude protein content (CP) and cellulose leaf content (Cel).

The analyzed data showed crude protein content (CP) was significantly ($P < 0.01$) affected by N, Cs, Cut, N×Cs, and Cs×Cut (Table 2). N fertilization resulted in a significant and linear increase in crude protein content. This increase was maintained during the two growing seasons. Maximum values were recorded at 60 kg N ha⁻¹, with an increase of 67% over the control. On the other hand, in unfertilized plots, there was a drop of 22% in the second year. The lowest value was recorded during the Cut2 (Figure 2, C).

Results showed a significant effect ($P < 0.01$) of all studied factors and interaction N×Cut×Cs on the organic matter content (OM) (Table 2).

N input has decreased the OM content of vetiver. This decrease was more marked under 60 kg N ha⁻¹. The minimum OM was recorded during Cut1 in first cropping seasons with 81.67%, the Maximum was observed during the Cut2 in the second cropping seasons for the control with 85.85%.

N and N×Cut interaction showed a significant effect ($P < 0.01$) on leaves calcium content (Ca) of vetiver (Table 2). Ca in vetiver leaves increased with a maximum of 48% under 60 kg N ha⁻¹ over the control. Moreover, variations between the cuts were only observed under 60 kg N ha⁻¹ (Data not Shown).

Vetiver phosphorus (P) content is significantly ($P < 0.01$) affected by N and Cs. P decreased with N fertilization. Maximum decrease (13.24%) was observed under 60 kg N ha⁻¹ (Table 2).

Vetiver extractible ether (EE) content is significantly ($P < 0.01$) affected by N and Cs. The maximum EE content was registered during the first cropping season, since 30 kg N ha⁻¹ with an increase of 51.32% compared to control (Table 2).

Correlation analysis of agronomic and forage quality parameters

Relationship between all agronomic and forage quality parameters were evaluated using Pearson’s correlation analysis. FY under 60 kg N ha⁻¹ were positively correlated with

Table 3. Multiple linear regression (stepwise) explaining fresh forage yield (FY) variation within nitrogen fertilization rate as a dependent variable, and all measured parameters as independent variables.

Treatments	Variable chosen	R ²
FY _{0 kg N ha⁻¹}	DY	0.97**
	DY, DM _p	0.99**
	DY, DM _p , DM _s	0.99**
FY _{30 kg N ha⁻¹}	DY	0.95**
	DY, DM _p	0.99**
	DY	0.98**
FY _{60 kg N ha⁻¹}	DY, DM _p	0.99**
	DY, DM _p , DM _l	0.99**
	DY, DM _p , DM _l , FW _s	0.99*

* $P < 0.05$; ** $P < 0.01$.

FW_p, DM_p, Nc and DY. A negative correlation was found between Ch and FY_{60 kg N ha⁻¹} ($r = -0.507$). Positive correlation showed between FY_{30 kg N ha⁻¹} and FW_p, Nc, and DY. While, FY_{0 kg N ha⁻¹} was negatively correlated with DM_l / DM_s ($r = -0.573$), EE ($r = -0.847$) and CP ($r = -0.604$). In the other hand, the lowest rate of nitrogen (0 kg N ha⁻¹) were positively correlated with Cel and Ca. A positive correlation was showed between Nt and three level of nitrogen fertilization with respectively, FY_{0 kg N ha⁻¹} ($r = 0.681$), FY_{30 kg N ha⁻¹} ($r = 0.799$) and FY_{60 kg N ha⁻¹} ($r = 0.755$) (Table 4).

Nt, FW_p, Nc, FY was positively correlated with DY under 30 and 60 (kg N ha⁻¹). A negative correlation was observed between DY_{0 kg N ha⁻¹} and Nt ($r = -0.769$), L/S ratio ($r = -0.733$) and Cel ($r = -0.617$). While, DY_{0 kg N ha⁻¹} was positively correlated with EE ($r = 0.529$) and CP ($r = 0.891$) (Table 4).

CP_{0 kg N ha⁻¹} was positively correlated with DM_l/DM_s ($r = 0.508$), DY ($r = 0.891$) and EE ($r = 0.680$). While a negative correlation was noted between CP_{0 kg N ha⁻¹} and Nt ($r = -0.771$), L/S ratio ($r = -0.550$), FY ($r = -0.604$), Cel ($r = -0.693$). A negative correlation was noted between EE and P under CP_{30 kg N ha⁻¹} with respectively ($r = -0.17$) and ($r = -0.506$) (Table 4).

Stepwise analysis

Stepwise analysis was released upon vetiver fresh forage yield (FY) most important forage yield components as dependent variable and DY, DM_p, DM_s, DM_l and FW_s as independent variables.

For FY under 0, 30 and 60 kg N ha⁻¹, the independent variable that was first chosen by the model was DY followed by DM_p. Both parameters accounts for 99% of the FY despite N fertilization (Table 3). Then, DM_s and FW_s are chosen by the model even if their contribution is low.

Discussion

Agronomic parameters

In the present investigation, N fertilization impacted growth and development of vetiver during the two cropping seasons (2015-2016) and (2016-2017). Plant height increased linearly with N increased rates. Similar results were highlighted by Mondyagu *et al.* [19] for *C. zizanioides*, where 200 mg N l⁻¹ lead the plant height to reach a maximum of 105.0 cm under controlled conditions. For forage species as oats, 100 kg N ha⁻¹ as urea increases height by 33% [20].

On the other hand, growth has also been affected by temperatures. During the second year and after mowing, plant height was significantly reduced in all three treatments, regardless the N rates. This decrease is attributable to low temperatures recorded from October to November ranging from 16.7 to 12.1°C. Temperature is one of the main factors driving growth kinetics of perennial forage species [21,22].

Table 4. Correlation coefficients for the relationships between fresh yield (FY), dry yield (DY) and crude protein (CP) under three nitrogen rates (N) and all measured parameters as vetiver height (H, cm), number of tillers per plant (Nt), fresh weight per plant (FW_p, Kg m⁻²), ratio of leaves fresh weight per stem fresh weight (L/S), plant dry matter content (DM_m, %), ratio of leaves dry matter per stems dry matter (DM_l/DM_s), fresh forage yield (FY, kg m⁻¹), dry forage yield (DY, kg m⁻¹), leaf chlorophyll content estimated by SPAD (Ch), and leaves nitrate content (Nc, ppm), cellulose content (Cel), extractable ether (EE), organic matter (OM), ashes (Ash), calcium (Ca), phosphorus (P) and crude

	H	Ch	Nt	Nt	FW _p	L/S ratio	DM _l /DM _s	Nc	DM _m	FY	DY	Cel	EE	Ash	OM	P	Ca	CP
FY _{0 kg N ha⁻¹}	0,1	-0,1	,779**	,779**	0,5	-0,2	-,742**	0,5	0,4	1,0	,989**	,765**	-,799**	-0,5	0,5	-0,2	-0,3	-,678**
DY _{0 kg N ha⁻¹}	0,0	-0,1	,768**	,768**	,567	-0,2	-,726**	,534*	,551*	,989**	1,0	,776**	-,772**	-,569*	,569*	-0,2	-0,2	-,622*
CP _{0 kg N ha⁻¹}	-0,4	-0,1	-,772**	-,772**	-0,2	-0,2	,658**	-0,2	0,1	-,678**	-,622*	-,680**	,675**	0,5	-0,5	0,4	,572*	0,0
FY _{30 kg N ha⁻¹}	0,405	-0,178	,799**	,799**	,756**	0,317	-0,071	,704**	0,174	1	,980**	-0,160	-0,015	-0,295	0,295	0,172	-0,080	0,005
DY _{30 kg N ha⁻¹}	0,336	-0,167	,848**	,848**	,819**	0,285	-0,067	,764**	0,356	,980**	1	-0,176	0,002	-0,235	0,235	0,117	-0,118	0,111
CP _{30 kg N ha⁻¹}	-0,356	-0,091	0,382	0,382	0,354	-0,476	-0,398	0,343	0,450	0,005	0,111	0,030	-0,617*	-0,160	0,160	-0,506*	0,164	1
FY _{60 kg N ha⁻¹}	0,115	-,507*	,755**	,755**	,721**	-0,217	-0,179	,708**	,814**	1	,991**	-0,236	0,053	-0,198	0,198	0,039	0,025	0,037
DY _{60 kg N ha⁻¹}	0,074	-0,473	,729**	,729**	,709**	-0,242	-0,233	,726**	,878**	,991**	1	-0,226	0,034	-0,136	0,136	0,034	0,001	0,048
CP _{60 kg N ha⁻¹}	-0,075	0,009	0,235	0,235	0,130	0,482	0,411	0,158	0,076	0,037	0,048	-0,204	-0,257	0,027	-0,027	0,050	-0,172	1

***, P<0.01; **, P<0.05; Ns: not significant.

Vetiver is a tropical specie adapted to areas with temperatures ranging from 21°C to 44.5°C [23,24]. In Mediterranean, temperatures varying between 21°C and 29°C stimulates optimal vetiver vegetative growth [10].

A significant decrease in height was recorded in the control during the second cropping season. Such result could be attributed to the significant increase of the number of tillers/plant. The same observation was registered in forage crop such as *Megathyrus maximus* [25]. Indeed, vetiver is a species known for its high tillering potential [26]. Moreover, vetiver well known as phytoremediation plant can uptake all soil nutrients content [27], to built-up its aerial biomass during the first cropping season, leading to poor soil during the second year of growth.

N have growth effect during vetiver first cropping year which is the installation growth stage for perennial crops. During spring growth restart, the N stored in vetiver long and developed roots from the first cropping season [29], are among the reborn of vegetative aerial part. The same observation was registered in forage crop such as *Lolium perenne* L. [30], *Cichorium intylys* [31] as well as grassland [32,33]. After last cutting concomitant with low temperatures, the suppression of photosynthetic tissues and resulting decrease of CO₂ assimilation are among a lack of available carbon to sustain regrowth [30]. Moreover, such conditions available impact negatively N mineral absorption and assimilation during the growth recovery stage [33].

N supply induced increase in vetiver fresh yield m⁻². This increase was maintained during the two growing seasons with a maximum reached in the second year across N rates. The same results were obtained for perennial forage species as *Brachiara brizantha* [34] *Phalaris arundinacea* [35], *Miscantus* [36] and *Miscantus×giganteus* [37]. In addition, N positively impacted FY components as fresh weight/plant and number of tillers/plant. Those results are in complete consistency of Lee et al. [38] studies on *Miscantus×giganteus* and *Panicum virgantum*. Moreover, studies on *Panicum virgantum* reached similar conclusions, emphasizing the importance of tiller/plant density as a selection criterion for increasing biomass production [39,40].

Interaction of N fertilization×Cs raised vetiver DY. N positive impact on forage crops dry matter production was well documented on *Leymus chinensis* grasslad [42], Sorghum bicolor [43,43] and hybrid Sorghum×Sudan [44]. Vetiver optimum DY appears to require lower N fertilization rate (60 kg N ha⁻¹) compared to other forage crops as Maize (*Zea mais*) which need 150 to 300 Kg N ha⁻¹ to reach maximum DY [45,46]. This fact is partially attributed to vetiver root N uptake ability from deep and large exploited soil volume. Thus, vetiver as phytoremediation species, can

uptake soil mineral elements N [19], heavy metals [47], Radiocesium [48] and crude-oil from contaminated soil [49]. In fact, vetiver use its long and developed roots as a Sink for all harmful components as for heavy metals leading to accumulate up to 24.5 mg kg⁻¹ plumb of roots dry matter [50]. Moreover, foliar nitrate (Nc) levels increase as N fertilization rates and was found to be correlated to DY as reported for perennial ryegrass (*Lolium perenne*) [51-52].

Forage quality

CP as well as quality components depends on soil N content [53], issued from mineral and/or organic origins. Vetiver were grown under the low organic matter content (OM) (1.8-2%) which limits mineralization and thus available N. Results showed that N fertilization rates improved vetiver forage quality mainly for crude protein content (CP). Same observations were registered by Coblenz et al. [54], on oat showing 37% increase of CP under 80 kg N ha⁻¹ and by Oliveira et al. [55], on *Megathyrsus maximus* showing 55.7 % increase of CP under 50 kg N ha⁻¹. In fact, N is the main constitutive component of plant proteins with an average of 1.5% of shoot dry matter [56]. This positive effect has been widely described in literature as for brome grass (*Bromus diandrus*) [56], reed canary grass (*Phalaris arundinacea*) [35], timothy (*Phleum pratense*) [57], and for oats (*Avena sativa*) [58]. Increased forage grass CP content promotes ruminant's ingestion. In fact, low CP limits the efficiency of microbial digestion, as well as the level of PDI intake [59].

Moreover, N fertilization increased vetiver shoot Cel content. The increase of Cel under N fertilization was previously reported for oat [60], and sorghum [61]. It's clear that N induced both proteins and cellulose biosynthesis process. Several authors have already described the relationships between the processes of protein and cellulose biosynthesis in plants as for *Lepidium sativum* [62], *Picea abies* [63], *Arabidopsis thaliana* [64-66]. At the anthesis, sorghum bicolor cellulose and hemicellulose contents varied between 20.5% - 27.5% and 18.7% - 23.2% respectively [67]. Moreover, cropping seasons, growth stages and cuts positively impacted Alfalfa crude protein content in leaves and stems as well as crude fiber content in stems [68].

N fertilization increased both leaves / plants ratio and plant dry matter content (DM_p). Meanwhile, results showed that N decreased ratio of fresh weight and dry matter leaves/ stems. Those results are due in part to vetiver perennial growth kinetics influenced by its old and new tissues composition. In fact, perennial plants, as *Lolium perenne*, have very complex carbon distribution models due at the presence of carbon in old tissues [69]. Thus, allocation and realloca-

tion of carbon in plants are strongly correlated to Source-Sink relationship mainly under stress conditions [70]. Increase in total leaves are considered as essential forage crops aptitude. Leaves had higher digestibly, lower fiber content and higher protein content [71]. At grazing, the total ruminant's ingestion is strongly correlated with green leaves biomass [72].

Forage mineral composition is dependent on plant growth stage and mineral fertilization [73,74]. The absorption of mineral elements must adjust to kinetic of development of new plant tissues and therefore to the absorption and metabolism dynamics of nitrogen and carbon [68]. Thus, ashes content (Ash) increased under N fertilization rates as already reported for *Sorghum bicolor* with 10% increase under 100 kg N ha⁻¹ [75]. However, for other species as *Sudan grass* no significant effect was found for N fertilization on leaves mineral content [76].

Results showed that N fertilization promoted calcium shoot accumulation and decreased total phosphorus content. It's well documented that Ca and P content decreased with plant growth [77]. N fertilization for fodder species as Bermuda grass, increased Ca and P levels [78]. In fact, N rate of 448 kg ha⁻¹ allowed an increase of P and Ca contents. The same trend of Ca increase was observed for vetiver under only 60 kg N ha⁻¹. These facts indicate the ability of vetiver to offer high level of Ca and mineral to feed qualitatively livestock.

Conclusion

Vetiver presents agronomic interest for the Mediterranean areas, due to its adaptability and very high yield potential compared to other forage crops. This two-year study proved that using the same technical package of other summer perennial forage crops as N fertilization rates, growing seasons and mowing significantly improved growth, yield and nutritional quality the vetiver and those since 30 Kg N ha⁻¹. Maximum N rate of 60 Kg N ha⁻¹ allowed vetiver to reach optimum development and spring regrowth after the winter dormant growth stage, as well as after each mowing. Compared with other fodder grasses such as sorghum or corn, the N requirements of vetiver are fairly contained, limiting production costs and N pollution. The introduction of this species into the fodder production systems of Mediterranean countries could have an agronomic and ecological interest.

Funding

This research was funded by North-Ouest Sylvo-Pastoral Development Office (ODESYPANO) and the laboratory of cereal breeding at INAT.

Acknowledgments

We would like to thank technical staff of Central Laboratory of Analyses of Aliments for the Cows.

Conflicts of interest

The authors declare that the research was conducted in the absence of any commercial or financial relationships that could be constituted as a conflict of interest regarding the publication of this paper.

References

- [FAO STAT] Food and Agriculture organization statistics. 2000. Are grasslands under threat Brief analysis of FAO statistical data on pasture and fodder crops.
- Huyghe C. 2003. Les fourrages et la production de protéines [Forages and protein production]. Fourrages. 174:145–162.
- [INS]. Institut National de la statistique [National Institut of statistics].2016. <http://www.ins.tn/fr/themes/agriculture>.
- [OEP] Office de l'Élevage et des Pâturages. Données sectorielles [Livestock and pasture office. Sector data].2017.
- <http://www.oep.nat.tn/index.php/fr/programmes-developpement/ressources-alimentaires>
- Khayouli C. 2000. Profil fourrager la Tunisie [Forage profile Tunisia]. http://www.fao.org/ag/agp/agpc/doc/counprof/frenchtrad/Tunisie_fr/Tunisia_fr.htm#6.1.
- Hafez EM, Abdelaal Kh AA. 2015. Impact of Nitrogen Fertilization Levels on Morphophysiological Characters and Yield Quality of Some Maize Hybrids (*Zea mays* L.). Egypt. J. Agron. 37 (1):35–48
- [A.P.I.A] Agence de Promotion des Investissements Agricoles. 2016. L'Agriculture tunisienne [Agency of Promoting Investments on Agriculture. Tunisia agriculture]. <http://www.apia.com.tn/agriculture-tunisienne.html>
- Mickovski SB, Van beek LPH, Salin F. 2005. Uprooting of vetiver resistance of vetiver grass (*Vetiveria zizanioides*). Plant Soil. 278:33–41.
- Ghotbizadeh M, Sepaskhah AR. 2015. Effect of irrigation interval and water salinity on growth of vetiver (*Vetiveria zizanioides*). Int J Plant Prod. 9:17–38.
- Dudai N, Putievsky E, Chaimovitch D, Ben-Hur M. 2006. Growth management of vetiver (*Vetiveria zizanioides*) under Mediterranean conditions. Journal of Environmental Management. 8: 63–71.
- Grimshaw, R.B. 1989. New Approaches to Soil Conservation. Rainfed Agriculture in Asia and the Pacific 1 (1):67-75.
- Truong PN. 2002. Vetiver grass Technology. “Vetiveria”, Ed. Massimo Maffei. Taylor & Francis, London and New York. Chapter 6:114–132.
- Truong PN, Loch R. 2004. Vetiver system for erosion and sediment control. ISCO 2004- Paper presented at: the 13th International Soil Conservation Organisation Conference; July 4–7; Brisbane, Australia.
- Datta R, Quispe MA, Sarkar D. 2011. Greenhouse study on the phytoremediation potential of vetiver grass *Chrysopogon zizanioides* L. in arsenic-contaminated soils. Bull Environ. Contam Toxicol. 86:124–128. Doi:10.1007/s00128-010-0185-8
- Raman JK, Edgard G. 2015. LCA of bioethanol and furfural production from vetiver. Bioresource Technology. 185:202–210.
- Liu JX, Cheng Y. 2002. issues of utilization and protection formative vetiver grass. Pratacultural Science. 19 (7): 13–16.
- Dindová, A., Hakl, J., Hrevušová, Z., Nerušil, P. 2019. Relationships between long-term fertilization management and forage nutritive value in grasslands. Agriculture, Ecosystems & Environment. 279: Pages 139-148.
- [AOAC] Association of Official Analytical Chemists International.1997. Official Methods of Analysis. 16th Edition, AOAC, Arlington.
- Mondyagu S, Kopsell DE, Steffen RW, Kopsell DA, Rhykerd RL. 2012. The Effect of nitrogen level and form on the growth and development of vetiver grass (*Chrysopogon zizanioides*). Transactions of the Illinois State Academy of Science. 105 (1&2):1-10.
- Coblentz WK, Jokela WE, Cavadini JS. 2016. Production and nitrogen-use efficiency of oat forages receiving slurry or urea. Agron. J. 108:1390–1404.
- Thomas H, stoddart J.1995.Temperature sensitivities of *Festuca arundinacea* as chreb. and *Dactylis glomerata* l. ecotypes. new Phytol.130:125–134
- Ferris R, Nijs I, Behaeghe T, Impens T. 1996. Contrasting CO₂ and temperature effects on leaf growth of perennial ryegrass in spring and summer. Journal of Experimental Botany. 47 (301):1033–1043.
- Greenfield, J.C. 1989. Vetiver Grass (*Vetiveria* spp.): The Ideal Plant for Vegetative Soil and Moisture Conservation. Asia Technical Department, Agriculture Division, The World Bank, Washington, DC. (TVN Newsletter1).
- Lavana UC. 2000. Primary and secondary centers of origin of vetiver and its dispersion. In: Chomchalow, N., Barang, N. (Eds.), Proceedings of the IInd International Conference on Veriver: Vetiver and Environment.

- Office of Royal Development Project Board, Bangkok, Thailand, pp. 424–427.
26. De Oliveira da Silva R, Chaves Miotto FR, Miranda Neiva JN, Monteiro da Silva LFF, De Freitas IB, Araújo VL, Reste L. 2020. Effects of increasing nitrogen levels in Mombasa grass on pasture characteristics, chemical composition, and beef cattle performance in the humid tropics of the Amazon. *Tropical Animal Health and Production*. 52, 3293–3300
 27. Xia HP, Bing YB. 2003. Study of screening better ecotypes of vetiver grass. 517–523. Proceedings of third international conference on Vetiver and exhibition. China Agriculture Press, Guangzhou, China.
 28. Truong PN. 2000. The global impact of vetiver grass technology on the environment. Proceedings of the second international Vetiver conference, Thailand. 46–47.
 29. Xia HP. 2004. Ecological rehabilitation and phytoremediation with four grasses in oil shale mined land. *Chemosphere*. 54:354–353.
 30. Avice JC, Louahlia S, Chanta Kim T, Jacquet A, Morvan-Bertrand A, Prudhomme MP, Ourry A, Simon JC. 2001. Influence des réserves azotées et carbonées sur la repousse des espèces prairiales [Influence of nitrogen and carbon reserves on the re-growth of pasture species]. *Fourrages, Association Française pour la Production Fourragère*. 165.3-22. <https://hal.inrae.fr/hal-02679188>
 31. Clement CR, Hopper MJ, Jones LHP. 1978. The uptake of nitrate by *Lolium perenne* from flowing solution. *J exp Bot*. 25:435–464.
 32. Hofer D, Suter M, Buchman N, Lüsher A. 2017. Nitrogen status of functionally different forage species explains resistance to severe drought and post-drought overcompensation. *Agriculture, Ecosystems and Environment*. 236: 312-322
 33. Jarvis SC, Macduff JH. 1989. Nitrate nutrition of grasses from steady-state supplies in flowing solution culture following nitrate deprivation and/or defoliation. *J Exp Bot*. 40: 965–975.
 34. Min DH, Vough LR, Reeves JB. 2002. Dairy slurry effects on forage quality of orchard grass reed canary grass and alfalfa–grass mixtures. *Anim Feed Sci Technol*. 95:143–157.
 35. Delevatti LM, Cardoso AS, Barbero RP, Leite RG, Remanzini EP, Ruggieri AC, Reis RA. 2019. Effect of nitrogen application rate on yield, forage quality, and animal performance in a tropical pasture. *Scientific reports*. 7596 (9).
 36. Clifton-Brown JC, Breuer J, Jones MB. 2007. Carbon mitigation by the energy crop, *Miscanthus*. *Glob. Change Biol*. 13:2296–2307. doi:10.1111/j.1365-2486-2007.01438.x.
 37. Christian DG, Riche AB, Yates NE. 2008. Growth, yield and mineral content of *Miscanthus giganteus* grown as a biofuel for 14 successive harvests. *Ind Crops Prod*. 28: 320–327. doi: 10.1016/j.indcrop.2008.02.009
 38. Lee MS, Wycislo A, Guo J, Lee DK, Voigt T. 2017. Nitrogen fertilization effects on biomass production and yield Components of *Miscanthus*×*giganteus*. *Front Plant Sci*. 8:544. doi:10.3389/fpls.2017.00544.
 39. Das MK, Fuentes RG, Taliaferro CM. 2004. Genetic variability and trait relationships in switchgrass. *Crop-Sci*. 44:443–448. doi: 10.2135/cropsci2004.4430
 40. Boe A, Beck DL. 2008. Yield components of biomass in switchgrass. *Crop Sci*. 48 :1306–1311. doi: 10.2135/cropsci2007.08.0482
 41. Ayub M, Nadeem MA, Tanweer A, Hussain A. 2002. Effect of different levels of nitrogen and harvesting time on growth, yield and quality of sorghum fodder. *Asian J. plant Sci*. 1:304–307.
 42. Afzal M, Ahmad A, Ahmad AUH. 2012. Effect of nitrogen on growth and yield of sorghum forage (*Sorghum bicolor* (L.) Moench cv.) under three cutting system. *Cercetări Agronomice în Moldova*. 4 (152) : 57–64.
 43. Shi Y, Wang J, Le Roux X, Mu C, Ao Y, Gao S, Zhang J, Knops JMH. 2019. Trade-off and synergies between seed yield, forage yield, and N-related disservices for a semi-arid perennial grassland under different nitrogen fertilization strategies. *Biology and Fertility of Soil* (2019) 55:497-509
 44. Mut H, Gulumser E, Dogrusoz MC, Basaran U. 2017. Effect of different nitrogen levels on hay yield and some quality of sudan grass and sorghum×sudan grass hybrids. *Animal nutrition and feed technology*. 17:269–278.
 45. Karasu A, Oz M, Bayram G, Turgut I. 2009. The effect of nitrogen levels on forage yield and some attributes in some hybrid corn (*Zea mays indentata* Sturt.) cultivars sown as second crop for silage corn. *African Journal of Agricultural Research*. 4 (3):166–170.
 46. Nadeem Ather M, Iqbal Z, Ayub M, Mubeen K, Ibrahim, M. 2009. Effect of nitrogen application on forage yield and quality of maize sown alone and in mixture with Legumes. *Pakistan journal life and social sciences*. 7 (2):161–167.
 47. Roongtanakiat N, Sanoh S. 2011. Phytoextraction of zinc, cadmium and lead from contaminated soil by vetiver grass. *Kasetsart J J (Nat. Sci.)* 45:603–612.
 48. Roongtanakiat N, Akharawutchayanon T. 2017. Evaluation of vetiver grass radiocesium absorption ability. *Agriculture and natural resources*. 51:173–180.

49. Brandt R, Merkl N, Schultze-Kraft R, Infante C, Broll G. 2006. Potential of Vetiver (*Vetiveria zizanioides* (L.) Nash) for phytoremediation of hydrocarbon-contaminated soils in Venezuela. *Int J Phytorem.* 8:273–284.
50. Alves JC, De Souza AP, Pôrto MLA, Fontes RLF, Arrund J, Marques LF. 2016. Potential of sunflower, castor bean, common buckwheat and vetiver as lead phytoaccumulation. *Revista Brasileira de Engenharia Agrícola Ambiental.* 20 (3) : 243-249. DOI : <http://dx.doi.org/10.1590/1807-1929/>
51. Sicard G. 1995. Nitrogen fertilization nitrogen uptake and seed yield in perennial ryegrass. *Proceedings of the Third International Herbage Seed Conference.* 286–290.
52. Gislum R, Rowarth JS, Boelt B. 1999. The relationship between applied nitrogen concentration of nitrogen in herbage and seed yield in perennial ryegrass (*Lolium perenne* L.), VI. Cv. Borvi in Denmark. *J Appl Seed Prod.* 17:89–92.
53. Gislum R, Boelt B, Jensen ES, Wollenweber B, Kristensen K. 2005. Temporal variation in nitrogen concentration of above ground perennial ryegrass applied different nitrogen fertilizer rates. *Field Crops Research.* 91:83–90.
54. Delaby L, Peyraud JL, Delagarde R. 1996. Utilisation des intrants azotés pour le pâturage des vaches laitières [Use of nitrogen inputs for grazing dairy cows]. *Revue suisse Agric.* 28 (5):276–280.
55. Coblenz WK, Jokela WE, Bertram MG. 2014. Cultivar, harvest date, and nitrogen fertilization affect production and quality of fall oat. *Agron. J.* 106:2075–2086.
56. De Oliveira JKS, Da C. Corrêa DC, Q. Cunha AM, Do Rêgo AC, Faturi C, Da Silva WL, Domingues FN. 2020. Effect of nitrogen fertilization on production chemical composition and morphogenesis of Guinea Grass in the humid Tropics. *Agronomy.* 10 (10), 1840
57. Brown WF, Phillips JD, Jones DB. 1987. Ammoniation or cane molasses supplementation of low quality forages. *J Anim Sci.* 64 (4): 1205–1214.
58. Messman M.A, Weiss WP, Erickson DO. 1991. Effects of nitrogen fertilization and maturity of brome grass on in situ ruminal digestion kinetics of fiber. *J Anim Sci.* 69:1151–1161.
59. Pelletier S, Tremblay GF, Bélanger G, Chantigny MH, Sequin P, Drapeau R, Allard G. 2008. Nutritive value of timothy fertilized with chloride or chloride-containing liquid swine manure. *J Dairy Sci.* 91:713–721.
60. Peyraud JL, Astigarraga L. 1998. Review of the effect of nitrogen fertilization on the chemical composition intake digestion and nutritive value of fresh herbage, consequences on animal nutrition and N balance. *Anim. Feed Sci. and Techn.* 72: 235–259.
61. Coblenz WK, Akins MS, Cavadini JS, Jokela WE. 2017. Net effects of nitrogen fertilization on the nutritive value and digestibility of oat forages. *J Dairy Sci.* 100:1–12. <https://doi.org/10.3168/jds.2016-12027>. © American Dairy Science Association®, 2017.
62. Yutaro M, Osamu U. 2018. Structural and physiological responses of the C4 grass *Sorghum bicolor* to nitrogen limitation. *Plant Production Science.* 21: (1)39–50. DOI:10.1080/1343943X.2018.1432290.
63. Herth W. 1985. Plasma-membrane rosettes involved in localized wall thickening during xylem vessel formation of *Lepidium sativum* L. *Planta.* 164:12–21.
64. Fernandes AN, Thomas LH, Altaner CM, Callow P, Forsyth VY, Apperley DC, Kennedy CJ, Jarvis MC, 2011. Nanostructure of cellulose microfibrils in spruce wood. *Proc Natl Acad Sci U.S.A.* 108:1195–1203.
65. Arioli T, Peng LC, Betzner AS, Burn J, Wittke W, Herth W, Camilleri C, Hofte H, Plazinski J, Birch R, et al. 1998. Molecular analysis of cellulose biosynthesis in *Arabidopsis*. *Science.* 279: 717–720.
66. Pearson S, Paredez A, Carroll A, Palsdottir H, Doblin M, Poindexter P, Khitrov N, Auer M, Somerville CR. 2007. Genetic evidence for three unique components in primary cell-wall cellulose synthase complexes in *Arabidopsis*. *Proc Natl. Acad Sci U.S.A.* 104:15566–15571.
67. Carroll, A., Mansoori, N., Li, S., Lei, L., Vernhettes, S., Visser, R.G., Somerville, C., Gu, Y., Trindade, L.M., 2012. Complexes with mixed primary and secondary cellulose synthases are functional in *Arabidopsis* plants. *Plant Physiol.* 160, 726–737.
68. Zhao YL, Dolat A, Steinberger Y, Wang X, Osman A. 2009. Biomass yield and production, impacts on the environment and best management strategies. *Nutr Cycl Agroecosyst.* 63:117-127. <http://dx.doi.org/10.1023/A:1021107026067>.
69. Popovic S, Grljusic S, Gupic T, Tucak M, Stjepanovic M. 2001. Protein and fiber content in alfalfa leaves and stems. In: Delgado I. (ed.), Lloveras J. (Ed). *Quality in lucerne and medic for animal production.* Zaragoza: CIHEAM, 2001.p.2015-2018 (Options Méditerranéennes: Série A. Séminaires Méditerranéens; n.45)
70. Bazot S. 2005. Contribution à l'étude de l'allocation des photassimilats récents dans la plante et la rhizosphère chez une graminée pérenne (*Lolium perenne* L.) [Contribution to the study of the allocation of recent photosynthates in the plant and the rhizosphere in a perennial grass (*Lolium perenne* L.)]. [dissertation]. Institut National Polytechnique de Lorraine-INPL. <https://tel.archives-ouvertes.fr/tel-00137743>

71. Farrar JF, Jones DL. 2000. The control of carbon acquisition by roots. *New Phytologist*.147: 43–53.
72. Collins M, Fritz JO. 2003. Forage quality. In: Barnes, R.F., Nelson, C.J., Collins, M., Moore, K.J. (Eds.), *Forages*. Vol. 1. An Introduction to Grassland Agriculture, 6th ed. Iowa State Press, Ames, IA, pp. 363–390.
73. Delaby L. 2000. Effet de la fertilisation minérale azotée des prairies sur la valeur alimentaire de l’herbe et les performances des vaches laitières au pâturage [Effect of nitrogen mineral fertilization of grasslands on the nutritional value of grass and the performance of dairy cows pasture]. *Fourrages*.164:421–436.
74. Hemingway RG. 1999. The effect of changing patterns of fertilizer applications on the major mineral composition of herbage in relation to the requirements of cattle: A 50-year review. *Animal Sci*. 69:1–18.
75. Salette J, Huché L. 1991. Diagnostic de l’état de nutrition minérale d’une prairie par l’analyse du végétal. Principes, mise en œuvre, exemples [Diagnosis of the state of mineral nutrition of a meadow by the analysis of the plant. Principles, implementation, examples]. *Fourrages*. 125: 3–18.
76. Joorabi S, Akbari N, Chaichi MR, Azizi KH. 2015. Effect of sowing date and nitrogen fertilizer on sorghum (*sorghum bicolor* l. var. speed feed) forage production in a summer intercropping system. *Cercetări Agronomice în Moldova*. vol. xlviii , no. 3 (163).
77. Glamočlija D, Janković S, Rakić S, Maletić R, Ikanović J, Lakić Ž. 2009. Effects of nitrogen and harvesting time on chemical composition of biomass of Sudan grass fodder sorghum and their hybrid. *Turk J Agric For*. 35:127–138.
78. Falola OO, Alasa MC, Amuda AJ, Babayemi OJ. 2013. Nutritional and Antinutritional Components of Vetiver Grass (*Chrysopogon zizanioides* L. Roberty) at Different Stages of Growth. *Pakistan Journal of Nutrition*. 12 (11):957–959.
79. Kering MK, Guretzky JA, Funderburg E, Mosali J. 2011. Effect of nitrogen fertilizer rate and harvest season on forage yield quality and macronutrients Concentrations in Midland Bermuda grass. *Agronomy & Horticulture -- Faculty Publications*. Paper 555.<https://digitalcommons.unl.edu/agronomyfacpub/555>



Received for publication: December, 07, 2021
Accepted: March, 10, 2022

Original paper

Comprehensive study on catfish (*Clarias gariepinus*) burger as affected by fortification using carrot and cauliflower

**ASMAA HAMMAD^{1*}, MOSTAFA AHMAD OWON¹, ABD ELBASET
ABD ELAZIZ SALAMA¹, BADIYA ABD ELRAHMAN BISAR¹**

¹Food Technology Department, Faculty of Agriculture, Kafrelsheikh University, Kafrelshiekh, Egypt.

Abstract

This work was conducted to prepare catfish burgers (CFB) using some fresh vegetables such as carrot, cauliflower and mixture of them. Vegetables were partially substituted of catfish meat at different levels of (2.5, 5, 10, 15 and 20%), compared with the control sample (without vegetables). Sensory properties were done in different sessions by a trained panel and generic consumers to assess product acceptability. The best samples were 2.5, 5 and 15% of cauliflower, carrots and mixture, respectively, which were selected from organoleptic values and analyzed. The addition of vegetables to catfish burger showed better cooking properties like decrease cooking loss, increase moisture retention, cooking yield and shrinkage. Proximate chemical composition, minerals, and vitamins (A, C and E) were determined. A little decrease in moisture and protein of prepared samples was reported compared with the control, furthermore, carrot and cauliflower improved the ash, fiber, fat and minerals content of CFB, except potassium (K) in burger fortified with 5% carrot as well as Mg, Zn and Fe in burger fortified with cauliflower and mixture vegetables. Also, adding investigated samples to CFB increased vitamin A and E compared with the control, but vitamin C was not defined in all samples including the control.

Keywords

Catfish burger; Carrot; Cauliflower; Vitamins; Minerals.

To cite this article: HAMMAD A., OWON MA., SALAMA AEAE, BISAR BAE. Comprehensive study on catfish (*Clarias gariepinus*) burger as affected by fortification using carrot and cauliflower. *Rom Biotechnol Lett.* 2022; 27(2): 3343-3351 DOI: 10.25083/rbl/27.2/3343.3351

✉ *Corresponding author: Asmaa Hammad, Food Technology Department, Faculty of Agric. Kafrelsheikh University, Egypt. E-mail: asmaa_hammad@agr.kfs.edu.eg

Introduction

Many studies have been demonstrated on high-quality fishery fast food products such as fish fingers, fish crackers, fish balls, fish cake and fish burgers. In recent years, consumers preference has significantly directed towards fast foods consumption since there has been rapid urbanization and an increase in the working women population. The working people along with new generation students and young people are now more interested in fast foods. Catfish (*Clarias gariepinus*) is mainly fresh water fish species that are well adapted to enclosed water and resistant to handling and diseases.

It is produced in Egypt in large quantities together with the Nile fishery, especially in Nasser's lake, in the first pond in Wadi El-Rayan Lake and together with fish farming and other freshwater lakes. Catfish is considered a good nutritionally food because it contains vitamins, minerals, protein and unsaturated fatty acids (Nelson *et al.*, 2016). However, many consumers do not prefer it in the fresh form because of its shape is undesirable for the consumer. One of the most important mince based products is the catfish burgers (CFB). CFB is a tasty and popular item in the fast foods industry.

Vegetables are vital among food crops because they provide humans with the necessary amounts of several vitamins and minerals. It is considered a rich source of folic acid, carotene, riboflavin, ascorbic acid and minerals (Van Duyn *et al.*, 2000; Woodside *et al.*, 2013 and Amao, 2018). Adding fresh vegetables to animal and fish meats is useful in providing them with some vitamins, minerals and dietary fiber, and reduces the fat content in them, in addition to being economically beneficial for the high prices of meat and fish.

Carrot (*Daucus carota*) is one of the important widely consumed root vegetables, a good source of beta carotene, iron, pectin, dietary fiber, minerals etc. It is known as a source of phenolic compounds and carotenoids, which inhibits lipid oxidation (Soria *et al.*, 2009). Cauliflower (*Brassica oleracea l. var. botrytis*) has been mentioned as a vital source of vitamin B6, dietary fiber, folic acid, vitamin B5 and minerals and contain many bioactive compounds, especially organo sulphur phytochemicals possessing anti-carcinogenic activity and other phytochemicals, which are known to have antioxidants activity (Hegazy and Ammar, 2019). Antioxidants included in these vegetables help the body against oxidative stress. Among Brassica vegetables, kale, broccoli and Brussels sprouts are satisfied sources of antioxidants, carotenoids and vitamins (Podsędek., 2007). They may protect humans from chronic diseases, such as cancer and cardiovascular disease.

The objectives of this work were to evaluate the effect of adding various levels of (cauliflower, carrot and mix of

them) as natural sources of antioxidants and dietary fiber on chemical composition, minerals content, vitamins, cooking properties and sensory characteristics of CFB.

Materials and methods

Materials

Fresh vegetables, such as carrot (carr) (*Daucus carota*), cauliflower (cauf) (*Brassica oleracea L. var. botrytis*), and food additives including rusk powder, sugar, salt, garlic, onion powder and spices mixture (black pepper, coriander, cumin, cardamon, red pepper, cubeb and clove) were bought from the local market in Kafr El-Sheikh, Egypt .

Fresh catfish (*Clarias gariepinus*) was bought from the local fish market in Kafr El-Sheikh, Egypt.

Chemicals and reagents (analytical grade) were purchased from El-Gomhoria Company for chemicals and drug, Tanta city, Egypt.

Proximate chemical composition of vegetables, minced catfish and CFB

The proximate chemical composition of vegetables, minced catfish and catfish burgers (CFB) was preformed depending on AOAC. (2011).

Total carbohydrate was estimated by difference as follows: Carbohydrates (%) = 100 - (crude protein + crude fat + ash).

The available carbohydrates were calculated by difference according to the sequence equation: Available Carbohydrates (%) = 100 - (crude fibers + ash + crude protein + crude fat).

Catfish burger preparation

All black membranes, viscera, blood and swim bladder were removed from catfish samples after they were beheaded, gutted and rinsed with tap water. Pure fillets were produced by removing skin and bones. Flesh parts (about 47%) were sliced into fillets. The fillets were dipped in 1.0% chilled brine solution contained 0.5% acetic acid for 5 min to clean and remove any fishy odor, and fillets were drained. A kitchen meat mincer with a 3 mm diameter plate was used to mince the drained fillets.

Minced catfish was blended with various additives that are contained in (Table 1) (Al-Bulushi *et al.*, 2005). Some modifications were done by replacing the catfish meat with five different levels (2.5, 5,10,15 and 20 %) of fresh carrot, cauliflower and the mix of carrot and cauliflower in the same proportions (1:1 w/w) of the previous five mixings, but equally between cauliflower and carrot.

Every prepared CFB formula was separated into equal parts separately (50 g weight), placed between two sheets of

Table 1. Substitution levels of the vegetables (Carrot, cauliflower and mixture of them) used in the preparation of catfish burger.

Substitution Level of Minced fish (%)	Carrot, cauliflower or mixture of them (g)	Minced catfish (g)
0	-	75.00
2.5	1.75	73.25
5	3.50	71.50
10	7.50	67.50
15	11.25	63.75
20	15.00	60.00

Table 2. Recipes of CFB.

%	Ingredients
75.0	Fish mince
9.0	Sunflower oil
8.0	Starch
2.0	Salt
0.40	Sod. Bicarbonate
2.50	Onion
0.08	Garlic
0.30	Polyphosphate
2.00	Spices mix

*Spices mixture composed of 32% black pepper, 22.5% coriander, 15% cumin, 10% cardamom, 9% red pepper, 7.5% cubeb and 4% clove.

transparent casings and gently pressed to reach the desired burger size. (8.5 cm and 1 cm of diameter and thickness, respectively) using forming machine (manually operated) (NOAW-Affetacrane, Italy). CFB cooked by frying with a little oil at 170 C° for 10 min (5 min per side).

Sensory properties of burgers

Sensory of properties prepared cooked CFB fortified by various levels (2.5, 5, 10, 15, and 20%) of Carrot, Cauliflower, and mixture of them were evaluated as described by Crehan et al., (2007).

Determination of minerals content

Minerals content of fresh vegetables and produced burgers were measured by using atomic absorption spectrophotometer (BB model Avanta Σ mar GBC, Australia) as described in the AOAC methods (AOAC 2008).

Determination of Vitamins

The method of AOAC. (2008) was used to determine vitamin A content of fresh vegetables, and CFB.

Vitamin C was analyzed for used fresh vegetables and produced CFB using HPLC reverse phase coupled with a Diode Array detector (DAD). A weight of 5 g from sample was weighted into a 0.1 L flask. In 20 ml of Tris (2-carboxyethyl)-phosphine hydrochloride acid solution the sample was dissolved and acidified. The solution was diluted to 100 mL with 1 % TCA solution and was shaken. The mixture was filtered by 0.45 mm membrane filter and

put into HPLC vial for VC determination (Brause et al., 2003). To analyse Vitamin E, HPLC (Diode Array and Fluorescent detector) was used. The sample (5 g) was put into a flask (250 ml). The pyrogallol acid was added, after that, 40 ml of 95% ethanol was added. Saponification process was done by 50% KOH (10 mL). 10 mL of glacial acetic acid was added to neutralize the KOH (Deveries and Silvera, 2002). Vitamin E was extracted into a mixture of tetrahydrofuran (THF) and ethanol (1:1) solution. The extract was filtered using a 0.45 1m membrane filter into a HPLC vial for analysis.

Cooking properties of different fish burgers

Cooking loss

The cooking loss of the prepared burgers was calculated using the formula of Essa and Elsebaie (2018). As following:

$$\% \text{ Cooking loss} = \frac{\text{Weight of raw burger (g)} - \text{Weight of cooked burger (g)}}{\text{Weight of raw burger (g)}} \times 100$$

Cooking yield and moisture retentions

Cooking yield fat, moisture retentions were measured as reported by Aleson et al., (2005) according to the following equations.

% Cooking yield = Weight of raw burger (g)/ Weight of cooked burger (g) × 100

% Moisture retention = moisture of raw burger /moisture of cooked burger × 100

Shrinkage and the thickness decrease measurements

Shrinkage and thickness increase were measured according to equations described by Berry, (1992) as follows:

$$\% \text{ Shrinkage} = \frac{\text{Diameter of uncooked sample (cm)} - \text{Diameter of cooked sample (cm)}}{\text{Diameter of uncooked sample (cm)}} \times 100$$

$$\% \text{ Thickness increase} = \frac{\text{Thickness of raw sample (cm)} - \text{Thickness of cooked sample (cm)}}{\text{Thickness of raw sample (cm)}} \times 100$$

Statistical analysis

All results were studied to analysis of variance by one-way ANOVA by Sigma Stat (v.3.5. Systat Software Inc.). The significant variance between the means of treatments was estimated at the $P \leq 0.05$ level by Duncan’s new multiple range test (Steel and Torrie, 1981).

Results and discussions

Chemical composition of fresh carrot cauliflower and minced catfish

Chemical composition of fresh carrot, cauliflower and minced catfish was shown in Table (3). The results reported that carrot contained 88.21, 5.52, 0.86, 4.57, 7.00 and 82.48 % for moisture, crude protein, fat, ash, crude fibers and available carbohydrates (on dry weight), respectively. These values are nearly with slight differences with those obtained by Karmoker *et al.*, (2011) and Sultana *et al.*, (2014).

Also, chemical composition in cauliflower were 91.54, 23.21, 7.75, 8.36, 12.06, 8.46 and 36.62% for moisture, crude protein, fat, ash, crude fibers and available carbohydrates (on dry weight), respectively. These results were very close to that found by Aamer and Emara, (2016) and Baloch *et al.*, (2015).

Additionally, the results showed that the chemical composition of fresh minced catfish were 62.23, 5.01, 23.15 and 9.61 for moisture, protein, fat and carbohydrates, respectively. These results were agreement with that found by Dale (2001), who found that the components of proximate composition in five samples to be quite consistent. The proximate composition ranged from 7.0 to 4.9 % moisture, crude

protein ranged from 59.2 to 61.9, fat 8.2-9.3 %, ash 22.8-24.1 % and crude fibers were 0.3-0.5 %.

Minerals and vitamins content of fresh carrot and cauliflower

Results in Table (4) showed that fresh carrot and cauliflower have high content of all minerals. The results revealed that carrot contained 929.80, 122.80, 7.19, 4.03, 17.85, 0.33, 6.09 and 109.41 mg/100g, for Na, Ca, Mg, Zn, Fe, K, Cu and P, respectively. These results were higher than the results noticed by Butnariu and Butu, (2015). Cauliflower contained 313.85, 125.55, 7.01, 3.32, 3.91, 304, 3.91 and 456.04 mg/100g for Na, Ca, Mg, Zn, Fe, K, Cu and P respectively. These results are nearly to the result obtained by Abou-Taleb (2015) and Aamer and Emara, (2016).

Moreover, carrot and cauliflower are rich in vitamins content, carrot had 15264.13, 689.95, 40.65, while cauliflower contains 2061.69, 1196.87, 26.01 IU, and mg/100g for vitamins A, C, and E, respectively. These results are higher than those obtained by Butnariu and Butu, (2015).

Sensory properties of CFB

Data presented in Fig. 1, showed the sensory properties of cooked burger samples prepared with different levels of vegetables (carrot, cauliflower and mixture of them). Results indicated that there were no significant differences at $p \leq 0.05$ for color, taste, odor, texture, tenderness, Juiciness and overall acceptability between prepared burgers fortified by vegetables and the control burger. Therefore, from these results supplemented burger with 5% carrot, 2.5% cauliflower and 15% mixture of them could be recommended to be produced as burger with good quality acceptable sensory quality attributes.

Chemical composition of cooked CFB

Moisture, protein, fat, ash and total carbohydrates contents of the cooked control and fortified CFB with different levels of carrot, cauliflower, and mixture of them (5, 2.5 and 15 %) were shown in Table (5). The results showed that the

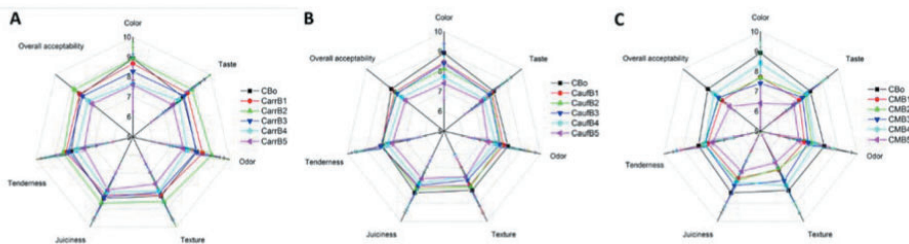


Figure 1. Hedonic sensory properties of cooked catfish burgers fortified by different levels of (A) carrot, (B) cauliflower and (C) mixture of them.

control of cooked burger (CB0) contained 47.06% moisture, 55.27 % protein, 28.14 % fat, 7.58 % ash and 9.01 % carbohydrates. From the tabulated data, it could be noticed that moisture content of cooked CFB decreased by adding vegetables. The decrease in moisture is due to the addition of fresh vegetables. These observation is in the line with Kassem and Emara, (2010), who stated that cooking of the burger patties reduced that there was about 5-7% less moisture, and Modi et al.(2004) reported that frying resulted in about 10% less moisture. The protein contents of cooked CFB had a trend like that of moisture. The decrease of protein contents in cooked CFB may be associated to the decrease in amount of catfish meat, and this is good to have burger rich in vegetarian protein. On the other hand, adding vegetables caused significantly increases in fat, fiber, and ash content in all samples including control. Increasing fat content may be related to the increase of fiber content by adding high ratio of vegetables that leads to absorb more oil when frying, or increasing fat content may be related to the oil used in frying process. A similar observation has been reported by (Dzudie et al.,2002). for beef patties prepared with common bean flour and in buffalo meat patties prepared using different legume flours (Modi et al.,2004). Increase both crude fiber and ash in this vegetable CFB due to the fact that vegetables are a rich source of crude fiber and minerals, and this is consistent with Aamer and Emara, (2016). Addition of dehydrated cauliflower powder with different levels to fish burger treatments led to increase in both of crude fibers and ash. Also, Kassem and Emara, (2010), who reported that 1% high ash depending on the formulation used in production of burger patties. Modi et al. (2004) reported that 0.4–1.2% higher ash content irrespective of binders.

Minerals content of CFB

Table (6) showed that adding fresh carrots at 5% in catfish burger CarrB2 caused increment in sodium (1395.0 to 1434.4 mg/100g), calcium (106.25 to 334.3 mg/100g), magnesium (95.625 to 120.0 mg/100g), Zinc (16.125 to 20.19 mg/100g), iron (7.0 to 7.15 mg/100g), and phosphorus (55.23 to 82.58 mg/100g) than control prepared without adding vegetables.

However, potassium content was decreased with little amount with adding fresh carrot from (1240.0 to 1238.75 mg/100g). In catfish burger fortified with 2.5 % cauliflower CaulfB1 there was also an excess of sodium, calcium and phosphorous, with a deficiency in magnesium, zinc, iron and potassium. As for the catfish burger fortified with a mixture of carrot and cauliflower CMB4 at a rate of 15%, with a ratio of 1: 1, an increase in the elements of sodium, calcium, potassium and phosphorus was observed with a decrease in the elements of magnesium, zinc and iron. As for the copper

content of the CFB, it was absent in all samples, including the control sample. High level of Na content in each fish burger treatments might be due to salt addition with 2% during manufacturing process. However, the studied fish burger still considered as a good source for minerals needed for human (Aamer and Emara, 2016).

Vitamins content of CFB

Table (7) illustrated vitamins content of CFB with adding vegetables comparing with control sample prepared from catfish meat only. CFB with 5% fresh carrot (CarrB2) was high in vitamin A content as the ratio increased from 694.81 to 1506.57 comparing with the control (CB0). In CFB fortified with 2.5% cauliflower (CaulfB1) was also increased in its content of vitamin A to 725.354, but with a smaller percentage than CFB fortified with carrot due to the higher vitamin A content of carrot than cauliflower as shown in Table (1). As for the sample containing 15% mixture of carrot and cauliflower in a 1:1 ratio, it increased in content of vitamin A, but by average rate in the previous samples. The vitamin E content of CFB had a trend like that of vitamin A. These results are in the same trend with the findings Sule et al.(2019). Incorporation of carrot powder into pasta resulted increase in beta carotene a pro-vitamin A and vitamin E. As beta carotene not detected in pasta from 100% wheat flour. Highest value of 6.13mg/100g was obtained for 30% carrot enriched pasta. Vitamin E increased from (0.68 to 1.54mg/100g). Also, these results were in conformity with those reported by Bell et al. (2006), and James & Nwabueze (2013).

Cooking properties of burgers

The cooking properties of fortified and non-fortified burgers are presented in Fig. 2A. The results showed that, the addition of vegetables to burgers affected cooking characteristics of the burgers. Cooking yield was increased in burgers with an increase in vegetables level compared to control. The cooking yield was increased from 53.66% for CB0 to 59, 52, 61.34 and 58.75 % for CarrB2, CaulfB1 and CMB4 burgers fortified with 5, 2.5 and 15 % carrot, cauliflower and mixture of them respectively. These results are in agreement with (Aleson-Carbonell et al., 2005 ; Naveena et al., 2006; Besbes et al., 2008; Alakali et al., 2010 and Al-Juhaimi et al., 2016) , who recorded similar results for the cooking yield in patties formulated with lemon albedo, finger millet flour, pea and wheat fiber concentrate, bambara groundnut seed flour and moringa seed flour, respectively. Also, El Zeny et al. (2019) found that cooking yield was increased in burgers with an increase in the chicory roots powder adding level compared to control. They explained this observation by the ability of these materials to the fat and water retention capacity and capability to keep moisture and fat in the patty matrix. As apparent in

Table 3. Chemical composition of fresh carrot, cauliflower and minced catfish (dry weight).

Materials	Moisture	Protein	Fat	Ash	Fiber	Dry matter	Total Carbohydrate	Available Carbohydrates
Fresh carrot	88.21±1.56	5.27±0.75	0.68±0.08	4.57±0.43	7.00±0.187	11.79±1.56	89.48±1.04	82.48±1.35
Fresh cauliflower	91.54±.54	23.21±0.14	7.75±0.91	8.36±0.55	12.06±1.56	8.46±0.68	48.62±1.31	36.62±1.36
Minced catfish	9.17±0.11	62.23±0.25	5.01±1.55	23.15±1.41	0.43±0.36	90.83±1.15	9.61±1.03	9.18±0.77

Data are represented as mean ± standard deviation (n=3). Values with the same superscript in the same column are not significant.

Table 4. Minerals (mg /100 g) and vitamins (IU and mg /100 g) content of fresh carrot and cauliflower.

vitamins (IU and mg /100 g)			Minerals (mg /100 g)								
Vitamin (E)	Vitamin (C)	Vitamin (A)	P	Cu	K	Fe	Zn	Mg	Ca	Na	Vegetable Sample
40.65	689.95	15264.13	109.41	6.09	.330	17.85	4.03	7.19	122.80	929.80	Fresh carrot
26.01	1196.87	2061.69	456.042	3.91	304	3.91	3.32	7.01	125.55	313.85	Fresh cauliflower

Table 5. Chemical composition of cooked burger fortified with different levels of carrot, cauliflower and mixture of carrot and cauliflower (dry weight).

Available Carbohydrates	Total Carbohydrate	Dry matter	Fiber	Ash	Fat	Protein	Moisture	Formulations
6.93±0.67	9.01±0.11	52.94±1.31	2.08±0.25	7.58±0.86	28.14±1.77	55.27±0.76	47.06±1.33	CB0 (control)
15.97±2.36	18.08±1.04	58.82±2.93	2.11±0.24	8.31±1.36	28.16±0.85	45.45±1.72	41.18±3.62	CarrB2
13.52±1.10	15.93±1.51	57.14±0.78	2.41±0.88	8.81±0.83	28.96±2.13	46.30±1.06	42.86±0.71	CaufB1
7.35±0.28	10.05±3.21	45.05±0.52	2.70±0.15	10.35±1.39	31.35±0.66	47.8±4.05	45.45±1.3	CMB4

Where: CB0, cooked cat fish burger (control); CarrB2, cooked cat fish burger fortified with 5 % carrot; CaufB1, cooked burger fortified with 2.5 % cauliflower and CMB4; cooked cat fish burger fortified with 15% mixture carrot and cauliflower. Data are represented as mean ± standard deviation (n=3).

Table 6. Minerals content of cooked catfish burgers fortified with different levels of carrot, cauliflower and mixture of carrot and cauliflower (mg/100g).

Formulations	Minerals (mg/100g)								
	Na	Ca	Mg	Zn	Fe	K	Cu	P	
CB0 (control)	1395.0	106.25	95.625	16.125	7.0	1240.0	Nd	55.23	
CarrB2	1434.4	334.3	120.0	20.19	7.15	1238.75	Nd	82.58	
CaufB1	1481.8	119.38	75.625	14.06	6.6	1231.25	Nd	106.78	
CMB4	1417.0	116.88	71.875	14.75	5.950	1263.75	Nd	77.32	

Where: CB0, cooked cat fish burger (control); CarrB2, cooked cat fish burger fortified with 5 % carrot; CaufB1, cooked burger fortified with 2.5 % cauliflower and CMB4; cooked cat fish burger fortified with 15 % mixture carrot and cauliflower.

Table 7 Vitamins content of cooked cat fish burger fortified with different levels of carrot, cauliflower and mixture carrot and cauliflower.

Formulations	Vitamin A (IU/100 g)	Vitamin C (mg/100 g)	Vitamin E (mg/100 g)
CB0 (control)	694.81	ND	23.916
CarrB2	1506.57	ND	30.28
CaufB1	725.354	ND	24.004
CMB4	850.90	ND	24.970

Where: CB0, cooked cat fish burger (control); CarrB2, cooked cat fish burger fortified with 5 % carrot; CaufB1, cooked burger fortified with 2.5% cauliflower and CMB4; cooked cat fish burger fortified with 15 % mixture carrot and cauliflower.

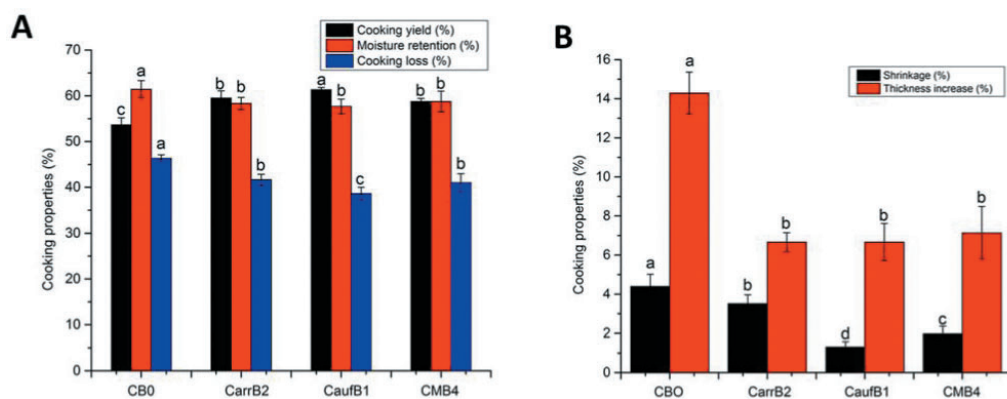


Figure 2. Cooking properties (%) of catfish burgers fortified with different levels of carrot, cauliflower and mixture of carrot and cauliflower (A) cooking yield, moisture retention and cooking loss, (B) shrinkage and thickness increase. Where: CBO, cooked cat fish burger (control); CarrB2, cooked cat fish burger fortified with 5 % carrot; CaulfB1, cooked burger fortified with 2.5 % cauliflower and CMB4; cooked cat fish burger fortified with 15 % mixture carrot and cauliflower. Data are represented as mean \pm standard deviation (n=3). Values with the same superscript in the same column are not significant.

Fig. 2A, the addition of fresh vegetables lessen the moisture retention of cooked burgers, where they were decreased with the increase of fresh vegetables level comparing to control sample. The decrease in moisture retention of the burgers may be caused to the decreases in the water absorption capacity of protein. Fig. 2B showed that the addition of fresh carrot, cauliflower and mixture of them at 5, 2.5, 15 %, respectively, was reduced the cooking loss compared to control CFB sample. The percentage of shrinkage was decreased with the fresh vegetables level and differed with the varying levels of fresh vegetables in burgers Fig. 2B. The control burger showed the highest shrinkage percent, 4.39 %, compared to 3.51, 1.3 and 1.97 % for CarrB2, CaulfB1 and CMB4 burgers, respectively. The denaturation of protein catfish, water evaporation and drainage of melted fat and juices during cooking process are related to the shrinkage (Alakali et al.,2010; Al-Juhaimi et al., 2016).

As in the case of cooking loss and reduction in diameter, the highest thickness increase was observed in the control beef burgers (14.29 %). The thickness increase decreased with increasing the amount of fresh vegetables added, where the burger fortified with 15 % mixture of fresh vegetables had the lowest thickness increase followed by fortified with 2.5 and 5 % cauliflower and carrot. These results are in the line with Selani et al. (2015), and Heydari, et al.(2016). This action could be attributed to the binding and the stabilizing properties of fresh vegetables.

Conclusion

Addition of vegetables to CFB showed improvement in the cooking properties such as increase cooking yield, de-

crease cooking loss, moisture retention and shrinkage. Proximate chemical composition, minerals, and vitamins (A, C and E) were determined to evaluate the nutritional value of prepared burger. It was observed that there are a little decrease in moisture and protein of prepared samples than control, further more carrot and cauliflower improved the ash, fiber, fat and minerals content of,CFB except potassium (K) in burger fortified with 5% carrot as well as Mg, Zn and Fe in burger fortified with cauliflower and mixture vegetables. Also, adding vegetables to CFB increased vitamin A and E than control, but vitamin C was absent in all samples including the control.

Acknowledgments

The study was enhanced by a project funded by the Priority Academic Program Development of Food Technology Department, Faculty of Agriculture, Kafrelsheikh University.

Conflict of interest

The authors have declared that there is no conflict of interest.

Highlights

- Carrot and cauliflower were added in a fresh form to the catfish burger.
- The cooking properties of fortified and non-fortified cooked catfish burgers were determined.
- The chemical composition, minerals and vitamins content of cooked catfish burger were measured.

- The sensory properties of prepared catfish burger fortified by vegetables and the control catfish burger were evaluated.

References

1. AOAC. Official Methods of Analysis of AOAC International. 18th ed. 2nd Revision . AOAC International, Maryland, USA (2008).
2. AOAC. Official Methods of Analysis of AOAC International. 18th Edition, AOAC International, Gaithersburg 2590. (2011).
3. Aamer, R. A. , Emara, H. H. Effect of Using Cauliflower (*Brassica oleracea*) to Improve Quality Characteristics of Tuna Fish Burger. *Alexandria Journal of Agricultural Sciences*. 2016; 61(6).
4. Abou-Taleb, A.A.M.A. Effect of Some Heat Treatments on nutritional and Health related constituents of Broccoli and Cauliflower as functional Foods. Master of Science in Food Science and Technology. Faculty of Agriculture, Alexandria university. (2015).
5. Alakali, J.S., Irtwange, S.V., Mzer, M.T. Quality evaluation of beef patties formulated with bambara groundnut (*Vigna subterranean L.*) seed flour. *Meat Science*, 2010; 85(2): p. 215-223. <http://dx.doi.org/10.1016/j.meatsci.2009.12.027>
6. Al-Bulushi, I.S., Stefan, K., Hamed, A., Sultan, A. Evaluating the quality and storage stability of fish burger during frozen storage. *Fish Sci* .2005;71: 648-654. DOI:[10.1111/j.1444-2906.2005.01011.x](https://doi.org/10.1111/j.1444-2906.2005.01011.x)
7. Aleson-Carbonell, L., Fernández-López, J., Pérez-Alvarez, J. A., Kuri, V. Characteristics of beef burger as influenced by various types of lemon albedo. *Innovative Food Science & Emerging Technologies*. 2005; 6(2), 247-255 <https://doi.org/10.1016/j.ifset.2005.01.002>
8. Al-Juhaimi, F., Ghafoor, K., Hawashin, M. D., Alsawmahi, O. N., Babiker, E. E. Effects of different levels of Moringa (*Moringa oleifera*) seed flour on quality attributes of beef burgers. *CyTA-Journal of Food*. 2016; 14(1), 1-9 <https://doi.org/10.1080/19476337.2015.1034784>
9. Amao, I. Health Benefits of Fruits and Vegetables: Review from Sub-Saharan Africa. *Vegetables - Importance of Quality Vegetables to Human Health*. 2018; 33-53. doi:10.5772/intechopen.74472
10. Baloch, A. B., Xia, X., Sheikh, S.A. Proximate and mineral compositions of dried cauliflower (*Brassica Oleracea L.*) grown in Sindh, Pakistan. *Journal of Food and Nutrition Research*. 2015; 3: 213-219. <http://dx.doi.org/10.12691/jfnr-3-3-14>
11. Bell, S., Becker, W., Vásquez-Caicedo, A., Hartmann, B., Møller, A., Buttriss, J. Report on Nutrient Losses and Gains Factors used in European Food Composition databases. *Federal Research Centre for Nutrition and Food*, Karlsruhe, Germany. 2006; 1–20.
12. Berry, B. Low fat level effects on sensory, shear, cooking, and chemical properties of ground beef patties. *Journal of food science*. 1992; 57(3): p. 537-537. <https://doi.org/10.1111/j.1365-2621.1992.tb08037.x>
13. Besbes, S., Attia, H., Deroanne, C., Makni, S., Blecker, C. Partial replacement of meat by pea fiber and wheat fiber: effect on the chemical composition, cooking characteristics and sensory properties of beef burgers. *Journal of Food Quality*. 2008; 31(4), 480-489 <https://doi.org/10.1111/j.1745-4557.2008.00213.x>
14. Brause, A.R., Woollard, D.C., Indyk, H.E. Determination of total vitamin C fruit juices and related products by liquid chromatography: interlaboratory study. *JAOAC Int*. 2003; 86, 367-374. <https://doi.org/10.1093/jaoac/86.2.367>
15. Butnariu, M., Butu, A. Chemical composition of Vegetables and their products. *Handbook of Food Chemistry*. 2015; 627-692 http://dx.doi.org/10.1007/978-3-642-36605-5_17.
16. Cakli, S., Taskaya, L., Kisla, D., Çelik, U., Ataman, C. A., Cadun, A., ... Maleki, R. H. Production and quality of fish fingers from different fish species. *European Food Research and Technology*. 2005; 220(5), 526-530 <http://dx.doi.org/10.1007/s00217-004-1089-9>
17. Crehan, C. M., Hughes, E., Troy, D. J., and Buckley, D. J. Effects of fat level and maltodextrin on the functional properties of frankfurters formulated with 5, 12 and 30% fat. *Meat science*. 2000; 55(4), 463-469 [https://doi.org/10.1016/s0309-1740\(00\)00006-1](https://doi.org/10.1016/s0309-1740(00)00006-1)
18. Dale, N. M. Nutrient value of catfish meal. *Journal of Applied Poultry Research*. 2001; 10(3), 252-254 <https://doi.org/10.1093/japr/10.3.252>.
19. DeVeries, J.W. , Silvera, K.R. Determination of vitamin A (retinol) and E (alpha-tocopherol) in foods by liquid chromatography: collaborative study. *J. AOAC Int*. 2002; 85, 424-434. <https://doi.org/10.1093/jaoac/85.2.424>
20. El Zeny, T., Essa, R. Y., Bisar, B. A., & Metwalli, S. M. (2019). Effect of using chicory roots powder as a fat replacer on beef burger quality. *Slovenian Veterinary Research*, 56(Suppl. 22), 509-514
21. Essa, R., & Elsebaie, E. M. (2018). Effect of using date pits powder as a fat replacer and anti-oxidative agent on beef burger quality. *Journal of Food and Dairy Sciences*, 9(2), 91-96.
22. Hegazy, A. E., Ammar, M. S. Utilization of cauliflower (*Brassica oleracea L. ssp. botrytis*) stem flour in im-

- proving Balady bread quality. *Al-Azhar Journal of Agricultural Research*. 2019; 44(1), 112-118. <https://dx.doi.org/10.21608/ajar.2019.59703>
23. Heydari, F., Varidi, M. J., Varidi, M., Mohebbi, M. Study on quality characteristics of camel burger and evaluating its stability during frozen storage. *Journal of Food Measurement and Characterization*. 2016; 10(1), 148-155. <https://doi.org/10.1007/s11694-015-9288-6>.
 24. James, S., Nwabueze, T.U. Quality Evaluation of Extruded Full Fat Blend of African Breadfruit–Soybean–Corn Snack. *International Journal of Scientific & Technology Research*. 2013; 2(9):212–216.
 25. Karmoker, P., Saha, T. ; Shams-Ud-Din, M. Processing and preservation of mixed chips from potato, papaya and carrot. *Bangladesh Journal of Agricultural Engineering* 22. 2011; (1&2): 53-60.
 26. Kassem, M. G., Emara, M. M. T. (2010). Quality and acceptability of value-added beef burger. *World Journal of Dairy and Food Sciences*, 5(1), 14-20. Lindsay, A., de Benoist, B., Dary, O., Hurrell, R. Guidelines on Food Fortification with Micronutrients. Geneva, Switzerland: WHO Library;. (2006). http://www.who.int/entity/nutrition/publications/guide_food_fortification_micronutrients.pdf. [Accessed: Oct 1, 2018]. Mahmoud, M.H., Abou-Arab, A.A., Abu-Salem, F.M. Quality Characteristics of Beef Burger as Influenced by Different Levels of Orange Peel Powder. *American Journal of Food Technology*. 2017; 12(4): p. 262-270. <http://dx.doi.org/10.3923/ajft.2017.262.270>
 27. Modi, V. K., Mahendrakar, N. S., Rao, D. N., Sachindra, N. M. Quality of buffalo meat burger containing legume flours as binders. *Meat science*. 2004; 66(1), 143-149. [https://doi.org/10.1016/S0309-1740\(03\)00078-0](https://doi.org/10.1016/S0309-1740(03)00078-0)
 28. Naveena, B. M., Muthukumar, M., Sen, A. R., Babji, Y., Murthy, T. R. K. Quality characteristics and storage stability of chicken patties formulated with finger millet flour (*Eleusine coracana*). *Journal of Muscle Foods* 2006; 17(1), 92-104. <https://doi.org/10.1111/j.1745-4573.2006.00039.x>
 29. Nelson, J.S., Grande, T.C., Wilson M.V.H. Fishes of the world. *Animal Science and Zoology*. 2016. John Wiley and Sons Inc. 5th Edition. DOI:10.1002/9781119174844
 30. Podsedek, A. Natural antioxidants and antioxidant capacity of Brassica vegetables: A review. *LWT-Food Science and Technology*. 2007; 40(1), 1-11. <https://doi.org/10.1016/j.lwt.2005.07.023>
 31. Rinaudo, M. Chitin and chitosan: properties and applications. *Progress in polymer science* . 2006; 31(7): p. 603-632. <https://doi.org/10.1016/j.progpolymsci.2006.06.001>
 32. Selani, M. M., Margiotta, G. B., Piedade, S. D. S., Contreras-Castillo, C. J., Canniatti-Brazaca, S. G. Physicochemical, sensory and cooking properties of low fat beef burgers with addition of fruit byproducts and canola oil. *Int Proc Chem Biol Environ Eng*. 2015; 81, 58-65. DOI: 10.7763/IPCBE. 2015. V81. 11
 33. Soria, A.C., Sanz, M.L., Villamiel, M. Determination of minor carbohydrates in carrot (*Daucuscarota*) by GC–MS. *Food Chemi* . 2009; 114:758–762. <https://doi.org/10.1016/j.foodchem.2008.10.060>
 34. Steel and Torrie, A. Principles and procedures of statistics, McGraw-Hill. 1981. <https://doi.org/10.4236/aid.2020.103001>
 35. Sule, S., Oneh, A. J. and Agba, I. M. Effect of carrot powder incorporation on the quality of pasta. *MOJ Food Process Technol*. 2019; 7(3), 99-103. <http://dx.doi.org/10.15406/mojfpt.2019.07.00227>
 36. Sultana, S., Iqbal, A., Islam, M. N. Preservation of carrot, green chilli and brinjal by fermentation and pickling. *International Food Research Journal*. 2014; 21(6).
 37. Van Duyn, M. A. S., Pivonka, E. Overview of the health benefits of fruit and vegetable consumption for the dietetics professional: selected literature. *Journal of the American Dietetic Association*. 2000; 100(12), 1511-1521. doi:10.1016/s0002-8223(00)00420-x
 38. Woodside, J. V., Young, I. S., McKinley, M. C. Fruits and vegetables: measuring intake and encouraging increased consumption. *Proceedings of the Nutrition Society*. 2013; 72(2), 236-245. <https://doi.org/10.1017/S0029665112003059>.



Received for publication: December, 07, 2021
Accepted: March, 10, 2022

Review

The contribution of manure to antibiotic resistance and the spread of antibiotic resistance genes in soil: a review

**JAGĂ IOANA MIHAELA^{1,*}, MANOLE ALINA^{2,*}, SÂRBU ECATERINA^{1,*},
MARUȚESCU LUMINITA GABRIELA⁴, POPA MARCELA⁴,
CHIFIRIUC MARIANA CARMEN^{4,5,6}, POSTOLACHE CARMEN^{1,3}**

¹University of Bucharest, Faculty of Biology, Doctoral School of Ecology, Romania

²University of Bucharest, Faculty of Biology, Doctoral School of Biology, Romania

³Department of Systems Ecology and Management of Natural Capital, University of Bucharest, Bucharest, Romania

⁴The Research Institute of the University of Bucharest, University of Bucharest, Romania

⁵Academy of Romanian Scientists, Bucharest, Romania

⁶The Romanian Academy, Bucharest, Romania

Abstract

The intensive use of antibiotics, worldwide, in animal husbandry, has led to the development and enrichment of different environments in antibiotic-resistant bacteria (ARB) and antibiotic-resistance genes (ARGs). Moreover, the subsequent application of manure contributes to the emergence of antimicrobial resistance (AMR) in soil. The spread of ARB and ARGs through trophic networks and potential human transmission indicate the need for innovative treatment approaches and strategies to reduce manure contaminants.

Keywords

antibiotic-resistant bacteria (ARB); antibiotic-resistance genes (ARGs)

To cite this article: JAGĂ IM, MANOLE A, SÂRBU E, MARUȚESCU LG, POPA M, CHIFIRIUC MC, POSTOLACHE C. The contribution of manure to antibiotic resistance and the spread of antibiotic resistance genes in soil: a review. *Rom Biotechnol Lett.* 2022; 27(2): 3352-3361 DOI: 10.25083/rbl/27.2/3352.3361

✉ *Corresponding author: Jagă Ioana Mihaela, Ecaterina Sîrbu, Manole Alina—University of Bucharest, Faculty of Biology, Romania; E-mail address: ioana.mihaela.jaga@drd.unibuc.ro; alina.manole@drd.unibuc.ro; monica.sarbu@cdi.unibuc.ro

Introduction

Excessive use of antibiotics in zootechnics poses a great risk to sustainable agriculture and human health worldwide. Antibiotic resistance (AR) is a typical “One Health” problem, affecting humans, animals and the environment [1,2,3]. In recent decades, the intensive use of antibiotics, worldwide, in livestock farming, has led to the development and enrichment of various environments in antibiotic-resistant bacteria (ARB) and antibiotic-resistance genes (ARGs), and the subsequent application of manure contributes to the high resistance to antibiotics in the soil [1]. Approximately 58% of the antibiotics consumed in the veterinary sector are excreted in the environment, more than half reaching the soil, where antibiotic residues can negatively affect microbial processes in the environment [4].

The development of large-scale animal feeding operations increased the need for widespread use of antibiotics in the treatment of veterinary infections, disease prevention and growth promotion. Antibiotics have been often included in the past in feed additives in small doses to promote the growth of animals used for meat, being excreted in non-metabolized forms or as active metabolites [5,6]. Antibiotics administered to animals offer selective advantages for ARB that develop in the animal intestine being eliminated in feces and possibly in the environment. The AR can rapidly spread among microbial populations by horizontal gene transfer (HGT), facilitated by mobile genetic elements (MGE), such as plasmids, integrons, transposomes and genetic tapes [5].

Manure composting is a common practice which could effectively reduce the relative abundance of ARGs and MGE, however, the field application of compost may still pose potential risks to humans and crops due to the presence of antibiotic residues, ARGs and pathogens.

In this context, in this paper we will present the diversity of resistant enteric pathogens with zoonotic potential present in manure, the determining factors for reducing the risks of human exposure to antimicrobial resistance (AMR) and the evaluation of different strategies of intervention on manure to reduce the risk of exposure to AMR.

Antibiotics, ARB and the abundance of ARGs in soil and manure

Antibiotics are a heterogeneous group of chemicals that have a low molecular weight, and are produced by microorganisms through biosynthesis processes, which stop or inhibit the microbial growth and multiplication [7]. The synthesis of antibiotics has thus evolved as an ecological competitive mechanism. Microorganisms from the group of actinomycetes, Gram-positive bacilli and microscopic fila-

mentous fungi are the main antibiotic producers [7]. Different antibiotics act differently, given the nature of their structure and the degree of affinity to certain target sites in the bacterial cell [8,7,9]. Some antibiotics inhibit the synthesis of cell walls (e.g., beta-lactams and vancomycin) blocking the functioning of enzymes involved in the synthesis of peptidoglycans. Another category of antibiotics changes the permeability of the plasma membrane (e.g., gramicidin, polymyxin, nystatin). Most classes of antibiotics interfere with protein synthesis (e.g., tetracyclines and aminoglycosides) disrupting bacterial metabolism, resulting in microbial death or growth and multiplication inhibition. There are also antibiotics that interfere with the synthesis of nucleic acids (e.g., fluoroquinolones, rifamycin) [10].

Since the early 50s, antimicrobials have been widely adopted for non-human applications, most importantly as feed additives [11].

Farm animal husbandry has intensified the need for widespread use of veterinary antibiotics in the treatment of infections, prevention of diseases and promotion of the growth of animals used for meat [12, 13, 14]. According to “The State of the World’s Antibiotics”, two-thirds of all antibiotics produced each year worldwide (65,000 tons out of 100,000 tons) are used to treat and raise farm animal [15]. In the global top of sales of antibiotics for animal use in 2009 are macrolides, penicillins and tetracyclines, which are very important for human medicine [16]. The most common antibiotics present in manure from pigs and turkeys are tetracyclines, tylosin, sulfamethazine, monesin, penicillin and nicarbazine [17,18, 19].

Antibiotic-resistant bacteria that are constantly found in animal feces can also be found in manure (e.g., *Extended-Spectrum Beta-Lactamase-producing E. coli* (ESB) and *Methicillin-Resistant Staphylococcus aureus* (MRSA) [20,21]. In soil and surface waters, antibiotics have been identified, such as macrolides, sulfonamides, sulfadimethoxine, tetracycline, lincomycins, chloramphenicol, chlortetracycline, sulfamethazine, trimethoprim [1]. The use of antibiotics in livestock production is equal to or even higher than in the human population, thus, the Union of Researchers reported that around 11 million kg of antibiotics were used for non-therapeutic purposes in the pig, poultry and cattle industries as growth promoters. This aggressive use clearly suggests the idea that large amounts of antibiotics end up in wastewater treatment plants and manure, and that is why environmental reservoirs are seen as the main hotspots for various microorganisms to achieve antibiotic resistance [22].

Manure from animals treated with antibiotics is a direct source of antibiotics and ARB, and thus the application of manure on the soil increases the level of BRA and ARGs in

the soil [23]. When animals consume antibiotics, they are released into the feces and up to 90% urine [12, 24]. In a study performed in the Netherlands on pig and cattle farms, the most common recovered antibiotics were oxytetracycline, doxycycline and sulfadiazine, followed by tetracycline, lincosycin and tylosin. More than a third of the fecal samples contained more than one antibiotic. The authors concluded that the sum of the concentrations of different antibiotics in a sample exceeded the concentrations required to select antibiotic resistance.

The indiscriminate and abusive use of antibiotics has led to the accumulation of higher concentrations of antibiotics in the environment. The sources by which antibiotics can be released into the environment are diverse, including human waste streams, as well as waste from veterinary use and animal husbandry [25,26]. Antibiotics used for prophylaxis or therapy in humans contaminate human waste streams, also antibiotics used in animals to promote growth, prevent and treat diseases, also contaminate animal waste streams. Thus, they are considered the main sources of antibiotic release into the environment [27, 15]. This is due to the fact that the administered antibiotics are not completely metabolized and are released unchanged in the environment, that is, water, manure or soils. Depending on the specific antibiotic and the dose administered, as well as the species and age of the animals, the amount and speed with which antibiotics are released into the environment are different [28], [29].

Antibiotics and their metabolites contained in manure from farm animals can leak through the pile to surface and groundwater, as well as into the soil. This phenomenon often occurs with antibiotics with high affinity in water or that are soluble in water, thus making their spread and ecotoxicity in the environment faster, and widely [30]. In fact, antibiotics can also be introduced into the environment by fertilizing the soil with raw animal manure, irrigation with wastewater generated from farmed activities or by accidental release through runoff from the farm [31,26]. Even the dust can be contaminated with antibiotics from farms and could serve equally as another way of their release into the environment [32]. Chee-Sanford et al. [33] also highlighted the release of antibiotics into the environment through the dispersion of food and the accidental spill of products [26].

Antibiotic resistance genes from the soil can enter the food chain through contaminated crops or groundwater, and can have serious consequences for human health. Studies evaluating the impact of fertilization with organic fertilizers have shown that excessive use of sulfonamides can lead to increase abundance of ARGs in the soil, but such increases are fleeting when manure is applied at recommended rates. The application of manure can affect the composition and functional

properties of microbial communities in the soil. A number of researches have been conducted using RT-qPCR on ARGs associated with agriculture to quantify several resistance genes groups, such as tetracycline resistance genes (e.g., *tetG*, *tetM*, *tetPB*) and sulfonamide resistance genes (e.g. *sul1*, *sul2*). Also based on quantitative PCR (HT-qPCR) analyses, it has been shown that hundreds of ARGs encoding resistance to aminoglycosides, tetracycline, macrolides, multidrug, chloramphenicol, beta-lactams and sulfonamide can be investigated simultaneously in manure and composts [34,35,5].

Antibiotics and heavy metals as selection agents for antimicrobial resistance in manure

The consumption of antibiotics is the main determinant of the emergence of new mechanisms of antimicrobial resistance. It should be noted that antimicrobial resistance is a natural phenomenon, preceding the modern selective pressure of the clinical use of antibiotics, as many BRA and ARGs have been identified in original environments [36]. Residues of antibiotics or other categories of substances (such as heavy metals and biocidal products) together with a large and diverse population of antimicrobial-resistant microorganisms, both both pathogens and environmental and commensal bacteria belonging to the intestinal microbiota, can also form an environment conducive to the emergence of new forms of resistance [37-43].

Resistance gives the bacterium the ability to survive at cytotoxic concentrations of antibiotic. In the presence of antibiotics, resistant bacteria can survive and even multiply. The bacteria have developed a remarkable ability to develop resistance to every antibiotic introduced into the clinic. With the introduction into the clinic of a new antibiotic, the development of resistance is inevitable, and the rate of appearance of bacterial strains resistant to new drugs is of the order of 1%, but after 8-12 years of intensive use of antibiotics in the human clinic and in animal husbandry, bacterial strains with multiple resistance have become very frequent [7]. After the application of fertilizers, the abundance of ARGs increased, which indicates a transfer of resistance genes from manure into the soil [44]. The vertical flow of genes involves the transmission of genetic information in successive generations of cells, along with the division, while the HGT is achieved by transferring genetic information between bacteria, in other ways than by division [7]. The HGT can be achieved between the donor bacterium, phages, free DNA or from dead cells and living cells through three different mechanisms, i.e. conjugation, transformation and transduction, occurring both in the clinic and in the natural environment [44,45,46].

The acquisition of resistance genes by human pathogens from environmental bacteria has been demonstrated in several cases, such as the *CTX-M*, a gene encoding for an extended spectrum β -lactamase, which originated from environmental bacteria [47,48,49,50].

An important reservoir for transferable plasmids carrying ARGs is the manure from pigs, used to fertilize the soil. A study by Binh et al. in Germany on pig manure demonstrated the frequent presence of plasmid *bla-TEM*, *sul1*, *sul2* and *sul3* [51]. The presence of selective agents such as antibiotics, heavy metals and disinfectants combined with ARGs, MGEs and various microorganisms create an ideal environment for generating resistance through mutation or genetic transfer [22].

The literature on investigating ARB and ARGs in manure has shown that most studies have focused on investigating pathogenic strains such as *Escherichia coli* and *Salmonella spp.*, and few studies have focused on investigating other genera such as *Campylobacter sp.* and *Enterococcus sp.* [52].

In cattle manure have been identified bacterial strains belonging to the *multi-resistant Enterobacteriaceae* (specifically *Salmonella spp.*), *Campylobacter*, *methicillin-resistant Staphylococcus aureus (MRSA)* and *vancomycin-resistant Enterococci (VRE)* (53-56).

Heavy metal contamination functions as a selective agent for AMR. The agricultural practices are a major source of soil contamination with moderate to highly toxic metals, such as mercury, lead, cadmium, copper, and zinc [5], which can accumulate at critical concentrations and may trigger co-selection of AMR [57]. Heavy metals such as iron, cobalt, manganese, copper and zinc are used as nutritional additives in animal feed.

Heavy metals together with antibiotics used in agriculture, discharged into the environment can cause a combined selection and co-selection effect for ARB, and therefore manure-enriched soils from antibiotic-treated animals can play an important role in evolution of ARB [58].

Antibiotics and heavy metal products are frequently used by farmers during feeding, in the treatment of infections and to limit the spread of infections to animals [59]. Exposure to these substances may increase the likelihood of RA selection and co-selection.

The toxicity of heavy metals differs from one bacterial species to another, being involved mainly in different physiological functions, but their toxicity depends very much on the concentration.

Environmental conditions greatly influence the toxicity of heavy metals. The pH value, the concentration of organic matter and the redox potential could affect the concentration and bioavailability of heavy metals in soil, sediments and

water. For example, the amount of O_2 influences the redox potential and therefore affects the solubility of some heavy metals. The decomposition in water of high concentrations of organic matter leads to a decrease in oxygen levels to anaerobicity, which decreases the solubility of cadmium and zinc. Low pH values increase the solubility of lead, cadmium and zinc [60].

It has been shown that bacteria in the environment can adapt to the ecological conditions of the environment, manifesting different degrees of sensitivity to toxic metals. The sensitivity of bacteria to the action of heavy metals is quite complex, studies having shown that Gram-positive bacteria are more sensitive to heavy metals than Gram-negative bacteria, but this sensitivity may differ even in bacteria belonging to the same genus [58].

To avoid cellular degradation caused by heavy metal toxicity, bacteria have developed tolerance mechanisms for heavy metals. The formation or complex sequestration of toxic metals shows that during metal binding, the concentration of free toxic ions in the cytoplasm is minimized. Biosorption of toxic metals takes place at the level of cell membranes, cell walls and extracellular polymeric substance (EPS) of biofilms [61, 62, 63].

Another mechanism of tolerance to heavy metals is detoxification by reducing the intracellular ions [64]. A well-understood example is the mercury reductase (*Mer A*) protein encoded by the *merA* gene. This *MerA* protein reduces Hg^{2+} to the less toxic Hg^0 , that will diffuse from the cell due to its low evaporation point [65, 66].

Extrusion of toxic ions by efflux systems is another mechanism by which bacteria tolerate the heavy metal [66]. The outflow of inorganic metal anionic arsenite is mediated by a membrane protein in Gram-positive bacteria, while in the Gram-negative ones it requires an additional ATPase subunit.

The relationship between soil resilience and human health

Human health has been directly correlated with the environment (i.e., habitat and its components, including plants, animals, microorganisms, and other human beings) and the food quality [67, 68]. Given the human population constant growing and living conditions changing, food shortages and growing demands for increased production of animal protein for human consumption around the world, there is an acute need for improving agricultural and industrial productivity [69]. The use of antibiotics in agriculture to meet the needs of the growing human population has been associated with several benefits and thus, it is anticipated that in the future almost all animals slaughtered and consumed as food will

be treated with antibiotics [70]. However, the consumption of meat, milk and eggs contaminated with antibiotic residues usually has an extraordinary negative impact on human health. Effects of antibiotic contamination can be direct or indirect, due to the high dose of residues, which could accumulate over an extended period [70]. They can manifest as hypersensitivity reactions to drugs, aplastic anemia, carcinogenic, mutagenic, immunological and teratogenic effects, nephropathy, hepatotoxicity, disruption of normal intestinal microbiota etc. [26].

The literature demonstrates the transmission of ARB and ARGs from animals to humans [71, 72, 73]. A recent review of the literature suggests that only 5% of the studies claim that there is no link between antibiotic use and AMR in humans, while 72% of the studies provided evidence in favor of transmitting AMR to humans [74].

Through the frequent use of the same antibiotics with similar modes of action, both for animal and human purposes, the transferability of AMR from animals to humans is very probable [75]. Resistance can be transferred from animal to animal or animal to human, either by direct contact or indirectly through the food chain, water, mud-fertilized soils and manure [76]. Contamination with ARB and ARGs can be achieved directly by immediate exposure to animals and biological substances, including urine, feces, milk, and saliva, or indirectly by contact or ingestion of contaminated animals and food derived from them [77, 26]. On the other hand, ARB can be transmitted from humans, including farm workers and their families, to food-bearing animals because it has been observed that the digestive tract and skin of these people contain a large number of commensal bacteria, especially *S. aureus* [78]. However, the risk of transmission depends on geographical location, ethnic / cultural practices, religion, hygiene status, farm size and type of integrated agriculture [79, 26].

Manure together with wastewater are among the main environmental reservoirs of AMR. Following direct spreading on the ground, ARB and ARGs may be released into the environment by penetration into surface waters, aerosolization or through crops (foodborne infections), all of which increasing the risk of human or animal exposure [14].

Animal husbandry operations on farms that use antibiotics are closely linked to the development of ARM in animal caregivers, meat processors and residents close to females [23].

After Woolhouse *et al.* [80], AMR in animal husbandry can be viewed from four different points of view considered as part of a farm described as an ecosystem [78]: farm animals (cattle, pigs, poultry, sheep), animal products, farm workers, farm environmental sites (water, soil, feed, wastewater, sewage, lagoon, manure and sludge after treatment).

Farm animals are an essential component in understanding the interaction between humans, animals and the environment in terms of bacteria, antibiotics and the movement of antibiotic resistance genes [80]. The digestive tract of animals and farm workers is colonized with various microorganisms, including bacteria and resistant forms, thus being the most important reservoir of microorganisms that play a vital role in disseminating and acquiring resistant bacteria and resistance genes [78, 26].

In a study conducted on a number of 1872 farmers and residents in the vicinity of farms in Germany, a country with a high density of closed animal farms, B. Bisdorff *et al.* demonstrated that 1% of the general population and 24 of the investigated farmers were positive for MRSA ST398. The risk factor for MRSA-ST398 strain colonization in the neighboring population was the repeated contact of a family member with animals, as well as regular visits to private farms. Contact with pigs has been the main risk factor for colonization among farmers [81]. The highest exposure for farmers was found in poultry farms [82].

Recent studies have shown that multi-drug-resistant *S. aureus* isolates have been identified in aerosols inside chicken farms, and over 80% of these isolates carry the *mecA* gene. For employees and local residents, inhaling bacteria from the air was the direct route of exposure, indicating a significant health risk associated with aerosol exposure [83].

The impact of manure treatment on the persistence and proliferation of AMR

Treatment methods used to limit the occurrence and spread of AMR should lead to inactivation of pathogens and, in addition, to the destruction of ARGs [84]. Composting and anaerobic digestion techniques are widely used for manure recycling.

Aerobic composting is a controlled process by which various groups of microorganisms decompose organic materials, producing secondary and inorganic organic compounds [85]. This method uses the biological oxidation process, an aerobic, thermophilic process of decomposition and microbial synthesis of organic substances from organic waste of plant or animal origin.

Aerobic composting lasts about 45 days, and the temperatures reached during this process are 65-70°C. Degradation of ARGs requires longer exposure to high temperatures. Laboratory studies have shown that temperatures above 70°C completely degrade bacterial DNA, ARGs are reduced, and therefore hyperthermophilic composting is more efficient than conventional composting, during which temperatures can reach 90°C [86].

Some studies have shown that exposure to higher temperatures and longer duration of the thermophilic phase greatly increases the effectiveness of reducing antibiotics during composting. Thus, composting has been suggested as a practical and economical intervention strategy to reduce the concentration of antibiotics in manure, before its application in the field [27]. In 2012, Kim showed in a study that composting reduced the concentration of extractable tetracycline by up to 96%, sulfonamides by 99% and macrolides by 95% [87].

There is limited information on the degradation of antibiotics during composting. A study conducted by Van Dijk and Keukens (2000) showed that the concentration of sulfochloropyramine in poultry manure decreased by 58-82% after 8 days of composting. Following the storage of the same manure after composting, for 3 months, an additional 33% reduction in the concentration of antibiotics was observed [27].

A study by Min Gou et al. in 2018 aimed to examine a broad spectrum of ARGs during the aerobic composting process and compare the effects of manure and compost application on the abundance, diversity and dynamics of these ARGs and bacteria associated with organic fertilizers and compost after a period of 4 months in the laboratory microcosm incubated in the soil taken from the field. Quantitative PCR analyzes detected a total of 144 ARGs in all soil samples, from untreated manure and composted manure, with multidrug-resistance and resistance to macrolide-lincosamide-streptogramin B, aminoglycosides, tetracycline, β -lactam. By incubating the microcosm for 120 days in the laboratory, the diversity and abundance of ARGs in manure-treated soils were significantly higher than in composted manure-treated soils. The level of AMR decreased rapidly over time in all samples of composted manure. The network analysis revealed interactions between ARGs and MGE in manure-treated soils compared to compost-treated soils, suggesting that the ARGs mobility potential was lower in compost-modified soils [88].

Anaerobic digestion is another biological method recommended to treat the manure before its application in the field. Elimination of the antibiotic during such an operation is due to temperature-dependent abiotic processes, such as adsorption and degradation [89, 90].

Another effective strategy to reduce the abundance and spread of ARGs in the soil is the application of biochar on the soil. Recently, the effects of biochar action on soil ARGs were studied and, based on the results, a significant change was observed in the microbial communities after the addition of biochar to soil. Different types of agricultural or household waste prepared from different raw materials cause different changes in the structures of the microbial commu-

nity. The change in bacterial phylogenetic compositions can result in a change in ARGs and, therefore, the addition of different biofuels to composting manure can have effects on the relative abundance of ARGs in the soil [91].

Conclusions

Soil is a natural source of antibiotics and ARGs, and their excessive use increases the risk of spreading AMR through manure. The presence and release of heavy metals in the environment trigger co-selection of antibiotic resistance in bacteria. Further, horizontal gene transfer mediated by mobile genetic elements increases the risk of spreading ARGs from soil microorganisms to human pathogens. Thus, well-managed aerobic compost treatments that reach higher peak temperatures ($> 60^{\circ}\text{C}$) are more effective in reducing antibiotic residues. Similarly, thermophilic anaerobic digesters that operate under steady state may be more effective at reducing antibiotic residues than mesophilic or anaerobic lagoons. ARGs often persist through these systems, although optimal management and higher temperature are a feasible method to more efficiently reduce the abundance of ARGs due to additional dehydration of the compost pile [92, 93].

Biochar added to a composting system favors the optimization of the composting process and its final quality, by stabilizing and reducing toxicity. Recent studies have shown that the combined application of biochar and compost decreases the bioavailability and absorption of contaminants in compost [94, 91].

Additional research leading to the development of sensitive and accurate analytical techniques to measure the concentrations of antibiotic residues, but also the clarification of the routes of antibiotic-associated contaminants in the ecosystem. In-depth research is required for optimization of the anaerobic digestion process of liquid manure, with emphasis on the elimination of antibiotic residues, streamlining the composting procedure to minimize AMR in manure and the subsequent dissemination of environmental ARGs in the food chain, as well the development of management programs for risk assessment regarding the research of minimum threshold concentrations that induce or support the spread of AMR in the environment.

Funding

This research was funded by COFUND-JPI-EC-AMR-ARMIS, Antimicrobial Resistance Manure Intervention Strategies, grant number 40/2018.

Conflicts of Interest

The authors declare no conflict of interest

References

1. Doma AO, Dumitrescu E, Muselin F, Teodor CR. 2015. Elements of bacterial structure and mechanisms of transmission of antibiotic resistance. *Veterinary medicinal product*, Vol. 9 (2), 4-27.
2. Hu H-W et al. 2016. Temporal changes of antibiotic-resistance genes and bacterial communities in two contrasting soil treated with cattle manure. *FEMS Microbiol Ecol* 92, fiv169.
3. Gelband H et al. 2015. The state of The World' S antibiotics. *Wound Healing Southern Africa* 8, 30-34.
4. Xie W-Y, Shen Q, Zhao FJ. 2018. Antibiotics and antibiotic resistance from animal manures to soil: a review. *European Journal of Soil Science*, 69, 181-195.
5. Zhu, YG, Timothy A, Johnson TA, Su JQ, Qiao M, Guo GX, Robert D, Stedtfeld RD Hashsham SA, Tiedje JM. 2013. Antibiotic resistance genes on Chinese pig farms. *PNAS*, 110 (9), 3435-3440.
6. Choffnes ER, Relman DA and Mack A. 2010. *Antibiotic Resistance: Implications for global health and novel Intervention Strategies: Workshop summary*, Washington, D.C.: National Academies Press.
7. Mihăescu G, Chifriuc MC, Dițu LM. 2007. *Antibiotics and antimicrobial chemotherapeutic substances*. Ed. Romanian Academy, ISBN: 9789732715734.
8. Sengupta S, Chattopadhyay MK, Grossart H-P. 2013. The multifaceted roles of antibiotics and antibiotic resistance in nature. *Front. Microbiol.* 4:47 10.3389/FMICB. 2013.00047.
9. Bayarski Y. 2006. *Antibiotics and their side effects*. http://hamiltoncountypreppers.org/Antibiotics_And_Their_Types.pdf
10. Ungureanu V. 2018. A brief history of the discovery of antibiotics and the evolution of resistance to antibacterial. *Medichub Media*.
11. Davies J. 2009. Antibiotic resistance and the future of antibiotics. In *Microbial Evolution and co-adaptation*. Iom. Washington, DC: The National Academies Press, pp. 160-72.
12. Sarmah AK, Meyer MT, Boxall AB. 2006. A Global Perspectives on the use, sales, exposure pathways, occurrence, fate and effects of veterinary antibiotics (VAs) in the environment. *Chemosphere* 65, 725-759 10.1016/J. Chemosphere. 2006.03.026.
13. Van Boeckel TP, Brower C, Gilbert M, and colab. 2015. Global trends in antimicrobial use in food animals. *Proc Natl Acad Sci USA*; 112 (18): 5649-5654.
14. Quaik S, Embrandiri A, Ravindran B, Hossain K, Al-Dhabi AN, Arasu MV, Ignacimuthu S, Ismail N. 2020. Review. Veterinary antibiotics in animal manure and manure laden soil: Scenario and challenges in Asian countries. *Journal of King Saud University-Science*, pg.1300-1305.
15. Gelband H et al. 2015. The state of the world's antibiotics. *Wound Healing Southern Africa* 8, 30-34.
16. World Health Organization. 2007. WHO List of important Important Antimicrobials 5th Revision. http://www.who.int/foodsafety/areas_work/antimicrobial-resistance/cia.
17. De Liguoro M, Cibir V, Capolong F, Halling-Sørensen B, and Montesissa C. 2003. Use of Oxytetracycline and tylosin in intensive calf farming: Evaluation of transfer to manure and soil. *Chemosphere*, 52:203-212.
18. Kumar K, Thompson A, Singh AK, Chander Y, and Gupta SC. 2004. Enzyme-linked Immunosorbent assay for ultratrace determination of antibiotics in stabcil aqueous samples. *J. Environ. Qual.* 33:250-256.
19. Kumar K, Gupta SC, Chander Y, and Singh AK. 2005. Antibiotic use in agriculture and its impact on the terrestrial environment. *Adv. Agron.* 87:1-54.
20. Dufour A and Bartram J. 2012 *Animal waste, water quality and human health*.
21. Huijbers PMC et al. 2015. Role of the Environment in the Transmission of Antimicrobial Resistance to Humans: A Review. *Environ. Sci. Technol.* 49, 11993-12004.
22. Hong P-Y, Al-Jassim N, Ansari MI and Mackie RI. 2013. Environmental and Public Health Implications of Water Reuse: Antibiotics, Antibiotic Resistant Bacteria, and Antibiotic Resistance Genes. *Antibiotics (Basel)*. Sep 2 (3): 367-399.
23. Udikovic-Kolica N, Wichmanna F, Brodericka NA and Handelsmana J. 2014. Bloom of resident antibiotic-resistant bacteria in the soil following manure fertilization. Edited by W. Ford Doolittle, Dalhousie University, Halifax, Canada.
24. Berendsen BJA, Wegh RS, Memelink J, Zuidema T and Stolker LAM. 2015. The analysis of animal faeces as a tool to monitor antibiotic usage. *Atalanta* 132, 258-268.
25. Gillings RM. 2013. Evolutionary consequences of antibiotic use for the resistome, mobilome and microbial pangenom. *Frontiers in microbiology*.
26. Manyi Loh C, Mamphweli S, Meyer E, Okoh A. 2018. The use of antibiotics in agriculture and its consequential resistance in environmental sources: potential implications of public health. *Molecule Logs*, Volume 23, Number 23 410.3390 / molecules23040795.
27. Dolliver H, Kumar K, Gupta SC, and Singh A. 2008. Application of enzyme-linked immunosorbent assay

- analysis for determination of monensin in environmental samples. *J. Environ. Qual.* 37:1220–1226.
28. Zhao L, Dong YH, Wang H. 2010. Residues of veterinary antibiotics in manures from feedlot livestock in eight provinces of China. *Science of Total Environment*, 1069–1075.
29. Martinez JL. 2009. Environmental pollution by antibiotics and by antibiotic resistance determinants. *Environ Pollut.*; 157:2893–2902. Two: 10.1016/J. Envpol. 2009.05.051.
30. Du L, Liu W. 2002. Occurrence, fate, and ecotoxicity of antibiotics in agro-ecosystems. A review. *Agron. Sustain. Dev.*, 32, 309–327.
31. Spiehl MJ, Goyal S. 2007. Best Management Practices for Pathogen Control in Manure Management Systems. University of Minnesota.
32. Hamscher G, Pawelzick HT, Sczesny S, Nau H, Hartung J. 2003. Antibiotics in dust originating from a pig-fattening farm: A new source of health hazard for farmers. *Environ. Health Perspect.*, 111, 1590–1594.
33. Chee-Sanford JC, Mackie R, Koike S, Krapac IG, Lin Y-F, Yannarell AC et al. 2009. Fate and transport of antibiotic residues and antibiotic resistance genes following land application of manure waste. *J. Environ. Qual.* 38 1086–1108.
34. Johnson TA, Stedtfield RD, Wang Q, Cole JR, Hashsham SA, Looft T et al. 2016. Clusters of antibiotic resistance genes enriched together stay together in swine agriculture. *MBio* 7, e02214–e02215. 10.1128/mBio.02214-15.
35. Xie WY, Yang XP, Li Q, Wu LH, Shen QR, Zhao FJ. 2016. Changes in antibiotic concentrations and antibiotic resistance during commercial composting of animal manures. *Environ. Pollut.* 219, 182–190.
36. D’Costa VM, King CE, Kalan L, Morar M, Sung WWL, Schwarz C et al. 2011, Antibiotic resistance is ancient, *Nature*, 477:457–61.
37. Tien Y-C et al. 2017. Impact of dairy manure pre-application treatment on manure composition, soil dynamics of antibiotic resistance genes, and abundance of antibiotic-resistance genes on vegetables at harvest. *Science of The Total Environment* 581-582, 32–39.
38. Schijven J F, Blaak H, Schets FM & de Roda Husman AM. 2015. Fate of Extended-Spectrum β -Lactamase-Producing *Escherichia coli* from Faecal Sources in Surface Water and Probability of Human Exposure through Swimming. *Environ. Sci. Technol.* 49, 11825–11833.
39. Slavcovici A. 2008. Antibiotic resistance of bacteria involved in severe infections, Romanian Review of Infectious Diseases. Vol. XI, nr. 4, pag. 255-264
40. Henderson DA. 1999. Ciprofloxacin resistance in *Campylobacter jejuni* isolates: detection of gyrA resistance mutations by mismatch amplification mutation assay PCR and DNA sequence analysis, *Journal of Clin Microbiology*, Record 108,8- 12.
41. Swartz NM. 2000. Minireview: Impact of antimicrobial agents and chemotherapy, from 1972 to 1998, *Antimicrobial Agents and Chemotherapy*, 2000- 2016.
42. Mărculescu A, Cernea M, Nucleanu V, Oros NA, Chereji R. 2007. Microbial resistance to antibiotics. *Veterinary Drug Volume 1*, pag. 44 -51.
43. Agero Y, Sandvang D. 2005. Class 1 integrons and tetracycline resistance genes in *Alcaligenes*, *Arthrobacter*, and *Pseudomonas* spp. isolated from pigsties and manured soil. *Appl. Environ. Microbiol.*, 71(12): 7941-7.
44. McKinney CW, Pruden A. 2012. Ultraviolet disinfection of antibiotic resistant bacteria and their antibiotic resistance genes in water and wastewater. *Environ. Sci. Technol.* 46, 13393–13400. 10.1021/es303652q
45. Sharma VK, Johnson N, Cizmas L, Mc Donald TJ, Kim H. 2016. A review of the influence of treatment strategies on antibiotic resistant bacteria and antibiotic resistance genes. *Chemosphere* 150, 702–714. 10.1016/j.chemosphere.2015.12.084.
46. Gases W, O’Neill C, Wellington E, Hawkey P. 2008. Antibiotic resistance in the environment, with special reference to MRSA. *Adv APPL Microbiol* 63C: 249-280.
47. Poirel L, Gerome P, De Champs C, Stephanazzi J, Naas T, Nordmann P. 2002. Integron, located in the oxa-32 gene box, encodes an extended-spectrum variant of beta-lactamase OXA-2 from *Pseudomonas aeruginosa*. *Antimicrobial. Chemotherapy agents.* 46 566-569.
48. Olson AB, Silverman M, Boyd DA, McGeer A, Willey BM, Pong-Porter V și colab. 2005. Identification of a progenitor of the CTX-M-9 group of extended-spectrum beta-lactamases from Georgian *Kluyvera* isolated in Guyana. *Chemotherapy antimicrobial agents.*; 49: 2112-2115.
49. Rossolini GM, D’Andrea MM, Mugnaioli C. 2008. The spread of beta-lactamases with an extended spectrum of CTX-M type. *Clin Microbiol Infect.*; 14 (suppliment 1: 33–41.
50. Kruse H, Sorum H. 1994. Transfer of Multiple Drug Resistance Plasmids between Bacteria of Diverse Origins in Natural Microenvironments, *Applied and Environmental Microbiology*, 60: 4015-4021.
51. Binh CTT, Heuer H, Kaupenjohann M, Smalla K. 2008. Piggery manure used for soil fertilization is a reservoir for transferable antibiotic resistance plasmids. *FEMS Microbiol Ecol* 66(1):25–37.

52. Feßler AT, Schwarz S. 2017. Antimicrobial Resistance in *Corynebacterium* spp., *Arcanobacterium* spp., and *Trueperella pyogenes*. *Microbiology Spectrum*, 5, (6).
53. Pornsukarom, S, Thakur S. 2016. Assessing the Impact of Manure Application in Commercial Swine Farms on the Transmission of Antimicrobial Resistant Salmonella in the Environment. *PLoS One.*, 11(10): e0164621.
54. Amador P, Fernandes R, Prudêncio C, Duarte I. 2019. Prevalence of Antibiotic Resistance Genes in Multi-drug-Resistant Enterobacteriaceae on Portuguese Livestock Manure. *Antibiotics* 13, 8(1), 23.
55. Peng S, Wang Y, Zhou B, Lin X. 2015. Long-term application of fresh and composted manure increase tetracycline resistance in the arable soil of eastern China. *Sci. Total Environ.* 506-507, 279–286.
56. Chen J, Ying GG, Wei XD, Liu YS, Liu SS, Hu LX *et al.* 2016. Removal of antibiotics and antibiotic resistance genes from domestic sewage by constructed wetlands: effect of flow configuration and plant species. *Sci. Total. Environ.* 571, 974–982. 10.1016/j.scitotenv.2016.07.085.
57. Nicholson FA, Smith SR, Alloway BJ, Carlton-Smith C, Chambers BJ. 2003. An inventory of heavy metal contributions to agricultural soils in England and Wales. *Sci. Total Environ.* 311205-219. 10.1016 / S0048-9697 (03) 00139-6.
58. Seiler C and Berendonk TU. 2012. Heavy metal driven co-selection of antibiotic resistance in soil and water bodies impacted by agriculture and aquaculture. *Frontiers in Microbiology*, vol.3.
59. Burrige L, Weis JS, Cabello F, Pizarro J and Bostick K. 2010. Chemical use in salmon aquaculture: a review of current practices and possible environmental effects. *Aquaculture* 306, 7–23.
60. Schulz-Zunkel C and Krueger F. 2009. Trace metal dynamics in flood plain soils of the River Elbe: a review. *J. Environ. Qual.* 38, 1349–1362.
61. Harrison JJ, Ceri H and Turner RJ. 2007. Multimetal resistance and tolerance in microbial biofilms. *Nat. Rev. Microbiol.* 5, 928–938.
62. Silver S and Phung LT. 1996. Bacterial heavy metal resistance: new surprises. *Annu. Rev. Microbiol.* 50, 753–789.
63. Teitzel GM and Parsek MR. 2003. Heavy metal resistance of biofilm and planktonic *Pseudomonas aeruginosa*. *Appl. Environ. Microbiol.* 69, 2313–2320.
64. Nies DH. 1999. Microbial heavy-metal resistance. *Appl. Microbiol. Biotechnol.* 51, 730–750.
65. Schiering N, Kabsch W, Moore MJ, Distefano MD, Walsh CT and Pai EF. 1991. Structure of the detoxification catalyst mercuric ion reductase from *Bacillus* sp. strain-RC607. *Nature* 352, 168–172.
66. Nies DH and Silver S. 1995. Ion efflux systems involved in bacterial metal resistances. *J. Ind. Microbiol.* 14, 186–199.
67. Sahoo KC, Tamhankar AJ, Johansson E, Lundborg CS. 2010. Antibiotic use, resistance development and environmental factors: A qualitative study among healthcare professionals in Orissa, India., *BMC Public Health*, 10, 629.
68. Ames BN. 1983. Dietary carcinogens and anticarcinogens. Oxygen radicals and degenerative diseases. *Science*, 221, 1256–1264.
69. Padol AR, Malapure CD, Dimple VD, Kamdi BP. 2015. Occurrence, Public Health Implications and Detection of Antibacterial Drug Residues in Cow Milk. *Environ. We Int. J. Sci. Technol.*, 10, 7–28.
70. Lee MH, Lee HJ, Ryu PD. 2001. Public health risks: Chemical and antibiotics residues. *Asian-Aust. J. Anim. Sci.*, 14, 402–413.
71. Khanna T, Prietena R, Dewey C, Weese JS. 2008. Colonization of *Staphylococcus aureus* resistant to methicillin in pigs and pig farmers. *Veterinar. Microbiol.* 128 298-303. 10.1016 / j. vetmic.2007.10.006.
72. Wulf MW, Sørum M, van Nes A, Skov R, Melchers WJ, Klaassen CH, and Voss A. 2008. Prevalence of methicillin-resistant *Staphylococcus aureus* among veterinarians: an international study. *Clin. Microbiol. Infect.* 14(1):29-34.
73. Smith R, Coast J. 2013. Costul real al rezistenței antimicrobiene. *British Medical Journal*; 346: f1493.
74. Singer AC, Shaw H, Rhodes V & Hart A. 2016. Review of Antimicrobial Resistance in the Environment and Its Relevance to Environmental Regulators. *Front Microbiol* 7, 407.
75. Phillips I, Casewell M, Cox T, De Groot B, Friis C, Jones R *et al.* 2004. Does the use of antibiotics in food animals pose a risk to human health? A critical review of published data. *J Antimicrob Chemother*; 53 :28–52. doi: 10.1093/jac/dkg483.
76. Marshall BM, Levy SB. 2011. Food and antimicrobial animals: the impact on human health. *Clin Microbiol Rev.*; 24 (4): 718-733.
77. Founou LL, Founou RC, Essack SY. 2016. Antibiotic resistance in the food chain: A developing-country perspective. *Front. Microbiol.*, 7, 1881.
78. Acar JF, Moulin G. 2006. Antimicrobial resistance at farm level. *Rev. Sci. Tech.* 2006, 25, 775–792.
79. Lozano C, Gharsa H, Slama KB, Zarazaga M, Torres, C. 2016. *Staphylococcus aureus* in animals and food: Methicillin resistance, prevalence and population struc-

- ture. A Review in the African Continent. *Microorganisms*, 4, 12.
80. Woolhouse M, Ward M, van Bunnik B, Farrar J. 2015. Antimicrobial resistance in humans, livestock and the wider environment. *Philos. Trans. R. Soc. B*, 370, 20140083
81. Bisdorff B et al. 2012. MRSA-ST398 in livestock farmers and neighbouring residents in a rural area in Germany. *Epidemiol. Infect.* 140, 1800–1808.
82. Radon K et al. 2002. Air contaminants in different European farming environments. *Ann Agric Environ Med* 9, 41–48.
83. Mazhar SH, Li X, Rashid A, Su JM, Xu J, Brejnrod AD, Su J-Q, Wu Y, Zhu Y-G, Zhou SG, Feng R, Rensing C. 2021. Co-selection of antibiotic resistance genes and mobile genetic elements in the presence of heavy metals in poultry farm environments. *Science of The Total Environment*, Volume 755, Part 2.
84. Barancheshme F and Munir M. 2017. Strategies to Combat Antibiotic Resistance in the Wastewater Treatment Plants. *Frontiers in Microbiol.*, 8: 2603.
85. Rynk R. 1992. On-farm composting handbook. Publ. NRAES-54. Natural Resource, Agriculture, and Engineering Service, Ithaca, NY.
86. Liao H, Lu X, Rensing C, Friman VP, Geisen S, Chen Z, Yu Z, Wei Z, Zhou S and Zhu Y. 2017. The Hyperthermophilic compound accelerates the elimination of antibiotic resistance genes and mobile genetic elements in sewage sludge. *Environ. Sci. Technol.*
87. Kim EB, Kopit LM, Harris LJ, Marco ML. 2012. Draft genome sequence of the quality control strain *Enterococcus faecalis* ATCC 29212. *J. Bacteriol.*, 194 (21), 6006–7.
88. Gou M, Hua H-Y, Zhang Y-J, Wang JT, Hayden H, Tang Y-Q, He J-Z. 2018. Aerobic composting reduces antibiotic resistance genes in cattle manure and the resistome dissemination in agricultural soils, *Science of the Total Environment* 612, 1300–1310.
89. Aust MO, Godlinski F, Travis GR, Hao X, McAllister TA, Leinweber P și colab. 2008. Distribution of sulfamethazine, chlortetracycline and tylosin in manure and soil of Canadian heath after subtherapeutic use in cattle *Environ. Pollut.* 156 1243-1251. 10.1016/j.envpol.2008.03.011.
90. Arikian OA, Mulbry W and Rice C. 2009. Management of antibiotic residues from agricultural sources: Use of composting to reduce chlortetracycline residues in beef manure from treated animals. *J. Hazard. Mater.* 164:483–489. doi:10.1016/j.jhazmat.2008.08.019.
91. Cui E, Wu Y, Zuo Y, Chen H. 2016. Effect of different biochars on antibiotic resistance genes and bacterial community during chicken manure composting. *Bioresour. Technol.* 203, 11–17. 10.1016/j.biortech.2015.12.030.
92. Pei R, Cha J, Carlson KH, Pruden A. 2007. Response of antibiotic-resistant (ARG) genes to biological treatment in milk lagoon water. *Environ. Sci. Technol.*; 41: 5108-5113. doi: 10.1021 / es070051x.
93. Bai H, He LY, Wu DL, Gao FZ, Zhang M, Zou HY, Yao MS, Ying GG. 2022. Spread of airborne antibiotic resistance from animal farms to the environment: Dispersal pattern and exposure risk. *Enviroment International*, Vol. 158.
94. Zheng H, Wang Z, Zhao J, Herbert S, Xing B. 2013. Sorption of antibiotic sulfamethoxazole varies with biochars produced at different temperatures. *Environ. Pollut.* 181, 60–67. 10.1016/j.envpol.2013.05.056.



Received for publication: December, 08, 2021
Accepted: March, 17, 2022

Original paper

Enzymatic extraction, characterization and biological properties of protein hydrolysates from freshwater fish waste

TOMA AGNES^{1,2}, CRACIUNESCU OANA², MOLDOVAN LUCIA², CIUCAN TEODORA², TATIA RODICA², ILIE DANIELA², MIHAI ELENA², SAVIN SIMONA², SANDA CATALINA², ANCA OANCEA², JURCOANE STEFANA¹, ISRAEL FLORENTINA¹, BALAN DANIELA¹, LUTA GABRIELA¹

¹University of Agronomic Sciences and Veterinary Medicine of Bucharest, 59 Marasti Blvd, District 1, Bucharest, Romania

²National Institute of Research and Development for Biological Sciences, 296, Splaiul Independentei, Bucharest, Romania

Abstract

Silver carp (*H. molitrix*) is one of the most popular species in fish farms around the world. In this paper, the bioactive properties of four protein hydrolysates from silver carp residues obtained with papain, flavourzyme, alcalase and combination of flavourzyme & alcalase treatment were analyzed. Physicochemical characterization showed that the alcalase extract had the highest extraction yield of 52.07%, presented 90.33% protein content and the highest degree of hydrolysis (76.23%). Gel electrophoresis pattern indicated that hydrolysate obtained with alcalase contains most peptides with a molecular weight below 15 kDa, while those present in the hydrolysate obtained with flavourzyme & alcalase had a molecular weight between 10-15 kDa. The effect of protein hydrolysates on DPPH free radicals inhibition varied between 47.37-50.14%, the highest value of antioxidant activity being recorded for hydrolysate obtained with papain. The hydrolysates presented antihypertensive potential determined as inhibition of angiotensin-converting enzyme, with the highest activity in the case of flavourzyme & alcalase extract. The fish protein hydrolysates were cytocompatible in a normal fibroblast culture, NCTC cell line showing cell viability over 80% for all variants. When cultivated in Hep-2 cancer cells at 10 mg/ml, the protein hydrolysates obtained by papain and flavourzyme & alcalase mixture decreased the cell viability, indication antitumoral potential. In conclusion, the fish protein hydrolysates demonstrated important bioactive properties, including antioxidant, antihypertensive and antiproliferative activity.

Keywords

bioactive peptides, fish hydrolysate, antioxidant, antihypertensive, antitumoral

To cite this article: TOMA A, CRACIUNESCU O, MOLDOVAN L, CIUCAN T, TATIA R, ILIE D, MIHAI E, SAVIN S, SANDA C, OANCEA A, JURCOANE S, ISRAEL F, BALAN D, LUTA G. Enzymatic extraction, characterization and biological properties of protein hydrolysates from freshwater fish waste. *Rom Biotechnol Lett.* 2022; 27(2): 3362-3367 DOI: 10.25083/rbl/27.2/3362.3367

✉ *Corresponding author: Agnes Toma, National Institute of Research and Development for Biological Sciences 296, Splaiul Independentei, 060031 Bucharest, Romania, Tel: +40-21-2200882, E-mail: agnes.toma@incdsb.ro

Introduction

Fish processing industry generates huge amount of wastes (skin, scales, bones, internal organs) that could be valorized to extract useful compounds, such as collagen, gelatin, bioactive peptides and minerals using physicochemical and enzymatic methods.

Fish protein hydrolysis can be performed by chemical (acidic, basic) or enzymatic treatment. The latter is easier to control, because enzymes cut proteins at certain sites resulting in certain peptides and the best results are obtained under specific conditions (pH, temperature, exposure time). The enzymes used for this purpose can have microbial (flavourzyme, alcalase, neutrase, protamex), plant (bromelain, ficin, papain) and animal (trypsin, pepsin, chymotrypsin) origin (Gao, 2021). Protein hydrolysates, resulting from the hydrolysis of native proteins, contain polypeptides and small bioactive peptides of 2-20 amino acids (Chalamaiah, 2012). Previous studies have showed that fish hydrolysates present antioxidant properties both *in vitro* and *in vivo*, antitumor, anti-inflammatory, antihypertensive, neuroprotective and antibacterial properties (Gao, 2021). The beneficial properties of the hydrolysates depend on the hydrolysis degree of the peptide extracts, composition and size of the constituent peptides.

Silver carp is a freshwater fish of the cyprinid family found in farms around the world. The by-products resulting from its processing could be used to obtain protein hydrolysates and bioactive peptides by enzymatic hydrolysis. It was previously showed that enzyme hydrolysates of silver carp white muscle obtained by alcalase, flavourzyme, neutrase, papain, pepsin, protamex and trypsin treatment presented antioxidant activity with the highest value in the case of pepsin hydrolysates (Zhong et al., 2011). Analyzing silver carp fins hydrolysates obtained with papain, alcalase, neutrase or trypsin, the highest antioxidant activity was reported in the case of alcalase and trypsin treatment (Zhang et al., 2020). Wang studied the enzymatic hydrolysates of silver carp muscle in terms of antioxidant properties assessed as free radicals inhibition and their biological properties in Caco2 cell cultures (Wang et al., 2021).

The present paper aimed to obtain enzymatic protein hydrolysates from silver carp waste tissues (bones, meat, skin) using the following types of enzymes: papain, flavourzyme, alcalase, and a combined treatment with flavourzyme & alcalase. The physicochemical characterization of the four hydrolysates was performed in terms of extraction yield, protein content, degree of hydrolysis and gel electrophoresis, then their antioxidant and antihypertensive activity assessment, while the biological evaluation consisted of

biocompatibility and antiproliferative activity testing using stabilized cell lines.

Materials and methods

Obtaining fish protein hydrolysates

Fish waste tissues were pretreated by washing, decalcification and delipidization and then subjected to hydrolysis with papain in phosphate buffer 7.5 µg/ml at pH 6, flavourzyme in phosphate buffer 4.5 µg/ml at pH 7, alcalase in phosphate buffer 4.5 µg/ml at pH 8 and a combined treatment with flavourzyme at pH 7 followed by alcalase at pH 8 (Zamora-Sillero, 2018).

Yield and protein concentration

The extraction yield was calculated as percentage reported to the amount of initial tissue put into work, based on the dry weight, according to the following formula.

Extraction yield (%) = final dry weight product / initial dry weight of raw material x 100

Protein quantification was done using Biuret assay based on reaction of CuSO₄ with peptide bonds resulting in a purple colored complex. The absorbance was read at 540 nm at a Spectrostar nano microplate reader (BMG Labtech). A standard curve was built using bovine serum albumin in a range of 0-200 µg/ml to calculate the protein concentration (Zheng et al., 2017)

Determination of the degree of hydrolysis using TNBS assay

The TNBS assay was used to quantify the free amino groups in the protein hydrolysate samples (Adler-Nissen 1969). Trinitrobenzenesulfonic acid (TNBS) reagent was prepared in 0.05 M Tris buffer, pH 8.3. A solution of L-leucine was used as standard. Absorbance was read at 346 nm at a V-650 UV-VIS spectrophotometer (Jasco, Japan).

Gel electrophoresis

Samples of protein hydrolysates were migrated in Tricine-SDS-polyacrylamide gel in 10-20% gradient of concentration, alongside a molecular weight marker. Before migration, the samples were mixed with Tricine SDS sample buffer and a reducing agent. After migration, the proteins were fixed in the gel by incubation in 85% o-phosphoric acid solution containing methanol, for 60 min. Then, the gel was stained by incubation in Coomassie blue solution, for 12 h and destained in 25% methanolic solution (Schagger, 2006).

Antioxidant activity assay

The antioxidant activity was analyzed using DPPH method (Zhang et al., 2011). This method is based on reducing

the DPPH radical in solution, which has red-purple color, turning to yellow colored solution. The absorbance was read at 520 nm using a V-650 UV-VIS spectrophotometer (Jasco, Japan). The degree of inhibition of the DPPH radical was calculated using the formula:

$$\% \text{DPPH inhibition} = (1 - \text{sample absorbance} / \text{blank absorbance}) \times 100$$

Determination of angiotensin-converting enzyme (ACE) inhibition

To determine the inhibitory potential of protein hydrolysates on the ACE, the samples were mixed with the substrate hippuryl-L-histidyl-L-leucine solution, dissolved in sodium borate buffer and NaCl, and then, with ACE. The absorbance was measured at 228 nm. The inhibition of the enzyme activity was expressed as percentage from initial activity (Papadimitriou *et al* 2012).

Cell cytotoxicity tests

The cytotoxicity evaluation of peptides samples was performed according to the standard SR-EN IS 10993. The samples were tested *in vitro* on normal mouse fibroblast NCTC cells and human tumor epithelial Hep-2 cells, using MTT cell viability assay. After 48 hours of treatment, the samples were treated with tetrazolium bromide salt solution (MTT) and isopropanol. The absorbance of resulted solutions was measured at the wavelength of 570 nm, using a Berthold plates reader (Germany). Cell viability was determined with the formula: $\% \text{cell viability} = (\text{sample O.D.} / \text{control O.D.}) \times 100$, where the viability of the Control culture is considered to be 100%.

Results and discussion

Yield and protein content

The extraction yield and protein content of the four enzymatic hydrolysates varied between 20.94-52.07% and 32.32-95%, respectively (Table 1). The lowest extraction yield was recorded in the case of papain hydrolysis (20.94%), but the extract had the highest protein content of 95%. These values were higher than those obtained by Noman *et al.* (2018) which reported values of 17.47% for yield and 79.67% for protein content as results of Chinese sturgeon hydrolysis with papain. The hydrolysate obtained by alcalase treatment had

the highest extraction yield (52.07%), which was 248.66% higher than the papain hydrolysate yield, while the protein content was 90.33%. In the case of hydrolysates prepared by flavourzyme and flavourzyme & alcalase treatment, the extraction yields were 48.4% and 50.4%, respectively, while the protein content was 32.32% and 58.11%, respectively.

Degree of hydrolysis

The degree of hydrolysis performed with different enzymatic treatments influences the peptides size and their biological properties. In our study, the degree of hydrolysis after treatment with papain, flavourzyme and alcalase varied between 61.4 -76.23% (Table 1). The highest degree of hydrolysis was obtained in the case of alcalase treatment. Similar results regarding the degree of hydrolysis of fish proteins after alcalase and papain treatment were reported by Je *et al.* (2007) in a study analyzing the hydrolysates from tuna backbone. Other researches noted higher hydrolysis degree of peptide extracts from fish by-products obtained with alcalase, compared to that of extracts obtained with other enzymes (papain, neutrase, flavourenzyme, protamex) (Idow *et al.*, 2018; Zhang *et al.*, 2021).

Gel electrophoresis

The pattern of protein hydrolysates migration in 10-20% gradient gels of SDS-tricine-polyacrylamide gel allowed the evaluation of their molecular weight. Following electrophoresis, polypeptides with a molecular weight between 10-15 kDa were observed in high proportion in all analyzed hydrolysates (Fig. 1). The hydrolysate obtained by flavourzyme treatment also presented peptides with molecular weight around 40 kDa. Instead, the hydrolyzate obtained by alcalase treatment contained mainly peptides with low molecular weight between 3-12 kDa. Previous studies of Roslan *et al.* (2014) reported the presence of low molecular weight peptides (below 3.5 kDa) in the protein hydrolysate obtained from tilapia by-products using alcalase, as showed the SDS-tricine-polyacrylamide electrophoresis analysis.

Antioxidant activity

In our study, the enzymatic hydrolysis of fish by-products resulted in bioactive peptides able to neutralize free radicals by donating an electron or a proton. Determination of the antioxidant activity by DPPH assay in the obtained hydrolysates showed that the values of DPPH radicals inhibition

Table 1. Extraction yield, protein content and hydrolysis degree of protein hydrolysates. The results are expressed as mean \pm SD (n=3).

	Papain hydrolysate	Flavourzyme hydrolysate	Alcalase hydrolysate	Flavourzyme & alcalase hydrolysate
Extraction yield [%]	20.94 \pm 2.52	48.45 \pm 2.77	52.07 \pm 2.31	50.40 \pm 2.64
Protein content [%]	95.00 \pm 0.035	32.32 \pm 0.02	90.33 \pm 0.013	58.11 \pm 0.021
Hydrolysis degree [%]	61.40 \pm 0.26	66.33 \pm 0.1	76.23 \pm 0.15	67.50 \pm 0.23

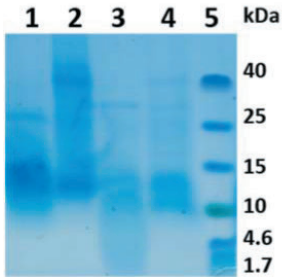


Figure 1. Gel electrophoresis of protein hydrolysates obtained by papain (1), flavourzyme (2), alcalase (3) and flavourzyme & alcalase (4) treatment. A low molecular weight marker (1.7-40 kDa) (5) was migrated in the same gel.

degree varied in a narrow range between 47.37-50.14%, at a concentration of 10 mg/ml enzyme fish hydrolysate (Fig. 2).

Numerous studies have demonstrated the antioxidant effects of different fish hydrolysates obtained with different enzymatic Peptides isolated from bones, meat, viscera and skin with alcalase, chymotrypsin, papain, pepsin, flavourzyme, protamex, neutrase have been shown to have antioxidant activity (Chalamaiah et al., 2012; Idow et al., 2018; Tacias-Pascacio et al., 2021). Je et al. (2007) analyzed the degree of inhibition of several hydrolysates obtained by treatment of tuna backbone with different enzymes and reported the highest value in the case of papain (36.72%) and the lowest in the case of alcalase (4.82%). Other studies analyzing the antioxidant activity of enzymatic hydrolysates from Alaska pollock skin by DPPH assay showed similar values of inhibition degree (32-50%) and the highest antioxidant activity for peptides extract obtained by flavourzyme treatment (Jia et al., 2010). Li et al (2012) reported that higher DPPH inhibition degree was noted in the case of hydrolyzate of grass carp meat obtained with papain compare to the one obtained with alcalase. (Li et al., 2012).

Antihypertensive activity

ACE inhibitors prevent the occurrence of high blood pressure by inhibiting the enzyme that catalyzes the conversion of angiotensin I to angiotensin II, which is a vasoconstrictor (Lee et al., 2010). In our study, the enzymatic hydrolysates showed ACE inhibition potential, whose values varied between 50.75-63.65% (Fig. 3). The enzymatic hydrolysate obtained with alcalase showed a slightly higher degree of ACE inhibition than that obtained with papain. Similar results were reported by Lee et al. (2010) for the hydrolysates obtained by treating the tuna skeleton with several enzymes, including papain and alcalase, observing that alcalase hydrolysate had a slightly higher antihypertensive

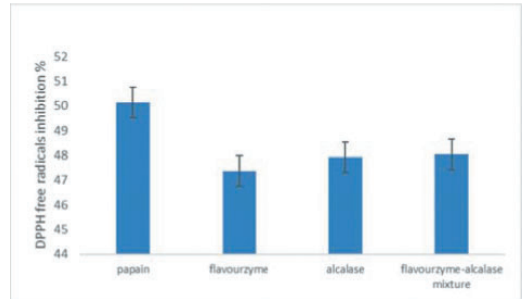


Figure 2. The antioxidant activity of the enzymatic hydrolysates determined as DPPH free radicals inhibition. The results are expressed as mean \pm SD (n=3).

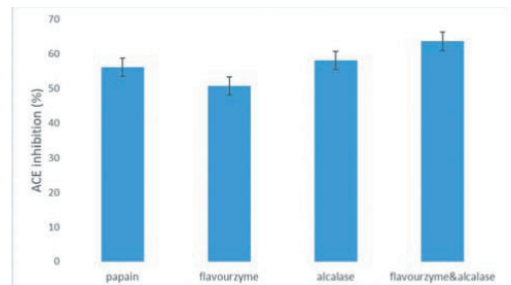


Figure 3. Inhibition potential of protein hydrolysates on ACE. The results are expressed as mean \pm SD (n=3).

activity than papain hydrolysate. As in our case, the degree hydrolysis of the alcalase extract was higher than that of papain, and this may influence the antihypertensive activity (Lee et al., 2010). Also Choonpicharn et al. (2015) found that gelatin hydrolysate from Nile tilapia skin obtained with alcalase exhibited an increased antihypertensive activity than papain hydrolysate.

Biocompatibility and antiproliferative activity

The results of biocompatibility test performed in normal fibroblast cells (NCTC cell line) have showed variable cell viability when cultivated in the presence of protein hydrolysates, depending on the samples concentration (3-6 mg/ml) (Fig. 4). In the case of papain hydrolysate, the values of cell viability were higher than 80% for all tested concentrations. The flavourzyme hydrolysate was cytocompatible (cell viability over 80%) at concentrations ranging between 3-6 mg/ml, and induced a decrease of cell viability down to 58.5% at a concentration of 10 mg/ml protein hydrolysate in the culture media. Similar variation was observed in the case of alcalase hydrolysate, but the cell viability values decreased to 73.94 and 48.7%, at 8 and 10 mg/ml, respectively, the last value representing the lowest viability in the experiment. The flavourzyme and alcalase hydrolysate induced an increase of the

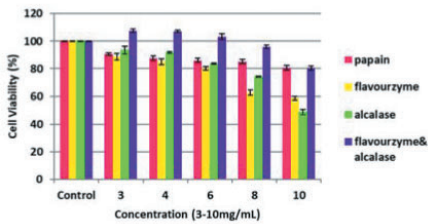


Figure 4. Cell viability of fibroblast cells (NCTC cell line) after 48 h of cultivation in standard conditions, in the presence of enzymatic hydrolysates. The results are expressed as mean \pm SD (n=3).

cell viability at concentrations between 3-6 mg/ml, showing stimulation of cell metabolism. Thus, the values of cell viability (103.12%-107.41%) were higher than that in the control sample (100%). At higher concentrations, the cell viability decreased down to 80.5%. All hydrolysates were cytocompatible, excepting the flavourzyme and alcalase extracts, at 8-10 mg/mL.

The evaluation of the antiproliferative activity was performed in a stabilized line of Hep-2 tumor cells in the presence of different samples concentrations (3-10 mg/ml). Antiproliferative activity of the analyzed fish protein hydrolysates increased proportionally with their concentration, thus reaching the maximum value at the concentration of 10 mg/ml. The protein hydrolysates obtained by combined treatment with flavourzyme and alcalase applied in the culture of Hep-2 cancer cells, at 10 mg/ml concentration, showed lower cell viability (29.58%) than the identical treatment in NCTC cell culture (80.5%) (Fig. 5).

The antiproliferative character was also observed in the case of papain extract at 10 mg/ml concentration, because the cell viability of Hep-2 cells was 39.8%, while in NCTC cells identically treated was 80.7%. In the case of hydro-

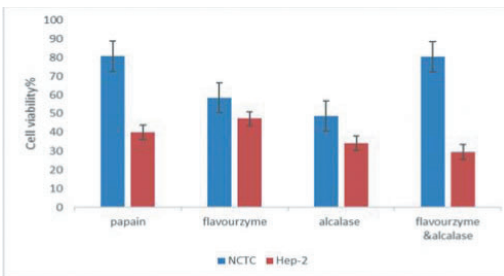


Figure 5. Cell viability of normal (NCTC cell line) and tumoral cells (Hep-2 cell line) after 48 h of cultivation in standard conditions, in the presence of enzymatic hydrolysates, at a concentration of 10 mg/ml. The results are expressed as mean \pm SD (n=3).

lysates obtained with separate alcalase and flavourzyme, the viability of Hep-2 cells was 34.7% and 47.2% at 10 mg/ml concentrations, but they were cytotoxic for normal NCTC cells. Thus, the protein hydrolysates obtained with papain and combined flavourzyme-alcalase treatment had antiproliferative activity in Hep-2 tumor cells.

Previous studies on the bioactive properties of roe or fish peptides showed their antiproliferative effect. Half-fin anchovy pepsin hydrolysate had antiproliferative effect on DU-145 human prostate cancer cell line, 1299 human lung cancer cell line and 109 esophagus cancer cell line (Song *et al.*, 2011). Rohu roe pepsin hydrolysate showed antiproliferative effect against Caco-2 cells (Chalamaiah *et al.*, 2015). Two peptides obtained from tuna dark muscle using papain and protease XXIII showed antiproliferative effect on human breast cancer cell line MCF-7 (Zamora-Sillero, 2018).

Conclusions

The protein hydrolysates obtained from silver carp tissue waste (skin, bones, meat) by enzymatic treatment with papain, flavourzyme and alcalase demonstrated important bioactive properties, including antioxidant, antihypertensive and antiproliferative activity. The study recommends their further analysis as ingredients of novel valuable nutraceuticals.

Acknowledgements

This work was supported by a grant of the Romanian Ministry of Education and Research, CCCDI - UEFISCDI, project number PN-III-P2-2.1-PTE-2019-0181, within PNCDI III

References

- Adler-Nissen J. Determination of the degree of hydrolysis of food protein hydrolysates by trinitrobenzenesulfonic acid. *Journal of Agricultural and Food Chemistry*. 1979;27(6): 1256–1262. doi:10.1021/jf60226a042
- Chalamaiah M, Dinesh K, Hemalatha R, Jyothirmayi T. Fish protein hydrolysates: Proximate composition, amino acid composition, antioxidant activities and applications: A review. *Food Chemistry*. 2012; 135: 3020–3038
- Chalamaiah M, Jyothirmayi T, Diwan PV, Dinesh K. Antiproliferative, ACE-inhibitory and functional properties of protein hydrolysates from rohu (Labeo rohita) roe (egg) prepared by gastrointestinal proteases. *Journal of Food Science and Technology*. 2015; 52(12):8300–8307 doi 10.1007/s13197-015-1969
- Choonpicharn S, Jaturasitha S, Rakariyatham N, Suree N, Niamsup H. Antioxidant and antihypertensive activ-

- ity of gelatin hydrolysate from Nile tilapia skin. *Journal of Food Science and Technology*.2015; 52(5):3134–3139 doi 10.1007/s13197-014-1581-6
5. Gao R, Yu Q, Shen Y, Chy Q, Chen G, Fen S, Yang M, Yuan L, McClements DV, Sun Q. Production, bioactive properties, and potential applications of fish protein hydrolysates: Developments and challenges. *Trends in Food Science & Technology*. 2021; 110:687-699
 6. Idowu AT, Benjakul S, Sinthusamran S, Sookchoo P, Kishimura H. Protein hydrolysate from salmon frames: Production, characteristics and antioxidative activity. *Journal of Food Biochemistry*. 2018; doi : 10.1111/jfbc.12734
 7. Je JY, Qian ZJ, Byun HG, Kim SK. Purification and characterization of an antioxidant peptide obtained from tuna backbone protein by enzymatic hydrolysis. *Process Biochemistry*. 2007; 42: 840-846
 8. Jia J, Zhou Y, Lu J, Chen A, Li Y, Zheng G. Enzymatic hydrolysis of Alaska pollack (*Theragra chalcogramma*) skin and antioxidant activity of the resulting hydrolysate. *Journal of the Science of Food and Agriculture*. 2010; 90: 635–640
 9. Lee SH, Qian ZJ, Kim SK. A novel angiotensin I converting enzyme inhibitory peptide from tuna frame protein hydrolysate and its antihypertensive effect in spontaneously hypertensive rats. *Food Chemistry*. 2010; 118:96-102
 10. Li X, Luo Y, Shen H, Youa J. Antioxidant activities and functional properties of grass carp (*Ctenopharyngodon idellus*) protein hydrolysates. *Journal of the Science of Food and Agriculture*. 2012; 92:292-298
 11. Noman A, Xua Y, Al-Bukhaiti W, Abed S, Ali A, Rhamadhan A, Xia W. Influence of enzymatic hydrolysis conditions on the degree of hydrolysis and functional properties of protein hydrolysate obtained from Chinese sturgeon (*Acipenser sinensis*) by using papain enzyme. *Process Biochemistry*. 2018; 67: 19-28
 12. Roslan J, Yunos KF, Abdullah N, Kamala MM. Characterization of Fish Protein Hydrolysate from Tilapia (*Oreochromis niloticus*) by-Product. *Agriculture and Agricultural Science Procedia*. 2014; 2:312-319
 13. Papadimitriou CG, Vafopoulou-Mastrojiannaki, A, Silva SV, Gomes, AM, Malcata FX, Alichanidis E. Identification of peptides in traditional and probiotic sheep milk yoghurt with angiotensin I-converting enzyme (ACE)-inhibitory activity. *Food Chemistry*. 2012; 105: 647- 656.
 14. Quetin-Leclercq J., Elias R., Balansard G. Cytotoxic activity of some triterpenoid saponins, *Planta Med*.1992; 58: 279-280
 15. Schägger H, Tricine SDS-PAGE. *Nature protocols*. 2006;1:16-23
 16. Tacias Pascacio V, Castaneda-Valbuena D, Morellon-Sterling R, Tavano O, Berenguer-Murcia A. Bioactive peptides from fisheries residues: A review of use of papain in proteolysis reactions. *International Journal of Biological Macromolecules*. 2021; 184:415-428
 17. Zamora-Sillero J, Gharsallaoui A, Prentice C. Peptides from Fish By-product Protein Hydrolysates and Its Functional Properties: an Overview. *Marine Biotechnology*. 2018; 20:118–130
 18. Song R, Wei R, Zhang B, Yang Z, Wang D. Antioxidant and Antiproliferative Activities of Heated Sterilized Pepsin Hydrolysate Derived from Half-Fin Anchovy (*Setipinna taty*). *Marine Drugs*. 2011; 9: 1142-1156; doi:10.3390/md9061142
 19. Zhang L, Shan Y, Hong H, Luo Y, Hong XYea W. Prevention of protein and lipid oxidation in freeze-thawed bighead carp (*Hypophthalmichthys nobilis*) fillets using silver carp (*Hypophthalmichthys molitrix*) fin hydrolysates. *LWT - Food Science and Technology*. 2020; 123: 109050
 20. Zhang X, Dai Z, ZhangY, DongY, Hu X, Structural characteristics and stability of salmon skin protein hydrolysates obtained with different proteases, *LWT - Food Science and Technology*. 2021; doi: <https://doi.org/10.1016/j.lwt.2021.112460>.
 21. Zheng K, Wu L, He Z, Yang B, Yang Y. Measurement of the total protein in serum by biuret method with uncertainty evaluation. *Measurement*. 2017; 112: 16–21
 22. Zhong S, Ma C, Lin Y, Luo Y, Antioxidant properties of peptide fractions from silver carp (*Hypophthalmichthys molitrix*) processing by-product protein hydrolysates evaluated by electron spin resonance spectrometry. *Food Chemistry*. 2011; 126:1636-1642
 23. Wang K, Han L, Hong H, Pan J, Liu H, Luo Y. Purification and identification of novel antioxidant peptides from silver carp muscle hydrolysate after simulated gastrointestinal digestion and transepithelial transport. *Food Chemistry*. 2021; 342: 128275.



Received for publication: March, 20, 2021
Accepted: September, 23, 2021

Original paper

Mesenchymal stem cells attenuate amiodarone-induced pulmonary fibrosis in rats via blockade of inflammation and TGF- β 1/Smad3/S100A4 signaling

ALYAA S. ABDEL HALIM, Ph.D.¹, HANAA H. AHMED, Ph.D.^{2,3},
HADEER A. AGLAN, Ph.D.^{2,3}, MOHAMED R. MOHAMED, Ph.D.¹

¹Department of Biochemistry, Faculty of Science, Ain Shams University, Cairo, Egypt;

²Hormones Department, Medicine and Clinical Studies Research Institute, National Research Centre, Giza, Egypt, Affiliation ID: 60014618;

³Stem Cells Lab, Center of Excellence for Advanced Sciences, National Research Centre, Giza, Egypt, Affiliation ID: 60014618

Abstract

Aim: This study aimed to clarify the anti-fibrotic potential of bone marrow-derived mesenchymal stem cells (BM-MSCs), compared to conditioned media (CM), in amiodarone (AD)-induced lung fibrosis. **Methods:** A total of 64 Wistar rats were categorized into eight groups: negative control group, positive control group, 3 AD-challenged-BM-MSCs-treated groups (1, 2 and 4 months) and 3 AD-challenged-CM-treated groups (1, 2 and 4 months). Serum macrophage inflammatory protein 2 (MIP-2) levels were measured. Gene expression levels of TGF- β 1, SMAD3 and S100A4, were estimated in the lung tissues. **Results:** Treatment with BM-MSCs/CM mediated a significant reduction in serum MIP-2 concentrations, while downregulating AD-induced up-regulation of lung TGF- β 1, SMAD3 and S100A4 gene expression levels. BM-MSCs transplantation revealed better effect than CM in mitigating lung fibrosis. **Conclusion:** BM-MSCs advance anti-fibrotic effect on lung fibrosis by targeting inflammatory response and TGF- β 1 signaling.

Keywords

Amiodarone; conditioned media; inflammatory response; lung fibrosis; mesenchymal stem cells; TGF- β 1 signaling

To cite this article: HALIM ASA, AHMED HH, AGLAN HA, MOHAMED MR. Mesenchymal stem cells attenuate amiodarone-induced pulmonary fibrosis in rats via blockade of inflammation and TGF- β 1/Smad3/S100A4 signaling. *Rom Biotechnol Lett.* 2022; 27(2): 3368-3378 DOI: 10.25083/rbl/27.2/3368.3378

✉ *Corresponding author: Mohamed R. Mohamed, Ph.D. Address: Department of Biochemistry, Faculty of Science, Ain Shams University, Abbassia, 11566, Cairo, Egypt. Fax: (+202) 26842123. Tel: (+2) 0102 384 4912. E-mail address: mohamed_elsotahi@sci.asu.edu.eg

Introduction

Stem cells are accounted as cells with unique biological nature owing to their capability to self-renewing and differentiation into multiple cell types. Stem cell-based therapy is emerging as a potential therapeutic opportunity for treatment of numerous disorders. Mesenchymal stem cells (MSCs) are multipotent adult stem cells that are derived from different tissues and can be utilized as an alternative to embryonic stem cells (Kang et al, 2019). Mesenchymal stem cells have emerged as promising therapeutic options in regenerative medicine (Motavaf et al, 2016) for the treatment of various diseases (Bianco et al, 2013; Farini et al, 2014), including lung fibrosis particularly on the experimental level (Gotts and Matthay, 2011; Akram et al, 2013). Mesenchymal stem cells transplantation has been reported to induce repair of the damaged lung tissues through suppressing inflammation and collagen deposition (Ortiz et al, 2003; Rojas et al, 2005). Since studies in animal models and patients indicated that low number of transplanted MSCs localized to the target tissue and transdifferentiate to appropriate cell lineage and the regenerative potential of MSCs has been found at least in part to be mediated *via* their paracrine actions, the use of MSC conditioned media has been suggested to improve tissue regeneration following injury (Ionescu et al, 2012).

Lung fibrosis is an aggressive and lethal form of interstitial lung diseases (Noble et al, 2012). This devastating disease is often fatal within 3-5 years after diagnosis (Ley et al, 2011), and the currently available treatment options are of unproven benefit with lung transplantation being the only definitive therapy (Aslam et al, 2009), emphasizing the urgent need for development of novel therapeutic strategies.

It is well known that the recruitment and activation of inflammatory cells leads to the release of inflammatory mediators that have an essential role in the stimulation and proliferation of cells involved in fibrotic processes (Noble et al, 2012). Further, it has been previously demonstrated that the angiogenic CXC chemokine, macrophage inflammatory protein 2 (MIP-2), is an important factor that regulates angiogenesis during the development of PF (Keane et al, 1999).

Transforming growth factor beta 1 (TGF- β 1), a pro-fibrogenic cytokine, has long been believed to be a central mediator of the lung fibrotic response (Allen and Spiteri, 2002). TGF- β 1 signals are transduced by transmembrane serine/threonine kinase receptors. The intracellular signaling pathway downstream of TGF- β 1 receptors has been found to be mediated by a family of transcription factors, known as the SMAD proteins, and among these, mothers against decapentaplegic homolog 2 (SMAD2) and SMAD3 are direct substrates of the TGF- β type I receptor (Flanders,

2004). The contribution of TGF- β 1 to fibrosis has been observed to be mediated mainly through the Smad-dependent signaling axis (Heldin and Moustakas, 2012). Of note, calcium-binding protein A4 (S100A4), a regulator of numerous cellular processes crucial to fibrotic progression (Donato et al, 2013), has been found to be a target of TGF- β 1 signaling (Matsuura et al, 2010).

The current study mainly focused on assessing the anti-fibrotic outcome of bone marrow mesenchymal stem cells (BM-MSCs) versus bone marrow mesenchymal stem cells conditioned media (BM-MSCs-CM) against amiodarone-induced lung fibrosis in rats, exploring their effect on inflammatory response and TGF- β 1/Smad3/S100A4 signaling.

Materials and methods

BM-MSCs isolation, propagation, characterization, and labelling

Bone marrow cells were collected from decapitated adult male Wistar rats by flushing the medullary cavity of the excised femur and tibia with Gibco Dulbecco's Modified Eagle's medium (DMEM)-high glucose (Biowest, France). Mononuclear cells were purified by density gradient centrifugation at 400 \times g for 30 minutes using GE Healthcare Ficoll-Paque Premium (Sigma-Aldrich, St. Louis, MO, USA). After three washes with phosphate-buffered saline (PBS) (Biowest, France), purified cells were plated into 25 cm² cell culture flasks in a complete culture medium (DMEM-high glucose supplemented with 30% fetal bovine serum [FBS], 1% non-essential amino acids and 1% penicillin/streptomycin (Biowest, France), and maintained at 37°C in a humidified incubator with 5% CO₂. After 48 hours, the culture medium was replaced with a fresh medium and non-adherent cells were discarded. The adherent cells (BM-MSCs) were grown in the complete culture medium to 80–90% confluency, defined as passage zero (P0) cells. The P0 cells were washed with PBS (Gibco, Thermo Fisher Scientific, Waltham, MA, USA) and harvested by incubation with 0.25 % trypsin-EDTA solution (Biowest, France) for 5 minutes at 37°C. The detached cells were centrifuged at 200 \times g for 10 minutes, resuspended in complete culture medium, counted, and plated as P1 in cell culture flasks at a density of 1 \times 10⁶ cells/flask. The culture medium was replaced every third day over a 10–14-day period. For each passage, the cells were seeded and grown similarly. As cells reached 80-90% confluency, cells were harvested and passaged by trypsinization (Alhadlaq and Mao, 2004). BM-MSCs were morphologically identified by their characteristic fibroblast-like spindle appearance. At the 3rd passage,

cells were immunophenotyped to determine the expression of various cell surface antigens. In brief, cells were harvested by trypsinization, washed by PBS, aliquoted at a concentration of 0.5×10^6 cells/mL, and stained for 30 minutes at room temperature in the dark with a set of monoclonal antibodies, including phycoerythrin-conjugated CD14, CD34 and CD44 (Invitrogen, Thermo Fisher Scientific, Waltham, MA, USA). Stained cells were washed twice with PBS, resuspended in PBS, and analyzed by the COULTER EPICS XL flow cytometer, using the SYSTEM II software (Beckman Coulter, Brea, CA, USA), according to the manufacturer's protocol (Dominici *et al*, 2006; Abdel Halim *et al*, 2020). Immunophenotyping demonstrated that the cells were positive for the typical MSC markers, CD44+ (90.4%), and negative for the hematopoietic lineage markers, CD14- (5.80%) and CD34- (4.59 %). The third passage BM-MSCs were incubated with Ferumoxides injectable solution (Feridex IV, Berlex Laboratories, Cedar Knolls, NJ, USA), a sterile aqueous colloid of dextran-coated superparamagnetic iron oxide nanoparticles, at a final concentration of 25 µg/mL, and poly-L-lysine (PLL, Sigma-Aldrich, St. Louis, MO, USA), at a final concentration of 375 ng/mL to boost the incorporation of the nanoparticles, for 24 hours. Feridex was mixed with PLL and shaken for 30 minutes at room temperature before being added to the cells in supplemented DMEM. After incubation with FePLL mixture, prussian blue staining was conducted to visualize the iron particles in Ferumoxides-labeled BM-MSCs. Briefly, BM-MSCs were harvested by trypsinization, washed twice with PBS, transferred to cytospin slides, fixed with 4% glutaraldehyde, washed with PBS, incubated for 30 minutes with 2% potassium ferric-ferrocyanide (Perl's reagent, Sigma-Aldrich, St. Louis, MO, USA) in 3.7% hydrochloric acid, washed 3 times with PBS, counterstained with nuclear fast red, and assessed for labelling efficiency using light microscopy (Balakumaran *et al*, 2010).

Generation of mesenchymal stem cells conditioned medium (MSCs-CM)

Passage 3 MSCs at 80–90% confluence was washed twice with PBS and maintained in supplemented FBS-free DMEM for 24 hours. The medium from equal numbers of cells in each culture (3×10^6 cells) was collected, centrifuged at $400 \times g$ for 20 minutes, and concentrated 10-fold using an Amicon Ultra Centrifugal Filter (Sigma-Aldrich, St. Louis, MO, USA) with a molecular weight cut-off of 10 kDa. Concentrated CM was filter-sterilized and stored at -80°C for later use (Ionescu *et al*, 2012).

Experimental model of lung fibrosis induced by amiodarone

Amiodarone hydrochloride (Cordarone) was obtained from Sanofi pharmaceutical company (Paris, France) as 200 mg tablets. A fresh solution was prepared by dissolving AD in Saline, 0.85% with 0.05% Tween 80 (Hardy Diagnostics, Santa Maria, CA, USA) before each administration. To induce PF, rats were given a daily dose of 30 mg/kg body weight AD by oral gavage for 3 months (Kolettis *et al*, 2007).

Study design

A total of 64 adult male Wistar rats, with a body weight of 100–120 g, procured from the holding company for biological products and vaccines, Giza, Egypt, were maintained in ventilated polypropylene cages in a specified pathogen-free air-conditioned (25°C and 50% humidity) room, with 12 hours-light/dark cycles and free access to a commercial standard pellet diet (PMI Nutrition, Shoreview, MN, USA) and fresh drinking water throughout the study period, in the animal care facility at the National Research Centre (NRC), Giza, Egypt. Rats were allowed to adapt in the animal care facility for one week before any experimentation. All procedures were done with proper approval of medical Research Ethics committee of the NRC, Giza, Egypt (Approval ID: 17-096), and in compliance with the guidelines of the National Institutes of Health (NIH) for the care and use of laboratory animals, 8th edition, 2011.

Rats were randomly allocated into 8 groups (8 rats/group), including a negative control (vehicle, saline) group, a positive control (AD) group, 3 BM-MSCs-treated groups (for post-treatment durations of 1, 2 and 4 months) and 3 CM-treated groups (for post-treatment durations of 1, 2 and 4 months).

The negative control rats were given 0.5 mL of Saline, 0.85% with 0.05% Tween 80/day by oral gavage for 3 months, whereas positive control rats as well as BM-MSCs- and CM-treated rats were orally given 0.5 mL of 30 mg/kg body weight AD once daily for 3 months. Following the 3-months AD administration, rats of the BM-MSCs- and CM-treated groups were given a single intravenous injection with 3×10^6 BM-MSCs in 0.5 mL PBS and 0.5 mL CM (Yu *et al*, 2015), respectively, whereas the positive control rats were given a single intravenous injection with 0.5 mL PBS, through the tail vein.

Blood collection, dissection, and tissues preparation

At the end of the experimental interval of 7 months, negative and positive control rats were sacrificed by decapitation, whereas rats of the 3 BM-MSCs- and 3 CM-treated groups were sacrificed by decapitation at 1, 2 and 4 months follow-

ing BM-MSCs or -CM injection. Blood samples were collected from the orbital sinus and serum samples were separated by centrifugation, snap-frozen in liquid nitrogen, and stored at -80°C for subsequent analysis. Both lungs were immediately excised and divided into four separate lobes. The largest lobe was fixed in 10% neutral buffered formalin for 24 hours, dehydrated through a graded alcohol, and embedded in paraffin wax for histopathological analysis. The remaining three lobes were snap-frozen in liquid nitrogen and stored at -80°C for later gene expression analysis.

Histopathological procedures

Paraffin-embedded lung tissues were cut into as $5\ \mu\text{m}$ thick slices by using microtome, mounted on glass slides, and stained with hematoxylin and eosin (H&E) (Sigma-Aldrich, St. Louis, MO, USA) according to the standard method (Mohamed et al, 2014) with little modification to visualize morphological deformation of the lung tissues, with Masson's trichrome (Sigma-Aldrich, St. Louis, MO, USA) to assess collagen fibers accumulation, and with prussian blue to track the Ferumoxides-labeled BM-MSCs, using light microscopy (Olympus BX51 microscope, Shinjuku, Tokyo, Japan).

Biochemical assay

Serum macrophage inflammatory protein 2 (MIP-2) levels were determined by a commercial "Sandwich" enzyme-linked immunosorbent assay (ELISA; Elabscience, Houston, TX, USA), according to the standard protocol provided by the manufacturer.

Quantitative genes expression analyses

Transforming growth factor beta 1 (TGF- β 1), mothers against decapentaplegic homolog 3 (SMAD3) and S100 calcium-binding protein A4 (S100A4) gene expression levels were determined in lung tissues using quantitative real-time polymerase chain reaction (qPCR). The sequences of forward and reverse primers used for qPCRs are listed in Table 1.

In brief, lung tissues total RNA was purified using Invitrogen PureLink RNA Mini Kit (Thermo Fisher Scientific,

Waltham, MA, USA) following the manufacturer's instructions. Complementary DNA (cDNA) was synthesized using SensiFAST cDNA Synthesis Kit (Bioline, London, UK) according to the manufacturer's instructions. Quantitative measurement of gene expression levels was conducted using QuantiNova SYBR Green PCR kit (Qiagen, Valencia, CA, USA) according to the manufacturer's recommendations. Stratagen Mx3000P Real-Time PCR System (Agilent, Santa Clara, CA, USA) was used for quantitative real-time analysis. Relative gene expression was analyzed by the comparative Ct method ($2^{-\Delta\Delta\text{Ct}}$) (Livak and Schmittgen, 2001), using β -actin (ACTB) as the endogenous control. For AD-treated rats, data were expressed as the fold change in gene expression in the AD-treated rats normalized to the expression levels of the endogenous control and relative to the saline-treated rats, whereas for the BM-MSCs- or CM-treated rats, data were expressed as the fold change in gene expression in the BM-MSCs- or CM-treated rats normalized to the expression levels of the endogenous control and relative to the AD-treated rats.

Statistics

The statistical package for the social sciences (SPSS Statistics for Windows, Version 23.0; IBM Corp., Armonk, NY, USA) was used for statistical analysis of data. Variables were expressed as mean \pm standard deviation (SD) if normally distributed and compared using the independent Student's t-test or one-way analysis of variance (ANOVA) as appropriate. On contrary, variables were expressed as median (interquartile range, IQR: 25th quartile to 75th quartile) if not normally distributed and compared using the non-parametric Mann-Whitney U test or Kruskal-Wallis test as appropriate. *P* values were two-sided, and a *P* value of less than 0.05 was considered statistically significant.

Results

Histological alteration of lung tissue

Our previously published manuscript (Abdel Halim et al, 2020) reported that hematoxylin and eosin (H&E) stained

Table 1. The sequence of forward and reverse primers used for qPCR

Gene	Gene ID	Primer type	Primer sequence (5' → 3')
ACTB	81822	FP	CCCATCTATGAGGGTTACGC
		RP	TTAATGTCACGCACGATTTTC
TGFB1	59086	FP	GGAGCCAAGTCCCATCGTCTACTAC
		RP	GGAGCGCACGATCATGTTGGAC
SMAD3	25631	FP	AGGGCTTTGAGGCTGTCTACC
		RP	ACCCGATCCCTTTACTCCCA
S100A4	24615	FP	AGCTACTGACCAAGGGAGCTG
		RP	TGCAGGACAGGAAGACACAG

FP, forward primer; RP, reverse primer.

lung tissue sections from rats given vehicle showed normal lung structure, while rats given AD exhibited the characteristic histological changes of AD-induced PF model, as indicated by notable pathological alterations of lung structure. BM-MSCs/CM treatment markedly improved the lung histology, with BM-MSCs/CM-treated rats possess less pathological alterations compared with AD-treated rats, demonstrating that the injection of BM-MSCs/CM exerted a considerable anti-fibrotic influence. Noteworthy, the alleviation of AD-induced histopathological changes was more apparent in BM-MSCs-treated rats than those treated with CM. At 1-, 2-, and 4-months following treatment with BM-MSCs/CM, fibrosis-associated histological alterations were ameliorated with differing degrees according to the time interval.

Collagen fibers deposition in lung tissue

In our previously published manuscript (Abdel Halim *et al*, 2020), vehicle-administered rats stained with Masson’s trichrome showed normal collagen fibers distribution surrounding the bronchioles and blood vessels as well as in between the air alveoli. On the other hand, lung tissue sections from AD-administered rats revealed intense collagen fibers accumulation, demonstrating that AD resulted in a signifi-

cant increase in collagen deposition. The AD-induced collagen accumulation was significantly reduced by treatment of the AD-administered rats with BM-MSCs/CM. Clearly, the collagen accumulation-reducing ability of BM-MSCs was more apparent than that of CM. At 2 and 4 months following BM-MSCs/CM treatment, the collagen amount determined in the lung tissue sections were remarkably decreased; however, at 1 month following BM-MSCs/CM treatment, the BM-MSCs/CM did not exhibit the same ability to decrease the collagen accumulation. These findings underscore the differing collagen accumulation-reducing influences of BM-MSCs and CM kept treating AD-administered rats for various time intervals.

Ferumoxides-labeled BM-MSCs tracking

As evidenced in our prior manuscript (Abdel Halim *et al*, 2020), at 1, 2 and 4 months post-BM-MSCs treatment, Prussian blue staining displayed slight, moderate, and extensive BM-MSCs homing, respectively, as manifested by mild, moderate, and highly positive blue staining, respectively. In fact, BM-MSCs homing at 4 months post-BM-MSCs treatment was significantly superior to that at 2 months’ post-treatment, which was considerably higher than that at 1-month post-treatment.

Impact of BM-MSCs/CM treatment on inflammatory response

To assess the effect of BM-MSCs/CM on inflammatory response, serum level of MIP2 was determined. As shown in Figure 1, AD administration resulted in a significant enhancement ($p<0.05$) in the serum concentration of MIP2 versus the saline-administered rats, as documented by marked increase in MIP2 concentration by 1165% in AD-administered rats. BM-MSCs or CM treatment attenuated AD-induced elevation in the serum concentration of MIP2. This finding is manifested by a significant reduction ($p<0.05$) in MIP2 concentration by 31%, 80% and 88% at 1, 2 and 4 months post-treatment with BM-MSCs respectively. Also, CM injection significantly suppressed ($p<0.05$) MIP2 concentrations by 16%, 43% and 69% at 1, 2 and 4 months post-treatment, respectively, when compared to AD group. Following AD administration, 4 months post-BM-MSCs or -CM treatment performed significantly better than 1 and 2 months post-treatment in reducing MIP-2 levels. Also, 2 months post-BM-MSCs or -CM treatment displayed significantly better than 1 month post-treatment in reducing MIP-2 concentrations. In general, BM-MSCs treatments were more efficacious than CM treatments in reducing MIP-2 concentrations.

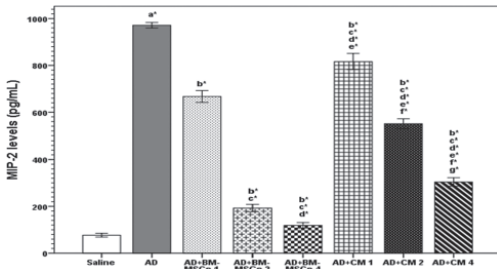


Figure 1. Serum concentrations of MIP-2 in vehicle- and AD-administered rats as well as at 1, 2 and 4 months post-BM-MSCs and -CM treatments. AD, amiodarone; BM-MSCs, bone marrow derived-mesenchymal stem cells; CM, conditioned media; MIP-2, macrophage inflammatory protein 2.

Data are represented as mean ± SD.

- a: statistical difference compared to the vehicle group.
 - b: statistical difference compared to the AD group.
 - c: statistical difference compared to the AD+BM-MSCs at 1 month group.
 - d: statistical difference compared to the AD+BM-MSCs at 2 months group.
 - e: statistical difference compared to the AD+BM-MSCs at 4 months group.
 - f: statistical difference compared to the AD+CM at 1 month group.
 - g: statistical difference between the AD+CM at 2 and 4 months groups.
- *, $P<0.05$.

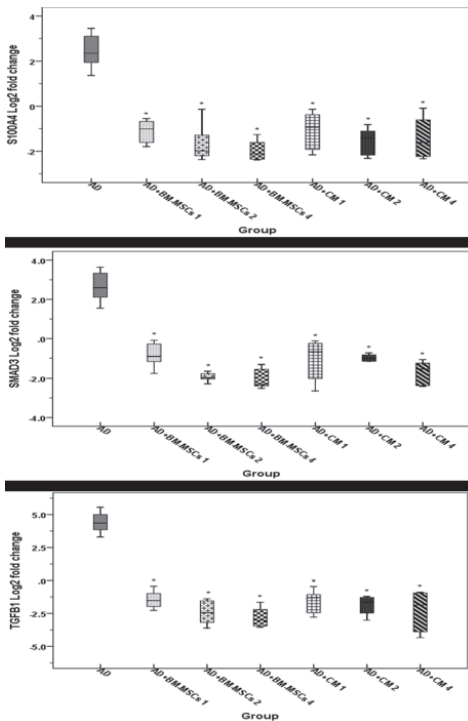


Figure 2. Lung tissue mRNA levels of S100A4 (A), SMAD3 (B) and TGF- β 1 (C) in AD-administered rats as well as at 1, 2 and 4 months post-BM-MSCs and -CM treatments. Data are expressed as median (interquartile range, IQR: 25th quartile to 75th quartile) of Log₂ fold change. For AD-treated rats, the fold change is the gene expression in the AD-treated rats normalized to the expression levels of β -actin and relative to the saline-treated rats, whereas for the BM-MSCs- or BM-MSCs-CM-treated rats, the fold change is the gene expression in the BM-MSCs- or BM-MSCs-CM-treated rats normalized to the expression levels of β -actin and relative to the AD-treated rats. AD, amiodarone; BM-MSCs, bone marrow derived-mesenchymal stem cells; BM-MSCs-CM, conditioned media; S100A4, S100 calcium-binding protein A4; SMAD3, mothers against decapentaplegic homolog 3; TGF- β 1, transforming growth factor beta 1. *: statistical significance when compared to the AD group ($P < 0.05$).

Effect of BM-MSCs/CM treatment on TGF- β 1/Smad3/S100A4 signaling

Gene expression levels of TGF- β 1, SMAD3 and S100A4 were determined in lung tissues to assess the effect of BM-MSCs/CM treatment on TGF- β 1/Smad3/S100A4 signaling pathway. As shown in Figure 2, after induction of lung fibrosis by AD, there was a significant upregulation ($P < 0.05$) in the lung expression level of genes encoding TGF- β 1, SMAD3 and S100A4 in comparison to vehicle-administered

group. Following infusion of BM-MSCs or BM-MSCs-CM, the lung expression level of TGF- β 1, SMAD3 and S100A4 genes were significantly downregulated at 1, 2 and 4 months post-treatments, versus the AD-administered group.

Noteworthy, 4 months post-BM-MSCs treatment produced significantly ($P < 0.05$) better performance than 1 month post-treatment in downregulating the expression level of TGF- β 1, SMAD3 and S100A4 in the lung, underscoring the various influences of BM-MSCs kept treating the AD-administered rats for various time intervals. However, the transcript levels of lung TGF- β 1, SMAD3 and S100A4 genes at 4 months post-BM-MSCs treatment were lower than those at the 2 months post-BM-MSCs treatment, but this difference did not meet the criteria for statistical significance ($P > 0.05$), demonstrating that both 2 and 4 months post-BM-MSCs treatments were equally effective in downregulating the mRNA level of TGF- β 1, SMAD3 and S100A4 genes. Except for SMAD3, the gene expression levels of TGF- β 1 and S100A4 at the 2 months post-BM-MSCs treatment did not differ significantly from those at the 1 month post-BM-MSCs treatment, indicating that both 1 and 2 months post-BM-MSCs treatments were of equal effect in downregulating the mRNA level of TGF- β 1 and S100A4 genes but not of SMAD3.

Concerning the infusion of BM-MSCs-CM, there was no significant difference ($P > 0.05$) in the transcript level of lung TGF- β 1, SMAD3 and S100A4 genes among 1, 2 and 4 months post BM-MSCs-CM treatment, suggesting that BM-MSCs-CM treatment at all time points were equally effective in downregulating the transcript level of TGF- β 1, SMAD3 and S100A4 genes.

Overall, BM-MSCs treatment displayed significantly ($P < 0.05$) better effect than BM-MSCs-CM treatment in downregulating AD-induced upregulation in the gene expression levels of TGF- β 1, SMAD3 and S100A4 in the lung.

Discussion

Current treatment options for PF are limited (Fernandez and Eickelberg, 2012) and there is no effective therapy capable of improving or at least suppressing the progressive course of the disease (King et al, 2011). MSCs have gained increasing interest as a promising cell-based therapeutic approach in several disease, including PF (Parekkadan and Milwid, 2010).

In the current research, BM-MSCs/ BM-MSCs-CM infusion evoked an obvious improvement in the architectural integrity of lung tissue. Moreover, treatment with BM-MSCs/ BM-MSCs-CM significantly blunted collagen deposition in the lung of AD-administered rats as evidenced by reduced

collagen deposition in Masson's trichrome-stained lung sections. At 1, 2 and 4 months post-treatment, BM-MSCs have been detected in damaged lung, as manifested by positive Prussian blue staining, emphasizing the concept that allogeneic or xenogeneic MSCs could accommodate in hosts after infusion (Javazon *et al*, 2004), thus, indicating the potentiality of BM-MSCs to relocate to the inflammatory sites and migrate into the lung tissue following the intravenous injection, to trigger repair and regeneration of lung tissue.

The production of humoral mediators by damaged lung that induce stem cell proliferation could cause local proliferation of stem cells mobilized from the bone marrow (or delivered as a stem cell transplant), or could be a signaling mechanism to the bone marrow to expand the pool of progenitor cells in response to tissue damage. The generation of substances chemotactic for stem cells by damaged lung may aid in explaining the selective accommodation of these progenitor cells to sites of tissue damage. In acute lung injury, a pro-inflammatory immune response has been initiated within the injured lung, and pro-inflammatory cytokines have been secreted, which can induce the homing of MSCs to the damaged lung (Yagi *et al*, 2010). Importantly, it has been proposed that most of the exogenously administered MSCs had disappeared shortly following administration, irrespective of the way of administration utilized; but these cells were able to stimulate longer-term paracrine effects that persisted long after they had been vanished, asserting that MSCs might still be able to alleviate lung damage despite gradually declining in numbers post-administration (De Becker and Riet, 2016). Another critical characteristic of MSCs linked to their retention in the lung following systemic administration. A previous study has mentioned that intravenous infusion of MSCs results in their homogeneous distribution into the lung parenchyma (Gao *et al*, 2001), ascribable to a well-defined cell-trapping phenomenon happening in the lung microvasculature (Schrepfer *et al*, 2007).

The studies advocated in the past two decades suggested that MSCs mediate their actions *via* engraftment in the lung and differentiation into alveolar cells. The notion of differentiation is supported by studies in which transplanted MSCs adopted lung cell phenotypes in lung injury models (Ortiz *et al*, 2003; Rojas *et al*, 2005). The anti-inflammatory activity of MSCs has also been suggested as a potential therapeutic mechanism in lung damage. It has been demonstrated that the inhibition of the prolonged local inflammatory response may furnish an environment more suitable to the normal repair process. Additionally, the decline in inflammatory cytokine expression supports the documentation that MSCs suppress the inflammatory reaction through the activation/inhibition of

critical cytokines, resulting in alterations in the local cytokine environment in favor of tissue repair (Matthay *et al*, 2010).

Few studies reported that the use of MSCs may carry some risks to the patient (Lepperding *et al*, 2008), therefore, the administration of MSCs-CM may confer an alternative therapeutic option for lung injury. The intratracheal administration of BM-MSCs-CM has shown to protect against PF in terms of lung inflammation and collagen accumulation in a lung fibrosis model induced by bleomycin. Furthermore, it has been stated that BM-MSCs-CM has the potential to reduce apoptosis of alveolar epithelial cells (AECs), stimulate AECs regeneration and suppress development of lung fibrosis. It has been suggested that the therapeutic impact of BM-MSCs-CM on AECs may be linked with the epithelial specific growth factors released by BM-MSCs and the synergistic effects of these factors (Shen *et al*, 2015). BM-MSCs-CM has shown to have dynamic influences relating to fibrotic therapy, stimulating both the migration and proliferation of AECs while inhibiting the activation and proliferation of pulmonary fibroblasts, supporting the potential role of BM-MSCs-CM in tissue repair (Akram *et al*, 2013). It has been mentioned that MSCs-CM contain multiple factors that may confer therapeutic benefit, remarkably resolving lipopolysaccharide (LPS)-induced lung injury by ameliorating lung inflammation. MSCs-CM have been found to mostly contribute to the reprogramming modulation of monocytes-macrophages, from a proinflammatory M1 phenotype to an anti-inflammatory M2 phenotype (Ionescu *et al*, 2012).

A growing body of evidence indicates that excessive cytokine-mediated inflammation plays a key role in the initiation of PF. In the present study, there was a significant elevation in the serum concentrations of MIP2 in AD-treated rats as compared to control rats. Treatment with BM-MSCs or CM produced a remarkable drop in serum MIP2 concentrations. In a mouse model of bleomycin-induced PF, the MIP-2 protein levels in lung tissue homogenates of bleomycin-treated mice have been found to be significantly increased, in comparison to saline-treated control mice (Keane *et al*, 1999). Additionally, in a model of endotoxin-induced lung injury in mice, the intrapulmonary administration of BM-MSCs has been shown to mediate a reduction of MIP-2 levels in the bronchoalveolar lavage (BAL) fluid and plasma, hence, mitigating lung injury, a beneficial effect that has been shown to be mediated by a shift from a proinflammatory to an anti-inflammatory response (Gupta *et al*, 2007). Furthermore, it has been documented that BM-MSCs have a profound anti-inflammatory effect in endotoxin-induced lung injury in mice by markedly blunting the BAL fluid MIP-2 levels (Hao *et al*, 2015).

Transforming growth factor beta 1 (TGF- β 1) has been shown to play a pivotal role in the pathogenesis of PF (Allen and Spiteri, 2002). It is widely reported that TGF- β 1 mediated fibrotic tissue remodeling by increasing the production and decreasing the degradation of connective tissue (Bartram and Speer, 2004). In a rat model of AD-induced lung fibrosis, TGF- β 1 (mRNA and protein) expression in the lung has been found to be upregulated relative to controls (Chung et al, 2001). In addition, in a rat model of bleomycin-induced lung injury, the TGF- β 1 mRNA levels have been recorded to be upregulated following intratracheal perfusion of bleomycin. The present results are in complete agreement with the previous report indicating that the engraftment of BM-MSCs attenuates lung injury and fibrosis as evidenced by significant reduction in the TGF- β 1 mRNA levels in injured rat lungs (Zhao et al, 2008). Moreover, in a double dose bleomycin-induced model of lung injury, intravenous infusion of BM-MSCs has been shown to reduce TGF- β 1 protein levels in lung tissue lysates (Moodley et al, 2013). It has been reported that the intratracheal administration of bleomycin causes an elevation in the lung protein levels of TGF- β 1. Treatment with BM-MSCs reduced TGF- β 1 protein levels, suggesting that the anti-fibrotic action of BM-MSCs might be mediated by down-regulating lung expression of TGF- β 1 protein (Yu et al, 2015). Smads comprise a family of structurally similar proteins that are the main signal transducers for receptors of the TGF- β superfamily, and TGF- β 1/Smad2/3 signaling is one of the main pathways involved in a variety of pulmonary fibrogenesis processes, including inflammation, epithelial to mesenchymal transition (EMT), and extracellular matrix deposition (Flanders, 2004). It has been demonstrated that the pro-fibrogenic TGF- β 1 signaling is mediated predominantly via the Smad-dependent pathways (Heldin and Moustakas, 2012). In a bleomycin-induced PF model in mice, induced pluripotent stem cells (iPSCs) intravenous administration remarkably suppressed bleomycin-mediated activation of TGF- β 1/Smad2/3 in lung tissues (Zhou et al, 2016). Calcium-binding protein A4 (S100A4), a calcium binding protein, is a regulator of a number of cellular processes important to the progression of fibrosis (Donato et al, 2013). In a prior genome-wide transcriptional analysis, idiopathic pulmonary fibrosis (IPF) mesenchymal progenitor cells (MPCs) have been shown to express higher levels of S100A4 compared with control MPCs (Xia et al, 2014). The mechanism by which S100A4 imparts fibrogenic properties to IPF MPCs has been proposed to involve high nuclear levels of S100A4, which function to promote p53 proteasomal degradation, stimulating IPF MPC proliferation and expansion of the IPF MPC population (Xia et

al, 2017). Previously, it has been documented that in the process of fibrosis, epithelial cells can be transformed into fibroblasts, a process called EMT, suggesting that EMT might be involved in many fibrotic diseases. Additionally, it has been reported that TGF- β 1 is a powerful mediator of EMT. Interestingly, S100A4 has been shown to be a target of TGF- β 1 signaling, suggesting that S100A4 might be a key factor in TGF- β 1-induced EMT (Matsuura et al, 2010). Recently, S100A4 expression has been found to be induced by the TGF- β 1 pathway (Ning et al, 2018).

It has been demonstrated that MSCs and MSCs-CM exert observable cytoprotective effects in a human relevant pre-clinical model of chronic obstructive pulmonary disease. These protective influences were mediated *via* MSCs secretion of soluble mediators. Of note, MSCs-CM has been shown to be less effective than MSCs and this is likely ascribed to the capability of MSCs to continually release soluble factors (Kennelly et al, 2016). These findings showed parallelism with our study as the infusion of BM-MSCs revealed more favorable impact than BM-MSCs-CM in attenuating lung fibrosis induced by AD. The therapeutic efficacy of BM-MSCs might be partly attributed to enhanced mobilization of BM-MSCs to the fibrotic lung tissue.

In the present approach, maintaining the rats in AD-induced lung fibrosis group with BM-MSCs for prolonged time intervals showed a better fibrosis-attenuating influence than of short time. Likewise, keeping the BM-MSCs-CM-treated rats for extended time intervals revealed a better effect in ameliorating lung fibrosis than in case of limited time.

Conclusions

Taken together, our data provide insight into the molecular mechanisms, namely, down-regulating inflammatory response and TGF- β 1 signaling, behind the potent effectiveness of BM-MSCs as anti-fibrotic candidates, and further reinforce the feasibility of BM-MSCs transplantation in the treatment of PF. Additionally, the present findings justify the optimal treatment period of BM-MSCs in PF induced by AD. BM-MSCs-based therapy may represent an innovative effective approach against lung fibrosis. Nevertheless, further studies using more pathologically oriented lung fibrosis models will be required in the advance towards clinical settings.

Acronyms and abbreviations

BM-MSCs- bone marrow-derived mesenchymal stem cells; CM -conditioned media; AD -amiodarone; TGF- β 1-transforming growth factor beta 1; SMAD3 -mothers against

decapentaplegic homolog; S100A4 -S100 calcium-binding protein A4; MIP-2 -macrophage inflammatory protein 2.

Conflict of Interest Statement

The authors have no conflicts of interest to declare.

Acknowledgments

The authors gratefully acknowledge the technical support of the Stem Cell Lab., Center of Excellence for Advanced Sciences, National Research Centre, Egypt, in providing all required facilities to accomplish the work of the current study. Also, the authors express sincere appreciation to Prof. Adel Bakeer Kholoussy, Professor of Pathology, Faculty of Veterinary Medicine, Cairo University for his kind cooperation in conducting histological examination in this study.

References

1. Abdel Halim AS, Ahmed HH, Aglan HA, Abdel Hamid FF et al. Role of bone marrow-derived mesenchymal stem cells in alleviating pulmonary epithelium damage and extracellular matrix remodeling in a rat model of lung fibrosis induced by amiodarone. *Biotechnic & histochemistry: official publication of the Biological Stain Commission*. 2020 Sep 10:1-13. doi: 10.1080/10520295.2020.1814966.
2. Akram KM, Samad S, Spiteri M, Forsyth NR. Mesenchymal stem cell therapy and lung diseases. *Adv Biochem Eng Biotechnol*. 2013;130:105-29. doi: 10.1007/10_2012_140.
3. Akram KM, Samad S, Spiteri MA, Forsyth NR. Mesenchymal stem cells promote alveolar epithelial cell wound repair in vitro through distinct migratory and paracrine mechanisms. *Respir Res*. 2013 Jan 25;14 (1):9. doi: 10.1186/1465-9921-14-9.
4. Alhadlaq A, Mao JJ. Mesenchymal stem cells: isolation and therapeutics. *Stem Cells Dev* 2004 Aug;13 (4):436-48. doi: 10.1089/scd.2004.13.436.
5. Allen JT, Spiteri MA. Growth factors in idiopathic pulmonary fibrosis: relative roles. *Respir Res*. 2002;3 (1):13. doi: 10.1186/rr162.
6. Aslam M, Baveja R, Liang OD, Fernandez-Gonzalez A et al. Bone marrow stromal cells attenuate lung injury in a murine model of neonatal chronic lung disease. *Am J Respir Crit Care Med*. 2009 Dec 1;180 (11):1122-30. doi: 10.1164/rccm.200902-0242OC.
7. Balakumaran A, Pawelczyk E, Ren J, Sworder B et al. Superparamagnetic iron oxide nanoparticles labeling of bone marrow stromal (mesenchymal) cells does not affect their "stemness". *PLoS One* 5. 2010 Jul 7;5 (7):e11462. doi: 10.1371/journal.pone.0011462.
8. Bartram U, Speer CP. The role of transforming growth factor beta in lung development and disease. *Chest*. 2004 Feb;125 (2):754-65. doi: 10.1378/chest.125.2.754.
9. Bianco P, Cao X, Frenette PS, Mao JJ et al. The meaning, the sense and the significance: translating the science of mesenchymal stem cells into medicine. *Nat Med* 2013 Jan;19 (1):35-42. doi: 10.1038/nm.3028.
10. Chung WH, Bennett BM, Racz WJ, Brien JF et al. Induction of c-jun and TGF-beta 1 in Fischer 344 rats during amiodarone-induced pulmonary fibrosis. *Am J Physiol Lung Cell Mol Physiol*. 2001 Nov;281 (5):L1180-8. doi: 10.1152/ajplung.2001.281.5.L1180
11. De Becker A, Riet IV. Homing and migration of mesenchymal stromal cells: How to improve the efficacy of cell therapy? *World J Stem Cells*. 2016 Mar 26;8 (3):73-87. doi: 10.4252/wjsc.v8.i3.73.
12. Dominici M, Le Blanc K, Mueller I, Slaper-Cortenbach I et al. Minimal criteria for defining multipotent mesenchymal stromal cells. The International Society for Cellular Therapy position statement. *Cytotherapy*.2006;8 (4):315-7. doi: 10.1080/14653240600855905.
13. Donato R, Cannon BR, Sorci G, Riuazzi F et al. Functions of S100 proteins. *Curr Mol Med*. 2013 Jan;13 (1):24-57.
14. Farini A, Sitzia C, Erratico S, Meregalli M et al. Clinical applications of mesenchymal stem cells in chronic diseases. *Stem Cells Int*. 2014;2014 Apr: 30:65-73. doi: 10.1155/2014/306573.
15. Fernandez IE, Eickelberg O. New cellular and molecular mechanisms of lung injury and fibrosis in idiopathic pulmonary fibrosis. *Lancet*. 2012 Aug 18;380 (9842):680-8. doi: 10.1016/S0140-6736 (12)61144-1.
16. Flanders KC. Smad3 as a mediator of the fibrotic response. *Int J Exp Pathol*. 2004 Apr;85 (2):47-64. doi: 10.1111/j.0959-9673.2004.00377.x.
17. Gao J, Dennis JE, Muzic RF, Lundberg M et al. The dynamic in vivo distribution of bone marrow-derived mesenchymal stem cells after infusion. *Cells Tissues Organs*. 2001;169 (1):12-20. doi: 10.1159/000047856.
18. Gotts JE, Matthay MA. Mesenchymal stem cells and acute lung injury. *Crit Care Clin* 2011 Jul;27 (3):719-33. doi: 10.1016/j.ccc.2011.04.004.
19. Gupta N, Su X, Popov B, Lee JW et al. Intrapulmonary delivery of bone marrow-derived mesenchymal stem cells improves survival and attenuates endotoxin-induced acute lung injury in mice. *J Immunol*. 2007 Aug 1;179 (3):1855-63. doi: 10.4049/jimmunol.179.3.1855.

20. Hao Q, Zhu YG, Monsel A, Gennai S et al. Study of Bone Marrow and Embryonic Stem Cell-Derived Human Mesenchymal Stem Cells for Treatment of Escherichia coli Endotoxin-Induced Acute Lung Injury in Mice. *Stem Cells Transl Med.* 2015 Jul;4 (7):832-40. doi: 10.5966/sctm.2015-0006.
21. Heldin CH, Moustakas A. Role of Smads in TGFbeta signaling. *Cell Tissue Res.* 2012 Jan;347 (1):21-36. doi: 10.1007/s00441-011-1190-x.
22. Ionescu L, Byrne RN, van Haafden T, Vadivel A et al. Stem cell conditioned medium improves acute lung injury in mice: in vivo evidence for stem cell paracrine action. *Am J Physiol Lung Cell Mol Physiol.* 2012 Dec 1;303 (11): L967-77. doi: 10.1152/ajplung.00144.2011.
23. Javazon EH, Beggs KJ, Flake AW. Mesenchymal stem cells: paradoxes of passaging. *Exp Hematol.* 2004 May;32 (5):414-25. doi: 10.1016/j.exphem.2004.02.004.
24. Kang J, Fan W, Deng Q, He H et al. Stem Cells from the Apical Papilla: A Promising Source for Stem Cell-Based Therapy. *Biomed Res Int.* 2019 Jan 29; 2019:6104738. doi: 10.1155/2019/6104738.
25. Keane MP, Belperio JA, Moore TA, Moore BB et al. Neutralization of the CXC chemokine, macrophage inflammatory protein-2, attenuates bleomycin-induced pulmonary fibrosis. *J Immunol.* 1999 May 1;162 (9):5511-8.
26. Kennelly H, Mahon BP, English K. Human mesenchymal stromal cells exert HGF dependent cytoprotective effects in a human relevant pre-clinical model of COPD. *Sci Rep.* 2016 Dec 6;6:38207. doi: 10.1038/srep38207.
27. King TE, Pardo A, Selman M. Idiopathic pulmonary fibrosis. *The Lancet.* 2017 May 13;389 (10082):1941-1952. doi: 10.1016/S0140-6736 (17)30866-8.
28. Kolettis TM, Agelaki MG, Baltogiannis GG, Vlahos AP et al. Comparative effects of acute vs. chronic oral amiodarone treatment during acute myocardial infarction in rats. *Europace.* 2007 Nov;9 (11):1099-104. doi: 10.1093/europace/eum196.
29. Lepperdinger G, Brunauer R, Jamnig A, Laschober G et al. Controversial issue: is it safe to employ mesenchymal stem cells in cell-based therapies? *Exp Gerontol.* 2008 Nov;43 (11):1018-23. doi: 10.1016/j.exger.2008.07.004.
30. Ley B, Collard HR, King TE Jr. Clinical course and prediction of survival in idiopathic pulmonary fibrosis. *Am J Respir Crit Care Med.* 2011 Feb 15;183 (4):431-40. doi: 10.1164/rccm.201006-0894CI.
31. Livak KJ, Schmittgen TD. Analysis of relative gene expression data using real-time quantitative PCR and the 2⁻(Delta Delta C (T)) Method. *Methods.* 2001 Dec;25 (4):402-8. doi: 10.1006/meth.2001.1262.
32. Matsuura I, Lai CY, Chiang KN. Functional interaction between Smad3 and S100A4 (metastatin-1) for TGF-beta-mediated cancer cell invasiveness. *Biochem J.* 2010 Feb 24;426 (3):327-35. doi: 10.1042/BJ20090990.
33. Matthay MA, Gooljaerts A, Howard JP, Lee JW. Mesenchymal stem cells for acute lung injury: preclinical evidence. *Crit Care Med.* 2010 Oct;38 (10 Suppl):S569-73. doi: 10.1097/CCM.0b013e3181ff1fd.
34. Mohamed MR, Emam MA, Hassan NS, Mogadem AI. Umbelliferone and daphnetin ameliorate carbon tetrachloride-induced hepatotoxicity in rats via nuclear factor erythroid 2-related factor 2-mediated heme oxygenase-1 expression. *Environ Toxicol Pharmacol.* 2014 Sep;38 (2):531-41. doi: 10.1016/j.etap.2014.08.004.
35. Moodley Y, Vaghjiani V, Chan J, Baltic S et al. Anti-inflammatory effects of adult stem cells in sustained lung injury: a comparative study. *PLoS One.* 2013 Aug 1;8 (8):e69299. doi: 10.1371/journal.pone.0069299.
36. Motavaf M, Pakravan K, Babashah S, Malekvandfar F et al. Therapeutic application of mesenchymal stem cell-derived exosomes: A promising cell-free therapeutic strategy in regenerative medicine. *Cell Mol Biol (Noisy-le-grand).* (2016) 62, 74-79.
37. Ning Q, Li F, Wang L, Li H et al. S100A4 amplifies TGF-beta-induced epithelial-mesenchymal transition in a pleural mesothelial cell line. *J Investig Med.* 2018 Feb;66 (2):334-339. doi: 10.1136/jim-2017-000542.
38. Noble PW, Barkauskas CE, Jiang D. Pulmonary fibrosis: patterns and perpetrators. *J Clin Invest.* 2012 Aug;122 (8):2756-62. doi: 10.1172/JCI60323.
39. Ortiz LA, Gambelli F, McBride C, Gaupp D et al. Mesenchymal stem cell engraftment in lung is enhanced in response to bleomycin exposure and ameliorates its fibrotic effects. *Proc Natl Acad Sci U S A.* 2003 Jul 8;100 (14):8407-8411. doi: 10.1073/pnas.1432929100.
40. Parekkadan B, Milwid JM. Mesenchymal stem cells as therapeutics. *Annu Rev Biomed Eng.* 2010 Aug 15;12:87-117. doi: 10.1146/annurev-bioeng-070909-105309.
41. Rojas M, Xu J, Woods CR, Mora AL et al. Bone marrow-derived mesenchymal stem cells in repair of the injured lung. *Am J Respir Cell Mol Biol.* 2005 Aug;33 (2):145-52. doi: 10.1165/rcmb.2004-0330OC.
42. Schrepfer S, Deuse T, Reichenspurner H, Fischbein MP et al. Stem cell transplantation: the lung barrier. *Transplant Proc.* 2007 Mar;39 (2):573-6. doi: 10.1016/j.transproceed.2006.12.019.
43. Shen Q, Chen B, Xiao Z, Zhao L et al. Paracrine factors from mesenchymal stem cells attenuate epithelial injury

- and lung fibrosis. *Mol Med Rep.* 2015 Apr;11 (4):2831-7. doi: 10.3892/mmr.2014.3092.
44. Xia H, Bodempudi V, Benyumov A, Hergert P et al. Identification of a cell-of-origin for fibroblasts comprising the fibrotic reticulum in idiopathic pulmonary fibrosis. *Am J Pathol.* 2014 May;184 (5):1369-83. doi: 10.1016/j.ajpath.2014.01.012.
45. Xia H, Gilbertsen A, Herrera J, Racila E et al. Calcium-binding protein S100A4 confers mesenchymal progenitor cell fibrogenicity in idiopathic pulmonary fibrosis. *J Clin Invest* 2017 Jun 30;127 (7):2586-2597. doi: 10.1172/JCI90832.
46. Yagi H, Soto-Gutierrez A, Parekkadan B, Kitagawa Y et al. Mesenchymal stem cells: Mechanisms of immunomodulation and homing. *Cell Transplant.* 2010;19 (6):667-79. doi: 10.3727/096368910X508762
47. Yu SH, Liu LJ, Lv B, Che CL et al. Inhibition of bleomycin-induced pulmonary fibrosis by bone marrow-derived mesenchymal stem cells might be mediated by decreasing MMP9, TIMP-1, INF-gamma and TGF-beta. *Cell Biochem Funct.* 2015 Aug;33 (6):356-66. doi: 10.1002/cbf.3118.
48. Zhao F, Zhang YF, Liu YG, Zhou JJ et al. Therapeutic effects of bone marrow-derived mesenchymal stem cells engraftment on bleomycin-induced lung injury in rats. *Transplant Proc.* 2008 Jun;40 (5):1700-5. doi: 10.1016/j.transproceed.2008.01.080.
49. Zhou Y, He Z, Gao Y, Zheng R et al. Induced Pluripotent Stem Cells Inhibit Bleomycin-Induced Pulmonary Fibrosis in Mice through Suppressing TGF-beta1/Smad-Mediated Epithelial to Mesenchymal Transition. *Front Pharmacol.* 2016 Nov; 15;7:430. doi: 10.3389/fphar.2016.00430.



Received for publication: April, 03, 2022
Accepted: April, 11, 2022

Original paper

Physicochemical, cooking and sensory properties of Mackerel fish burger fortified with globe artichoke *Cynara scolymus* L.

WALAA ELMESHAD¹, MOHAMMED ABDELGALEEL¹, ESMAIL BORIY², BADAWEY W.Z.^{1*} AND MOSTAFA ALI^{1*}

¹Department of Food Technology, Faculty of Agriculture, Kafrelsheikh University, Egypt

²Food Sciences and Technology Department, Faculty of Agriculture, Damanhur University, Egypt

Abstract

The present study aims to characterize the globe artichoke parts, receptacle (AR) and bracts (AB), and to evaluate the quality characteristics of fish burger formulated by partial substitution of Mackerel fish meat with different level of both AR and AB. Physicochemical, cooking measurements and sensory characteristics of fish burgers were analyzed. The study results showed that the used artichoke parts had high protein, crude fiber, inulin and ascorbic acid contents. Total phenolics content of AR and AB was 43.1 and 38.2 (mg galic acid equivalent/g), respectively. The addition of artichoke parts to fish burger showed improvement in the cooking properties for instance increase cooking yield and decrease cooking loss and shrinkage, without noteworthy differences in sensory properties. Moreover, it was concluded that artichoke parts could be a great source of health-promoting phenolic compounds with high antioxidant activity. Therefore, our results could promote the consumption of artichoke parts and their using in different industrial food applications.

Keywords

Globe artichoke, receptacle, bracts, fish burger, cooking and sensory properties

To cite this article: ELMESHAD W, ABDELGALEEL M, BORIY E, BADAWEY WZ, ALI M. Physicochemical, cooking and sensory properties of Mackerel fish burger fortified with globe artichoke *Cynara scolymus* L. *Rom Biotechnol Lett.* 2022; 27(2): 3379-3388 DOI: 10.25083/rbl/27.2/3379.3388

Introduction

The globe artichoke (*Cynara scolymus* L.) is a large thistle and herbaceous perennial plant, that belongs to the family of *Asteraceae* (sunflower family). It is an ancient crop and medicinal plant, the therapeutic potential of artichoke was known to the ancient Egyptians, Greeks and Romans (Lattanzio *et al.*, 2009). As of 2017, the total production/yield quantities of artichokes in the world were 1505328 tons over an area of 122390 ha. Top globe artichoke producers in 2017 were Italy (387803 ton), Spain (223150 ton) and Egypt (185695 ton) (FAO, 2017). In addition, in 2018, Italy, Egypt and Spain recorded the highest volumes of artichoke consumption with 394.000, 319.000 and 196.000 K tons, respectively, which represents about 54% of global consumption. In 2019, the total world production of artichokes was approximately 1.6 million tons (FAOSTAT, 2019).

The artichoke fruit can be consumed in many ways, raw, steamed, fried, boiled, and used as ingredient in many recipes (Pandino *et al.*, 2011). The edible part, lower part (receptacle), of artichoke accounts 10–18% of the total weight head whereas, the core parts (inner bracts and receptacle) represent about 40%. The by-products of artichoke fruit (stems, leaves, outer bracts) account around 80% of the biomass. They can be used to extract nutraceuticals and food additives (Lattanzio *et al.*, 2009; Ciancolini *et al.*, 2013). Fresh artichokes have a low calories and fat content (Fратиanni *et al.*, 2007; Pandino *et al.*, 2011), are an excellent source of vitamins and rich in dietary fiber, polyphenolic compounds, hydroxycinnamates, flavones, antioxidants and minerals (potassium, sodium, phosphorus). These compounds help to improve the body's immunity against many diseases (Lattanzio *et al.*, 2009; Abd-Elhak *et al.*, 2014). Plant polyphenolic compounds are the richest source of antioxidants in our diet (Manach *et al.*, 2004). El-Sohaimy (2014) found that classic globe artichoke contain 72% moisture, 14 % protein, 2% lipids, 73% carbohydrates and 30 mg GAE/g DM total phenolic compounds. Artichoke parts (receptacle and bracts) are good source of inulin. Inulin, a highly water-soluble carbohydrate, is used in human nutrition and food industry due to its healthy and long chain length inulins (López-Molina *et al.*, 2005; Clifford & Brown, 2006; Lattanzio *et al.*, 2009; Costabile *et al.*, 2010).

Burgers are one of the most preferred fast foods, which contain more trans fatty acids, so it can cause obesity, coronary disease and diabetes. Vegetables and fruits are part of a healthy diet, which could help prevent major diseases, if consumed daily in sufficient amounts. They are an excellent and cheap source of minerals. Dietary fiber intake through meat replaced with fruits and vegetables is related to prevent against the risk of major dietary problems and many

diseases (Abd-Elhak *et al.*, 2014). Recently, the usage of natural plant parts in improving the shelf-life of foods is a promising technology due to its substances that have nutritional and functional properties (Burt, 2004; Badawy & Ali, 2018). Meat replacement with added non-meat constituents has been applied in meat industries. This replacement is used for several reasons for example, health, quality and economic purposes. Egbert and Payne (2009) and Badawy and Ali, (2018) replaced the animal meat source with plant parts in food industry such as burger. To our knowledge, the bracts and receptacle of artichoke were not thoroughly researched. Therefore, the goal of this study was to characterize two different parts of artichoke fruit (bracts and receptacle). Moreover, incorporation of these parts with different quantities in fish burger preparation by replacing of meat to test its effect on their chemical, cooking, nutritional and sensory properties.

Materials and methods

Materials

The globe artichoke fruits, *Cynara scolymus* variety, were obtained from a farm at Kafr El-Dour origin, EL-Behera, Egypt. Mackerel fish and ingredients of burger such as: spices, starch onion, salt, garlic, and refined sunflower oil were bought from Kafr El-Sheikh local market, Egypt. Standards phenols, 1,1 Diphenyl-2-Picrylhydrazyl (DPPH) and 6-hydroxi-2,5,7,8-tetramethylchromane-2-carboxylic acid (Trolox, TE), were acquired from Sigma company, St. Louis, MO, USA.

Methods

Preparation of artichoke powders

Artichoke fruits were washed with water and manually cleaned. Subsequently artichoke receptacle and bracts were manually separated and dried in an electric oven at 50±2 °C for 48h. Afterwards, these parts were cut into small pieces and powdered in a Moulinex hammer mill. Finally, the powders were stored in polyethylene airtight bags at refrigerated temperatures (4 °C) until analysis and use in burger formulations.

Preparation of fish burgers

Four Mackerel fish burger formulations were designed according to Yousefi *et al.*, (2018) with minor modifications. The fish meat was replaced with different levels (2.5, 5 and 10 %) of artichoke parts. All ingredients (2% NaCl, 2% oil, 2% spices, onion, ginger, hot spices, garlic, green chili paste) were mixed together in a blender and the prepared paste was added to minced fish and mixed with artichoke parts. After that, samples with a weight of 60 g, thickness of around one cm and diameter of around seven cm were

prepared. The burger samples were stored at -18 ± 2 °C until further analyses.

Thermal treatment

Fresh prepared burgers were fried using sunflower oil in stainless steel pan at 160 ± 10 °C for about 6 min (3 min for each side).

Determination of chemical composition of AR and AB and burgers

Moisture content was determined as the loss in weight after drying in an electrical air oven at 105 °C to reach a constant weight. Crude protein content was determined by the Micro-Kjeldahl method using the nitrogen- to protein conversion factor of 6.25. Ether extract was performed in a Soxhlet apparatus for 6 hours using petroleum ether (40-60 °C) as a solvent. Ash content was determined using the muffle at 550 °C. The crude fiber was determined in sample free from moisture and fat that remained after digestion with weak acid and base. All the above mentioned determinations were carried out followed the methods described in the AOAC (2011). The total carbohydrates were calculated as follows: Total carbohydrates (%) = 100 - (protein + ash + fat). All analyses were carried out in triplicate determinations.

Preparation of AR and AB extracts

Methanolic extracts were obtained from dried powders as follows: 1.5 g of dried powders was mixed with 20 ml of absolute methanol. The mixtures were stirred at 100 rpm for 24 h at room temperature. Then, the mixtures were filtrated and stored at refrigerated temperatures (4 °C) till analysis (Ziada, 2002).

Determination of total polyphenolics content

The total polyphenolics content of extracts were evaluated as described in Bonoli et al., (2004). one gram of sample was macerated in 50 ml of different solvents (99% methanol, 95% ethanol, 70% aqueous methanol, 70% aqueous ethanol and water) at room temperature for 1, 2, 3, 4, 6, 8 and 24 hrs. Moreover, 60 and 90 °C for 5 and 10 min were used. The extracts were filtrated. 300 µl of filtrates were added to 300 µl of Folin Ciocalteu's reagent, then 2.4 ml of 7.5% sodium carbonate solution was added and the mixture was incubated in the dark for half hour. Absorbance was then read at 760 nm using a UV spectrophotometer (Varian, Melbourne, VIC, Australia). Gallic acid was used as the standard. The content of total polyphenolics was calculated as mg gallic acid equivalent (GAE)/ g dried powders.

Determination of antioxidant capacity of artichoke parts

Antioxidant capacity of artichoke parts was determined using DPPH assay as illustrated in details in Badawy and

Ali, (2018). One mL of 0.15 mM DPPH solution in 95% ethanol was added to one mL extract. The mixture was stored for 30 min in the dark at room temperature. The absorbance was measured at 517 nm using PG Instruments T80 UV/VIS Spectrophotometer. Trolox (TE) was used to make the standard curve and the antioxidant activity was calculated as µM TE/100g dried powders.

Determination of inulin in artichoke parts

The procedure recommended by Prosky and Hoebregs (1999) was used to determine the inulin content in artichoke receptacle and bracts. One gram of dried powder was extracted with 25 ml distilled water at 40 oC. The extract was mixed with 5 ml of 1.0 N lead acetate solution and 5 ml saturated solution of sodium phosphate dibasic then filtered and the supernatant was removed. The residue was washed again with distilled water after that, the combined supernatant and washing water were diluted to 100 ml using distilled water. Two ml of the extract was added to 2 ml of folin reagent and the mixture was heated for 90 minutes in a water bath. After heating, the mixture was titrated with 0.01 N standard potassium-permanganate solution until a faint rose colour appeared. The inulin content was estimated using the following equation:

$$1.85 \text{ ml of } 0.01 \text{ N potassium permanganate solution} = 1 \text{ mg inulin}$$

Determination of ascorbic acid in AR and AB

Ascorbic acid content of artichoke receptacle and bracts was evaluated using Folin- Ciocalteu Reagent depending on the method reported by Dashman et al., (1991). Twenty ml of extract was transferred into 100 ml volumetric flask followed by 2 ml of 10% TCA solution and diluted to 100 ml with distilled water. The mixture was swirled gently for 1 minute and left to stand for 1 minute and filtered with Whatman filter (no 542). Briefly 30 mg of ascorbic acid were added to 10 ml distilled water to prepare the standard solution. One ml of the standard solution and extract was mixed with 3 ml of distilled water and 0.4 ml of Folin reagent. After that, the mixture was incubated for 10 min at room temperature. The absorbance of the mixtures was read at 760 nm using a UV spectrophotometer (Varian, Melbourne, VIC, Australia). The results were expressed as g per 100g fresh weight.

Determination of mineral contents:

Mineral contents (Ca, Mg, Na, Fe, P, Zn, and Mn) were determined depending on the methods of AOAC (2011). Five grams of dried sample were dry ashed in muffle furnace maintained at 550°C for 2 hr. The ash was cooled in desiccators and then weighed. After weighing, the ash was dissolved in a solution of 1:1 ratio of H₂O: HCl, in which

the concentration of the final mixture was 6N HCl. Calcium, Magnesium, iron and zinc were determined using the atomic absorption spectrophotometer (Zeiss FMD3). Sodium and potassium were determined by flame photometer. Phosphorus (P) was estimated photometrically of phosphorus molybdate complex by spectrophotometer at a wavelength of 650 nm, using a standard curve according to the methods described in the AOAC (2011).

Energy value of prepared burgers

Energy value of prepared burgers (on wet weight basis) was calculated as reported in AOAC (2011). Where, one gram of protein, lipid and available carbohydrates gives 4.27, 9.02 and 4.10 Kcal, respectively.

Physical properties of prepared burgers

Protein-water-fat coefficient (PWFC), water-protein coefficient (WPC) and protein - water coefficient (PWC) were calculated as reported by Tsuladze (1972) and Feder value as reported by Pearson (1970).

Cooking properties of burgers

The percentage of burger shrinkage, cooking yield, moisture retention and the cooking loss of the prepared burgers were calculated according to equations planned by Berry (1992), Aleson-Carbonell *et al.*, (2005) and Akwetey and Knipe (2012), respectively and found in Badawy and Ali (2018).

Sensory evaluation of prepared fish burgers

Sensory properties of cooked fish burgers fortified with artichoke parts were evaluated through hedonic test, by 25 panelists from the staff members of the Food Industry Department, Faculty of Agriculture, Kafrelsheikh University, as mentioned in Meilgaard *et al.*, (2007). Panelists were asked to give numerical values ranging from 0 to 10 for the sample's characteristics, taste, odor, texture, color, appearance and overall. The panelists were asked to have mouths rinsed with water between each sample.

Statistical Analysis

The results were statistically analyzed using T test analysis of variance (ANOVA) procedure by SPSS (Version 16.0) software.

Results and Discussion

Chemical composition of AR and AB

The chemical composition of studied artichoke parts (AR and AB) was determined, and the results are shown in Table (1). The results reported that receptacle from artichoke contained 84.4, 11.50, 2.6, 4.1, 9.51 and 81.8 % for moisture, crude protein, fat, ash, crude fibers and total carbohydrates (on dry weight basis), respectively. While, the chemical composition of bracts was 74, 5.2, 2.1, 3.9, 10.6 and 88.8 % for moisture, crude protein, fat, ash, crude fibers and total carbohydrates, respectively. Shalaby (2000) found that chemical composition of artichoke bracts was 85.32±0.4 moisture, 69.11±1.2% total carbohydrates, 11.10±1.0% crude protein, 2.85±0.2% ether extract, 26.0±2.1% crude fibers, 16.10±1.2% ash (on dry weight basis). While, Gomaa (2010) and Claus *et al.*, (2015) stated that artichoke receptacle was found to have 12.90 and 24.27% protein, 1.41 and 1.34 % fat and 6.20 and 12.32 % ash and artichoke bracts recorded low protein (11.60 and 10.35%), fat (1.31 and 2.04 %) contents, where ash content was (10.10 and 5.37 %), respectively. These differences may be related to the varieties, origin and conditions of agriculture.

The results presented in Table (1) show that inulin and ascorbic acid were found in two studied parts. Furthermore, Table (1) indicated remarkable differences in inulin and ascorbic acid contents among the different parts, where receptacle showed 32.9 and 0.89%, while bracts showed 21.8 and 0.34 %, respectively. These data are in the line with (Lattanzio *et al.*, 2000; Sharara & Ghoneim, 2011) who reported that inulin content in artichoke is more than 30%. Shalaby (2000) re-

Table 1. Chemical composition (on dry weight basis) of some artichoke parts

Parameters	AR	AB
Moisture %	84.5± 0.10 ^a	74±1.20 ^b
Crude Protein %	11.5±1.10 ^a	5.2±0.17 ^b
Ether extract %	2.6±1.30 ^a	2.1±1.11 ^b
Ash %	4.1±0.23 ^a	3.9±1.00 ^a
Crude fibers %	9.5±0.19 ^b	10.6±0.30 ^a
Total carbohydrates %	81.8±2.7 ^b	88.8±3.21 ^a
Inulin %	32.9±0.22 ^a	21.8±0.31 ^b
Ascorbic acid %	0.89±0.23 ^a	0.34±0.21 ^b
Total phenolics mg GAE/g	43.1±0.12 ^a	38.3± 0.21 ^b
Total flavonoids mg QE/g	8.6±0.14 ^a	7.8±0.17 ^b
Antioxidant activities (µM TE/g sample)	53.5± 1.10 ^a	31.9± 1.14 ^b

Where: AR; Artichoke Receptacle and AB; Artichoke Bracts.

Values followed by the same letter in a row are not significantly different $P \leq 0.05$

ported that the inulin content of bracts was 10.89±1.1%. The results of assays of total phenolics and flavonoids content and antioxidant activity assays of receptacle and bracts are also listed in Table (1). The results of total phenolics content are in agreement with El Sohaimy (2014), who found that the total phenolic content (TPC) in methanol extract of globe artichoke was 30.70±1.87 mg GAE/g dry sample). While, they are higher than the results reported by Rejeb et al., (2020), who found that the TPC content for the bracts of two different artichoke varieties was (15.262 and 10.726 mg GAE/ g DW). These differences may be related to the varieties, origin and conditions of agriculture. As shown in Table (1) the total flavonoids and antioxidant activity contents differ also depending on the fruit parts. The highest values were recorded for receptacle compared to bracts. The significant differences between the results were found, where it was clear that receptacle had the highest phenolics and flavonoids content and antioxidant activity compared to bracts part. This trend is similar to the results found by El Sayed et al., (2018). The highest antioxidant activity content of receptacle compared to bracts is related to the total phenolic and flavonoids content.

Minerals content of some artichoke parts

The results in Table (2) indicate that artichoke is a great source of minerals such as potassium, sodium, manganese and calcium. Potassium presented as the highest value of mineral, 1807.5 and 1875.0 (mg/100g DM) by receptacle and bracts, respectively. While, sodium existing as 1285.0 and 365.3 mg/100 g DM by receptacle and bracts, respectively. Moreover, trace elements such as iron and copper were detected in both artichoke parts. These results are similar to the findings of El Sayed et al., (2018) who reported that macro elements of artichoke extract contained high contents of Na, Ca, and Mg and traces from Zn, Fe, Mn, and Cr.

Table 2. Minerals content (mg/100g on dry weight basis) of some artichoke parts

Elements	Amounts			
	AR	% of total	AB	% of total
K	1807.5	45	1875.0	68.5
Na	1285.0	32	365.3	13.4
Mg	713.7	17.7	387.8	14.2
Ca	191.3	4.8	89.4	3.2
P	9.6	0.24	5.6	0.24
Fe	8.0	0.21	10.1	0.38
Cu	1.9	0.05	1.9	0.08
Total	4016	100	2735	100

Where: AR; Artichoke Receptacle and AB; Artichoke Bracts.

Values followed by the same letter in a column are not significantly different $P \leq 0.05$

Influence of the artichoke parts level on chemical composition of prepared fish burgers

The moisture, protein, fat, ash, crude fiber and total carbohydrates contents of the raw and cooked controls and fortified fish burgers with different levels (2.5, 5 and 10 %) of some artichoke parts (receptacle and bracts) were listed in Tables (3 and 4). The results exposed that the control of uncooked burger contained 71.7 % moisture, 46.1 % protein, 12.27% fat, 3.74 % ash, 0.5 crude fiber and 37.89 % carbohydrates, while the control of cooked burger contained 68.3 % moisture, 45.6 %protein, 19.29 % fat, 3.71 % ash, 0.4 crude fiber and 31.4 % carbohydrates.

From the presented data, it could be observed that the moisture content of uncooked burgers decreased as the level of receptacle and bracts increased, but the decreasing rate was not significant. Serdaroglu (2006) stated a reduction in moisture content of beef burgers formed with the flour of oat due to an increase in solid contents., In contrary, the moisture content of cooked burgers increased slowly as the level of artichoke parts increased, but the increasing rate was not significant between the levels of artichoke powders. It has been informed that during cooking, fish burgers lose moisture during evaporation and drip (Sheridan & Shilton, 2002), which could be because the adding of receptacle and bracts decreases evaporation and drip causing a significant increase in the content of moisture of fortified cooked burgers. In addition, protein and ether extract contents of raw burgers decreased as the amount of artichoke parts increased, while, ash, crude fiber and carbohydrates increased with the increasing of artichoke parts. These could be related to the lower content of crude fat and protein in Artichoke parts than in fish. On the other hand, in cooked samples, all determined constituents except protein content increased with the increasing of Artichoke parts. Hassaballa et al., (2009), Al-Juhaimi , (2016) and Badawy and Ali (2018) reported that an increase in protein, fat and ash contents in burgers, fortified with moringa and mashed pumpkin and potato and marjoram after cooking processes was observed.

Influence of the artichoke parts level on physicochemical properties of fish burgers

The results showed that, PWC, PWFC and Feder value of fish burgers were gradually decreased by increasing levels of dried Artichoke parts compared to control sample. While WPC increased with increasing levels of dried Artichoke parts. So that, tenderness of burger was increased. This result might be due to the decrease in protein content of all prepared burgers as a result to denaturation and aggregation of protein. These results are in the line with the results of Hegazy (2004) and El - Refai et al., (2014). Moreover, the

Table 3. Chemical composition (on dry weight basis) of raw fish burgers

Formulations	Moisture	Protein	Fat	Ash	Crude fiber	Total Carbohydrates
Control	71.7±0.12 ^{ms}	46.1 ^a ±0.22 ^a	12.27±0.03 ^a	3.74±0.05 ^c	0.5±0.05 ^d	37.89
2.5% AR	71.6±0.06	45.3±0.07 ^a	12.17±0.08 ^a	3.81±0.07 ^c	0.7±0.03 ^c	38.72
5.0% AR	71.5±0.14	44.2±0.09 ^b	12.04±0.12 ^a	4.06±0.02 ^b	0.9±0.18 ^c	39.7
10% AR	71.3±0.70	43.1±0.03 ^b	11.83±0.04 ^b	4.14±0.09 ^b	1.2±0.07 ^b	40.93
2.5% AB	70.2±0.01	44.9±0.11 ^a	12.21±0.02 ^b	4.05±0.10 ^b	1.1±0.04 ^b	38.84
5.0% AB	70.1±0.09	43.6±0.05 ^b	12.10±0.09 ^b	4.41±0.18 ^a	1.7±0.15 ^a	39.89
10% AB	69.8±0.00	42.3 ^c ±0.01 ^c	12.00±0.05 ^a	4.75±0.14 ^a	2.1±0.09 ^a	40.95

Where: AR; Artichoke Receptacle and AB; Artichoke Bracts.

Values followed by the same letter in a column are not significantly different $P \leq 0.05$

Table 4. Chemical composition (on dry weight basis) of cooked fish burgers

Formulations	Moisture	Protein	Fat	Ash	Crude fiber	Total Carbohydrates
Control	68.3±0.08 ^{ms}	45.6±0.05 ^a	19.29±0.01 ^{ms}	3.71±0.21 ^c	0.4±0.02 ^d	31.4
2.5% AR	68.5±0.11	44.7±0.19 ^a	19.47±0.08	3.86±0.06 ^c	0.6±0.05 ^c	31.97
5.0% AR	68.7±0.06	43.9±0.08 ^b	19.71±0.18	3.96±0.02 ^c	0.8±0.03 ^c	32.68
10% AR	68.9±0.02	42.8±0.03 ^c	19.88±0.01	4.10±0.09 ^b	1.1±0.01 ^b	33.22
2.5% AB	68.7±0.09	45.0±0.16 ^a	19.38±0.07	4.10±0.00 ^b	1.0±0.22 ^b	31.52
5.0% AB	69.2±0.20	43.7±0.11 ^b	19.63±0.13	4.51±0.11 ^a	1.6±0.03 ^a	32.16
10% AB	69.6±0.07	42.5±0.11 ^c	19.87±0.00	4.86±0.06 ^a	2.0±0.02 ^a	32.77

Where: AR; Artichoke Receptacle and AB; Artichoke Bracts.

Values followed by the same letter in a column are not significantly different $P \leq 0.0$

Table 5. Physicochemical properties and energy value of fish burger fortified with different levels of artichoke

Formulations	PWC	PWFC	WPC	Feder value	Energy value
Control	0.18±0.03 ^b	0.17±0.07 ^b	5.49±0.17 ^b	3.02±0.12 ^a	154.07
2.5% AR	0.18±0.02 ^b	0.17±0.05 ^b	5.56±0.15 ^b	2.99±0.14 ^a	155.56
5.0% AR	0.18±0.02 ^b	0.17±0.04 ^b	5.67±0.16 ^a	2.98±0.15 ^a	155.28
10% AR	0.17±0.01 ^c	0.17±0.07 ^b	5.76±0.17 ^a	2.96±0.11 ^a	153.53
2.5% AB	0.19±0.04 ^a	0.18±0.06 ^a	5.51±0.12 ^b	2.81±0.13 ^b	154.02
5.0% AB	0.19±0.03 ^a	0.18±0.02 ^a	5.54±0.13 ^b	2.80±0.14 ^b	154.28
10% AB	0.18±0.05 ^b	0.17±0.03 ^b	5.58±0.11 ^b	2.77±0.15 ^b	147.98

Where: AR; Artichoke Receptacle and AB; Artichoke Bracts.

Values followed by the same letter in a column are not significantly different $P \leq 0.05$

results showed that the feder numbers of prepared burgers were less than 4. Therefore, they are in good quality (Pearson, 1970).

Influence of the artichoke parts level on cooking properties of fish burgers

The cooking properties of fortified and unfortified fish burgers are presented in Table (6). The data exposed that, the addition of artichoke parts (receptacle and bracts) to fish burgers influenced on the cooking characteristics of prepared burgers. The cooking yield was increased in burgers with an increase in the artichoke amount compared to control. The cooking yield was increased from 95.24 % for control to 96.12, 96.32 and 97.76 % for burgers fortified with 2.5, 5 and 10 % receptacle, and to 94.30, 94.74 and 95.55 % for ones fortified with 2.5, 5 and 10 %, bracts, respectively. These results agree with Al-Juhaimi *et al.*, (2016) and Badawy and Ali (2018), who stated similar trends for the

cooking yield in burgers fortified with moringa seed powder and marjoram leaves, respectively. Alakali *et al.*, (2010) also found the same results for the cooking yield of beef fortified with groundnut seed powder. They explained this observation by the ability of these materials to the water and fat retention capacity, in addition to ability to maintain fat and moisture in the patty matrix.

As apparent in Table (6), the addition of receptacle and bracts of artichoke improved the moisture retention of cooked burgers, where they were increased with the increase of artichoke level compared to control. This results can be explained by the increasing of the water absorption capacity of protein and the gelatinization of starch during cooking process in addition to the swelling of the fiber (Modi *et al.*, 2004). This result is important since high water retention positively influences properties of meat or fish products such as juiciness and texture. The results obtained for fat uptake

Table 6. Cooking properties of fish burgers fortified by different levels of Artichoke

Formulations	Cooking yield (%)	Cooking loss (%)	Shrinkage (%)	Moisture retention (%)	Oil uptake %
Control	95.24±1.67 ^d	4.72±0.16 ^a	7.14±0.12 ^a	95.25±1.07 ^c	57.2±0.37 ^c
2.5% AR	96.12±1.38 ^c	3.80±0.21 ^b	5.71±0.15 ^b	95.67±1.21 ^c	59.98±0.39 ^d
5.0% AR	96.78±1.34 ^b	3.52±0.25 ^b	3.57±0.17 ^c	96.08±1.17 ^b	63.70±0.32 ^b
10% AR	97.87±1.42 ^a	2.68±0.18 ^c	2.85±0.13 ^d	96.63±1.31 ^b	68.47±0.34 ^a
2.5% AB	96.45±1.51 ^b	4.64±0.17 ^a	4.28±0.18 ^c	97.86±1.27 ^a	58.72±0.37 ^d
5.0% AB	96.10±1.33 ^c	4.53±0.15 ^a	2.86±0.14 ^d	98.71±1.31 ^a	62.23±0.41 ^c
10% AB	96.66±1.61 ^b	4.34±0.18 ^a	1.34±0.16 ^c	99.71±1.19 ^a	65.58±0.38 ^b

Where: AR; Artichoke Receptacle and AB; Artichoke Bracts.

Values followed by the same letter in a column are not significantly different $P \leq 0.05$

Table 7. Sensory evaluation of cooked fish burgers fortified by different levels of artichoke

Overall Acceptability	Sensory properties				Formulations
	Texture	Odor	Taste	Color	
8.42±0.67 ^a	8.58±0.51 ^a	8.67±0.49 ^a	8.08±0.90 ^b	8.75±0.8 ^a	Control
8.83±0.39 ^a	8.75±0.45 ^a	8.67±0.50 ^a	8.92±0.29 ^a	8.67±0.9 ^a	2.5% AR
8.43±0.90 ^a	8.25±0.97 ^b	8.25±0.82 ^b	8.17±0.94 ^b	8.17±1.1 ^a	5.0% AR
7.93±0.79 ^b	7.67±1.83 ^c	8.00±1.51 ^b	8.30±1.22 ^b	8.33±0.7 ^a	10% AR
8.50±0.74 ^a	8.17±0.94 ^b	8.00±0.95 ^b	7.92±1.00 ^b	8.81±1.1 ^a	2.5% AB
7.92±0.90 ^b	7.83±0.83 ^c	8.00±0.82 ^b	7.25±1.24 ^c	7.16±0.7 ^b	5.0% AB
7.17±1.40 ^c	7.08±1.38 ^d	7.42±1.51 ^c	7.08±1.78 ^c	6.83±1.3 ^b	10% AB

Where: AR; Artichoke Receptacle and AB; Artichoke Bracts.

Values followed by the same letter in a column are not significantly different $P \leq 0.05$

of cooked fish burgers (Table 6) showed the same result that observed for moisture retention. The raise in fat retention may be related to the fact that the swelling of the fiber and starch in addition to the fat absorbed by the fiber can be interact with the protein of the crushed meat matrix to avoid migration of fat from the product (Alakali et al., 2010). Table (6) also shows that the addition of artichoke parts was decreased the cooking loss compared to control burger sample with values of 4.72 for control burger and 3.80, 3.52 and 2.86 % for burgers fortified with 2.5, 5 and 10 % receptacle, while the values decreased to 4.64, 4.53, 4.34 % for burgers fortified with 2.5, 5 and 10 %, bracts, respectively. This improvement in cooking loss was occurred by the addition of orange peel and marjoram leaves which is able to bind water and fat (Eldemery, 2010; Mahmoud et al., 2017; Badawy & Ali, 2018). Fibers decreased the cooking loss of burgers because of their high ability to retain moisture and fat in the medium (Besbes et al., 2008). The percentage of shrinkage was decreased with the artichoke level increased (Table 6).

Bracts part showed more decrease than receptacle part, where the control burger showed the highest shrinkage percent, 7.14 %, compared to 5.71, 3.57 and 2.85 % for burgers fortified with 2.5, 5 and 10 %receptacle, and to 4.28, 2.86 and 1.34 % for burgers fortified with 2.5, 5 and 10 %, bracts, respectively. The denaturation of protein meat, water evaporation and juices during cooking process is associated to

the shrinkage (Alakali et al., 2010; Al-Juhaimi et al., 2016). The lower shrinkage observed in fish burgers fortified with artichoke parts compared to the unfortified burgers might be due to the stabilizing and binding characteristics of portions used, which retain the meat particles together and banned changes in the juice losses, moisture and accordingly the shape of the product as reported by Naveena et al., (2006) and Al-Juhaimi et al., (2016).

Influence of the artichoke parts level on sensory properties of cooked fish burgers

Results presented in Table (7) show the mean sensory scores of cooked fish burger samples prepared with different levels of artichoke parts. The addition of non-meat ingredient to fish usually decreases its quality and the main problem is to keep it at the level as close as possible to the full-meat product. Results indicated that there were no significant differences at $p \leq 0.05$ for color, odor, texture, flavor and overall acceptability between cooked burgers fortified by different levels of artichoke and the control burger. Fish burgers which were not fortified with dried artichoke or were fortified with 2.5 and 5% dried artichoke parts had better organoleptic properties compared to burgers fortified with 10%. Therefore, supplemented burger with Artichoke till 5 % could be recommended to be produced as burger with good quality acceptable sensory quality attributes.

Conclusions

The results of this study showed that powders of artichoke parts (receptacle and bracts) are important sources of minerals (K, Na, Mg and Ca), bioactive compounds (phenolic compounds), inulin and vitamin C. In addition, these powders have antioxidant potential being beneficial in a healthy diet for prevention of diseases caused by free radicals. Dried receptacle and bracts of artichoke can be used for food fortification and as functional food in fish products. Fortification with dried artichoke at levels 2.5, 5 and 10% caused good effects on all physicochemical properties and cooking properties of fish burgers at zero time. Fish burgers which were not fortified with dried artichoke or were fortified with 2.5 and 5% dried artichoke had better organoleptic properties compared to burgers fortified with 10%. Therefore, powders prepared from artichoke parts can be used as functional ingredients and can be used to fortify food products (fish, bakery and pastry products, especially) in order to increase the nutritional and their antioxidant potential, but also as sweetening agent for products for diabetics. The results indicated that used artichoke parts has high potential as a binder for use in burger production in addition to its health and nutritional benefits. Further studies are needed to characterize artichoke parts.

Conflict of Interest

The authors have declared no conflicts of interest for this article.

References

1. Abd-Elhak, N. A., Ali, S. E., & Zaki, N. L. (2014). Innovative modification of traditional burger. *Egypt. J. Agric. Res.*, *92*(3).
2. Akwetey, W. Y., & Knipe, C. L. (2012). Sensory attributes and texture profile of beef burgers with gari. *Meat Science*, *92*(4), 745-748. doi:https://doi.org/10.1016/j.meatsci.2012.06.032
3. Al-Juhaimi, F., Ghaffoor, K., Hawashin, M. D., Alsawmahi, O. N., & Babiker, E. E. (2016). Effects of different levels of Moringa (*Moringa oleifera*) seed flour on quality attributes of beef burgers. *CyTA-Journal of Food*, *14*(1), 1-9.
4. Alakali, J., Irtwange, S., & Mzer, M. (2010). Quality evaluation of beef patties formulated with bambara groundnut (*Vigna subterranean* L.) seed flour. *Meat Science*, *85*(2), 215-223.
5. Aleson-Carbonell, L., Fernandez-Lopez, J., Perez-Alvarez, J. A., & Kuri, V. (2005). Characteristics of beef burger as influenced by various types of lemon albedo. *Innovative Food Science & Emerging Technologies*, *6*(2), 247-255. doi:https://doi.org/10.1016/j.ifset.2005.01.002
6. AOAC. (2011). Official Methods of Analysis of AOAC International. 18th Edition, AOAC International, Gaithersburg, 2590.
7. Badawy, W., & Ali, M. (2018). Improvement of some Functional and Nutritional Characteristics of the Beef Burger Using Marjoram Herb. *Journal of Food and Dairy Sciences*, *9*(7), 263-271.
8. Berry, B. (1992). Low fat level effects on sensory, shear, cooking, and chemical properties of ground beef patties. *Journal of food science*, *57*(3), 537-537.
9. Besbes, S., Attia, H., Deroanne, C., Makni, S., & Blecker, C. (2008). Partial replacement of meat by pea fiber and wheat fiber: effect on the chemical composition, cooking characteristics and sensory properties of beef burgers. *Journal of Food Quality*, *31*(4), 480-489.
10. Bonoli, M., Marconi, E., & Caboni, M. F. (2004). Free and bound phenolic compounds in barley (*Hordeum vulgare* L.) flours: Evaluation of the extraction capability of different solvent mixtures and pressurized liquid methods by micellar electrokinetic chromatography and spectrophotometry. *Journal of Chromatography A*, *1057*(1-2), 1-12.
11. Burt, S. (2004). Essential oils: their antibacterial properties and potential applications in foods—a review. *International journal of food microbiology*, *94*(3), 223-253.
12. Ciancolini, A., Alignan, M., Pagnotta, M. A., Miquel, J., Vilarem, G., & Crinò, P. (2013). Morphological characterization, biomass and pharmaceutical compounds in Italian globe artichoke genotypes. *Industrial Crops and Products*, *49*, 326-333.
13. Claus, T., Maruyama, S. A., Palombini, S. V., Montanher, P. F., Bonafé, E. G., Junior, O. d. O. S., . . . Visentainer, J. V. (2015). Chemical characterization and use of artichoke parts for protection from oxidative stress in canola oil. *LWT-Food Science and Technology*, *61*(2), 346-351.
14. Clifford, M., & Brown, J. (2006). Dietary flavonoids and healthbroadening the perspectives In: Flavonoids: Chemistry, Biochemistry and Applications. Andersen; OM, Markham; Eds. In: CRC Press, Boca Raton, FL.
15. Costabile, A., Kolida, S., Klinder, A., Gietl, E., Bäuerlein, M., Froberg, C., . . . Gibson, G. R. (2010). A double-blind, placebo-controlled, cross-over study to establish the bifidogenic effect of a very-long-chain inulin extracted from globe artichoke (*Cynara scolymus*)

- in healthy human subjects. *British journal of nutrition*, 104(7), 1007-1017.
16. Dashman, T., Blocker, D. E., & Baker, N. (1991). *Laboratory manual for human nutrition*: Harwood Academic Publishers GmbH.
 17. Egbert, W., & Payne, C. (2009). Plant Proteins in Ingredients in Meat Products: Properties, Functionality and Applications. . In: Springer New York.
 18. El-Refai, A., El-Zeiny, A. R., & Rabo, E. (2014). Quality attributes of mushroom-beef patties as a functional meat product. *Journal of Hygienic Engineering and Design*, 6, 49-62.
 19. El Sayed, A. M., Hussein, R., Motaal, A. A., Fouad, M. A., Aziz, M. A., & El-Sayed, A. (2018). Artichoke edible parts are hepatoprotective as commercial leaf preparation. *Revista Brasileira de Farmacognosia*, 28(2), 165-178.
 20. El Sohaimy, S. A. (2014). Chemical composition, antioxidant and antimicrobial potential of artichoke. *The Open Nutraceuticals Journal*, 7(1).
 21. Eldemery, M. E. (2010). *Effect orange albedo as a new source of dietary fiber on characteristics of beef burger*. Paper presented at the The 5th Arab and 2nd International Annual Scientific Conference on: Recent Trends of Developing Institutional and Academic Performance in Higher Specific Education Institutions in Egypt and Arab World. Mansoura University–Egypt.
 22. FAO. (2017). Major Food and Agricultural Commodities and Producers - Countries By Commodity". FAO. Org. Retrieved Dec 1, 2019.
 23. FAOSTAT. (2019). Crops and livestock product. Food and Agriculture Organization of the United Nations. (World+Total; Production Quantity; Crops Primary; 2019). . Retrieved 2021-11-02.
 24. Fratianni, F., Tucci, M., De Palma, M., Pepe, R., & Nazaro, F. (2007). Polyphenolic composition in different parts of some cultivars of globe artichoke (*Cynara cardunculus* L. var. *scolymus* (L.) Fiori). *Food chemistry*, 104(3), 1282-1286.
 25. Goma, M.A.H. (2010). *Chemical and technological studies on some foods chemical, technological and biological studies on Artichoke (Cynara scolymus L.)*. PhD Thesis ,Dept. of Food Technol., Fac. Of Agric., Kafrelsheikh, Univ ., Egypt.,
 26. HassabAlla, A., Mohamed, G., Ibrahim, H., & AbdEl-Mageed, M. (2009). Frozen cooked catfish burger: effect of different cooking methods and storage on its quality. *Global Veterinaria*, 3(3), 216-226.
 27. Hegazy, N. (2004). *Chemical, Microbiological and Technological Studies on some Poultry Meat Products*. M. Sci. Thesis, Food Industry Dept., Faculty of Agric., El-Mansoura Univ., Egypt,
 28. Lattanzio, V., Cicco, N., & Linsalata, V. (2000). *Antioxidant activities of artichoke phenolics*. Paper presented at the IV International Congress on Artichoke 681.
 29. Lattanzio, V., Kroon, P. A., Linsalata, V., & Cardinali, A. (2009). Globe artichoke: a functional food and source of nutraceutical ingredients. *Journal of functional foods*, 1(2), 131-144.
 30. López-Molina, D., Navarro-Martínez, M. D., Rojas-Melgarejo, F., Hiner, A. N., Chazarra, S., & Rodríguez-López, J. N. (2005). Molecular properties and prebiotic effect of inulin obtained from artichoke (*Cynara scolymus* L.). *Phytochemistry*, 66(12), 1476-1484.
 31. Mahmoud, M., Abou-Arab, A., & Abu-Salem, F. (2017). Quality characteristics of beef burger as influenced by different levels of orange peel powder. *American Journal of Food Technology*, 12(4), 262-270.
 32. Manach, C., Scalbert, A., Morand, C., Rémésy, C., & Jiménez, L. (2004). Polyphenols: food sources and bio-availability. *The American Journal of Clinical Nutrition*, 79(5), 727-747.
 33. Meilgaard, M. C., Civileand, G. V., & Carr, B. T. (2007). *Sensory Evaluation Techniques* (4 ed.): 4th Ed. CRC Press: New York.
 34. Modi, V. K., Mahendrakar, N. S., Narasimha Rao, D., & Sachindra, N. M. (2004). Quality of buffalo meat burger containing legume flours as binders. *Meat Science*, 66(1), 143-149. doi:[https://doi.org/10.1016/S0309-1740\(03\)00078-0](https://doi.org/10.1016/S0309-1740(03)00078-0)
 35. Naveena, B., Muthukumar, M., Sen, A., Babji, Y., & Murthy, T. (2006). Quality characteristics and storage stability of chicken patties formulated with finger millet flour (Eleusine coracana). *Journal of Muscle Foods*, 17(1), 92-104.
 36. Pandino, G., Lombardo, S., Mauromicale, G., & Williamson, G. (2011). Profile of polyphenols and phenolic acids in bracts and receptacles of globe artichoke (*Cynara cardunculus* var. *scolymus*) germplasm. *Journal of Food Composition and Analysis*, 24(2), 148-153. doi:<https://doi.org/10.1016/j.jfca.2010.04.010>
 37. Pearson, D. (1970). *The chemical Analysis of Food* (6th ed.) (6 ed.). Churchill, London, UK.
 38. Prosky, L., & Hoebregs, H. (1999). Methods to determine food inulin and oligofructose. *The Journal of nutrition*, 129(7), 1418S-1423S.
 39. Rejeb, I., Dhen, N., Gargouri, M., & Boulila, A. (2020). Chemical Composition, Antioxidant Potential and Enzymes Inhibitory Properties of Globe Artichoke By-

- Products. *Chemistry & Biodiversity*, 17. doi:10.1002/cbdiv.202000073
40. Serdaroglu, M. (2006). The characteristics of beef patties containing different levels of fat and oat flour. *International Journal of Food Science & Technology*, 41, 147-153. doi:10.1111/j.1365-2621.2005.01041.x
41. Shalaby, S. (2000). *Extraction of Inulin from Some Plant Source and Its Utilization in Preparing Some Diabetic Foods*. Ph.D. Thesis, Faculty of Agriculture., Kafr El-Sheikh, Tanta University, Egypt.
42. Sharara, S. M., & Ghoneim, M. I. (2011). Inulin in Some Artichoke By-Products :Determination and Effects of Some Technological Processes Thereon. *Alexandria Journal of Food Science and Technology*, 8(1), 1-8. doi:10.12816/ajfs.2011.20182
43. Sheridan, P. S., & Shilton, N. C. (2002). Analysis of yield while cooking beefburger patties using far infra-red radiation. *Journal of Food Engineering*, 51(1), 3-11. doi:https://doi.org/10.1016/S0260-8774(01)00029-2
44. Tsuladze, E. A. (1972). The relationship between the tenderness of fish meat and its protein water and protein water fat coefficient. *Fish Industry*, 48(7), 68-69.
45. Yousefi, N., Zeynali, F., & Alizadeh, M. (2018). Optimization of low-fat meat hamburger formulation containing quince seed gum using response surface methodology. *Journal of Food Science and Technology*, 55(2), 598-604. doi:10.1007/s13197-017-2969-x
46. Ziada, N. (2002). *Studies on natural antioxidants effectiveness in oils*. Ph. D. Thesis, Faculty of Agriculture, Saba Bacha, Alexandria University,



Received for publication: January.10, 2022
Accepted: May, 02,2022

Original paper

Study of use sewage sludge compost as fertilizer on the sandy soil in a plum orchard

**IRINA TITIRICĂ¹, MILICA DIMA^{1*}, GEORGETA TEMOCICO²,
CLAUDIA NICOLA³**

¹Dăbuleni Research-Development Station for Plant Cultivation on Sandy Soil, Romania

²University of Agronomic Sciences and Veterinary Medicine of Bucharest, Romania

³Research Institute for Fruit Growing Pitesti-Maracineni, Romania

Abstract

To the Research and Development Station for Plants Culture on Sands, Dăbuleni, in the period 2020-2021, in a plum orchard, different doses of compost were applied obtained from sludge resulting from the processing of domestic wastewater. Soil analyzes, in the second year after the application of compost, showed an improvement in the content of nitrogen, phosphorus and potassium, with higher values at doses of 60-80t / ha compost. Organic carbon showed values between 0.13% in the control version and 0.69% in the fertilized variant with 80t / ha compost. Regarding the soil reaction, a slight reduction of pH was observed with increasing amount of compost. The results obtained regarding the heavy metals in the soil showed increases in all the analyzed elements, with the increase of the amount of compost, but the values obtained do not exceed the maximum allowed limits in EU countries. The highest values were determined to dose of 60t / ha of compost, at which the manganese content increased from 180 mg to 414 mg, copper from 10.1 mg to 43.9 mg, and zinc from 15.6 mg to 39.3 mg. These results lead to the premise of the careful use of composts obtained from sludge resulting from the processing of domestic wastewater as fertilizer in the orchards.

Keywords

urban sludge, sandy soils, heavy metals

To cite this article: TITIRICĂ I, DIMA M, TEMOCICO G, NICOLA C. Study of use sewage sludge compost as fertilizer on the sandy soil in a plum orchard. *Rom Biotechnol Lett.* 2022; 27(2): 3389-3397 DOI: 10.25083/rbl/27.2/3389.3397

Introduction

The use in agriculture of the sludge resulting from the processing of domestic wastewater is one of the methods of their release and a form of enhancement of their content in organic matter and nutrients. Many studies have been published on the beneficial effects of changes in sewage sludge on crop production and the physical and chemical properties of the soil. The addition of sludge to the soil is known to improve the physical properties of the soil, increasing water content, increasing water retention, increased aggregation, soil increased aeration, higher permeability, increasing water infiltration and decreasing surface crust (HUSSEIN [12]). The application of sewage sludge by mixing it with the 30 cm soil layer has proven to be effective in improving the physical, chemical and fertility properties of the soil. Also, the use of residual sludge as organic manure is considered as a necessary source of nutrients for plants (HUSSEIN [12]).

Some studies reported that the application of sewage sludge decreased soil pH and increased the quantity of total soluble salts, organic carbon and soil cation exchange capacity (ANTOLIN & al., [2]). They also found that the application of sewage sludge increased the content of heavy metals extractable from the soil (Cd, Cu, Mn, Pd and Zn) and increased the N-NH₄⁺ content from the soil.

MENDOZA & al., [18] reported that organic and extractable matter increased with the addition of sludge to the soil, while soil pH decreased.

Globally, researches on the application of sludge composts to fruit trees is much more numerous, and the results obtained argue for their use in agriculture. The application of sludge (biosolids) over several years in apricot (*Prunus armeniaca* L.) plantations, on sandy soils, did not lead to a reduction in fruit production, although fruit ripening was generally delayed, but the percentage of ripened fruit at the same time was higher at higher biosolids doses. Although the C and N content of the soil has increased with the long-term application of biosolids, it is recommended prudence on its negative effect on fruit production (GARY & al., [11]). Researches conducted by ANGIN (& al., [1]) in a cherry plantation showed that the application of sewage sludge not only improved the chemical properties of the soil, but also led to an increase in nutrient content of cherry leaves. The application of sewage sludge has increased the content of heavy metals in the soil. However, the critical values were not exceeded and was not reflected in the heavy metal content of the leaves. The most effective application rate was 7.5 kg per tree. Studies should be continued to evaluate the effects of residual sludge on trees throughout the growing season,

as well as on the parameters of vegetative growth, yield and fruit quality.

MEHMET (& al., [17]), after a study on the apple species, showed that the application of sewage sludge in installments of 0, 10, 20, 40 and 60 kg / tree for four years, led to an increase in the production of fruits, annual growth, and leaves content in N, Mg, Fe, Mn, Zn and Cu at the end of the study. The results indicated that the repeated application of sludge in apple plantations did not cause toxicity to leaves and fruits. However, long-term application of sludge can lead to the accumulation of Zn, Cu and Ni in the soil and plant.

The high content of organic matter and the amount of residual sludge nutrients are a guarantee of agronomic benefits. At the same time, the use of sludge from wastewater makes possible reusing the organic waste and has many advantages. There is insufficient organic matter in agricultural soil, a serious problem in areas with a Mediterranean climate where high summer temperatures promote high annual mineralization of organic matter (ANTOLIN & al., [2]). Turkey's agricultural lands, especially the eastern ones, the soils of the Anatolian region are generally low content in organic matter. Therefore, these soils favor the application of sewage sludge as an organic amendment and the provision of nutrients for these soils with a relatively low risk of pollution (BOZKURT & al., [5]). An increase in soil organic matter and other nutrients after the application of sewage sludge has been observed by other researchers (BROFAS G., & al., [6], GARCIA-GILL[9]).

The use of sewage sludge improves soil structure by increasing the stability of aggregates, which leads to improve water retention capacity, aeration and reduction erosion (SORT & al., [25]), BARGEZAR., & al., [4]). Similarly, many researches have shown the beneficial effects of applying sewage sludge on production to different crops (VIATOR & al., [28], BARBOSA & al., [3]), Korboulewsky [15], MATA- GONZALES[16]).

PINAMONTI & al., [22] tested the compost of sludge in different apple orchards. The resulted data showed that the sludge can be used for soil fertilization without any short/ medium term danger to the environment or crops. NEILSEN & al., [20], they initiated an experiment to evaluate the effects of municipal biosolid on an 8-year-old plantation. The application of biosolid often increased in the leaves the concentration of Zn, Cu and Mn, but the increases were modest.

At the national level, researches have been carried out in fruit growing on the use of compost from sludge. For fruit trees are relevant the researches undertaken by SUMEDREA & al., [27], and NICOLA & al., [21], on the apple species, which showed that the application of the

same amounts of manure and sludge per volume of planting substrate at 0-30 cm compared to the depth of 0-60 cm did not show a significant difference in tree growth. At the same application rates, manure induced a more intense and earlier growth of annual shoots and cross-section of tree trunks compared to urban sludge. Also, in the apple orchard, IANCU & al., [13], showed that the use of sludge as a fertilizer in agriculture prevents environmental pollution, which is mainly caused by some infestations of pathogens or the high content of chemicals above the maximum limits admitted by law. SMITH, & al., [24] shows that the long-term accumulation of heavy metals in the soil is an important concern, as they can have important consequences on the quality of the human food chain, plant toxicity and soil microbial processes and, once applied, have long-lasting effects in the ground.

In the present study was evaluated the sandy soil chemical compounds after use of urban sludge as fertilizer in a plum orchard.

Materials and Methods

Study area

The study was conducted in a plum experimental plot of the Research and Development Station for Plants Culture on Sands, Dăbuleni. The orchard was established in 2014 year, with Stanley cultivar. The experimental plot was located at 43 80 60 N and 24 05 97 East on a sandy soil poor in nitrogen (0.02-0.06%), medium to well supplied with phosphorus 24-107 ppm and low supplied with exchangeable potassium (15-38ppm). The organic carbon content was low (0.07-0.49%), characteristic of sandy soils, and the soil reaction was moderately acidic to neutral ($\text{pH}_{\text{H}_2\text{O}} = 6.36-7.10$). To evaluate the effect of urban sludge compost as fertilizer, in 2020 year in the first decade of April, a single factor experiment was designed (five experimental variants with four replicates) the experimental factors with the following graduations: V1=0 tons/hectar; V2=20 tons/hectar; V3=40 tons/hectar; V4 = 60 tons/hectar; V5=80 tons/hectar (t/ha) of urban sludge compost obtained at the Mioveni wastewater treatment plant applied as fertilizer, the doses was mixing to the 30 cm soil depth. The compost was applied in compliance with the Environmental Acquis [*** 29, 30, 31]).

Soil sampling and laboratory analysis

In the study period 2020-2021, for evaluated the soil chemical characteristics the following determinations were made: total nitrogen by Kjeldahl method (KJELDAHL [14]); the extractable phosphorus (P-AL) by

Egner - Riem Domingo method, by which phosphates are extracted from the soil sample with a solution of acetate - ammonium lactate at pH - 5.75, and the extracted phosphate anion is determined calorimetrically as - molybdenum blue; the changeable potassium (K-AL) by Egner-Riem Domingo method which the hydrogen and ammonium ions of the extraction solution replace by exchange the potassium ions in exchangeable form from the soil sample which are thus passed into the solution (EGNER & al.[8]). The potassium dosing in the solution thus obtained is done by flame emission photometry; the organic carbon by the method of wet oxidation and titrimetric dosing (gogoasa modification); the soil pH by the potentiometric method; the determination of the content of heavy metals in the soil, before the application of the compost and after the application was performed at National Research and Development Institute for Soil Science, Agrochemistry and Environment Bucharest. The geoaccumulation index of heavy metal in soil (I_{geo}) was calculated after formula: $I_{\text{geo}} = \log_2 (C_n / 1.5 \times B_n)$ (MULER [19]) where C_n is the measured concentration of the element in sewage sludge (mg/kg) and B_n is the geochemical background value in soil. The constant value 1.5 is introduced for better analysis of the natural variability of the content of the chosen substance in the environment.

Vegetable material sampling and laboratory analysis

After the administration of the compost, during the period of intense growth of the shoots, leaves samples were collected to determine the nitrogen, phosphorus and potassium content of the plants. The chemical content in the leaves during the period of intense growth of shoots was evaluated by the following methods: the total nitrogen by the Kjeldahl method; the total phosphorus by the colorimetric method; the total potassium by method of dosing by flame emission photometry.

Statistical analyses

The obtained results were statistically analyzed using the analysis of variance (ANOVA). Means were compared using Duncan's multiple range test at 0.05 probability levels.

Results and discussion

The chemical composition of the soil before the application of the sewage sludge compost

The results obtained regarding the chemical composition of the soil before the application of the sewage sludge compost used as fertilizer, show that soil is poorly provisioned in total nitrogen (0.03%), also the average soil content in

Table 1. Chemical composition of the soil in the plum, before applying the compost

Dose of compost applied (t/ha)	Depth (cm)	Total nitrogen content Nt (%)	Extractable phosphorus (ppm)	Exchangeable potassium (ppm)	Organic carbon (%)	pH
V1-0	0-30	0.04	62	38	0.38	6.66
	30-60	0.05	53	26	0.21	6.36
	60-90	0.03	40	20	0.18	6.70
V2-20	0-30	0.06	65	26	0.46	6.56
	30-60	0.01	52	20	0.35	7.00
	60-90	0.02	46	20	0.43	6.87
V3-40	0-30	0.04	46	26	0.41	6.87
	30-60	0.02	24	15	0.07	7.10
	60-90	0.02	34	15	0.21	6.86
V4-60	0-30	0.02	73	32	0.07	6.96
	30-60	0.04	77	26	0.21	7.00
	60-90	0.03	62	20	0.42	6.95
V5-80	0-30	0.04	82	20	0.49	6.87
	30-60	0.03	72	20	0.21	6.80
	60-90	0.02	107	20	0.17	6.76
Average		0.03	87	20	0.29	6.81

Table 2. Analysis of heavy metals and microelements (mg/kg dry soil) from sandy to plum soil

Depth (cm)	Cd	Cu	Co	Mn	Ni	Pb	Zn
0-30	0.066	10.1	4.03	180	7.50	6.12	15.6
30-60	0.043	8.56	3.13	147	7.78	5.47	14.6
Normal limits after Order 756/1997	1-3	20-100	15-30	900	20-75	20-50	100-300

phosphorus (87 ppm), potassium (20 ppm) is normal after RĂUȚA & CHIRIAC [23] the organic carbon content was low (0,29 %) (Table 1). The heavy metals content before sewage sludge compost applied in plum orchard was under the normal limits after Order 756/1997 (Table 2).

The influence of compost application on plum leaves chemicals characteristic

The values of the total nitrogen content from plum leaves, after fertilization in the plantation, divided the 5 fertilization variants into 3 statistical classes. The differences registered

between the fertilization variants are between 5.50-12.3%. The highest values of leaf content in total nitrogen and potassium were recorded in plants of variant V5, respectively 80t compost/ha in 2020 year and in 2021 year the highest value were registered on V4 variant. In our case, the differences between the total nitrogen values in leaf registered in first and in the second year were between 0.42% - 9.1%. Regarding the phosphorus content of the leaves, the highest value was registered for fertilized plants with a dose of 20t/ha (0.33%) in 2020 year and in the second year, 2021 the highest value was registered on V5 variant (0.44%). The

Table 3. The influence of compost application on the nitrogen, phosphorus and potassium content of the plum leaves in 2020-2021 year

Dose of compost applied (t/ha)	Total nitrogen (%)		Total phosphorus (%)		Total potassium (%)	
	2020	2021	2020	2021	2020	2021
V1-0	2.06 c*	1.96 e	0.26 b	0.24 d	2.05 d	1.38 e
V2-20	2.05 c	2.23 d	0.33 a	0.29 c	2.19 cd	1.87 d
V3-40	2.18 b	2.40 b	0.25 b	0.37 b	2.28 c	1.99 c
V4-60	2.23 b	2.80 a	0.29 ab	0.39 b	2.71 b	2.79 b
V5-80	2.35 a	2.36 c	0.29 ab	0.44 a	2.92 a	2.96 a

*Different letters indicate significant differences for the probability $P \leq 0.05$ according to Duncan's multiple range test.

Table 4. The chemical composition of sandy soil profile, in plum orchard after compost application, 2021 year

Dose of compost applied (t/ha)	Depth (cm)	Total nitrogen (%)	Extractable phosphorus (ppm)	Exchangeable potassium (ppm)	Organic carbon (%)	pH
V1-0	0-30	0.04 c	53gh	32 i	0.35 i	6.70 ab
	30-60	0.03 c	51 h	38 h	0.49 g	6.60 b
	60-90	0.03 c	47 i	36 h	0.13 k	6.62 b
V2-20	0-30	0.04 c	66 e	32 i	0.63 c	6.29 c
	30-60	0.04 c	59 f	42 g	0.35 i	6.95 a
	60-90	0.03 c	52 h	30 i	0.24 j	6.70 ab
V3-40	0-30	0.05 bc	66 e	32 i	0.58 d	6.54 bc
	30-60	0.05 bc	76 cd	45 f	0.66 b	6.64 b
	60-90	0.03 c	64 e	50 e	0.55 e	6.48 bc
V4-60	0-30	0.07 bc	78 c	38 h	0.70 a	6.51 bc
	30-60	0.06 bc	86 b	57 d	0.60 d	6.66 b
	60-90	0.04 bc	56 fg	63 c	0.45 h	6.57 b
V5-80	0-30	0.10 a	74 d	57 d	0.69 a	6.48 bc
	30-60	0.07 bc	96 a	77 b	0.57 de	6.77 ab
	60-90	0.06 bc	73 d	84 a	0.52 f	6.65 b

*Different letters indicate significant differences for the probability $P \leq 0.05$ according to Duncan's multiple range test.

differences assured statistically, in the case of the phosphorus content in the leaves, vary between 12.1-21.2%, and between 17.2%-44.5% in 2021 (table 3). The values recorded to the potassium leaves content showed the highest value in the study period on the V5 variant (2.92 % in 2020 year, and 2.96 in 2021 year) (table 3).

The influence of compost application on the chemical characteristics of sandy soil profile, in plum orchard.

The total nitrogen content of the soil after sewage sludge compost applied as fertilizer in the plum orchard, presented in table 4, was between 0.03% for the control variant (V1) and 0.10% for the V5 (80t/ha). That show, an increase of total nitrogen with differences between the studied variants till 30%. The differences between the analyzed variants are statistically assured, the same situation is with the content of extractable phosphorus and exchangeable potassium were the differences between V1 variant and the other studied variants rise progressively with the sewage sludge compost dose till 47%.

The organic carbon showed values between 0.13% in the depth of 60-90 cm for the control variant (V1) and 0.69% in the depth of 0-30 cm for the variant fertilized with 80 t/ha compost (V5). As for the soil reaction, a slight decrease in pH can be observed with increasing amount of compost (table 4).

Between the amount of nitrogen in the compost and the content of total nitrogen, extractable phosphorus and exchangeable potassium in the soil, polynomial correlations were established, given by second degree equations, with

significant correlation factors. Nitrogen and potassium (average content per profile 0-90cm) accumulate in the soil with increasing amount of compost, and phosphorus increases with increasing of nitrogen content in compost to the nitrogen values in compost of 1000 kg/ha (Figure 2 1).

In the second year after sewage sludge compost applied used as fertilizer in plum orchard, the heavy metals soil content show for five from seven elements analyzed the highest content in the v4 variant, on the deep 0-30 cm, with differences between 30.4 and 2.2% (table 5). Also, the highest value in soil cobalt content was recorded on V4 variant to the depth 60-90 cm. In case of soil nickel content the highest values (20.7 mg/kg) was recorded on variant V5, on 30-90cm depth. For all the heavy metals analyzed, the differences between the fertilizer variants applied, were ensured from a statistical point of view (Table 5).

The geoaccumulation index according to MULDER [19] cited by DÍAZ-DE-ALBA & al.[7], is associated with a qualitative scale of pollution status: $I_{geo} < 0$ indicates practically unpolluted status; $I_{geo} = 0-1$ denotes unpolluted to moderately polluted status; $I_{geo} = 1-2$ is moderately polluted status; $I_{geo} = 2-3$ represents moderately to strongly polluted status; $I_{geo} = 3-4$ is strongly polluted status; $I_{geo} = 4-5$ is strongly to extremely strong polluted status; and $I_{geo} > 5$ is extremely polluted status. In our study, after I_{geo} was calculated for all seven metals studied, for Cd heavy metal, the sandy soil was high polluted on V4 and moderate polluted on others studied variants. For the other heavy metals analyzed after I_{geo} calculated the soil was characterized as no polluted (table 6).

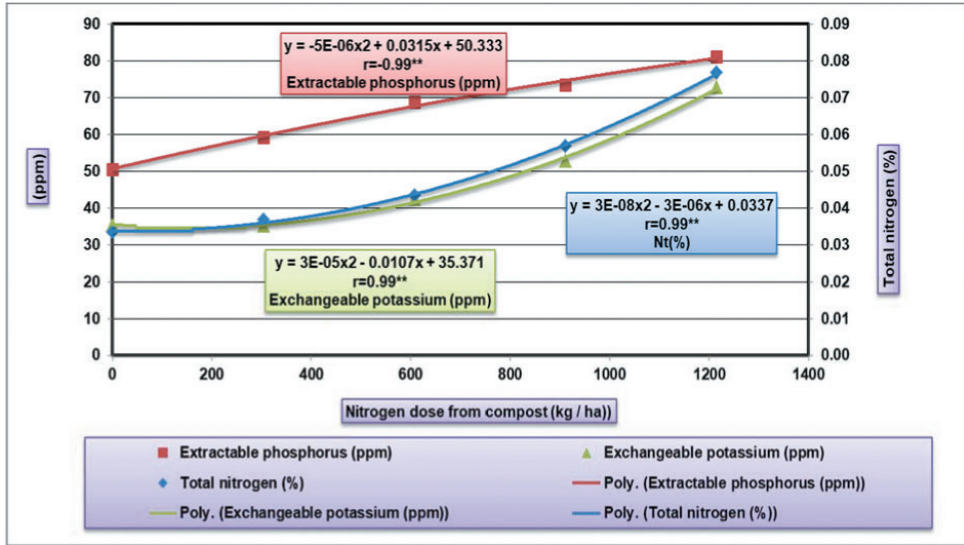


Figure 1. Correlation between the amount of nitrogen in the compost and the content of total nitrogen, extractable phosphorus and exchangeable potassium in the soil for the plum species, 2021

The results obtained by NICOLA & PARASCHIV [19], in an apple orchard, show that in the first year after sludge compost applied the soil contamination with Cd, Pb, Zn appeared to a dose of 60t/ha, versus to the second year after compost applied, when the pollution moderately was identify to a dose of 40 t/ha compost. So, they show that heavy

metals are trapped in soluble compounds and are made available with changing environmental conditions.

In whatever way, after the studies made by ANTOLIN & al.[2], IANCU & al. [13], Bozkurt & al.[15], ANGIN & al. [1] long-term application of sludge compost can lead to the accumulation of Zn, Cu and Ni in the soil and in plant, also.

Table 5. The sandy soil heavy metals content (mg/kg dry soil) in the second year after the application of the urban sludge as fertilizer

Dose of compost applied (t/ha)	Depth (cm)	Cd (mg/kg)	Cu (mg/kg)	Co (mg/kg)	Mn (mg/kg)	Ni (mg/kg)	Pb (mg/kg)	Zn (mg/kg)
V1-0	0-30	0.066 e	10.01i	4.03 b	180 l	7.50 i	6.12 b	15.6 j
	30-60	0.043 g	8.56 k	3.13 c	147 n	7.78 i	5.47 d	14.6 k
	60-90	0.035 h	5.36 e	2.15 d	120 o	7.80 i	4.32e	13.82 l
V2-20	0-30	0.064 e	39.8 b	n.d**	316 f	6.67 j	4.41e	23.2 f
	30-60	n.d**	23.8 e	n.d**	250 k	9.40 g	3.11g	18.6 h
	60-90	0.081 d	8.9 jk	3.01 c	306 h	11.6 f	4.97d	31.8 b
V3-40	0-30	n.d**	24.0 e	1.63 c	323 e	7.83 i	5.71c	24.9 e
	30-60	n.d**	21.3 f	1.55 e	274 j	8.95 h	4.43e	20.7 g
	60-90	n.d**	13.9 h	3.02 c	175 m	12.9 e	4.01 f	13.6 e
V4-60	0-30	0.201a	43.9 a	1.51 e	414 a	17.6 b	6.63a	39.3 a
	30-60	0.118 b	25.8 d	3.07 c	352 b	17.7 b	6.42ab	30.1 c
	60-90	n.d**	9.7 ij	4.21 a	297 i	17.1 c	3.27g	16.9 i
V5-80	0-30	0.091 c	33.5 e	n.d**	346 c	15.7 d	4.59 e	26.4 d
	30-60	0.088 c	19.3 g	1.48 e	311 g	20.7 a	4.24ef	26.3 d
	60-90	0.056 f	14.5 h	2.23 d	332 a	20.7 a	3.35g	26.8 d

*Different letters indicate significant differences for the probability $P \leq 0.05$ according to Duncan's multiple range test; n.d** - not detected

Table 6. The degree of sandy soil heavy metals pollution in the second year after the application of the urban sludge compost as fertilizer

Dose of compost applied (t/ha)	The analyzed metal	Heavy metal content of fertilized soil (mg/kg)	Heavy metal content of compost (mg/kg of d.m)	The Igeo index	Degree of heavy metal pollution in the soil
V1=0	Cd	0.066			
	Cu	10.1			
	Co	4.03			
	Mn	180			
	Ni	7.50			
	Pb	6.12			
	Zn	15.6			
V2=20	Cd	0.064	1.04	1.0	moderate pollution
	Cu	39.8	72.36	0.0	pollution no
	Co	0.021	38.75	0.0	pollution no
	Mn	316	446.14	0.0	pollution no
	Ni	6.67	29.53	0.2	pollution no
	Pb	4.41	32.21	0.3	pollution no
	Zn	23.2	557.0	0.1	pollution no
V3=40	Cd	0.091		2.0	moderate pollution
	Cu	24.0		0.1	pollution no
	Co	1.63		0.8	pollution no
	Mn	323		0.0	pollution no
	Ni	7.83		0.2	pollution no
	Pb	5.71		0.2	pollution no
	Zn	24.9		0.1	pollution no
V4=60	Cd	0.201		3.2	high pollution
	Cu	43.9		0.0	pollution no
	Co	1.51		0.8	pollution no
	Mn	414		0.0	pollution no
	Ni	17.6		0.1	pollution no
	Pb	6.63		0.2	pollution no
	Zn	39.3		0.1	pollution no
V5=80	Cd	0.091		2.3	moderate pollution
	Cu	33.5		0.0	pollution no
	Co	0.001		0.0	pollution no
	Mn	346		1.2	moderate pollution
	Ni	15.7		0.1	pollution no
	Pb	4.59		0.3	pollution no
	Zn	26.4		0.1	pollution no

Conclusion

Soil analyzes in the second year after the application of compost to the plum orchard showed an improvement in the content of nitrogen, phosphorus and potassium, with higher values at doses of 60-80 t/ha compost. The organic carbon showed values between 0.13% in the depth of 60-90 cm for the control variant and 0.69% in the depth of 0-30 cm for the variant fertilized with 80 t/ha compost, results that indicate a reduced to middle states. Regarding the soil reaction, a slight reduction of pH was observed with increasing amount of compost.

The results obtained regarding the heavy metals in the soil in the second year after the application of the com-

post, showed increases to all the analyzed microelements, with the increase of the amount of compost, but the values obtained do not exceed the maximum allowed limits. The highest values were determined at a dose of 60t/ha of compost, for which the manganese content increased from 180 mg to 414 mg, copper from 10.1 mg to 43.9 mg, and zinc from 15.6 mg to 39.3 mg. The values obtained for the analyzed microelements, in the conditions of sandy soils, in the second year from the compost administration lead to the premise of the careful use of composts obtained from sludges resulting from domestic wastewater treatment in orchards. Regarding the analysis of the macroelements in the leaves, the results obtained show that the increase in

the amount of compost led to the increase of the content of the three macroelements, both in the first year and in the second year, and the highest values were recorded in fertilized variants with 60 and 80 t/ha.

Acknowledgements

The research from this paper was supported from the project ADER 7.3.10. *Research on the use of compost obtained from sludge resulting from the treatment of domestic wastewater as fertilizer in fruit growing in compliance with the Environmental Acquis*, funded by the Ministry of Agriculture and Rural Development.

References

1. ANGIN, R. ASLANTAS, M. KOSE, H. KARAKURT, G. OZKAN. Changes in chemical properties of soil and sour cherry as a result of sewage sludge application I. Hort. Sci. Vol. 39, No. 2: 61–66 (2012).
2. ANTOLIN M.C., PASCUAL I., GARCIA C., POLO A., SANHEZ-DIAZ M. Growth yield and solute content of barley in soils treated with sewage sludge under semiarid Mediterranean conditions. *Field Crops Res.* 94, 224 (2005).
3. BARBOSA G.M., FILHO T. Agriculture utilization of sewage sludge: effect on the chemical and physical properties of soils and on the productivity and recovery of degraded areas. *Ciencias Agrarias (Londrina)* 27, 565 (2006).
4. BARGEZARA.R., YOUSEFIA., DARYASHENAS A. The effect of addition of different amounts and types of organic materials on soil physical properties and yield of wheat. *Plant And Soil* 247, 295 (2002).
5. BOZKURT M.A., CIMRIN K.M. The effects of sewage sludge applications on nutrient and heavy metal concentration in a calcareous soil. *Fresen Environ Bull.* 12, 1354 (2003).
6. BROFAS G., MICHPOULAS P., ALIFRAGIS D., Sewage sludge as an amendment for calcareous bauxite mine spoils reclamation. *J. Environ. Qual.* 29,811 (2000).
7. DÍAZ-DE-ALBA M., GRANADO-CASTRO M.D., GALINDO-RIÑOM.D., CASANUEVA-MARENCO M.J. Comprehensive assessment and potential ecological risk of trace element pollution (as, ni, co and cr) in aquatic environmental samples from an industrialized area. *Int. J. Environ. Res. Public Health* , 18, 7348. <https://doi.org/10.3390/ijerph18147348> (2021)
8. EGNER, H., RIEHM, H., DOMINGO, W.R. Untersuchungen über die chemische bodenanalyse als Grundlage für die beurteilung des nährstoffzustandes der böden. ii. chemische extraktionsmethoden zur phosphorund kaliumbestimmung. *Annals Royal Agricultural College, Sweden*, 26: 199-215 (1960).
9. GARCIA-GILL J.C., PLAZA C., SENESI N., BRUNETTI G., POLO A. Effects of sewage sludge amendment of humic acids and microbiological properties of semiarid mediterranean soil. *Biol. Fertil. Soils* 39, 320 (2004)
10. GARCIA-GILL J.C., PLAZA C., SENESI N., BRUNETTI G., POLO A. Effects of sewage sludge amendment of humic acids and microbiological properties of semiarid mediterranean soil. *Biol. Fertil. Soils* 39, 320 (2004).
11. GARY S. BANUELOS, SAJEEMAS PASAKDEE, SHARON E. BENES, CRAIG A. Long-term application of biosolids on apricot production, *Communications in Soil Science and Plant Analysis*, 38: 1533-1549 (2007).
12. HUSSEIN A.H.A. Impact of sewage sludge as organic manure on some soil properties, growth, yield and nutrient contents of cucumber crop. *Journal of Applied Sciences*, 9: 1401-1411 (2009).
13. IANCU M., SUMEDREA D., DUMITRU M., EUGENIA GAMENT, PREDESCU C., MIHAELA ULMEANU, MIRELA SOCACIU, TOGOE I., TUDOR L. Influence of the urban sludge used as fertilizer on the chemical components of soil and leaves of Idared apple, *Fruit growing research*, vol. XXIV, p. 187-195 (2008).
14. KJELDAHL J. New method for the determination of nitrogen. *Chemistry News.*, 48(1240):101-102 (1983).
15. KORBOULEWSKY N., BONIN G., MASSIANI C. Biological and ecophysiological reactions of white wall rocket grown on sewage sludge compost. *Environ Poll.* 117, 36 (2002).
16. MATA-GONZÁLEZ, R. SOSEBEE RE. WAN C. Nitrogen in desert grasses as affected by biosolids. their time of application and soil water content. *Arid Land Research and Management*; 18(4):385–395 (2004).
17. MEHMET A. B., TARIK Y., AYŞE Y. The use of sewage sludge as an organic matter source in apple trees, *Pol. J. Environ. Stud.*, 19(2):267–274 (2010).
18. MENDOZA, J., G. TATIANA, C. GABRIELA AND S.M. NILSA. Metal availability and uptake by sorghum plants grown in soils amended with sludge from different treatments. *Chemosphere*, 65: 2304-2312 (2006).
19. MULLER G. Index of geoaccumulation in sediments of the Rhine River. *GeoJournal*, 4, 108-118(1969).
20. NEILSEN G.H., HOGUE E.J., FORGE T., NEILSEN D., KUCHTA S. Nutritional implications of biosolids

- and paper mulch applications in high density apple orchards. *Can J Plant Sci.* 87, 551 (2007).
21. NICOLA C., PARASCHIV M. Use of urban sludge compost as fertilizer on apple orchards. *Fruit growing research, vol. XXXVII, p: 103-114. doi10.33045/fg: v37.2021.15* (2021).
 22. PINAMONTI F., STRINGARI G., GASPERI F., ZORZI G. The use of compost: its effects on heavy metal levels in soil and plants. *Resour Conserv Recy.* 21, 129 (1997).
 23. RAUȚA, C., CHIRIAC A. Metodologia de analiză a plantei pentru evaluarea stării de nutriție minerale. *Ed. Academiei Române de Științe Agricole și Silviculte* (1980).
 24. SMITH S. R. A critical review of the bioavailability and impacts of heavy metals in municipal solid waste composts compared to sewage sludge, *Environment International* 35, 142–156 (2009).
 25. SORT X., ALCANIZ J.M. Effects of sewage sludge amendment on soil aggregation. *Land Degrad. Develop.* 10, 3 (1999).
 26. STILES W.C. Nitrogen management in orchard. Cap. IV in “Tree Fruit Nutrition”. Shortcourse proceedings. *Ed. by Peterson A.B. and Stebens R.G.. Yakima. Washington* (1994).
 27. SUMEDREA D. IANCU M. CHITU E. Influence of urban sludge used as fertilizer on Idared apple behavior, *Fruit growing research, vol XXIV, p. 178-186* (2008).
 28. VIATOR R.P., KOVAR J.L., HALLMARK W.B, Gypsum and compost effects on sugarcane root growth, yield and plant nutrients. *Agron J.* 94, 1332 (2002).
 29. ***1999. Council Directive 1999/31/EC of 26 April 1999 on the landfill of waste.
 30. ***2006 Commission Regulation (EC) No.1881/2006 of 19 December 2006 setting maximum levels for certain contaminants in foodstuff (Text with EEA relevance).
 31. *** 2008 Commission Regulation (EC) No.834/2007 on organic production and labeling of organic products with regard to organic production, labeling and control.



Received for publication: January.10, 2022
Accepted: April, 11,2022

Original paper

Performance of fungus-tolerant grapevine cultivars in different production systems

Fungus-tolerant grapevine cultivars

DRAGOSLAV IVANIŠEVIĆ¹, MLADEN I. KALAJDŽIĆ^{1*}, PREDRAG BOŽOVIĆ¹, NEMANJA BRZAKOVIĆ

¹Department of Fruit growing, Viticulture, Horticulture and Landscape architecture, Faculty of Agriculture, Trg Dositeja Obradovića 8, Novi Sad 21000, Serbia

Abstract

Several fungus-tolerant grapevine cultivars have been created and have already found their place in vineyards in Serbia and Hungary. The aim of this work was to investigate the differences in yield, grape quality and wine sensory properties obtained in two different production systems of pathogen-tolerant white grapevine cultivars Backa and Panonia over the 2015-2018 period. The paper showed differences in harvest parameters between the Conventional and NoPes&MinFert (without use of pesticides and mineral fertilizers) production systems. Fruitfulness and bud tolerance to low temperatures in these production systems were also examined. The results suggest that grape quality obtained by NoPes&MinFert was at the same level as that achieved by conventional methods, while the yield loss in NoPes&MinFert was on average <20% compared to the conventional system. Although the number of inflorescences per node and yield were higher in conventional production, NoPes&MinFert production showed satisfied yield that exceeded 10 t/ha. Wine sensory analyses showed that production NoPes&MinFert achieved better wine score compared to the wines derived from the Conventional production.

Keywords

fungus tolerant cultivars; yield; grape quality

To cite this article: IVANIŠEVIĆ D, KALAJDŽIĆ MI, BOŽOVIĆ P, BRZAKOVIĆ N. Performance of fungus-tolerant grapevine cultivars in different production systems. Fungus-tolerant grapevine cultivars. *Rom Biotechnol Lett.* 2022; 27(2): 3398-3406 DOI: 10.25083/rbl/27.2/3398.3406

✉ *Corresponding author: MLADEN KALAJDŽIĆ, e-mail: mladen.kalajdzic@polj.uns.ac.rs

Introduction

Application of the synthetic fungicides is a common practice in the conventional grape production. According to PETERLUNGER & al [1] viticulture in Europe accounts 3% of the total agricultural land and applies 65% of all fungicides used in whole agriculture. Due to increasing concern for the human health and the protection of the environment, nature friendly production systems should be applied instead of conventional.

In last few decades, organic viticulture has been intensively promoted (BARTOLUCCI [2]; MEISSNER & al. [3]) but it seems without success (MASSON & al. [4]). Most producers are reluctant to grow grapes organically due to the need to comply with integrated pest management schemes (GEIER [5]). Also, limiting factors in organic production is yield reduction by 8 to 16% (GUESMI & al., [6]).

On the other hand, organic viticulture enhances microbial diversity (HENDGEN & al. [7]) and floral diversity (NASCIMBENE & al [8]). Moreover, organic vineyards have been shown to host consistently richer communities of both vascular plants and butterflies compared to their conventional counterparts (PUIGMONTERRAT & al. [9]). In organic production the grape quality is enhanced and without fungicides residues, compared to conventional (CRINION [10]). Also, organic products have better nutritional and sensory characteristics (GRANATO & al. [11]), and higher antioxidant activity (TASSONI & al. [12]).

However, organic viticulture approaches are very strict and in many cases difficult to apply.

Cultivars such as Merlot and Chardonnay are very sensitive to pathogens and therefore alternative cultivars should be cultivated.

The main goal of grapevine breeding stations around the world is creation of cultivars that are resistant to fungal diseases while yielding adequate grape quality (PETERLUNGER & al. [1], TÖPFER & al. [13]). Resistant grapevine cultivars can be grown without use of pesticides or, in some years, require only a small portion of the fungicide applications that are necessary for cultivating traditional cultivars. Grapevine breeding in Serbia has been conducted since the middle of the 20th century, aiming to develop grape cultivars with improved grape quality, higher yield and enhanced tolerance to stress factors. As a result, several new grapevine cultivars suitable for organic production have been created. Some fungus tolerant cultivars such as Backa and Panonia have already found their place in vineyards in Serbia, Hungary, and some other countries.

The aim of the present study was to investigate the effects of Conventional and NoPes&MinFert production sys-

tems on productive characteristics of grape cultivars Backa and Panonia in the 2015-2018 period.

Material and methods

The experiment was performed, at the Experimental field of University of Novi Sad, Faculty of Agriculture situated in Sremski Karlovci (45°10' N, 20°10' E), 150 m, above sea level during four consecutive seasons (2015-2018), on the two Serbian wine grape cultivars: Backa (VIVC number 21272) and Panonia, (VIVC number 23765) which are less susceptible to fungal diseases. Backa (Petra x Bianca), released in 2004, is highly vigorous cultivar with mid-compact bunches. Wines made of Backa are light bodied wines, Panonia (one Hungarian tolerant genotype -(Kunbarat x Traminer) x Bianca) x Riesling), also released in 2004, is less vigorous compared to Backa with loose bunches. Moreover, Panonia has ideal shoot positioning in the canopy with small laterals. Panonia has full body wines similar to Riesling.

The vines were pruned to a modified Guyot (one arched cane of 12 buds and one spur of 2 buds), with an average of 14 buds per vine. Vines were planted in 2000 with 2.8 m space between rows and 1.6 m separation between pair of vines in a row. Rows had an East-West orientation.

Two production systems were performed:

NoPes&MinFert—without use of pesticides and mineral fertilizers; Grass mixture was established as cover crop in between the rows. Every second row was ploughed. Weeds in between the vines were controlled mechanically.

Conventional- pesticides and mineral fertilizers were applied as is usual in modern viticultural practice. Grass mixture was established as cover crop in between the rows. Every second row was ploughed. Weeds in between the vines were controlled by Glyphosav, herbicide produced by the company Chemical Agrosava (Belgrade, Serbia). The average amount of 50 kg N, 50 kg P and 70 kg K per hectare was applied each autumn.

The experiment was designed as a randomized complete block, in which a total of 24 vines of each cultivar/production system combination (Backa/NoPes&MinFert, Backa/conventional, Panonia/NoPes&MinFert and Panonia/conventional) were grouped into 3 blocks of 8 vines.

The climate conditions at the experimental site, including mean monthly air temperatures (°C) and mean monthly precipitation (mm) for the period 2015-2018 are presented in Figure 1.

Phenological observations

Three key phenological stages of the grapevine were examined. BBCH scale was used to identify the development stage.

BBCH-07- the beginning of budburst i.e. the date when green shoot tips became visible; BBCH-60- the beginning of flowering i.e. the date when first flower hoods were detached from the receptacle; and BBCH-80-the beginning of veraison i.e. the date when berries begun to develop cultivar-specific color (COMBE [14]).

Fruitfulness parameters

In the season 2015 fruitfulness of the nodes and shoots on 10 vines per combination cultivar/production were evaluated. Percentage of the nodes that arose in the shoot/s were calculated by dividing number of the bud-burst nodes with total nodes. The number of inflorescences per node and number of inflorescences per shoot were recorded when the shoot's length was approximately 15-20 cm.

Harvest parameters

Yield was determined at harvest by weighing all the grapes. Average cluster weight was obtained by dividing the weight of all clusters in replicate with the number of clusters.

$$\text{Average cluster weight (g)} = \frac{\text{Weight of all clusters (g)}}{\text{Number of clusters}}$$

After crashing, the sugar content in the must was measured with Oechsle hydrometer. Titratable acidity was measured by titration of grape juice sample (10 ml) against 0,1 M NaOH, in the presence of bromothymol blue as an indicator, until changing color of the indicator. The *Botrytis* incidence was determined by visual assessment of the health status of the clusters at harvest time, expressed as percentage of infected clusters.

Tolerance to low winter temperatures

The bud tolerance to low winter temperatures was examined under laboratory conditions. Samples of 10 canes (one-year old wood, with 10 nodes) were collected three times during the winter 2017/2018 (end of December, end of January and middle of February). The canes were stored in cold chamber for 24 h at -5 °C. After that, the temperature was decreased for 3 °C each hour, until the temperature reached -21 °C. After 12 hours the cold chamber was turned off. The canes were left until the temperature in cold chamber reached the room temperature (CINDRIĆ & al. [15]) and after 7 days the bud asession was performed. The buds exposed to low temperatures were classified in three categories: alive, partially alive and frozen.

Microvinification and wine sensory analysis

From each replicate, grapes were destemmed and crushed. The liquid phase was separated and 10 mg L⁻¹ SO₂ was added. Then the liquid phase was left for one day and

then racked before being inoculated with *Saccharomyces cerevisiae* (Uvaferm BDX). Fermentation was conducted in 5 L glass fermenters. After the end of fermentation, the wines were racked in the bottles.

Wine sensory analysis was performed five months after the end of fermentation by five trained academic staff members of the Faculty of Technology and Faculty of Agriculture from the University of Novi Sad. Buxbaum method was used to score the wine samples (0-20 points), assessing appearance (maximum 2 points), color (2), aroma and bouquet (4) and other characteristics, such as sugar, acidity, and astringency (scoring maximum of 12 points in total for these traits related to taste). All samples were presented to each assessor at the same time. The order of sample presentation was completely randomized, and individual samples were identified by assigning each a random number. Bread cubes were provided to cleanse the palate between samples during evaluation.

Statistical analyses

Statistical analyses (multifactorial ANOVA) were performed using R software. Duncan's test was used to test the significance of differences ($p < 0.05$) among the mean values of measured parameters. Graphs were generated using the *ggplot2* package.

Results

Weather conditions varies among the years (Figure 1). In general, summers were hot and dry, particularly in 2015 and 2017. Precipitation amount was the highest in May and June; cumulative precipitation value for these months was the highest in 2016 (268 mm).

Phenological stages, including beginning of budburst, flowering, veraison and harvest date differed among cultivars (Table 1). However, different production systems did not affect the phenology and harvest date, therefore grapes from both NoPes&MinFert and conventional plots were harvested same day.

Conventional production of Panonia had a higher percentage of the nodes that arose in the shoot/s compared to

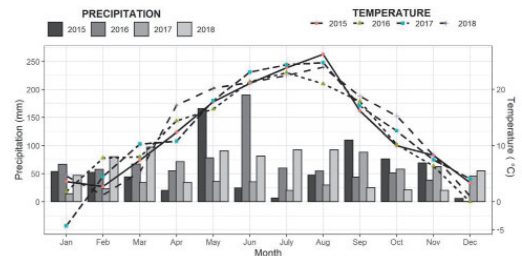


Figure 1. Variations of weather conditions among the years.

Table 1. Dates for the beginning of the main phenological stages and harvest (2015-2018).

Year	GDD* (°C)	Cultivar	Beginning of bud-burst	Beginning of flowering	Beginning of veraison	Harvest date
2015	1925	Backa	8 April	19 May	15 July	31 August
		Panonia	8 April	19 May	15 July	31 August
2016	1740	Backa	2 April	22. May	14 July	05 September
		Panonia	1 April	20. May	03 July	05 September
2017	1880	Backa	27 March	25 May	18 July	23 August
		Panonia	25 March	25 May	18 July	23. August
2018	2074	Backa	3 April	06 May	8 July	20 August
		Panonia	2 April	06 May	7 July	20 August
2015-2018	1904	Backa	4 April	18 May	13 July	29 August
		Panonia	3 April	17 May	9 July	29 August

*GDD- Growing Degree Days is a temperature derived index using average temperatures above a 10 °C base (April - October)

Table 2. Shoot fruitfulness of Backa and Panonia in NoPes&MinFert and conventional production systems in 2015.

Cultivar	Production system	Nodes that arose in the shoot (%)	Number of developed shoots		Number of fruitful shoots		Fruitful shoots (%)	
			Spur	Cane	Spur	Cane	Spur	Cane
Backa	NoPes&MinFert	85.1 ^{ab}	2.0	7.2 ^b	1.7	6.0 ^b	86.7	83.4 ^b
	Conventional	94.9 ^a	1.8	9.0 ^a	1.8	8.6 ^a	100.0	96.2 ^a
Panonia	NoPes&MinFert	75.8 ^b	1.8	6.5 ^b	1.7	5.4 ^b	95.8	86.4 ^b
	Conventional	88.1 ^a	1.7	6.6 ^b	1.6	5.8 ^b	85.8	89.7 ^{ab}

Different letters in superscript indicate significant difference among the mean values (Duncan’s test, p<0.05).

Table 3. Number of inflorescences per node, shoot and fruitful shoot depend on the production system in 2015.

Cultivar	Production system	Number of inflorescences		
		per node	per shoot	per fruitful shoot
Bačka	NoPes&MinFert	1.19 ^c	1.47 ^b	1.74 ^b
	Conventional	1.69 ^a	1.67 ^{ab}	1.73 ^b
Panonia	NoPes&MinFert	1.44 ^b	1.84 ^a	2.11 ^a
	Conventional	1.73 ^a	1.92 ^a	2.16 ^a

Different letters in superscript indicate significant difference among the mean values (Duncan’s test, p<0.05).

NoPes&MinFert counterpart (Table 2). In the conventional production of Backa, the number of developed shoots and number of fruitful shoots were significantly higher compared to all other treatments.

Conventional production system of booth cultivars had significantly higher number of inflorescences per node compared to NoPes&MinFert production (Table 3). NoPes&MinFert production of Backa had significantly lower number of inflorescences per shoot (irrespective to its fruitfulness) compared to booth production systems of Panonia. Panonia had more inflorescences per fruitful shoot compared to Backa, while no difference was observed between production systems.

In booth cultivars the number of inflorescences per node was higher in a vine treated through conventionally methods compared to NoPes&MinFert (Figure 2). In conventional production of Backa number of inflorescences per node showed an increase from the beginning (1) until the node number 7. Then, the slight decrease in number of inflorescences per node was observed. In NoPes&MinFert production system of Backa number of inflorescences per node showed higher variation.

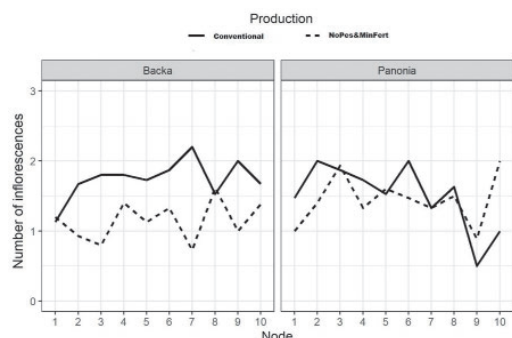


Figure 2. Comparison between number of inflorescences per node in a vine treated through conventionally methods and NoPes&MinFert.

Table 4. Yield and grape quality of Backa and Panonia in NoPes&MinFert and conventional production systems, in 2015-2018 years.

Cultivar	Production systems	Yield (kg m ⁻²)	Cluster weight (g)	Total soluble solids (%)	Titrateable acidity (g l ⁻¹)	<i>Botrytis</i> sp. incidence (%)
2015.						
Backa	NoPes&MinFert	0.86 ^b	269.9 ^a	21.47	6.07	0.0
	Conventional	1.41 ^a	163.3 ^b	20.73	6.53	0.0
Panonia	NoPes&MinFert	0.97 ^b	240.3 ^a	23.97	8.37	0.0
	Conventional	1.43 ^a	220.0 ^{ab}	24.13	7.97	0.0
2016.						
Backa	NoPes&MinFert	1.90 ^{ab}	270.0 ^a	22.4	7.27	0.33
	Conventional	1.66 ^{ab}	266.7 ^a	19.2	7.83	3.00
Panonia	NoPes&MinFert	1.54 ^b	156.7 ^b	24.9	9.43	0.00
	Conventional	2.14 ^a	223.3 ^{ab}	23.2	8.76	2.33
2017.						
Backa	NoPes&MinFert	1.90 ^a	313.3 ^a	21.36	6.13	0.33
	Conventional	1.28 ^{bc}	326.7 ^a	23.86	5.67	0.00
Panonia	NoPes&MinFert	1.54 ^{ab}	186.7 ^b	24.13	7.83	0.00
	Conventional	0.77 ^c	190.0 ^b	27.06	6.90	0.00
2018.						
Backa	NoPes&MinFert	1.18 ^b	253.3 ^b	21.53	5.80	3.33
	Conventional	2.19 ^a	356.7 ^a	21.40	5.63	0.00
Panonia	NoPes&MinFert	1.05 ^b	241.7 ^b	25.63	6.93	0.00
	Conventional	1.13 ^b	195.0 ^b	25.10	7.63	0.00
2015-2018 (average)						
Bačka	NoPes&MinFert	1.46	276.4	21.69	6.32	1.00
	Conventional	1.63	278.3	21.29	6.41	0.75
Panonia	NoPes&MinFert	1.27	206.3	24.67	8.15	0.58
	Conventional	1.37	207.1	24.86	7.81	0.00

Different letters in superscript indicate significant difference among the mean values (Duncan's test, $p < 0.05$). If the interaction (Year x Cultivar x Production) was not observed multiple comparisons was not performed; the effects of other factors are present in Table 5.

Table 5. Statistical significance of the following experimental factors: year, cultivar and production system.

Factor	Yield (kg m ⁻²)	Cluster weight (g)	Sugar (%)	Titrateable acidity (g l ⁻¹)	<i>Botrytis</i> sp. incidence (%)
Year	**	*	**	**	**
Cultivar	**	**	**	**	*
Production system	ns	ns	ns	ns	ns
Year x Cultivar	**	**	ns	ns	ns
Year x Production system	**	*	**	ns	**
Cultivar x Production system	ns	ns	ns	ns	ns
Year x Cultivar x Production system	**	**	ns	ns	ns

*, **, ns indicate significant at $p < 0.05$, 0.01, or non significant, respectively.

In conventional and NoPes&MinFert production systems of Panonia, number of inflorescences showed an increase from the base until second and third node, respectively. Then, in booth production systems of Panonia a slight decrease in number of inflorescences was detected.

In 2015, both Backa and Panonia, had significantly higher yield in the conventional compared to the NoPes&MinFert production (39 and 32 %, higher respectively) (Table 4). In 2016 in the conventional production of Panonia the yield was 28% higher compared to NoPes&MinFert production. In 2018, Backa showed 46% higher yield in the conven-

tional compared to the NoPes&MinFert production, while no difference was observed for Panonia. Moreover, Backa showed higher yield compared to Panonia.

In the seasons 2015 and 2018, Backa had significantly higher cluster weight in the conventional compared to NoPes&MinFert production. The highest cluster weight was recorded in the conventional production of Backa in 2018. On average, Backa had 70 g heavier clusters compared to Panonia.

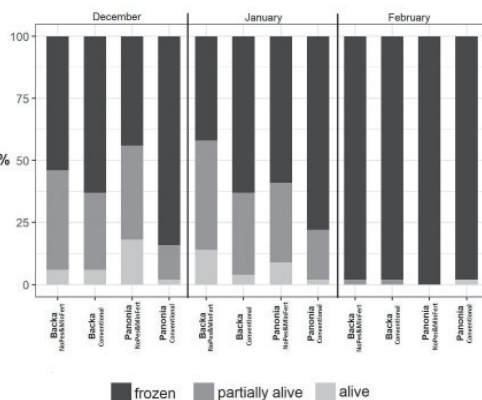
The cultivars showed satisfied tolerance to the incidence of *Botrytis* sp.(Table 4). However, Backa was more sensitive particularly in the organic production during 2017 and 2018, while in 2016 both cultivars were more sensitive in conventional production.

In 2016, higher sugar percentage was recorded in the NoPes&MinFert production. Contrary, in 2017 both Backa and Panonia had higher sugar percentage in the conventional compared to NoPes&MinFert production. Panonia accumulated significantly higher sugar in the grape juice (24.8%) compared to Backa (21.5%).

Titrate acidity varies particularly among the seasons and between cultivars. Thus, the highest titrate acidity (8.32 on average) was observed in 2016, while the lowest

in 2018 (6.5 g l⁻¹). During the experiment Panonia had significantly higher titrate acidity (7.98 g l⁻¹) compared to Backa (6.37).

Both cultivars, Backa and Panonia, had less frozen buds in NoPes&MinFert compared to conventional production (Figure 3.). The highest difference in frozen buds between



Comparison between frozen buds of cultivars Backa and Panonia in NoPes&MinFert and conventional production.

Table 6. Total wine score of Backa and Panonia in NoPes&MinFert and conventional production systems, in 2015-2018 years.

Cultivar	Production systems	Color	Clarity	Aroma	Taste	Total score
2015.						
Backa	NoPes&MinFert	2.0	2.0	3.3	10.6	17.9
	Conventional	2.0	2.0	3.0	10.1	17.1
Panonia	NoPes&MinFert	2.0	2.0	3.2	10.2	17.4
	Conventional	2.0	2.0	2.9	10.2	17.1
2016.						
Backa	NoPes&MinFert	2.0	2.0	3.0	11.2	18.2
	Conventional	2.0	2.0	3.0	10.9	17.9
Panonia	NoPes&MinFert	2.0	2.0	3.3	11.4	18.7
	Conventional	2.0	2.0	3.3	11.3	18.6
2017.						
Backa	NoPes&MinFert	2.0	2.0	3.4	10.7	18.1
	Conventional	2.0	2.0	3.5	10.5	18.0
Panonia	NoPes&MinFert	2.0	2.0	3.4	10.9	18.3
	Conventional	2.0	2.0	3.3	10.6	17.9
2018.						
Backa	NoPes&MinFert	2.0	2.0	3.2	10.8	18.0
	Conventional	2.0	2.0	3.2	10.7	17.9
Panonia	NoPes&MinFert	2.0	2.0	3.1	11.3	18.4
	Conventional	2.0	2.0	3.1	11.1	18.2
2015-2018 (average)						
Backa	NoPes&MinFert	2.0	2.0	3.2	10.9	18.1
	Conventional	2.0	2.0	3.1	10.8	17.9
Panonia	NoPes&MinFert	2.0	2.0	3.2	10.8	18.0
	Conventional	2.0	2.0	3.2	10.5	17.7

Buxbaum method was used to score the wine samples (0-20 points), assessing appearance (maximum 2 points), color (2), aroma and bouquet (4) and other characteristics, such as sugar, acidity, and astringency (scoring maximum of 12 points in total for these traits related to taste).

production systems was observed in Panonia at the end of December 2017 (44% necroted buds in NoPes&MinFert compared to 84 in Conventional production). Moreover, both cultivars showed the lowest cold hardiness at the end of the winter. In the February 2018, in NoPes&MinFert production of Panonia all bud categories (primary and secondary) in the winter buds were damaged.

The wines of both cultivars achieved higher score in the NoPes&MinFert production compared to the conventional counterpart (Table 6). There were no differences among the treatments in the scores for wine color and clarity and each wine achieved a maximum (2 points) for these traits. The wine of Backa had a slightly better scores for and taste in the NoPes&MinFert compared to conventional production. The taste of the wine of Panonia, which is similar to the wine of its ancestor Riesling, achieved higher score in the NoPes&MinFert compared to the conventional production.

Discussion

Production without use of pesticides and mineral fertilizers - NoPes&MinFert, was similar to organic viticulture practices. Higher percentage of developed shoots and fruitful shoots in conventional compared to NoPes&MinFert production, results in higher number of inflorescences per node. Our results are in agreement with (DÖRING & al. [16]) who found that organic production, had significantly lower growth and yield compared to integrated system. The lower yield in NoPes&MinFert compared to conventional production can be the result of the significantly lower cluster weight in the organic system and aligns with the findings reported by DÖRING & al. [16]. Moreover, it could be the result of lower bunch compactness (MEIBNER [17]). DÖRING & al. [18] posted that a decrease in soil moisture content under organic and biodynamic viticulture is likely to be responsible for the lower yield. However, POOL & ROBINSON [19] did not observe any differences in the number of berries/clusters and the average cluster weight between different management systems. It is speculated that difference in yield between conventional and organic production may be due to yield losses due to pests. Meta-analysis of 362 paired sets of organic-conventional yield data, noting that organic yields are on average 80% of conventional yields, but variation is substantial (21% standard deviation) (DE PONTI & al. [20]). In that research, authors also observed that the organic yield gap significantly differed between crop groups and regions (DE PONTI & al. [20]).

In a number of experiments (TASSONI & al. [12]; DÖRING & al. [16]) the grape juice sugar concentration of organically managed vines was almost same as that of conventionally managed vines. In our experiment the effect of

production system on sugar concentration in the grape juice was inconclusive and depends on the interaction of weather conditions during the season (year) and cultivar. Titratable acidity in the grape juice was not affected by the production system which is in agreement with DÖRING & al. [16].

Our results for Backa and Panonia are supported by those obtained by DANNER [21], who observed a higher *Botrytis* sp. incidence in the production without spraying compared to conventional production. Conversely, some authors (PIKE [22], MEIBNER [17]) reported lower incidence of *Botrytis* sp. in organic vineyards. However, PIKE [22] conducted the experiment in Australian climate conditions where the disease pressure is low. In our experiment, the lower number of developed shoots could result in lower canopy density and better aeration around clusters which prevents *Botrytis* incidence (IVANIŠEVIĆ & al. [23]). Backa and Panonia are early ripening cultivars (end of the August) that can be harvested before the onset of unfavorable weather conditions in September and October.

NoPes&MinFert production showed higher bud freezing tolerance compared to the conventional production. Enhanced tolerance to low temperatures in organic production can be related to lower yield. WAMPLE & WOLF [24] observed that Chardonnay had a greater freezing tolerance in the low than in the high crop load vines. CINDRIĆ & al. [15] observed that in the conditions of North Serbia (Vojvodina) majority of the cultivars have the highest tolerance to low temperatures in the last decade of January and in the middle of February. However, some cultivars tolerant to fungal diseases are the most susceptible to low temperatures in the middle of February (CINDRIĆ & al. [15]), as it was the case in our study.

In our study we observed enhanced wine aroma in the NoPes&MinFert production of Backa compared to conventional counterpart. Satisfied sensory properties of the organic wines, such as flavor intensity, wine body and a general acceptance were also observed in Italy (LANTE & al. [25]). Organic grapevines, grown with reduced pesticides, are more stressed by pathogens compared to conventionally grown grapevines and produce more aroma related compounds (MARTIN & RASMUSSEN [26]). In one study that presents differences between organic and conventional production in central Italy, organic wines had higher overall acceptance by the sensory panel (BENI & ROSSI [27]). Wines of Trebbiano and Sangiovese from the conventional production in the same study, were described as unbalanced and acidic, compared to the organic wines (BENI & ROSSI [27]). In our study, sugar-acid ratio in the grape juice was improved by the NoPes&MinFert production system of Panonia (lower sugar and higher acidity-Table 4). Therefore,

it seems that better sugar-acid ratio in the NoPes&MinFert production improves the wine balance which is particularly important in hot and dry seasons.

Conclusions

Findings yielded by the present study show that fungus-tolerant grape cultivars Backa and Panonia are suitable for the production without use of pesticides. Although the number of inflorescences per node and yield were higher in conventional production, NoPes&MinFert production showed satisfied yield that exceeded 10 t/ha. Moreover, NoPes&MinFert production showed enhanced bud tolerance to low winter temperatures compared to conventional counterpart. Grape chemical composition was similar in both productions while the wines from NoPes&MinFert production achieved higher score in the wine sensory analyses. Differences between cultivars in yield and grape chemical composition were also observed. The studied cultivars allow sustainable grape production in the moderately continental climate conditions.

Source of research fundings

the research was supported by The Ministry of Education, Science and Technological development of the Republic of Serbia and its project TR 31027 and Contemporary technology in organic viticulture - supported by Autonomous Province of Vojvodina, Provincial Secretariat for higher education and scientific research.

Acknowledgments

We are grateful to our professor emeritus Petar Cindric (creator of the cultivars Backa and Panonia), prof Nada Korać and dr Vlada Kovač. We are also grateful to enologist Siniša Ostojić for his support of this work.

References

1. E. PETERLUNGER, G. DI GASPERO, G. CIPRIANI, P. SIVILOTTI, L. ZULINI, M.T. MARRAZZO, D. ANDRETTA, R. TESTOLIN. Breeding strategy for the introgression of disease resistance genes into European grapevine. *Acta Hortic.*, 603: 665-670 (2003).
2. R. BARTOLUCCI. Philosophical considerations in converting to organic vineyard production. *Am J Enol Vitic*, 43: 294-295 (1992).
3. G. MEISSNER, M.E. ATHMANN, J. FRITZ, R. KAUSER, M. STOLL, H.R. SCHULTZ. Conversion to organic and biodynamic viticultural practices: impact on soil, grapevine development and grape quality. *OENO One*, 53(4) (2019).
4. J.E. MASSON, I. SOSUSTRE-GACOUNGOLLE, M. PERRIN, C. SCHMITT, M. HENAU, C. JAUGEY, E. TEILLET, M. LOLLIER, J.F. LALLEMAND, F. SCHERMESSER, G. WESTHALEN. Transdisciplinary participatory-action-research from questions to actionable knowledge for sustainable viticulture development. *Humanit. Soc. Sci. Commun.*, 8(24): 1-9 (2021).
5. B. GEIER. Organic grapes - More than Wine and Statistics. *The World of Organic Agriculture: Statistics & Emerging Trends 2016*. H. Willer, & M. Yussefi, (Eds.): International Federation of Organic Agriculture Movements (IFOAM), pp. 62-65. Bonn, Germany. (2006).
6. B. GUESMI, T. SERRA, Z. KALLAS. The productive efficiency of organic farming: the case of grappe sector in Catalonia. *SJAR*, 10(3): 552-566 (2012).
7. M. HENDGEN, B. HOPPE, J. DÖRING, M. FRIEDEL, R. KAUER, M. FRISCH, A DAHL, H. KELLNER. Effects of different management regimes on microbial biodiversity in vineyard soils. *Sci Rep*, 9393: 1-13 (2018).
8. J. NASCIMBENE, L. MARINI, M.G. PAOLETTI. Organic farming benefits local plant diversity in vineyard farms located in intensive agricultural landscapes. *Environ Manage*, 49: 1054-1060 (2012).
9. X. PUIGMONTSERRAT, C. STEFANESCU, I TORRE, J. PALET, E FABREGAS, J. DANTART, A ARIZ-ZABALAGA, C FLAQUER. Effects of organic and conventional crop management on vineyard biodiversity. *Agr Ecosyst Environ*, 243 : 19-26 (2017).
10. W.J. CRINNION. Organic foods contain higher levels of certain nutrients, lower levels of pesticides, and may provide health benefits for the consumer. *Altern. Med. Rev.*, 15(1): 4-12. (2010).
11. D. GRANATO, T. MARGRAF, I. BROTZAKIS, E. CAPUANO, S.M. VAN RUTH. Characterization of conventional, byodynamic and organic purple grape juices by chemical marker, antioxidant capacity, and instrumental taste profile. *J. Food. Sci.*, 80: C55-C65 (2015).
12. TASSONI, N TANGO, M. FERRI. Comparison of biogenic amine and polyphenol profiles of grape berries and wines obtained following conventional, organic and biodynamic agricultural and oenological practices. *Food Chem*, 139: 405-413 (2013).
13. R. TÖPFER, L. HAUSMANN, M HARST, E. MAUL, E. ZYPRIAN, R. EIBACH. New horizons for grapevine breeding. *Fruit, vegetable and cereal science and biotechnology*. H. Slochowsky, & M.V. Hanke, (Eds.): Global Science Books, Isleworth, pp. 79-100. (2011).
14. B.G. COMBE. Growth stages of the grapevine: Adoption of a system for identifying grapevine growth stages. *Aust J of Grape Wine R*, 1(2): 104-110 (1995).

15. P. CINDRIĆ, N. KORAC, V. KOVAČ. Sorte vinove loze, Prometej, Novi Sad. (2000).
16. J. DÖRING, M. FRISCH, S. TITTMANN, M STOLL, R. KAUER. Growth, yield and fruit quality of grapevines under organic and biodynamic management. *PLoS ONE*, 10(10): 1-28 (2015).
17. G. MEIBNER. Untersuchungen zu verschiedenen *Bewirtschaftungs systemen* im Weinbau unter besonderer Berücksichtigung der biologisch-dynamischen Wirtschaftsweise und des Einsatzes der biologisch-dynamischen Präparate. Justus-Liebig-Universität Gießen. (2015).
18. J. DÖRING, C. COLLINS, M. FRISCH, R. KAUER. Organic and biodynamic viticulture affect biodiversity and properties of vine and wine: A systematic quantitative review. *Am J Enol Vitic*, 70: 221-242 (2019).
19. R.M. POOL, J.A. ROBINSON. The SARE–Cornell organic grape project. In 3rd Organic Grape and Wine Production Symposium. Pool RM (Eds): pp. 7–14. (1995).
20. T. DE PONTI, B. RIJK, M.K ITTERSUM. The crop yield gap between organic and conventional agriculture. *Agr Syst*, 108: 1–9 (2012).
21. R. DANNER. Vergleichende Untersuchungen zum konventionellen, organisch-biologischen und biologisch-dynamischen Weinbau. PhD Thesis, Universität für Bodenkultur Wien. (1985).
22. B.P.A. PIKE. Effect of organic, biodynamic and conventional vineyard management inputs on grapevine growth and susceptibility to powdery mildew and *Botrytis* bunch rot. Thesis, School of Agriculture, Food and Wine. The University of Adelaide. (2015)
23. D. IVANIŠEVIĆ, M. KALAJDŽIĆ, M. DRENJANČEVIĆ, V. PUŠKAŠ, N. KORAC. The impact of cluster thinning and leaf removal timing on the grape quality and concentration of monomeric anthocyanins in Cabernet-Sauvignon and Probus (*Vitis vinifera* L.) wines. *OENO One*, 54(1): 63–74 (2020).
24. R.L. WAMPLE, T.K.WOLF. Practical consideration that impact vine cold hardiness. Proc. for the 4th Int. Symposium on Cool Climate. pp. 23-38 (1996).
25. LANTE, A. CRAPISI, G. LOMOLINO, P SPETTOLI. Chemical parameters, biologically active polyphenols and sensory characteristics of some Italian organic wines. *J Wine Res*, 15(3): 203-209 (2004).
26. K.R. MARTIN, K.K. RASMUSSEN. Comparison of sensory qualities of geographically paired organic and conventional red wines from the southwestern US with differing total polyphenol concentrations: a randomized pilot study. *Food Nutr. Sci*, 2: 1150–1159 (2011).
27. C. BENI, G. ROSSI. Conventional and organic farming: Estimation of some effects on soil, copper accumulation and wine in a Central Italy vineyard. *Agrochimica*, 53:145–159 (2009).



Received for publication: February,10, 2021

Accepted: May, 10,2022

Original paper

Early detection of breast cancer using robust back propagation neural network classifier

**DR.S. VIJAYALAKSHMI^{1*}, DINESH VALLURU²,
MR.A.MANIKANDAN³, DR.P.MATHIYALAGAN⁴**

¹Associate Professor, Department of ECE, Sona College of Technology,Salem

²Research scholar, Department of Information and communication Engineering
Anna University, Chennai-600025, Tamil Nadu, India

³Assistant Professor, Department of ECE, Vivekanandha College of Technology for Women, Namakkal

⁴Associate Professor, Dept. of CSE, Sri Ramakrishna Engineering College, Coimbatore

Abstract

Breast cancer is the most widely recognized malignancy in women and is the second most common and important cause of cancer death in women. Currently, there is no effective approach to avoid breast cancer, as its motivation is not yet fully understood. The common problems of women in recent years are breast cancer. The problem of breast cancer classification has been the main problem in recent years. This article gives a reasonable idea of the readiness of the mammogram image to find out the area affected by cancer, which is a vital advance in breast cancer detection. Therefore, the research focuses on examining and analyzing the image processing of cancerous diseases, especially breast cancer. When detecting breast cancer, images are obtained from a mammogram and subjected to treatment. The artificial neural network (ANN) plays an important role in this regard, in particular in the application of biomedical image processing for the early diagnosis of breast cancer. It is actually detected by these steps. Preprocessing, image splitting, attribute extraction and categorization. An average vector filter is used to perform the preprocessing operation. Helps eliminate noise and turn RGB image into grayscale image. Vessel segmentation is used to segment the image. To perform entity extraction, the technique of the Binary Local Scale Model (MLBP) method is used and optimized using the Robust Propagation Neural Network Classifier (RBPNN). Using MLBP, 12 functional derivatives were extracted. The extraction is performed on the basis of color, texture and shape. It plays an important role in detection. Finally, for the classification of the extracted function, RBPNN is performed and then analyzes the test data with the trained data. To prove its usefulness, it produces great precision compared to other current games. The accuracy of this suggested analysis is 97%.

Keywords

Vector Median filter, Vessel segmentation, Robust back Propagation Neural Network (RBPNN), Multiscale Local Binary Pattern(MLBP)

To cite this article: VIJAYALAKSHMI S, VALLURU D, MANIKANDAN A, MATHIYALAGAN P.
Early detection of breast cancer using robust back propagation neural network classifier. *Rom Biotechnol Lett.* 2022; 27(2): 3407-3415 DOI: 10.25083/rbl/27.2/3407.3415

Introduction

Breast cancer is the leading cause of death among women and the most frequently reported non-dermal cancer in women [1]. Breast cancer occurs when breast tissue becomes abnormal and uncontrollable and decomposes. These abnormal cells form a large tissue and are transformed into tumors. The diagnosis can soon be cured normally. Therefore, it is important to provide an adequate procedure to detect the initial symptoms of breast cancer. The first symptoms of breast cancer are scaly and small lumps, which can only be determined by advanced technology. Micro calcifications are fragments of very small calcium deposits present in the soft tissues of the breast [2]. Tumor detection in breast tissue is often more difficult than microcalcification. The reason is not only the large difference in size and shape, but also the fact that mammography tumors usually show contrast with poor images [3]. The difficulty in classifying benign and malignant microcalcification also poses serious problems for medical imaging. The radiologist's automatic classification can help distinguish between benign and malignant tendencies. Therefore, this article investigates artificial neural networks (ANNs) that can be used as automated classifications. In medical imaging, artificial neural networks are applied to various data classification and pattern recognition activities [4]. As far as diagnostic and medical detection techniques are concerned, X-ray mammography is currently in common use in clinical practice [5] due to its low cost and ease of use. Although there are some limitations in the mammography detection process, since reliability is low in the dense breasts of young women or women, they resist the surgical invention, which is the most effective recommendation method that can be detected. first in breast cancer. The sensitivity of the fatty breast is also high and the detection performance of microcalcification is excellent [6]. In the part of the results, the mammogram is very large, which is necessary to examine the number of radiologists who can cause eye fatigue due to incorrect diagnoses.

In many degrees, they can reflect subtle variations. Therefore, the specific choice of image characteristics can lead to separate classification decisions. It can be classified as 1. The statistically dependent form, such as Support Vector Machine. 2. Basic form of Don's rule, how to determine trees and approximate sets. 3. Artificial neural network [5]. Medical research on breast cancer is not true because a challenge is early recognition of the lack of the appropriate method [6]. By improving in the field of advancement, the contributions of information technology offer a new dimension in terms of medical

imaging. By investing in the distinctive feature that cannot be in the cancer area, there are other areas as well. In terms of imaging techniques, it can be easy to detect the cancerous mass that may be affected in the breast region. In the diagnosis phase, three steps are to be performed for cancer detection and classification. (1) Initial step is done in pre-processed mamogram image to detect the Region of Interest and hence locating the tumor region. (2) Extracting the feature by using expert knowledge such as texture, color, shape and density of the tumor (3) and finally by classifying the feature vector analyse whether it is a malignant or benign tumor. To obtain the accurate result, Researchers have used several techniques for detection and processing of image. Gaussian filter and median filter are used in this proposed work to perform pre-processing. Pre-processing is done to transform a color image to a gray scale image, and its main function is to remove the salt and pepper smell. After pre-processing it undergoes segmentation using threshold-based technique and GLCM uses the function extracted. It describes the gray distribution over all pixels which is a second order joint condition probability. The main purpose of feature extraction algorithm is to minimize the original dataset image by measuring ensured features. In GLCM, the gray scale textual features were extracted. From the extracted feature, computation is to be performed to obtain mean, standard deviation, entropy, auto correlation, correlation etc. The feature which is extracted can be classified by using classifier [6]. Various supervised techniques were used for identifying the abnormalities which occurs in the breast cancer, Artificial Neural network is used [8]. It relates the test data to an accurate outcome with qualified collection.

Related Works

In Lashkari [7], to classify the tissues as normal and abnormal using the Gabor wavelet and therefore the ANN that can maximize precision, the radiologist's moment is recorded. In artificial vision, as well as in image processing technique, it transforms the factor into wavelet Gabor. The result of combinations of neural networks has great potential for unknown cases with an accuracy of 97%.

The Vikas Chaurasia and Saurabh Pal classification of supervised learning performance is compared with some classification techniques to find the breast cancer, such as the SVM-RBF core, decision trees (J48), RBF neural networks, Naïve Bayes, therefore simple CART. The SVM-RBF core achieves a better precision result than the other classification techniques proposed in the Wisconsin breast cancer datasets (original) that achieve an accuracy of 96.84%.

Xin-Sheng Zhang (2014) illustrates the detection and classification of microcalcification (MC) groups. Classification problems result from poor learning functionality for test samples among the set of learning samples called visual parts vocabulary. A rich vocabulary of training samples for visual information is created manually with a series of samples consisting of MC parts, therefore not MC parts[9].

Liyang Wei (2009) propose, the exam is the means of using retrieved comparative and to improve the presentation of a digital classifier. The reasoning method is that by adapting the addition of adjacent adjacent data to the classifier, the accuracy of the characteristics on these lines can be improved, and a “second score” beyond the radiologist can be obtained. The results of mammography tests in a database show that the recovery-based methodology proposed with a multipurpose support vector machine (SVM) can improve the performance from 0.78 to 0.82[10].

Ayman A. AbuBaker 2015, proposes a strategy capable of improving exposure to computer-aided diagnosis (CAD) by distinguishing and consequently organizing microcalcifications (MC) in the mammographic image with precision and competence using multiple channels of facts and a change in deterioration wavelet. . This new method has proven to be difficult to recognize CM in mammography images reaching a high evident positive level of 98.1% and a low false positive rate of 0.63 groups / image for MIAS and USF databases [11].

Identifying the effectiveness of microcalcification can be prohibited because the contrast of the mammography image is low, as is the amount of lower breast tissue. using the spatial dependency matrix of the gray level (GLSDM) and the methods based on the Gabor channel. A total of 120 regions of interest (ROI) extracted from 55 mammographic images from the miniMias database, including ordinary and microcalcification images[12]

Proposed Methodology

The proposed system proposes a simple and orderly procedure for detecting cancer sites from mammograms. Our goal was to divide the cancer site into the mammogram images. Therefore, the research focuses on examining and analyzing the image processing of cancer diseases, especially breast cancer. Mammographic images are produced and processed in breast cancer imaging. Breast cancer image data is collected and processed using the proposed approach. Figure 1 presents a summary of the flow chart of the proposed approach. In the primary stage of image processing, image data is collected using the mammography image acquisition method, followed by a filtering approach to eliminate noise.

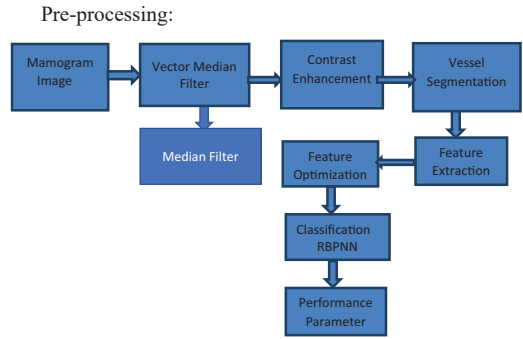


Figure 1. Block diagram of RBPNN classifier

Image Pre-processing:

Gaussian Filter:

Used to emphasize pixel values for accurate cancer detection. It mainly consists of two processes, namely noise reduction and improvement. A central vector filter is used to eliminate denoising of the coronary artery image, and adaptive histogram equalization technology is used to further enhance the denoised image.

Step 1: Update the center pixel value based on the surrounding pixels using the following equation (1) as,

$$xc = \sum_{i=1}^N |xc - xi| \quad (1)$$

Where

xc = Center pixel in 3x3 sub window

xi = Surrounding pixels

N = Number of pixels in 3x3 sub window.

Step 2: After updating the center pixel in the 3x3 sub-window, adjust the surrounding pixels above the center pixel with respect to the intensity value, and then the 3x3 sub window will calculate the median of the center pixel replacement.

Step 3: Continue this process until there are no more pixels in the image.

Based on the discussions, the preprocessed echocardiogram images are depicted in figure 3.

RGB Image Conversion into Gray scale image

The methods used in converting color image to gray scale image is (1) Average method Weighed method. While converting RGB to grayscale image, we have to compute the average of three colors and make as a result a single value reflecting the brightness of that pixel. Computing the average from each pixel is performed by using the equation,

$$\text{Average of three colors} = \frac{(R+G+B)}{3} \quad (3)$$

Since the obtained brightness is often dominated by the green component. So “human oriented” method is taken to compute a weighted average. It is calculated by using,

$$0.3R+0.59G+0.11B \quad (4)$$

after conversion. To provide an enhanced image brightness error can be achieved by using the

$$g(i,j) = \frac{f(i,j)}{e(i,j)} = \frac{cf(i,j)}{fc(i,j)} \quad (5)$$

$g(i,j)$ is the reference image and $fc(i,j)$ indicates the degraded result.

Extracting ROI

Images can be segmented into constituent objects or regions. In image analysis, segmentation plays the main role. The goal of segmentation is that the regions of interest isolate the problem and its characteristics. By suddenly dividing the image, the intensity changes, like the edges of the image, as well as the region that is divided, which can be similar depending on the set of predefined criteria. In medical imaging, the cancer-based application uses efficient segmentation [15].

Linear Iterative Vessel Segmentation

Operation for segmentation requires identifying and evaluating the features. The purpose of the linear iterative vessel segmentation is to adjust the medium k by two essential differences to produce superpixels: Limit the search space to an area proportional to the size of the superpixel, and significantly reduce the number of calculations for optimal distance. This reduces linear complexity regardless of the number of pixels N and the number of superpixels k . Weighted distance measurement combines color and spatial proximity while controlling the size and miniaturization of superpixels.

Efficient pixel compression and constant pixel size determine the performance of the blood vessel separation algorithm. The efficiency of the algorithm is measured by detecting the limit and measuring the error in between.

The maximum possible color distance between two adjacent colors in space (assumed as an RGB input image) is limited and determined according to the size of the spatial distance image. To apply the Euclidean distance to this space, you need to normalize the spatial distance. Therefore, a new distance measurement (D) was applied to take into account the size of the superpixels, improving the color uniformity and proximity of the pixels in this space and the expected cluster size and range is described in the following equations (2), (3) and (4).

$$D = \sqrt{\left(\frac{d_c}{S}\right)^2 + \left(\frac{d_s}{S}\right)^2} \quad (2)$$

$$d_c = \sqrt{(R_a - R_b)^2 + (G_a - G_b)^2 + (B_a - B_b)^2} \quad (3)$$

$$d_s = \sqrt{(a_i - a_j)^2 + (b_i - b_j)^2} \quad (4)$$

Where

D = Distance measurement of cluster

d_c = Represent Color of distance between pixel a and b

d_s = Represent Spatial distance between pixel a and b

S = Size of pixel ($S \times S$)

R_a, G_a, B_a = Color Components of Pixel a

R_b, G_b, B_b = Color Components of Pixel b

Algorithm for image segmentation

```

step1: begin
step2: initialize clusters H.
step3: Read feature graph G.
step4: read preprocessed image Img.
step5: for each group Hi of H
Select Random Nodes from G.
H =  $\int_1^N \text{Rand}(G, 1..X)$ 
X- Available nodes of G.
End.
step6: for each cluster Hi from H
For each Node Ni from Hi
Compute Energy  $E = \sqrt{Ni \cdot Gm - \frac{Hi \cdot Ni \cdot Gm}{\phi}}$ 
If  $E \leq Eth$  then // Eth- Energy threshold
Assign Ni with Hi
Else
Continue;
End
End
End
step7: read user feedback
Read Eth.
Go to step 4.
step8: stop.
    
```

Based on the previous steps of the algorithm, the regions affected by the tumor are extracted and processed using the local binary model on multiple scales to derive their actual characteristics.

Feature extraction using GLCM

GLCM stands for Gray Level Co-occurrence Matrix which examines the statistical method when examining the spatial relationship of pixels. GLCM calculates the pair of pixels with specific values as well as a specific spatial relationship that occurs in the image, as well as extracting the statistical measurements from the matrix. This type of statistics provides information on the texture of the images [16].

Algorithm:

Step 1: Quantizing the data, the specimen being taken is treated as a single image pixel and the specimen value is the intensity of that pixel.

Step 2: (i) Construct the GLCM as a square N×M matrix.

- (ii) Render symmetric GLCM
 - (a) Make a transposed copy of the GLCM.
 - (b) Include the copy in the GLCM itself.
- (iii) Normalize the GLCM.

(a) Divide every component by the sum of all elements.

(b) The elements of the GLCM are considered as probabilities of finding the relationship i, j in window size W .

Step 3: Calculate the role you chose. This tests by using the GLCM values. Those four characteristics aid in deciding.

Energy:

It is also known to be second moment uniformity, or angular. In the GLCM it generates the number of square elements. It reckoned as follows,

$$\text{Energy} = \sum_{i,j=0}^{N-1} (P_{ij})^2 \quad (5)$$

Contrast:

This analyses the local differences in the gray level co-occurrence matrix.

$$\text{Contrast} = \sum_{i,j=0}^{N-1} p_{ij} (i - j)^2 \quad (6)$$

Correlation:

It tests the occurrence of joint probability of specified pairs of pixels.

$$\text{Correlation} = \sum_{i,j=0}^{N-1} p_{ij} \frac{(i-\mu)(j-\mu)}{\sigma^2} \quad (7)$$

Homogeneity:

It tests the proximity of element distribution within the GLCM

$$\text{Homogeneity} = \sum_{i,j=0}^{N-1} \frac{p_{ij}}{1+(i-j)^2} \quad (8)$$

Where p_{ij} denotes the element i, j . N represents the number of measures. Using the equation to estimate the strength of all reference pixels,

$$\mu = \sum_{i,j=0}^{N-1} i p_{ij} \quad (9)$$

Enhanced ANN Feature Optimisation

In this paper, the Enhance Artificial Neural Network (ANN) classifier is used for the classification of breast cancer. The simple elements are made up of neural networks inspired by biological neurons that work in par-

allel. The neural network is trained to perform specific functions that are adapted to the weight of the elements [17]. To get the desired output that can be driven by the neural network. The computational model works similarly to neurons calculated in the human brain. Based on the output comparison, the network is adjusted and the target that corresponds to the network output. Training and testing are two steps to the enhanced ANN classifier. The accuracy of the classification depends on the training. The features are extracted from selected mammography images which are used for inputs that can be trained with the improved ANN classifier to classify the images as malignant and therefore benign.

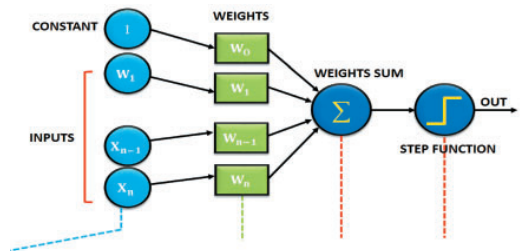


Figure 2. Structure of feature optimization

Robust Back Propagation Neural Network Classifier

In testing / recognition, the Robust Back Propagation Neural Network Classifier(RBPNN) is used to classify new images by comparing the extracted characteristics with the characteristics of the unknown sample image from mammography. RBPNN has been configured, which is to load trained data or test data to correct the problem, namely the classification problem and the clustering problem. To solve problems, the neural network is highly capable of solving complex data for the derivation of meaning. Sometimes it is very common to find the use of trends, but it is complex and cannot be solved even by machines. A neuron is a true function of the input vector ($V_1, V_2 \dots V_k$). The output obtained is

$$V_h = \sum_{n=1}^{N_{Hid}} w_{nh} y_n \quad (10)$$

$$\text{Where, } y_n = \sum_{j=1}^{N_l} \frac{w_{jn}}{1+e^{-ikl}}$$

where N_{Hid} is the number of hidden neurons, w_{nh} is the assigned weight of the n - h link of the network and V_h is the output of the h^{th} output neuron and y_n is the output of the n^{th} hidden neuron.

Performance Metric:

The performance measures metrics of the algorithm is calculated by:

Accuracy–The accuracy of Classification is the percentage of instances which is classified correctly by the model. The formula for accuracy is:

$$Accuracy(\%) = \frac{TP+TN}{TP+TN+FP+FN} \tag{11}$$

Specificity–Commonly used in two class problems which is measures as particular class. It is negative class propagation which is predicted negatively as well as called as true negative rate. The formula is

$$Specificity = \frac{TN}{TN+FP} \tag{12}$$

Recall / Sensitivity- Classification model ability measures for certain selective class instance from the dataset. It is actually positive propagation, the prediction is positive one. The formula used for:

$$Sensitivity = \frac{TP}{TP+FN} \tag{13}$$

Results & Discussion

In this section, discuss the results breast cancer detection of different sample images. The following figure shows the output of the preprocessed image, i.e. the input image of breast cancer is preprocessed using a medium filtering technique to eliminate noise. The preprocessed image is provided as input for the extracting part of the function. ROI extraction is used for the feature extraction process. Figure 3 as shown below. The segmented image is shown in Figure 4. The image extracted from the function can be used for the segmentation process. The image of breast cancer is segmented into images without ROI and ROI. The image without ROI is shown below in Figures 2–4.

Thus, the segmented breast images and the accuracy of the tumor is recognized by using preprocessing and convolu-

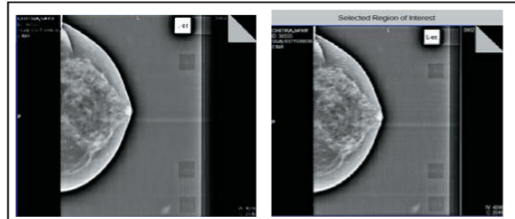


Fig.2: Median Filter Image

Fig.3: ROI extracted Image

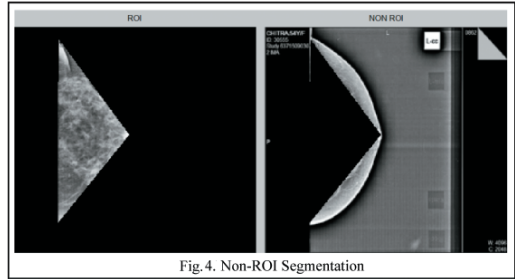


Fig. 4. Non-ROI Segmentation

tional neural techniques where it classifies the the type of the tumor whether it is malignant or benign tumor. The simulated results are shown below.

By using GLCM, 12 feature derivatives were extracted. Extraction is done based on color, texture and shape. Those parameters are given Table 1.

Output Results

Due to the successful calculation of 12 different features, it helps to recognize the tumor of the mammogram images with the maximum precision (91.69%) compared to other classifiers. The method efficiently calculates the output value also minimizes the deviation in calculating the output value. Based on the discussion, the graphical analysis of the classification accuracy obtained is shown in Figure 5. In terms of energy, entropy, comparison correlation and homogeneity,

Table 1. Parameters of GLCM

Parameters	Fig 1	Fig 2	Fig 3	Fig 4	Fig 5	Fig 6	Fig7	Fig 8
Contrast	0.808	0.508	0.304	0.224	0.507	0.335	0.4975	0.810
Correlation	0.825	0.880	0.919	0.936	0.894	0.924	0.8920	0.829
Cluster Prominence	154.06	185.2	78.61	71.12	125.8	113.1	180.97	127.68
Cluster Shade	18.99	25.88	1.07	3.98	7.599	6.797	24.17	11.175
Dissimilarity	0.235	0.154	0.123	0.094	0.190	0.136	0.144	0.241
Energy	0.264	0.320	0.264	0.282	0.218	0.234	0.299	0.243
Entropy	1.567	1.380	1.547	1.456	1.701	1.646	1.409	1.629
Homogeneity(1)	0.935	0.962	0.96	0.968	0.943	0.956	0.966	0.943
Homogeneity(2)	0.935	0.955	0.95	0.965	0.936	0.951	0.960	0.932
Maximum Probability	0.347	0.426	0.35	0.335	0.299	0.346	0.386	0.364
Variance	31.61	28.41	40.12	42.54	36.03	36.13	30.22	35.21
Autocorrelation	31.38	28.38	40.07	42.54	35.91	36.14	30.124	35.048

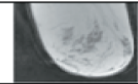
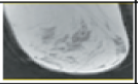
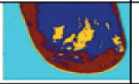
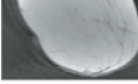
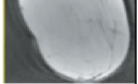
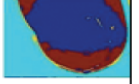


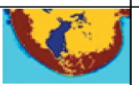
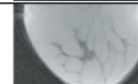
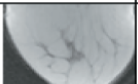










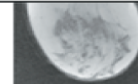
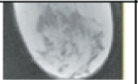
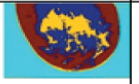
Image no	Input image	Preprocessing image	Segmented image	Type of tumor	Accuracy
1				Malignant	89.64
2				Malignant	86.31
3				Malignant	90.76
4				Malignant	91.69
5				Malignant	89.48
6				Malignant	92.22
7				Malignant	88.81
8				Malignant	89.13

Figure 5. Classification of RBPNN Classifier

the proposed segmentation algorithm is superior to the current RBPNN algorithm [11-12].

From Table 2, it is clearly demonstrated that the RBPNN approach achieves the maximum accuracy value while selecting the exact tumor location from the breast cancer images. The effectiveness of the discussed system is assessed on 6 different mammogram images.

From the Table 3 analysis, the RBPNN attains the maximum sensitivity results when compared to other classifiers such as Enhanced ANN, Regression, with adaboost and support vector machine. Based on the tabular value, sensitivity results graphical analysis is illustrated in figure 8.

From the Table 4, it clearly depicted that introduced robust backpropagation neural network (RBNN) approach at-

Table 2. Accuracy of different classifiers

Classifier	Accuracy (%)					
	Image 1	Image 2	Image 3	Image 4	Image 5	Image 6
RBPNN	89.64	86.31	90.76	91.69	89.48	92.22
Enhanced ANN	86.73	85.29	87.01	86.79	86.89	87.02
Regression	84.29	82.78	84.9	85.28	84.38	86.309
Adaboost	82.72	83.28	85.82	84.89	84.93	85.03
SVM	86.33	86.92	88.56	89.36	86.12	88.76

Table 3: Sensitivity of different classifiers

Classifier	Sensitivity (%)					
	Image 1	Image 2	Image 3	Image 4	Image 5	Image 6
RBPNN	97.30	96.37	97.35	97.452	96.76	97.32
Enhanced ANN	96.73	96.89	96.01	95.79	94.89	94.02
Regression	92.29	91.78	94.9	92.28	91.38	91.309
Adaboost	88.3	89.28	87.82	90.89	90.93	89.03
SVM	94.56	95.24	93.67	94.26	93.45	92.15

Table 4. Specificity of different classifiers

Classifier	Specificity (%)					
	Image 1	Image 2	Image 3	Image 4	Image 5	Image 6
RBPNN	96.42	97.46	97.89	98.13	98.44	97.97
Enhanced ANN	94.02	95.9	94.97	95.65	96.03	94.13
Regression	89.34	91.89	89.39	89.82	91.47	91.03
Adaboost	82.72	84.89	82.29	83.78	87.9	83.345
SVM	93.30	92.45	92.76	92.31	94.54	93.21

tains the high specificity value while classifying the exact tumor location from the mamogram images. The discussed system efficiency is evaluated on the 6 different mamogram images. Based on the tabular value, sensitivity results graphical analysis is illustrated in figure 9.

Table 5. Performance of Various Classifiers

Classifier	Accuracy	Sensitivity	Specificity
RBPNN	91.69	97.452	98.13
Enhanced ANN	86.79	95.79	95.65
Regression	85.28	92.28	89.82
Adaboost	84.89	90.89	83.78
SVM	89.36	94.26	92.31

According to the Table 5, the breast cancer detection in mammogram images, efficiency is determined using different metrics. From the discussion, the RBPNN attains the maximum results on mammogram images compared to the other methods.

Conclusion

The main cause of death for women is breast cancer. To prevent cancer, early detection is important, which has been proven; Diagnosis can be timely treatment and periodic detection. When detecting breast cancer, images are obtained from a mammogram and subjected to treatment. The main objective is to examine the effectiveness of the data mining technique for classifying breast cancer data. In this work, image processing involves several stages, such as preprocessing, segmentation, feature extraction, classification of mammographic images. The results can therefore be used to improve the RBPNN method for detecting cancer and also to easily distinguish between malignant and benign. Compared to conventional classifiers, the proposed RBPNN accuracy is 91.69%, sensitivity is 97.452%, and specificity is 97.452%. The results can therefore be used to improve the RBPNN method for detecting cancer and also to easily distinguish between malignant and benign. This can help the doctor analyze the stage of cancer so that the suffering patient also takes the necessary treatment. In the future, apply breast cancer survival prediction models to two parameters for cancer patients: benign and malignant.

Conflict of interest

The authors declare that they have no conflict of interest.

References

1. B.Sahiner, M.A.Helvie, L.Hadjiiski, "Breast masses of computer aided diagnosis with serial Mammograms", published in journal of Radiology, vol.240, no.2, pp.343-356, 2006.
2. Darakhshan, Ghanbari, "Erratum to: Tranilast enhances the anti-tumor effects of tamoxifen on human breast cancer cells in vitro", Journal of Biomedical Science, SP. 89, Vol. 20, no. 1, pp 1423-0127, DEC 2013. <https://doi.org/10.1186/1423-0127-20-89>
3. N Albert singh, S Tamil selvi, "Computer aided detection of breast cancer mammograms, a swarm intelligence Optimized Wavelet Neural network approaches".Journal of biomedical informatics, volime-49, pp.45, 2014
4. S.K.Mun, M.T.Freedman, H.Li, J.S Lin, "Artificial convolution neural network for medical image pattern recognition", published in journal of Neural Networks, Vol.8, no.7-8, pp.1201-1214, 1995.
5. Falah H.Ali, Tengfei Yin, 2015, "A Robust and artefact resistant algorithm of UWB system for breast cancer detection", published in IEEE transactin on biomedical engineering, pp.1514-1525, volume.62, no.06.
6. Baran, A., Kurrant, D., Zakaria, A., Fear, E., & LoVetri, J. (2014, July). Breast cancer imaging using microwave tomography with radar-derived prior information. In IEEE Radio Science Meeting (Joint with AP-S Symposium), 2014 USNC-URSI, pp. 259-259
7. [7] Lashkari, "Full automatic micro calcification detection in mammogram images using artificial neural network and Gabor wavelets, " in *Proceedings of the 6th Iranian Conference on Machine Vision and Image Processing (MVIP '10)*, Isfahan, Iran, October 2010
8. V. Chaurasia and S. Pal, "Data Mining Techniques: To Predict and Resolve Breast Cancer Survivability, " vol. 3, no. 1, pp. 10–22, 2014
9. M.M Mehdy, E.FShair and C.Gomes, 2017, "Artificial neural networks in image processing for early detection of Breast Cancer"published in computational andmathematical methods inmedicine, volume2017, ID2610628.

10. Xin-Sheng Zhang, A New Approach for Clustered MCs Classification with Sparse Features Learning and TWSVM, Hindawi Publishing Corporation, the Scientific World Journal, Volume 2014.
11. Tariq N (2018) Breast Cancer Detection using Artificial Neural Networks. J Mol Biomark Diagn 9: 371. doi: 10.4172/2155-9929.1000371
12. Yousif M.Y Abdallah, Sami Elgak, Hosam Zain, Mohammed Rafiq, Elabbas A. Ebaid, Alaeldein A. Elnaema, "Breast cancer detection using image enhancement and segmentation algorithms", Biomedical Research, Vol. 29, Issue.20: Pg. 3732-3736, 2018
13. Hong Lu, Xia Xiao , 2015, "Direct Extraction of Tumor responses based on ensemble empirical mode de-composition for image reconstruction of early breast cancer detection by UWB", IEEE transactions on biomedical circuits and systems, volume.9, pp 710-724.
14. P.Xu, H.Li, "Anew ANN Based detection Algorithm of the masses in digital mammograms", in proceedings of the IEEE International Conference on Integration technology, pp.26-30, IEEE, Shenzhen, china, March 2007.
15. I.L.A Vennila, C.G Shankar and T.Balakumaran, "Detection of micro calcification in Mammograms using Wavelet transform and fuzzy shell clustering", published in International journal of computer science and information technology, pp.121-125, vol.7, no.1, 2010.



Received for publication: May, 16, 2022
Accepted: May, 20, 2022

Review

Anti-cancer alternative therapies: from inorganic nanoparticles to tumor-killing bacteria

GRIGORE MIHĂESCU¹, MARIAN CONSTANTIN^{2,3*}, OCTAVIAN ANDRONIC, ALEXANDRA BOLOCAN⁴, ROXANA FILIP^{5,6}

¹Faculty of Biology, University of Bucharest, 030018 Bucharest, Romania

²Institute of Biology Bucharest of Romanian Academy, 296 Splaiul Independentei, 060031 Bucharest, Romania

³Fellow of the Research Institute of the University of Bucharest, ICUB, Bucharest, Romania

⁴General Surgery, University of Medicine and Pharmacy “Carol Davila”, 020021 Bucharest, Romania

⁵Faculty of Medicine and Biological Sciences, Stefan cel Mare University of Suceava, 720229 Suceava, Romania

⁶Regional County Emergency Hospital, 720284 Suceava, Romania

Abstract

Cancer affects an increasing number of people every year, affecting many families and representing a major problem for health systems in all countries. As chemotherapy is one of the most widely used therapeutic approaches, usually following surgical resection of the tumour mass, its adverse effects have made it necessary to find alternative, less toxic ways for treating cancer. These include nanoparticles, especially those containing Ag and/or Pt, some nonpathogenic, attenuated or genetically engineered bacteria can exhibit a destructive potential on tumors, especially when they carry antitumor genes or antineoplastic agents, cationic antimicrobial peptides, modified to mitigate their harmful effects, and immunotherapy, such as immune checkpoint inhibitors.

Keywords

chemotherapy, cancer treatment, nanoparticles, nonpathogenic bacteria, cationic antimicrobial peptides, immune checkpoint inhibitors

To cite this article: MIHĂESCU G, CONSTANTIN M, ANDRONIC O, BOLOCAN A, FILIP R. Anti-cancer alternative therapies: from inorganic nanoparticles to tumor-killing bacteria. *Rom Biotechnol Lett.* 2022; 27(2): 3416-3421 DOI: 10.25083/rbl/27.2/3416.3421

Introduction

One of the main public health problems affecting society today is the high incidence of cancer. In addition to complications caused by the primary tumour and possible metastases, cancer patients are more susceptible to complications after infections caused by *Streptococcus pneumoniae*, *Staphylococcus* spp., *Escherichia coli*, *Klebsiella pneumoniae*, *Pseudomonas aeruginosa*, *Helicobacter pylori* and *Candida* spp.. On the other hand, the patients chronically infected with *S. aureus*, *A. baumannii*, *P. aeruginosa* and *Enterobacter* are immunosuppressed and have a higher risk of developing cancer (Rodriguez et al., 2019). In the treatment of cancer, standard therapeutic management requires surgical resection, chemotherapy and radiotherapy. Tumour resection is an invasive method and ensures the removal of the primary tumour and possible metastases, and in some cases can ensure a cure. Most of the time, however, after resection, the cancer patient undergoes chemotherapy. This involves the administration of a platinum-based or other chemical agents, either by infusion or orally, which inhibits the multiplication of tumoral cells. It has also non-specific toxic effects on normal cells, causing symptoms such as sickness, vomiting, numbness in the extremities, hair loss, etc. Since tumour cells exposed to chemotherapeutic agents increase their enzymatic capacity to detoxify drugs and repair DNA, they could become drug resistant, leading to tumour recurrence. Some patients cannot tolerate the treatment for the entire period of administration and it has to be stopped prematurely. In case of tumors resistant to chemotherapy, radiotherapy is prescribed. The standard treatment involves irradiating the site of the tumour cell deposits with a dose high enough to destroy them, especially when they are therapeutically sensitised. Because radiation affects any tissue it passes through, healthy tissues are affected by radiation. Unfortunately, none of these therapeutic approaches can always permanently eliminate the pool of tumour cells; so, the risk of neoplasm recurrence remains, especially in very aggressive tumours such as mucinous tumours, whose cells are extra-protected by their mucus secretion. Alternative strategies such as nanoparticles (NPs), non-pathogenic bacteria, antimicrobial cationic peptides, *immunotherapy*) have been developed to at least partially eliminate its side effects.

NPs in cancer treatment

Nanotechnology is a multidisciplinary domain of chemistry, microengineering, biology and medicine with applications in therapy and fighting against bacterial resistance and neoplasia (Tudose et al., 2016). Against bacteria, Ag NPs

act by perforating the bacterial cell wall, forming reactive oxygen species (ROS), inhibiting aerobic respiration and damaging DNA. Ag NPs are also active on transforming cell lines and tumors by altering mitochondrial function, blocking the cell cycle and activating apoptosis (Tianyuan Shi et al., 2018; Albulę et al., 2017). The effect depends on the concentration, size and coating material of the NPs. NPs consisting of Ag-Pt inhibit glioblastoma and melanoma cell lines. Platinum binds to DNA and kills the cells by apoptosis or necrosis. Like all chemotherapeutic agents, cisplatin is not selective for malignant cells, and, because lower toxicity, NPs with Pt are more efficient in stopping cancer development (Lopez Ruiz et al., 2020).

Therapy with nonpathogenic bacteria

Some bacteria are potentially carcinogenic promoters by stimulation of the inflammatory reaction in infective process: *H. pylori* is a potentially gastric carcinoma inductor; *Salmonella typhi* can induce hepatobiliary carcinoma, *Campylobacter jejuni* leads to small intestine lymphoma; *Chlamydia psittaci* is an inductor for eye lymphoma; *Mycobacterium tuberculosis* can lead to lung cancer; *Citrobacter rodentium* induces human colorectal cancer (CRC); *Porphyromonas gingivalis*, which is present in the oral cavity is a potentially inductor for pancreatic cancer (Song et al., 2018).

On the other side, bacteria reported to have potential anti-cancer activity include species of *Salmonella*, *Clostridium*, *Bifidobacterium*, *Lactobacillus*, *Escherichia*, *Pseudomonas*, *Caulobacter*, *Listeria*, *Proteus*, BCG and *Streptococcus*. The routes of action and their use in treating cancer are diverse. Nonpathogenic or genetically modified bacteria with tropism for neoplastic tissue can have direct anticancer action through oncolytic activity, by secreting toxins and enzymes (proteases and lipases). Tumour produces attractant molecules for bacteria that penetrate ECM to the central region of the tumour, where hypoxic medium is favorable to obligate and facultative anaerobes: *Clostridium* spp., *Bifidobacterium* spp., *E. coli*. After tumour colonization, quorum sensing commutes the genetic program that changes the tumour microenvironment and produces cell lysis (Zargar et al., 2019). BCG is used for treating bladder tumours (Morales et al., 1976; Maffezini, 2006). In anaerobic conditions, *E. coli* stimulates cell immune response mediated by TCD8 cytolytic lymphocytes (Song et al., 2018) and the monocytes (macrophages) from the tumor tissue containing bacteria release TNF-innate immunity factor with cytolytic effect.

Molecules synthesized and released by bacteria can inhibit tumour growth (enzymes such as lipases and proteases) or have toxicologically specific anti-tumour potential (bacteriocins). *P. gingivalis* is one of the few bacteria that syn-

thesize peptidyl arginine deiminase (PAD), an angiogenic agent efficient in leukemia treatment (Ye Ni *et al.*, 2008) and against arginine auxotroph neoplasia-hepatocellular carcinoma and melanoma. Bacteriocins (piocines, colicines, pediocins, microcines) are antimicrobial cationic peptides produced by many bacterial species, with specific toxic potential against different malignant cell lines: breast, colon, HeLa (Cornnut *et al.*, 2018; Song *et al.*, 2018).

Some of the bacterial toxins, such as diphtheria toxin (TD), bind to antigens on the surface of tumor cells, inhibiting the EGF production. The TD-HB-EGF complex is released by endocytosis, and the lytic A subunit (activity) of TD is eliminated inside the cell. Ligand-conjugated toxins (*Pseudomonas* exotoxin, ricin DT) can be therapeutically effective, but must be targeted to specific cell membrane sites. *C. novyi* spores have a non-lethal toxin (Patyar *et al.*, 2010) and when injected in mice with neoplasia produce lytic destruction of tumors (Baindara & Mandal, 2020);

Live attenuated or genetically engineered bacterial cells have the ability to carry and spread tumorigenic molecules, releasing them mainly in hypoxic and anaerobic regions of solid tumors, with a potentially destructive effect on primary neoplasia (Patyar *et al.*, 2010; Song *et al.*, 2018). They can

also be modified to carry genes for anti-cancer lytic proteins or can be used as vehicles for antineoplastic agents to be released into solid tumors (Patyar *et al.*, 2010). Genetically engineered *Salmonella* cells synthesize LPS that do not stimulate proinflammatory cytokines and thus lower the risk of septic shock. Oral administration of genetically modified probiotics or enteric administration of heterologous bacteria, either probiotics or fecal transplantation, can be used for treating blood neoplasia, sarcoma and melanoma.

The main limiting factors in the use of bacteria for the treatment of cancer stem from the fact that, in the dose required for therapy, bacteria become toxic, with systemic infection posing a major risk of toxicity. Also, bacteria incompletely lyse the tumour mass and act only in hypoxic regions without affecting metastases that do not have anaerobic conditions (Patyar *et al.*, 2010).

Antimicrobial cationic peptides

Although chemotherapeutic agents produce side effects on normal cells and tissues, they continue to be the main therapeutic option in cancer, but a new therapeutic approach with less toxicity is emerging. This is represented by new molecules with selective action and anti-infective and anti-tumour specificity: toxins, immunotoxins, enzymes, peptides, bacteriocins (also peptides) and a wide range of proteins (Karpinski & Adamczak, 2018). Of particular importance are antimicrobial peptides (AMPs) with antitumor activity, which can specifically target tumor cells and are classified into two categories: (a) peptides active on bacteria and malignant cells with no side effects on mammalian cells, and (b) peptides that are toxic on tumor cells, bacterial cells, but also on healthy cells (Rodriguez *et al.*, 2019). Antimicrobial peptides are synthesized by plants, invertebrates, vertebrates and represent a major part of their innate immunity in thousands of chemical variants (Wu *et al.*, 2010). Antimicrobial peptides from animal sources are small molecules, with chains of 6-100 amino acids, and very diverse chemically. They are classified according to their secondary structure into β -fold peptides, α -helical loop peptides and linear peptides (Grădișteanu Pircălăbioru *et al.*, 2021). The discovery of the therapeutic effects of cationic antimicrobial peptides began with the observation that they favor the restoration of the balance of the resident microbiota. Synthesized by probiotic bacteria, they have antimicrobial and immunomodulatory effects and antimicrobial properties, inhibiting the synthesis of LPS-induced proinflammatory cytokines and recruiting antigen presenting cells. A family of antimicrobial peptides, defensins, are important players in innate immunity and play a role in defense (Hancock & Sahl, 2006; Giuliani & Nicoletto, 2007). The lytic properties of AMPs allow them to be

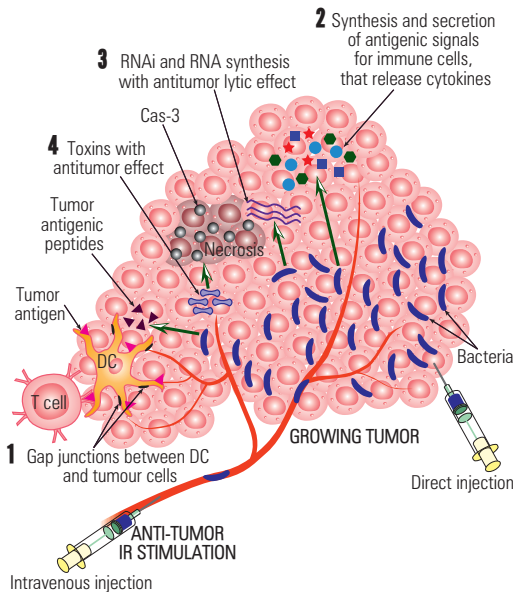


Figure 1. Anti-neoplastic effect of genetically modified bacteria. Anti-tumor IR stimulation by: 1. Gap junctions between DC and tumour cells, that facilitates the transfer of tumour antigenic peptides to DC and then recruitment of T1 and T2, T3 lymphocytes; 2. Synthesis and secretion of antigenic signals for immune cells, that release cytokines; 3. RNAi and RNA synthesis with antitumor lytic effect; 4. Toxins with antitumor effect (modified after Baindara & Mandal, 2020).

considered as a therapeutic option in the treatment of malignancies: magainins from *Xenopus* skin lyse hematopoietic cells and solid tumour cells, with limited effect on normal lymphocytes (Zasloff, 1987; Makovitzki et al., 2009). The next level of investigation is the chemical synthesis of cationic AMPs with therapeutic potential in cancer. AMPs are positively charged and have amphipathic properties, making it possible for them to bind, via electrostatic interaction, to intensively negatively charged membrane of malignant cells due to the rich presence of phosphatidyl serine, glycoproteins and glucosamines. By penetrating into the intracellular space, AMPs reach mitochondria, which they inactivate and cause cell death through necrosis or apoptosis. Thus, amphipathic cationic AMPs can be an efficient source of antineoplastic agents (Giuliani & Nicoletto, 2007; Hung Lun Chu et al., 2015; Deslouches & Di, 2017).

Therapeutic use of AMPs is limited by in vivo instability at the internal pH, high price and toxicity against normal cells (Giuliani & Nicoletto, 2007). Also, AMPs could eventually resistant tumour cells. Peptidomimetics synthesized by coupling AMPs with a substituted amine have a significant anti-tumour activity and a low toxicity on normal cells (Huan Li et al., 2021). Another attempt to overcome the limitation in the therapeutic use of AMPs was the replacement of amino acids with D forms in vivo and in vitro (Papo et al., 2009), or association of AMPs with nanomaterials (titanium padded with calcium sulphate), which increases their stability (Kazemzadeh-Narbat et al., 2010).

Anti-metabolites

Next-generation sulphonamides inhibit the activity of matrix metalloproteinases (MMPs). Their discovery led to the synthesis of TNF α converting enzyme inhibitors (TACE) with great potential for reducing inflammation. MMP and TACE have a synergistic action in the pathophysiology of tumour invasion (Supuran et al., 2003, Cierpial et al., 2020).

Immunotherapy

Malignant cells have evolved various strategies to overcome host immunity, and the basic concept of immunotherapy (IT) is the immune checkpoint inhibition (ICI). ICI immunotherapy methodology is considered to be particularly successful in solid tumours (Martins Lopes et al., 2020). One of the checkpoints is PD binding to the L1 ligand (PD-1 programmed cell death protein 1; L1-ligand 1). PD1 is expressed on lymphocytes, and PD-L1 is expressed on tumor cells and APCs. Binding of PD1 to ligand 1 inactivates T lymphocytes and blocks the immune response (IR). The anti PD-1 and anti PD-L1 monoclonal antibodies (MAB) abrogates the inhibitory effect of anti-tumor cytotoxic T lymphocyte activation and has been introduced in advanced non-small cell lung cancer (NSCLC). Patient survival was significantly improved. The outcome after ICI treatment is heterogeneous, being beneficial for a small number of patients. One explanation could be the physiology of the microbiota acting on the anti-tumour effect of therapy targeting an ICI checkpoint. Chronic mitomy-

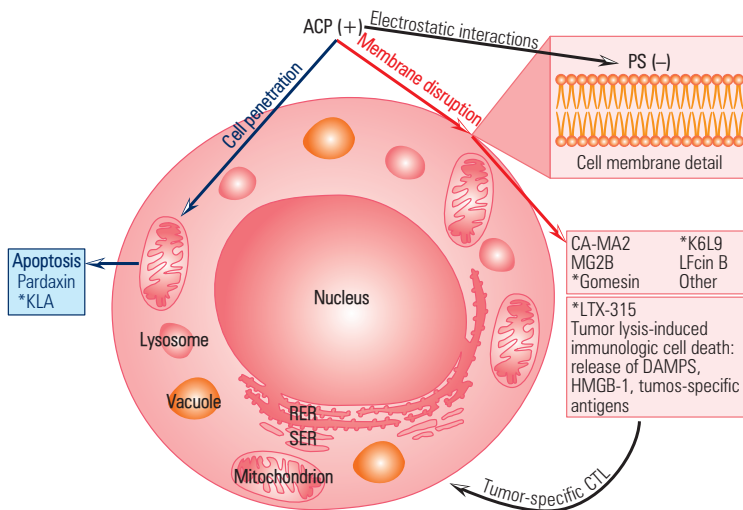


Figure 2. Common anti-tumour mechanisms for cationic AMPs. Negatively charged anti-cancer cationic peptides selectively recognize malignant cells by electrostatic interaction with negatively charged Ek (PS–phosphatidyl serine) cell membrane phospholipids. Some AMPs are efficient in vivo (MG2B, Gomesin, K6L9, other). CAP can kill tumour cell by membrane disruption (red), and others (KLA, pardaxin) can penetrate the target cell and break the mitochondrial membrane (blue) (modified after Deslouches & Y Peter Di, 2017).

cin (anthracycline antibiotic) therapy indicates dysbiosis and greatly diminishes the effect of AMC immunotherapy targeting the PD-1-L1 checkpoint (Reed *et al.*, 2019; Schett *et al.*, 2020; Derosa *et al.*, 2020). Another checkpoint for IR is CTL-4 (cytotoxic T lymphocyte-associated protein 4=CD152). CTL-4 is a cytotoxic T lymphocyte membrane receptor that is activated upon binding of CD80 (or CD86) ligand expressed on CPA. The CTL-4 receptor triggers an inhibitory signal in activated T lymphocytes. Specific anti-CTL-4 mAbs are used in metastatic melanoma therapy. The therapeutic effect of MAB is diminished or reversed in germ-free animals or animals treated with broad-spectrum antibiotics (Pianbianco *et al.*, 2018; Dubin *et al.*, 2016). The efficacy of anti PD-1 anti PD-L1 and anti CTL-4 immunotherapy is influenced by the physiological status of the microbiota. Bifidobacterium stimulates T lymphocytes. Antibiotics, through changes in microbiota have reversed the favorable effect of treatments targeting ICI in most cancer patients (Bertrand *et al.*, 2018; Vetzou & Trinchieri, 2018, Gopalakrishnan *et al.*, 2018; Ming Yi *et al.*, 2018; Elkrief *et al.*, 2019; Garajova, 2021).

Conclusions

Finding alternative routes to chemotherapy in the treatment of cancer is a great challenge for researchers in the field of human biology and in this regard there are several promising research directions, represented by the use of metal nanoparticles, nonpathogenic bacteria with direct anti-tumor effect or which transport and release various compounds into the tumor microenvironment, cationic antimicrobial modified peptides and immunotherapeutic methods inhibiting the immune checkpoints.

Acknowledgements

This research was funded by ICUB, grant number 2153/01.02.2022, the Ministry of Research, Innovation and Digitalization through Program 1—Development of the national R&D system, Subprogram 1.2—Institutional performance—Financing projects for excellence in RDI, Contract no. 41 PFE/30.12.2021 and UEFISCDI-FDI 2022-0675. The funders had no role in the design of the study; in the collection, analyses, or interpretation of data; in the writing of the manuscript or in the decision to publish the results.

Bibliography

1. Albuleț *et al.*, Nanostructures for Cancer Therapy 2017. Book chapter *Part of* DOI: 10.1016/B978-0-323-46144-3.00001-5EID: 2-s2.0-8504062037
2. Baidara P., Mandal M.S., Bacteria and bacterial anticancer agents as a promising alternative for cancer

- therapeutics. *Biochimie*, vol. 177, 2020, pag. 164/189, 2018. doi:10.1016/j.biochi.2020.07.020
3. Bertrand R. *et al.*, Gut microbiome influences efficacy of PD-1 based immunotherapy against epithelial tumors. *Science*. 2018 jan 5; 359 (6371): 91-98. doi:10.1126/Science.aan3706
4. Cierpial T. *et al.*, Fluoroaryl analogs of sulforaphane—A group of compounds of anticancer and antibacterial activity. *Bioorg chem*.2020 jan; 94:103454. doi:10.1016/j.bioorg.2019.103454
5. Cornut G *et al.*, Antineoplastic properties of Bacteriocins: revisiting potential active agents. *Am J Clin Oncol*. 2008, 31(4): 399-404. doi:10.1097/COC.=B=13e31815e456d
6. Derosa L. *et al.*, Negative association of antibiotics on clinical activity of immune checkpoint inhibitors in patients with advanced renal cell and non-small-cell lung cancer. *Onco-Immunology*, vol 29, issue 6, P 1437-1444, 2018. doi:https://doi.org/10.1093/onco/ndy103
7. Deslouches B.&Peter DiY., Antimicrobial peptides with selective antitumor mechanisms: project for anticancer applications. *Oncotarget*.2017, jul 11;8(28):46651. doi:18632/oncotarget.16743
8. Dubin K *et al.*, Intestinal microbiome analysis identify melanoma patients at risk for checkpoint-blockade-induced colitis. *Nat Commun*. 2016;7:10391. doi:10.1038/ncomms10391
9. Elkrief A. *et al.*, The intimate relationship between microbiota and cancer immunotherapy. *Gut microbes*. 2019; 10(3):424.428. doi:10.1080/19490976.218.1527167
10. Garajova Ingrid *et al.*, The role of the microbiome in drug resistance in gastrointestinal cancers. doi.org/10.1080/14737140.2021.1844007
11. Giuliani A.P.G.&Nicoletto S.F., Antimicrobial peptides: an overview of a promising class of therapeutics. *Central European Journal of Biology*. 2007; 2(1):1-33)
12. Gopalakrishnan *et al.*, Gut microbiome modulates response to anti-PD-1 immunotherapy in melanoma patients. *Science*.2018 Jan 5; 359(6371) 97-103. Doi:10.1126/science.aan4236.Epub2017 Nov 2.
13. Gradisteanu Pircalabioru G., Popa L.I., Marutescu L., Gheorghe I., Popa M., Czobor Barbu I., Cristescu R., Chifiriuc M.C., Bacteriocins in the Era of Antibiotic Resistance: Rising to the Challenge. *Pharmaceutics*. 2021 Feb 2;13(2):196. doi: 10.3390/pharmaceutics13020196. PMID: 33540560; PMCID: PMC7912925.
14. Hancock R.E.W.&Sahl H.G., Antimicrobial and host defense peptides as new anti-infective therapeutic strategies. *Nature Biotechnology* 24, 1551-1557 (2006)

15. Huan Li et al., Antimicrobial and antitumor activity of peptidomimetics synthesized from amino acids. *Bioorganic chemistry*, vol 106, January 2021. doi: 10.1016/j.bioorg.2020.104506
16. Hung-Lun Chu et al., Novel antimicrobial peptides with high anticancer activity and selectivity. May 13, 2015. doi:10.1371/journal.pone.0126390
17. Karpinski T., Adamczak A., Anticancer Activity of Bacterial Proteins and Peptides. *Pharmaceutics*, 2018 Jun;10(2):54 doi:10.3390/pharmaceutics10020054
18. Kazemzadeh-Narbat M. et al., Antimicrobial peptides on calcium phosphate coated titan for the prevention of implant-associated infections. *Biomaterials*. 2010; 31:9519-26. 10.1016/j.biomaterials.2010.08.035
19. Lopez Ruiz A. et al., Novel Silver-Platinum Nanoparticles for Anticancer and Antimicrobial Applications. *Int J Nanomedicine*. 2020; 15:169-179. doi:10.2147/IJN.S176737
20. Maffezini M.R., Intravesical BCG versus Mitomycin C for Ta and T1 bladder cancer. *European Urology* 2006, 50:613-710
21. Makovitzki A et al., Suppression of Human solid tumor growth in mice by intratumor and systemic inoculation of histidine-rich and pH-dependent host defense-like lytic peptides. *Can Res*.2009;69(8):3458-63. doi:10.1158/0008-5472.CAN-08-3021
22. Martins Lopez M.S. et al., Antibiotics, cancer risk and oncologic treatment efficacy: a practical review of the literature. *Ecancermedalscience*. 2020;14:1106. doi:3332/cancer.2020.1106
23. Ming Yi et al., Gut microbiome modulates efficacy of immune check point inhibitors. *Hematol Oncol*. 2018 Mar 27; 11(1):47. doi:10.1186/s13045-018-0592-6
24. Morales A et al., Intracavitary BCG in the treatment of superficial bladder tumors. *J Urol*. (1976), 10.1016/s0022-5347(17)58737-6.10.1016/j.juro.2016
25. Papo N et al., A Novel lytic peptide composed of DL-aminoacids selectively kills cancer cells in culture and in mice. *J. Biol Chem*.2009; 30(4):660-8. 10.1016/j.peptides.2008.12.019
26. Patyar S. et al., Bacteria in Cancer therapy: a novel experimental strategy. *J. Biomed Sci*. 2010 Mar 23; 17(1). doi:10.1186/1432-0127-17-21
27. Pianbianco C. et al., Pharmacomicrobiomics: exploiting the drug-microbiota interactions in cancer therapies–Microbiome. 2018;6:92. doi:10.1186/s40168-018-0483-7
28. Reed J.P. et al., Gut microbiome, antibiotic use and immunotherapy responsiveness in cancer. *Ann Transl Med*. 2019; 7(suppl 8):S309. doi:10.21037/atm.21037.2019.10.27
29. Rodriguez G et al., Bacterial Proteinaceous Compounds with multiple activities toward Cancers and Microbial Infection. *Front Microbiol*. 2019; 10:1690. doi:10.3389/fmicb.2019.01690
30. Schett Anne et al., Predictive impact of antibiotics in patients with advanced non small lung cancer receiving immune checkpoint inhibitors. *Cancer Chemother Pharmacol*. 2020; 85(1): 121-131. doi:10.1007/s00280-019-03993-1
31. Song Shiyu et al., The role of bacteria in cancer therapy- enemies in the past, but allies at present. *Infectious Agents and Cancer* 13, Article number 9 (2018)
32. Supuran T. Claudiu et al., Protease inhibitors of the sulfonamide type: Anticancer, antiinflammatory and antiviral agents–9 May 2003. doi.org/10.1002/med.10047
33. Tianyuan Shi et al., Cytotoxicity of Silver Nanoparticles against Bacteria and Tumor Cells. *Current Protein & Peptide Science* vol 19, issue 6, 2018. doi:10.2174/1389203718666161108092149
34. Tudose M et al., Multifunctional Silver Nanoparticles-Decorated Silica Functionalized with Retinoic Acid with Anti-Proliferative and Antimicrobial Properties. *Journal of Inorganic and Organometallic Polymers and Materials*2016 | Journal article DOI: 10.1007/s10904-016-0407-6EID: 2-s2.0-8497815334
35. Vetzizou Marie, Trinchieri G., Anti-PD-1 in the wonder gut-land. *Cell Res*, 2018 Mar; 28(3):263-264.
36. Wu Dongdong et al., Peptide-based cancer therapy: opportunity and challenge. *Cancer Lett*. 2014; 351(1):13-22. 10.1016/j.canlet.2014.05.002
37. Ye Ni et al., Arginin deiminase–a potential anti-tumor drug. *Cancer Lett*. 2008 Mar; 261(1):1-11. doi:10.1016/j.canlet.2007.11.038
38. Zargar Amin et al., Overcoming the challenges of cancer drug resistance through bacterial-mediated therapy. *Chronic Diseases and Translational Medicine*, vol 5, issue 4, December 2019, pag 258-266. doi:org/10.1016/j.cdtm.2019.11.001
39. Zasloff M., Magainins–a class of antimicrobial peptides from *Xenopus* skin: isolation, characterization of two active forms and partial cDNA sequence of a precursor. *Proc Natl Acad. Sci. USA* 84, 5449-5453 (1987)



Received for publication: May, 16, 2022
Accepted: May, 20, 2022

Review

Antitumor antibiotics: representatives, mechanisms of action and side effects

GRIGORE MIHAESCU¹, MARIAN CONSTANTIN^{2,3*}, OCTAVIAN ANDRONIC⁴, ALEXANDRA BOLOCAN⁴, ILINCA VLAD⁵, ROXANA FILIP^{6,7}

¹Faculty of Biology, University of Bucharest, 030018 Bucharest, Romania

²Institute of Biology Bucharest of Romanian Academy, 296 Splaiul Independentei, 060031 Bucharest, Romania

³Fellow of the Research Institute of the University of Bucharest, ICUB, Bucharest, Romania

⁴General Surgery, University of Medicine and Pharmacy “Carol Davila”, 020021 Bucharest, Romania

⁵Department of Pharmaceutical Chemistry, Faculty of Pharmacy, “Carol Davila” University of Medicine and Pharmacy, 6 Traian Vuia, 020956 Bucharest, Romania

⁶Faculty of Medicine and Biological Sciences, Stefan cel Mare University of Suceava, 720229 Suceava, Romania

⁷Regional County Emergency Hospital, 720284 Suceava, Romania

Abstract

Bacteria and fungi synthesize various compounds necessary for their own metabolism, as well as compounds that kill other microbial strains and species from the environment in which they grow, to ensure their access to sufficient supplies. Since the discovery of their antitumor effect, three main classes of antibiotics are used in cancer therapy: anthracyclines (secondary metabolites, mainly produced by members of Streptomyces group, or semisynthetic derivatives containing the 7,8,9,10-tetrahydro-tetracen-5.12 quinone structure), peptide antibiotics and quinolones. In this minireview, we will present the mechanisms of action, main representatives and side effects of these anti-cancer agents.

Keywords

antitumor agents, anthracyclines, peptide antibiotics, quinolones

To cite this article: MIHĂESCU G, CONSTANTIN M, ANDRONIC O, BOLOCAN A, VLAD I, FILIP R. Antitumor antibiotics: representatives, mechanisms of action and side effects. *Rom Biotechnol Lett.* 2022; 27(2): 3422-3428 DOI: 10.25083/rbl/27.2/3422.3428

Introduction

Bacteria and fungi synthesize various compounds necessary for their own metabolism, as well as compounds that kill other microbial strains and species from the environment in which they grow, to ensure their access to sufficient supplies. In 1909, American bone surgeon and cancer researcher William Coley (1909) has prepared native supernatants from pure culture of *Streptomyces pyogenes* and *Serratia marcescens*, which he administered to 1200 neoplastic patients. The results were encouraging: tumour regression in 52 of them, and out of these, 30 patients were completely recovered. Its discovery preceded with 19 years the discovery of the very first antimicrobial compound, penicillin, by Alexander Fleming, in 1928, which opened a new era in infections treatment. Since then, the antibiotic classes of anthracyclines, peptides and quinolones, were proved to have specific inhibitory effects on tumour cells and anti-bacterial cells, some of their members being used as anti-cancer agents with high clinical importance (Rao et al., 1962). The purpose of this minireview is to present the mechanisms of action, main representatives and side effects of these anti-cancer agents.

Anthracyclines

Anthracyclines are polyketides (condensed planar heterocycles) containing anthracene as core structure (fig.1). Polyketides are complex molecules, belonging to the group of actinobacteria secondary metabolites, mainly synthesized by members of *Streptomyces* group, or to the semisynthetic derivatives containing 7,8,9,10-tetrahydrotetracen-5,12 quinone structure. According to Katz & Donadio (1993), there are two classes of polyketides: aromatic and complex. They have both antitumor and antibacterial activity. The first members of this group of compounds were reported by Brockman and Bauer (1950) and their use as anti-tumour agents started with daunorubicin discovery. Natural anthracyclines are isolated from fungal species, while the synthetic ones are obtained by glycosylation with rodosamine (including amino sugars), *daunosamine* and neutral glycosides. Some of them, such as aglycon, are usually inactive, but amongst hundreds of anthracyclines molecular analogues with antitumoral and antimicrobial activity, FDA approved a small number for clinical administration: *actinomycin D* (dactinomycin), *daunorubicin*, *doxorubicin*, *epirubicin*, *idarubicin*, *mitomycin*, *mitoxantrone*, *plicamycin*, *valrubicin*, *enediyne*, *guanorycin*, etc. (Saeidnia, 2015). Some of these are active, especially after chemical change, irrespective of cell cycle stage, even in G₀, inhibiting proliferation, acting as pro-apoptosis and anti-epithelial-mesenchymal transition factors, thus inhibiting metastasis (Zhou J, 2013). Anthracy-

clines inhibit oxidative phosphorylation in mitochondria, inhibit DNA and RNA polymerases, DNA repairing enzymes, metallothionein synthesis (a protein synthesized by intestinal epithelial cells that inhibits Cu absorption, its synthesis being stimulated by Zn), topoisomerase I and II, helicase, stimulates free radicals release and the non-nucleolytic cleavage (Robert J & Gianni L, 1993).

Doxorubicin (adriamycin) was isolated from *Str. peucetius* and is a cytotoxic antibiotic with major importance in different types of neoplasia, including pediatric cancer (Hayward et al., 2013; Preet et al., 2015; Gao Yuan et al., 2020; Cheng et al., 2017). It has an amphiphilic (amphipathic) molecule; the water insoluble anthracycline ring is lipophilic and the saturated end of the cycle with numerous -OH groups associated with aminated carbohydrate daunosamine forms a hydrophilic center. The molecule is amphoteric because contains acid functions in phenolic groups and alkaline ones in the amino group of the carbohydrate. Doxorubicin binds to the cell membrane and plasmatic proteins and disturbs numerous cell functions. Enzymatic reduction of doxorubicin, by electron acceptance under the action of oxidases, dehydrogenases and reductases generates extremely active species, including free OH[•] radicals. Doxorubicin is also a DNA intercalating agent, blocking DNA and RNA replication and transcription and thus protein synthesis in cells with high growth and division rate. It also interacts with topoisomerase II forming complexes that break the DNA molecule. Cardiotoxicity of doxorubicin is explained by the inhibitory activity on topoisomerase and glutathione peroxidase, leading to increased oxidative stress in the absence of catalase in these cells (Thorn et al., 2011; Cagel et al., 2017; Hayward et al., 2013; Takemura & Fujiwara, 2007; Minotti et al., 2004).

Daunorubicin (daunomycin) is a glycoside derivative of anthracycline fermentation which contains an anthraquinone ring and daunosamine (an amino sugar). Daunorubicin rapidly penetrates cell, it accumulates in nucleus, intercalates in the DNA strand and daunosamine stabilizes the complex by additional interactions making the difference between daunorubicin and other intercalation agents as ethidium bromide – which establishes interactions only in the intercalation site. Another probable target being topoisomerase II, daunorubicin is an efficient inhibitor of DNA replication and transcription. By oxidation and reduction of anthraquinone, daunorubicin can generate cytotoxic free O₂^{•-} radicals, explaining the cumulative cardiotoxicity (Bloomfield et al., 1973; Marco et al., 1977).

Epirubicin is a DNA intercalating chemotherapeutic agent and also a topoisomerase II inhibitor (Cragg & Newman, RAPT vol 33) (Waters et al., 1999).

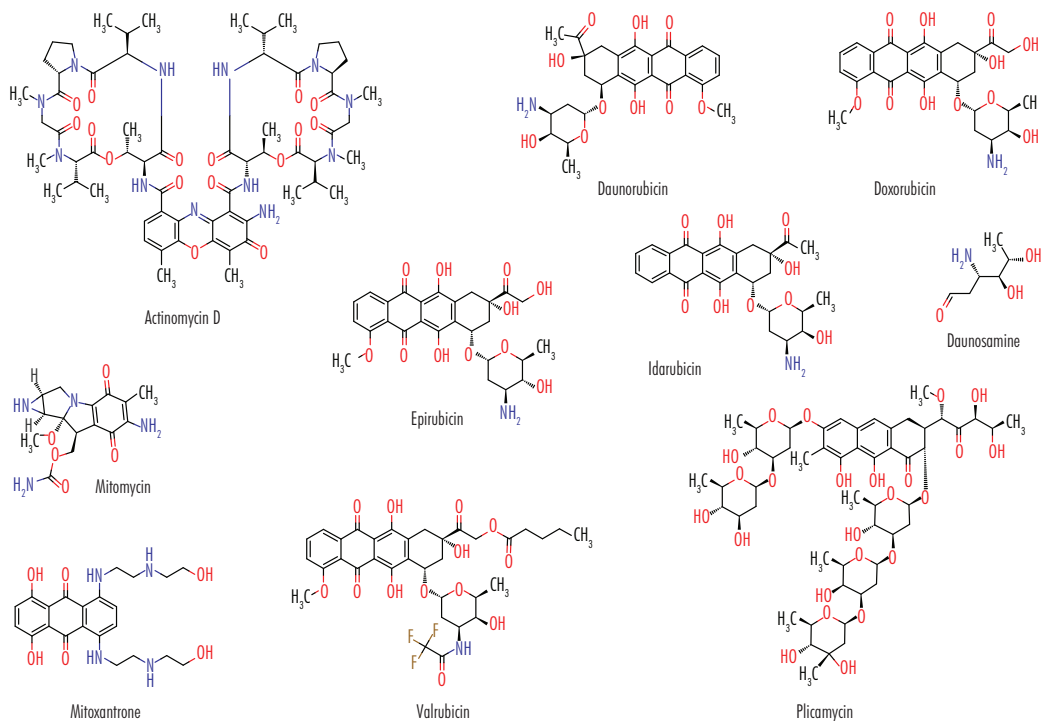


Figure 1. Chemical structures of some members of the anthracycline family, synthesized by microorganisms and having antimicrobial and antitumor activity. Actinomycin D is also a member of the peptide class of antibiotics which act as antimicrobial and antitumor agents.

Mitoxantrone (anthracenedione) inhibits lipid peroxidation, has a low toxicity to cardiac muscle, it contains no carbohydrate groups and produces no reactive oxygen species (Fox *et al.*, 1986).

Plicamycin has inhibitory effect against several neoplasia. It binds DNA sequences rich in GC in any stage of cell cycle, inhibits RNA and protein synthesis (Thurlimann *et al.*, 1992).

Idarubicin is an anthracycline antibiotic with antimetabolic and cytotoxic activity acting by DNA intercalation and topoisomerase II inhibition (Robert J & Gianni L, 1993).

The three members of mitomycin family: mitomycin A, mitomycin B, and mitomycin C are isolated from *Str. caespitosus*. After activation inside the cell by a reductase, mitomycin binds on a DNA single chain by alkylation, but also forms transversal links between chains. The effect is DNA depolymerization, with replication, transcription and protein synthesis inhibition (Verweij *et al.*, 1990; Tomasz & Palom, 1997, Bradner, 2001).

Peptide antibiotics

Actinomycines are a family of 50 chromopeptide antibiotics, but only two have therapeutic value. Actinomycin D

(dactinomycin) is synthesized by *Str. antibioticus* on a variety of chemically defined media and on complex organic media, and it is the first antibiotic which was proved to have antitumor activity (1943). Its molecule contains an aromatic group (polyphenolic ring) that binds with two cyclic polypeptide chains (fig. 2). Actinomycin D interacts with absolute specificity with deoxyguanine in DNA, similarly in eukaryotic and prokaryotic cells: the aromatic ring intercalates inside the DNA double helix at GC pairs, and the cyclic peptide remains outside and induces single and double strand breaks. Actinomycin D also inhibits RNA polymerase (inhibiting replication and transcription) and has played an important role in mRNA discovery. After RNA polymerase-catalyzed transcription is blocked, the synthesis of all forms of RNA, including those undergoing synthesis, is stopped. The antibiotic is not active on Gram negative bacteria because of reduced permeability, but spheroplasts are sensitive. Actinomycin D does not bind to RNA or mcDNA, and its affinity for double-stranded DNA depends on the guanine content, as synthetic double-stranded polynucleotides do not interact with the antibiotic (Farhane *et al.*, 2018; Koba & Konopa, 2005). Actinomycin D has cytotoxic and antineoplastic effects, inducing P53-independent

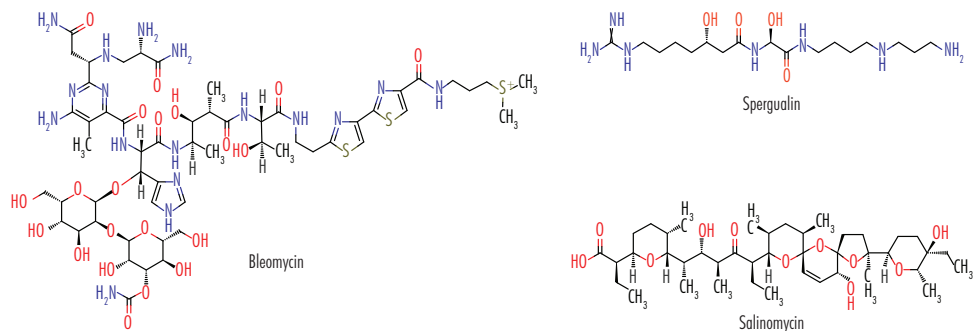


Figure 2. Chemical structures of some members of the peptide class of antibiotics as antimicrobial and antitumor agents, synthesized by microorganisms.

cell apoptosis (Prouvot et al., 2018; Dactinomycine accessed 20 February 2018; Hazel et al., 1983).

Sparguadin is a water-soluble peptide possessing a special chemical structure: it has a C-terminal guanidyl group and a C-terminal polyamine. It stimulates T-cell-mediated cytotoxic immunity (Umezawa K & Takeuchi T, 1987; Umezawa H et al., 1987, Nishikawa et al., 1986).

Bleomycin's molecule consists of a central heptapeptide that represents the binding site of different groups under the action of halogenases and transferases therefore generating a large structural diversity. Bleomycin was discovered by Hamao Umezawa (1962) in *Str. verticillus* cultures filtrates bacterium. All bleomycins have the same general structure, but differ by function group attached to the terminal amino group (ACS - Chemistry for life, 2020). The natural form is a mixture of two glycopeptide antibiotics: Bleomycin A2 and Bleomycin B2, bound with 3 carbohydrate residues. Bleomycin binds DNA and possibly RNA. In the presence of Fe^{+2} forms a *pseudoenzyme* that interacts with O_2 resulting in the release of superoxide (*in vitro* O_2^-) and OH^- groups that cleave DNA resulting single and double strand breaks (Segerman et al., 2013). Bleomycin sulfate is used to treat Hodgkin and non-Hodgkin lymphoma, squamous cell carcinomas and cancer-related pleural effusion. Some bacterial and tumour cells encode a bleomycin-inactivating hydrolase, which hydrolyses the amide group attached to beta-amino alanine. The protection degree against bleomycin depends on hydrolase level (Sugiyama & Kugamai, 2002; Bayer et al., 1992; Baidara & Mandal, 2020, Latta et al., 2015; Egger et al., 2013).

Salinomycin is a monocarboxylic polyether isolated from *Str. albus* (Miyazaki et al., 1974) and is used as an antibacterial, antifungal, antiparasitic and antitumoral drug (Hyun-Gyo Lee et al., 2017, Zhou et al., 2013, Gupta et al., 2009). The polyether skeleton acts as a cationic ionophore, forming complexes with metal cations and interfering with

the ion exchange function of the cell membrane. It binds to monovalent cations ($Na > K > Cs$) and divalent cations ($Sr > Ca > Mg$), having high affinity for K ions, and interferes with its transmembrane potential. Both *in vivo* and *in vitro*, it induces ROI (extracellular reactive oxygen intermediates) release and apoptosis of leukemic CD4 cells, but not of CD4 cells sampled from healthy individuals (Piperno et al., 2016). Salinomycin is EMT and metastases inhibitor (Chen 2014).

Quinolones

Quinolones (also called 4-quinolones) are a family of molecules that share the quinolinic nucleus. They are the first synthetic antimicrobial agents obtained by synthesis. Changes in the chemical structure of nalidixic acid have given rise to the new generation quinolones or fluoroquinolones

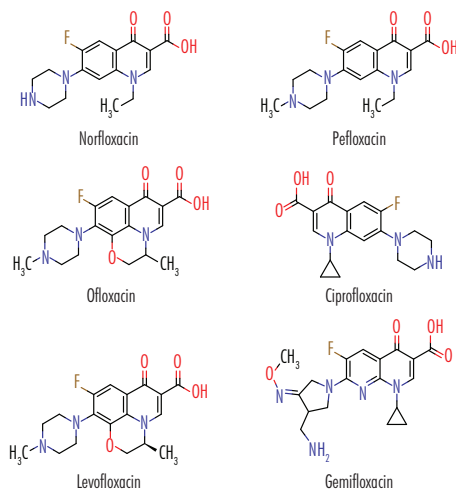


Figure 3. Chemical structures of some members of the quinolone class of antibiotics as antimicrobial and antitumor agents, synthesized by microorganisms.

(norfloxacin, pefloxacin, ofloxacin, ciprofloxacin, levofloxacin etc.) which have an extended antibacterial spectrum. Along with beta-lactams and macrolides, quinolones are one of the most widely used antimicrobial agents used in humans. Quinolones inhibit the DNA gyrase quickly stopping the replicative DNA synthesis. Quinolones are toxic to mammalian cells *in vitro* and *in vivo* experimental models (Goto & Wang 1985; Warren, 1985; Liu, 1989).

Among fluoroquinolones, the most used is ciprofloxacin, which has a wider antibacterial spectrum compared to nalidixic acid. In ciprofloxacin molecule, fluorine ensures activity on Gram-positive bacteria, piperazine group increases anti-enterobacteria activity and piperazine and cyclopropyl groups enable anti-*Pseudomonas* activity. Ciprofloxacin is widely used in the therapy of urinary, respiratory and gastrointestinal infections. It is also active on cell lines from human and animal bladder neoplasia. Ciprofloxacin has anti-proliferative and pro-apoptosis effects, since *gemifloxacin* is EMT (anti-epithelial-mesenchymal transition) and metastases inhibitor (Chen 2014).

Conclusions

Since the discovery of their antitumor effect, three main classes of antibiotics were used as adjuvants in cancer therapies: anthracyclines, peptide antibiotics and quinolones. They have both antimicrobial and antitumoral activity, being able to induce DNA breaks and to inhibit DNA and RNA synthesis and protein synthesis. Through these mechanisms, the antitumor antibiotics inhibit EMT and metastases formation (salinomycin, gemifloxacin), induce P53-independent cell apoptosis, stimulate T-cell-mediated cytotoxic immunity, thus exhibiting anti-proliferative and pro-apoptosis effects.

Conflict of interest

The authors declare that they have no conflict of interest.

Acknowledgements

This research was funded by ICUB, grant number 2153/01.02.2022, the Ministry of Research, Innovation and Digitalization through Program 1—Development of the national R&D system, Subprogram 1.2—Institutional performance—Financing projects for excellence in RDI, Contract no. 41 PFE/30.12.2021 and UEFISCDI-FDI 2022-0675. The funders had no role in the design of the study; in the collection, analyses, or interpretation of data; in the writing of the manuscript or in the decision to publish the results.

Bibliography

1. ACS chemistry for life – Bleomycin –Molecule of the week Archive, 2020)

2. Baidara P & Mandal M S - Bacteria and bacterial anticancer agents as a promising alternative for cancer therapeutics - Biochimie, vol. 177, 2020, pag. 164/189, 2018. doi:10.1016/j.biochi.2020.07.020
3. Bayer R A et al. – Bleomycin in non-Hodgkin's lymphoma. Semin.Oncol.1992;19(suppl.5):46-53
4. Bloomfield C D et al. – Daunorubicin-prednisone remission induction with hydroxyurea maintenance in acute non-lymphoblastic leukemia – Cancer, 1973-Wiley On line Library
5. Bradner W. T -Mitomycin C: A clinical update. Cancer Treat. Rev. 2001; 27(1):35-50. doi:10.1053/ctrv.2000.0202
6. Brokman H, Bauer K – Rhodomycin, ein rotes antibiotikum aus actinomyceten – Naturwissenschaften.1950; 37(21):492-493. doi:10.1007/BF00623151
7. Cagel M. et al. – Doxorubicin: Nanotechnological overviews from bench to bedside. Drug Discov. Today.2017; 22:270-281. doi:10.1016/j.drudis.2016.11.005
8. Chen T C et al. – Gemifloxacin inhibits migration and invasion and induces mesenchymal-epithelial transition in human breast adenocarcinoma cells. J Mol Med (Berl) 2014; 92(1):53-64
9. Cheng M et al. – Molecular Effects of Doxorubicin on choline Metabolism in Breast Cancer[J] Neoplasia. 2017; 19(8):617-627
10. Coley W. B. – The treatment of inoperable by bacterial toxins (the mixed toxins of the *Streptococcus erysipelas* and *Bacillus prodigiosus*) Proc. R. Soc. Med. Surg. 1909;3:1-48
11. Cragg G M et al. – Natural Product Drug Discovery and Development - Recent Advances in Phytochemistry, RAPT, vol 33, pp 19-32
12. Cragg G M and Newman D J – Natural Products discovery and development at the United States National Cancer Institute – Recent Advances in Phytochemistry, RAPT, vol 33, pp 1-19
13. Cragg G M, Newman D J, Snader K M – Natural products in drug discovery and development – J Nat Prod. 1997;60(1):52-60. doi:10.1021/np9604893
14. Dactinomycine.[(accessed on 20 February 2018)]; Available on line: <http://medycyna.anauk.net/101-0393-Encyklopedia.Lekow.html>
15. Egger C. et al. – Administration of bleomycin via the oropharyngeal aspiration route leads to sustained lung fibrosis in mice and rats as quantified by UTE-MRI and histology. PLoS ONE. 2013; 8:e63432. doi:10.1371/journal.pone.0063432
16. Farhane Z. et al.- An in vitro study of the interaction of the chemotherapeutic drug Actinomycin D with lung cancer

- cell lines using Raman micro-spectroscopy. *J. Biophotonics*.2018;11:e2001700112. doi:10.1002/jbio.201700112
17. Gao Yuan et al. – Antibiotics for Cancer Treatment: A double-edged sword – *J Cancer*. 2020;11(17):5135-5149. doi:107150/jca.47470
18. Goto T & Wang JC, 1985 - Cloning of yeast Topo I, the gene encoding DNA Topo I and construction of mutants defective in both DNA Topo I and DNA Topo II. *Proc. Natl. Acad. Sci. USA* 82, 7178/7182
19. Gupta B Piyush et al. - Identification of Selective Inhibitors of Cancer Stem Cells by High-Throughput Screening – *Cell*, 645-659, 2009. doi:10.1016/j.cell.2009.06.034
20. Hayward R et al. – Tissue retention of Doxorubicin and its effects on cardiac, smooth and skeletal muscle function. *J Physiol Biochem*. 2013; 69(2):177-87. doi:10.1007/s13105-012-0200-0
21. Hazel G A et al. – Treatment of metastatic carcinoid tumor with dactinomycin or dacarbazine – *Cancer Treat Rep*. 1983 jun; 67(6):583-5
22. Hyun-Gyo Lee et al. – Salinomycin reduces stemness and induces apoptosis on human ovarian cancer stem cell - *J Ginecol Oncol*; 2017 Mar; 28(2):e14. doi:10.3802/jgo.2017.28.e14
23. Katz L, Dnadio S – Polyketide synthesis: prospects for hybrid antibiotics – *Annu Rev Microbiol*.1993; 47:85-912. doi:10.1146/annurev.mi.47.100193.004303
24. Koba M.& Konopa J. – Actinomycin D and its mechanism of action. *Postepy Hig. Med. Dosw*. 2005;59:290-298
25. Latta V. D., et al. – Bleomycin in the setting of lung fibrosis induction: From biological mechanisms to contraindications. *Pharmacol.Res* 2015; 97:122-130. doi:10.1016/j.phrs.2015.04.012
26. Liu L F- DNA topoisomerase poisons as antitumor drugs. *Annu. Rev. Biochem*. 1989; 58:351-375
27. Marco A D et al. – Changes of activity of daunorubicin, adriamycin and stereoisomers, following the induction or removal of hydroxyl groups in the amino sugar moiety [J] – *Chemico-Biological Interactions*, 1977; 19(3):291-302
28. Minotti G et al. – Anthracyclines: Molecular Advances and Pharmacologic Developments in Antitumor Activity and Cardiotoxicity. *Pharmacol. Rev*. 2004; 56:185-229
29. Miyazaki Y et al. – *J. Antibiot. (Tokyo)* 1974, 27, 814
30. Nishikawa N et al. – Antitumor activity of Spergualin, a novel antibiotic. *The Journal of Antibiotics (Tokyo)*, 1986; 39(10): 1461-1466. doi:10.7164/antibiotics.39.1461
31. Piperno Anna et al. – Chemistry and Biology of salinomycin and its analogues. doi:http://dx.medra.org/10.17374/targets.2016.19.177
32. Preet S et al.-Effect of nisin and Doxorubicin on DMBA-induced skin carcinogenesis-A possible adjunct therapy. *Tumor Biol*. 2015; 36:8301-8308 doi:10.1007/s13277-015-3571-3
33. Prouvot C et al. – Efficacy and safety of Second line 5-Day Dactinomycin – *Int J Gynecol Cancer*. 2018 Jun; 28(5):1038-1044. doi:10.1097/IGC.0000000000001248
34. Rao K V et al. – Chemotherapy. New antibiotic with antitumor properties. 1962; 12:182-186
35. Robert J & Gianni L – Pharmacokinetics and metabolism of Anthracyclines. *Cancer Surv*. 1993; 17:219-252
36. Saeidnia S.- Anticancer Antibiotics [M]/New Approaches to Natural Anticancer Drugs. 2015
37. Segerman J Z et al. – Characterization of bleomycin-mediated cleavage of a hairpin DNA library. *Biochemistry*. 2013; 52, 31, 5315-5327. doi:10.1021/bi400779r
38. Sugiyama M & Kugamai T - Molecular and structural biology of bleomycin and its resistance determinants. *J of Bioscience and Bioengineering*, vol 93, issue 2, 2002, pages 105-116. https://doi.org/10.1016/S1389-1723(02)80001-9
39. Takemura G & Fujiwara H –Doxorubicin induced cardiomyopathy from the cardiotoxic mechanisms to management. *Prog Cardiovasc Dis*. 2007;49(5):330-352. doi:10.1016/j.pcad.2006.10.002
40. Thorn et al.- Doxorubicin pathway: Pharmacodynamics and adverse effects. *Pharmacogenet.Genom*.2011; 21:440-446. doi:10.1097/FPC.0b013e32833ffb56
41. Thurlimann B et al. – Plicamycin and pamidronate in symptomatic tumor-related hypercalcemia: a prospective randomized crossover trial [J]- *Anal of Oncology: official journal of the European Society for Medical Oncology*. 1992; 3(8):619
42. Tomasz M & Palom Y – The mitomycin bioreductive antitumor agents. Cross linking and alkylation of DNA as the molecular basis of their activity. 1997;76(1-3):73-87. doi:10.1016/s0163-7258(97)00088-0
43. Umezawa K & Takeuki T –Spergualin: a new antitumor antibiotic –*Biomed Pharmacother*. 1987; 41(5):227-32.
44. Umezawa H et al. – Involvement of Cytotoxic T-lymphocytes in the antitumor activity of Spergualin against L1210 cells – *Can Res*. 1987 jun;47(12):30-62-5
45. Verweij J, Pinedo H.M. – Mitomycin C: Mechanism of Action, usefulness and limitations – *Anticancer Drugs*. 1990; 1:5-13. doi:10.1097/00001813-199010000-00002
46. Warren E R – DNA topoisomerases as Targets for Cancer Therapy. *Biochemical Pharmacology*. Vol 34. No 24, pp 4191-4195. 1985

47. Waters J S et al. – Long term survival after epirubicin, cisplatin and fluorouracil for gastric cancer: results of a randomized trial. *Br J Cancer*. 1999;80(1-2):269-272
48. Zhou J et al. – Salinomycin induces apoptosis in cisplatin-resistant CRC cells by accumulation of reactive oxygen species. *Toxicol Lett*. 2013; 222(2):139-145



Received for publication: May, 06, 2021
Accepted: May, 26, 2022

Original paper

The connection between nicotinic and adenosinic system in analgesia

**CLAUDIA MARIANA HANDRA¹, ISABEL GHIȚĂ², DANIELA GEORGESCU²,
MARINELA CHIRILĂ³**

¹Department of Occupational Medicine, Faculty of Medicine, “Carol Davila” University of Medicine and Pharmacy Bucharest, 8, Eroilor Sanitari Street, 050474, Bucharest, Romania

²Department of Pharmacology and Pharmacotherapy, Faculty of Medicine, “Carol Davila” University of Medicine and Pharmacy Bucharest, 8, Eroilor Sanitari Street, 050474, Bucharest, Romania

³„Titu Maiorescu University”, Faculty of Pharmacy, Bucharest, Romania

Abstract

Determination of analgesic effects of different substances is important since this a very complex process that occur in the human body. The purpose of the present study was to evaluate the analgesic effect of caffeine and nicotine, both alone and in combination, using writhing test and hot plate test. The study used Swiss albino strain male mice, weighting 25 to 35 grams. The substances were administered subcutaneously. In the first experiments caffeine was administered in doses of 1 mg/kg and 5mg/kg and nicotine in doses of 1 mg/kg and 4 mg/kg. The last experiment evaluated the association between caffeine 5 mg/kg and nicotine 4 mg/kg. 30 minutes after administration, both doses of caffeine caused an antinociceptive effect, while nicotine induced analgesia only when the dose was increased to 4 mg/kg bw. Furthermore, when administered simultaneously, the two substances behaved like potentiating each other's effect, but additional research is needed in order to understand the mechanism of action.

Keywords

Nicotine, caffeine, analgesia

To cite this article: HANDRA CM, GHIȚĂ I, GEORGESCU D, CHIRILĂ M. The connection between nicotinic and adenosinic system in analgesia. *Rom Biotechnol Lett.* 2022; 27(2): 3429-3433
DOI: 10.25083/rbl/27.2/429.3433

✉ *Corresponding author: Assoc. Prof. Isabel Ghiță MD, PhD. Address: Blvd. Eroii Sanitari Nr. 8.
Telephone: 0744887571. Email address: isabelghita@yahoo.co.uk

Introduction

Pain is defined, according to the International Association for the Study of Pain, as an unpleasant sensory and emotional experience associated with actual or potential tissue damage or described in terms of such damage [1]. Each individual describes pain differently, according to his past experiences and particular genetic background, but it is generally accepted that the human body uses this unpleasant sensation as an alarming signal to remove the injurious stimuli.

Physiologically, pain is classified as slow and fast pain, both categories serving different transmission pathways, but identical receptors, respectively the free nerve endings. One essential characteristic of nociceptive receptors is the lack of adaptation towards distress which massively influences the perception of pain.

Existing studies show that natural plant extracts are able to influence nociception, among other biological properties, like the antioxidative, anti-inflammatory, antiulcerogenic or immunomodulatory ones. *Plantago* species is a good example with its biologically active agents: flavonoids, iridoids, caffeic acid derivatives, polysaccharides, glycosides and terpenoids. Radu N and the team investigated the analgesic effects of various *Plantago* species. The study conducted of N. Radu et al. [2] proved the existence of a connection between polysaccharide extracts of *Plantago* species and pain perception; this study showed that polysaccharide extracts of *Plantago* species decreased analgesia. Further research showed that flavonoid extracts have no analgesic effects [3]. Moreover, a study that assessed the antinociceptive effect of iridoid extracts showed a partial analgesic response during writhing tests [4].

Caffeine is the most popular psychostimulant in the world, mostly consumed as coffee. It is a natural methylxanthine which stimulates the central nervous system, increases clinical alertness and generates restlessness by acting as a phosphodiesterase inhibitor, adenosine receptor antagonist and intracellular calcium modulator [5]. However, the biological effects of caffeine are predominantly provided by antagonizing adenosine receptors and affecting the adenosinergic tonus, which explains its effects when used acutely [6].

As mentioned above, caffeine inhibits adenosine receptors (A1, A2A, A2B, A3) which all show effects on spinal glial cells regarding the adjustment of nociception. However, recent studies indicate caffeine has more affinity at A1, A2A and A3 receptors compared to the A2B ones [7]. Even if adenosine receptors have similar distributions, they modulate nociception differently and, consequently, these complex mechanisms influence the way caffeine behaves

towards analgesia. Nevertheless, recent data indicates occurrence of differences between genders that should be considered while assessing the efficacy of adenosine-based analgesics [7].

Nicotine, a highly addictive alkaloid found in tobacco plants, has both stimulatory and inhibitory effects on acetylcholine release. The mechanism of action depends on the administered dose and the predominance of either sympathetic or parasympathetic innervation of the selected organ system. Regarding the central nervous system (CNS), nicotine causes stimulation, thus improving concentration and reaction time. It diminishes stress and anxiety levels, while recent studies suggest nicotine could also have analgesic effects [8].

Several studies that investigated the role of nicotine in inducing antinociception by modulating the release of neurotransmitters, such as acetylcholine [8, 9, 10], glutamic acid [11] and other neuromodulators (dopamine, serotonin, noradrenaline) [8]. Hormonal signaling is implied as well, as in the case of corticotropin-releasing hormone [12].

Most importantly, nicotine, commonly consumed as cigarettes, is toxic and highly addictive, the addiction potential being influenced by genetic factors [13]. Considering these, nicotine is considered as it one of the most dangerous drugs available for everyday use.

Based on these literature data, our aim was to assess the way caffeine and nicotine affect analgesia and if both substances influence each other throughout the three experiments we conducted.

Material and methods

The analgesic effects of caffeine and nicotine were evaluated in three experiments on mice. The purpose of the first experiment was to study the sensitivity to pain 30 minutes after the administration of one dose of caffeine. The second experiment aimed to assess the analgesic effect of a single dose of nicotine 30 minutes after administration and the last experiment studied the identical behavior 30 minutes after administering simultaneously caffeine and nicotine.

The hot-plate and writhing tests were used to determine the analgesic effect of caffeine and nicotine. Pre-administered analgesic drugs, such as opioids, increase pain tolerance, the animal thus spending more time on the heated plate and writhing less compared to the control group.

3 groups of 12 albino male mice were used for conducting the experiments with caffeine and nicotine alone, while the third experiment, which combined both substances, used 4 groups of 12 albino male mice. All the animals weighted between 25 and 30 grams and were provided by the "Carol Davila" University of Medicine and

Pharmacy Bucharest bio-base. The mice were brought to the laboratory 24 hours prior to the start of the tests and were kept in standard environmental conditions with *ad libitum* access to food and water. The animals were housed in plexiglass cages (bed of wood chips), 12 mice per cage. The ambient temperature was set between 21°C and 24°C while the relative humidity was maintained between 45% and 60%.

The first experiment implied the administration of one dose of caffeine - 1 mg/kg bw or 5 mg/kg bw compared to the second experiment where nicotine was used in single doses of 1 mg/kg bw or 4 mg/kg bw. Finally, the third stage of our study combined caffeine 5 mg/kg bw and nicotine 4 mg/kg bw. Both substances were provided by Sigma Aldrich and were dissolved in 9‰ sodium chloride in order to administer 0.1 mL/10 g bw of solution. Additionally, all control groups received 0.1 mL/10 g bw of saline solution and each writhing test required 0.15 mL/10 g of acetic acid in concentration of 0.75%. The acetic acid was injected intraperitoneally while the other substances were administered subcutaneously.

All three experiments implied conducting hot-plate and writhing tests 30 minutes after injecting subcutaneously caffeine, nicotine or sodium chloride.

In the hot-plate test, the mouse is placed individually on a plate previously heated to 55°C and maintained at this temperature. Physiologically, after feeling the excessive heat, the animal starts licking its paw or attempts escaping by jumping on the side of the plate. The timer was started when all 4 paws of the mouse touched the plate and stopped when the animal began licking its paw. The cut-off time for the reaction was 30 seconds. In the writhing test, after injecting intraperitoneally an irritant such as acetic acid, the abdominal muscles start contracting and the animal acquires antalgic positions by pressing its back on the floor. We chose to measure the number of contortions performed in 5 minutes. If a substance increases the average amount of time spent on the hot-plate and decreases the number of contortions, compared to the control, it is considered to have analgesic effects.

The study was approved by the local ethics committee of "Carol Davila" University of Medicine and Pharmacy, Bucharest. The ethical agreement obtained was in concordance with the European Directive 86/609/EEC/24.11.1986 and with Governmental Decision 37/30.01.2002 referring to protection of experimental animals.

The obtained data was analyzed using *Microsoft Office-Excel*. Means and standard deviations were calculated for each group and then, the *Student-t test* was applied. Results were considered statistically significant if $p < 0.05$.

Results and Discussion

Evaluation of antinociceptive effect 30 minutes after administering caffeine

During the writhing test, the group that received 1 mg/kg bw of caffeine had a decreased number of contortions, with an average of 14.33 writhings, compared to the control group which presented an average of 22.25 ($p < 0.05$). The 5 mg/kg bw dose determined mice to behave similarly, the average number of contortions being 15.16, lower than the result of 22.25 obtained by the control group ($p < 0.05$) (Fig.1).

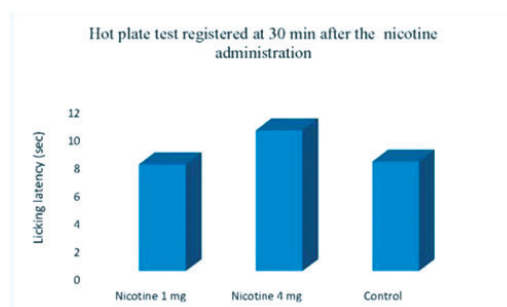


Figure 1. Writhing test: evaluation of antinociceptive effect 30 minutes after administering caffeine 1mg, 5mg and control.

In the hot-plate test, animals that were administered 1 mg/kg bw of caffeine spent, on average, 9.48 seconds on the heated surface, in contrast with the 7.88 seconds registered by those belonging to the control group ($p < 0.05$). Also, the dose of 5 mg/kg bw of caffeine caused an increased average amount of time, 9.52 seconds (Fig. 2), in comparison to control group's 7.88 seconds ($p < 0.05$).

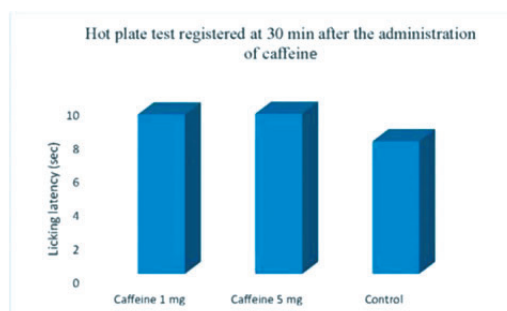


Figure 2. Hot-plate test: evaluation of antinociceptive effect 30 minutes after administering caffeine 1mg, 5mg and control

Evaluation of pain relief 30 minutes after administering nicotine

The writhing test conducted with the group which received 1 mg/kg bw of nicotine showed a diminished average number

of contortions, respectively 21.25, but the result is statistically insignificant considering the 22.5 average of the control group (Fig. 3). The batch injected with 4 mg/kg bw of nicotine performed, on average, 14.58 writhings, well below the average of the control group – 22.5 contortions ($p < 0.05$).

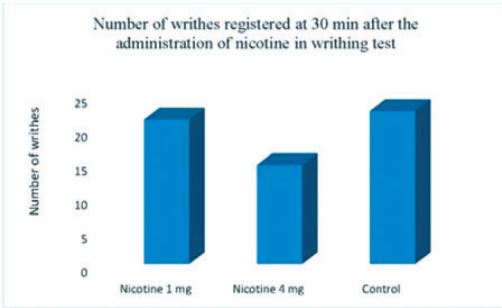


Figure 3. Writhing test: evaluation of antinociceptive effect 30 minutes after administering nicotine 1mg, 4mg and control

The hot-plate test revealed that 1 mg/kg bw of nicotine had induced a slight decrease - 7,64 seconds - in the average period of time the animals spent on the heated surface, which is statistically insignificant compared to the mean achieved by the control group – 7.84 seconds. In contrast, the mice treated with 4 mg/kg bw of nicotine (Fig. 4) resisted for an average of 10.08 seconds, far greater than the control group – 7.84 seconds ($p < 0.05$).

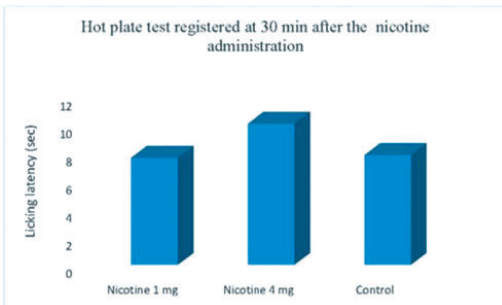


Figure 4. Hot-plate test: evaluation of antinociceptive effect 30 minutes after administering nicotine 1mg, 4mg and control

Evaluation of analgesia 30 minutes after administering caffeine and nicotine together

Regarding the writhing test, 5 mg/kg bw of caffeine determined an average number of 14.5 contortions, 4 mg/kg bw of nicotine obtained a mean of 13.5, while the control group recorded an average of 22.08 ($p < 0.05$ for each substance). Injecting simultaneously the previous doses of both drugs, the average number of contortions was 11.5 compared to the control group – 22.08 contortions ($p < 0.05$) (Fig. 5).

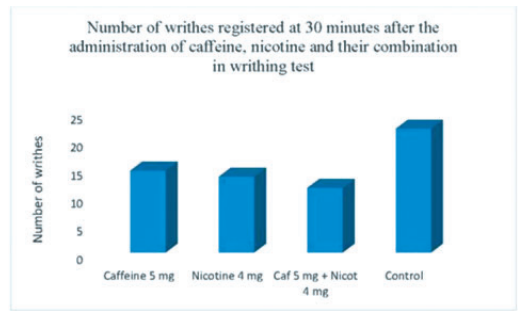


Figure 5. Writhing test: evaluation of analgesia 30 minutes after administering the combination of caffeine and nicotine

During the hot-plate test, 5 mg/kg bw of caffeine increased the average amount of time to 9.56 seconds, 4 mg/kg bw of nicotine did it to 10.37 seconds, while the control group managed to stay only 8.45 seconds on the plate ($p < 0.05$). As expected, combining the two substances led to a better outcome, which was 11.19 seconds, well above the average of 8.45 seconds achieved by the control ($p < 0.05$) (Fig. 6).

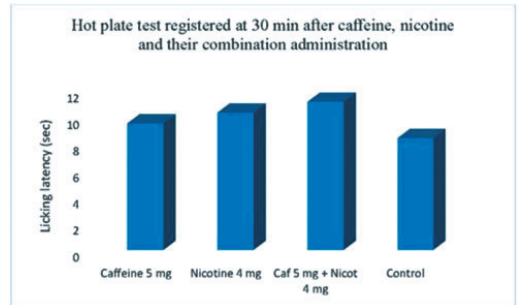


Figure 6. Hot-plate test: evaluation of analgesia 30 minutes after administering the combination of caffeine and nicotine

Conclusions

The results of the present study showed that, 30 minutes after administration, both doses of caffeine (1 mg/kg bw, 5 mg/kg bw) caused an antinociceptive effect by increasing pain tolerance throughout all experiments while only the high dose of 4mg/kg bw of nicotine induced analgesia. When administered simultaneously, the two substances behaved like potentiating each other’s effect, but additional research is needed in order to understand the mechanism of action.

In addition, lower dose of caffeine proved to have similar or even better antinociceptive effect than the higher dose which could represent a starting point for further studies.

References

1. INTERNATIONAL ASSOCIATION FOR THE STUDY OF PAIN, <https://www.iasp-pain.org/Education/Content.aspx?ItemNumber=1698>, accessed in 28.06.2020.
2. RADU N, GHITA I, RAU I. Therapeutic Effect of Polysaccharides from Plantago Species. *Mol. Cryst. Liq. Cryst.* 2010; 523: 236/[808]–246/[818].
3. NICOLETA R, GHITA I, COMAN O, RAU I. Therapeutic Effect of Flavonoids Derived from Plantago Species. *Mol. Cryst. Liq. Cryst.* 2010; 273/[845]–281/[853].
4. NICOLETA R, GHITA I, RAU I. Therapeutic Effect of Iridoid Compounds from Plantago Species. *Mol. Cryst. Liq. Cryst.* 2010; 523: 289/[861]–296/[868].
5. LAMARINE RJ. Selected health and behavioral effects related to the use of caffeine. *J Community Health* 1994; 19 (6): 449-66.
6. VOICULESCU M, GHIȚĂ I, SEGĂRCEANU A, FULGAI, COMAN O. Molecular and pharmacodynamic interactions between caffeine and dopaminergic system. *Journal of Medicine and Life* 2014; 7(4): 30-38.
7. SAWYNOK J. Adenosine receptor targets for pain. *Neuroscience* 2016; 338: 1–18.
8. CHIRILA M, GHITA I, FULGA I. Current knowledge on bupropion and varenicline clinical efficacy in nicotine dependence. *Farmacia* 2015; (1):1-7.
9. DAMAJ MI, FONCK C, MARKS MJ. Genetic Approaches Identify Differential Roles for $\alpha 4\beta 2$ Nicotinic Receptors in Acute Models of Antinociception in Mice. *J Pharmacol Exp Ther* 2007; 321:1161-1169.
10. UMANA IC, DANIELE CA, MCGEHEE DS. Neuronal nicotinic receptors as analgesic targets: It's a winding road. *Biochem Pharmacol.* 2016; 86(8): 1208-1214.
11. SCHROEDER JA, QUICK KF, LANDRY PM. Glutamate transporter (GLT-1) activation enhances nicotine antinociception and attenuates nicotine analgesic tolerance. *Neuroreport* 2011; 22(18): 970-973.
12. BAIAMONTE BA, VALENZA M, ROLTSCH EA. Nicotine Dependence Produces Hyperalgesia: Role of Corticotropin-Releasing Factor-1 Receptors (CRF1Rs) in the Central Amygdala (CeA). *Neuropharmacology* 2014; 77: 217-223.
13. MARINELA CHIRILĂ, ISABEL GHIȚĂ, CLAUDIA MARIANA HANDRA, ION FULGA: Genetic variants influencing smoking behavior and efficacy of smoking cessation therapies. *Romanian Biotechnological Letters Vol. 19, No. 5, 2014*
- 14.



Received for publication: May, 17, 2022
Accepted: May, 27, 2022

Original paper

Current status on in vitro propagation of sea buckthorn (*Hippophae* sp.)

**DUȚĂ-CORNESCU GEORGIANA^{1*}, CONSTANTIN NICOLETA¹,
POJOGA MARIA DANIELA¹, SIMON-GRUIȚA ALEXANDRA¹**

¹ University of Bucharest, Faculty of Biology, Department of Genetics, Intr. Portocalelor 1-3, sector 6, Bucharest, Romania

Abstract

Sea buckthorn, *Hippophae* spp., a dioecious shrub, is considered for a very long time a wonder plant, due to the fact that the leaves and berries contain a myriad of biological compounds which have been used in many domains related to human and animal health. For that reason, there is a huge market demand for elite varieties, resistant to biotic and abiotic stress. Because the traditional breeding and propagation methods are limited in their ability to produce such varieties so, plant biotechniques, encompassing plant tissue culture and genetic engineering have been applied. However, the development of optimal *in vitro* multiplication strategies of *Hippophae* spp. is very difficult, because sea buckthorn explants are sensitive to their sterilization treatment, plant growth regulators and nutrient composition of the culture medium. This paper is a review of the progress made in the application of the modern biotechnological tools in order to preserve genetic resources for mass production of sea buckthorn and create new varieties.

Keywords

Hippophae spp., in vitro, micropropagation, biotechnologies

To cite this article: DUȚĂ-CORNESCU G, CONSTANTIN N, POJOGA MD, SIMON-GRUIȚA A.
Current status on in vitro propagation of sea buckthorn (*Hippophae* sp.). *Rom Biotechnol Lett.* 2022; 27(2):
3434-3442 DOI: 10.25083/rbl/27.2/3434.3442

✉ *Corresponding author: georgiana.duta-cornescu@bio.unibuc.ro

Introduction

Sea buckthorn, *Hippophae spp.*, is a dioecious shrub-wide-spread in the temperate zone of Europe and Asia particularly in the Himalayas, at an altitude ranging between 2,100–3,600 m (CHAUHAN & al. [1]). It is considered a unique medicinal and aromatic plant, used from the most ancient times, many researchers considering that it has “momentous economic potential” and is predicted as the “next major health food” (SMALL & al [2]). In addition, due to the strong root system it is used in the recovery of areas affected by erosion and landslides; in symbiosis with *Frankia sp.* it fixes the atmospheric nitrogen with 2-fold higher rate than soya (CHEN & al. [3]).

Leaves and fruits of sea buckthorn biological compounds yields many important, with tremendous medicinal and pharmacological applications (Yang & Kallio [4], Zeb [5], CSERNATONI & al. [6], RĂCHIERIU & al. [7]). Not only that sea buckthorn berry vitamin content is much higher than in any other cultivated fruit or vegetable, but also these are rich in carotenoids, flavonoids, steroids, tannins, minerals, enzymes, amino acids, essential oils, and essential fatty acids (BARL & al. [8]). The leaves contain considerable amounts of proteins (averaging 20–21%) (LI & al. [9]) and triacylglycerols, free fatty acids, carotenoids, aldehydes, and triterpenes, which exhibit pharmacological properties. Tannins, flavonoids and other secondary metabolites have also been isolated from sea buckthorn leaves (GARCIA-GONZALES & al [10], TOLKACHEV & SHEICHENKO [11]).

The vulnerability of sea buckthorn to a variety of biotic and abiotic stress factors and the limitations of conventional breeding and propagation methods (KALIA & al. [12]) require the application of plant biotechniques, encompassing plant tissue culture and genetic engineering. The purpose of these actions is to create and preserve elite planting material for species of the genus *Hippophae*. *In vitro* tissue culture and micropropagation assays; of *Hippophae sp* have been reported since 1988 (MONTPETIT & LALONDE [13]), but from the beginning, it has been shown that clonal multiplication in sea buckthorn raised some difficulties, like low micropropagation ability, lower rooting rates and serious browning (YANG & al. [14]). During the past few years considerable progress has been made in the callus, organ and embryos cultures, regarding aspects related to selection and sterilization of explants, choosing of optimal media to induce callus, roots, somatic embryos, preventing browning, transplanting and acclimatization of the seedling (KALIA & al. [12])

This paper is a review of the progress made in the application of the modern biotechnological tools in order to preserve genetic resources for mass production of sea buckthorn and create new varieties.

Organogenesis, embryogenesis and callus formation

Two strategies can be used for *in vitro* plant cultivation in order to regenerate a new individual: using explants (like roots, leaf, stems, flower) to obtain organs (either shoots or roots) and/or inducing the formation of embryos (namely somatic embryos) from different plant materials (BHATIA & BERA [15]).

Organogenesis can be either direct or indirect. The direct organogenesis refers to the direct formation of buds or shoots from plant tissue with no intermediate callus stage. This regeneration strategy is used to reduce operational costs for plant propagation (because it generates high number of plant/explant), to produce transgenic plants and for clonal propagation since it ensures the production of uniform planting material without genetic variation (MUGUERZA & al. [16]). Indirect organogenesis refers to process in which plant organs are derived from a calli mass and is usually used for production of transgenic plant either by regeneration of a plant from transformed callus or by developing callus and shoots from an initial transformed explant (FRUGIS [17]).

The *in vitro* embryogenesis is the process in which a bipolar structure embryo-like can regenerate from somatic cells (any plant cell other than a gamete or germ cell) (ARNOLD & al. [18]). Because of the embryo origin in tissue culture, this process is named somatic embryogenesis (SE) and it can be direct or indirect. In direct somatic embryogenesis the embryo-like structures are formed from already differentiated cells, without intermediate callus generation. Indirect SE involves the formation of callus, which is then treated with different phytohormone combinations in order to form embryos (HUANG & al. [19])

Factors influencing *in vitro* plant cell culture

There are three main factors influencing *in vitro* plant regeneration, either by organogenesis or embryogenesis: explant type and age, phytohormone balance and growth conditions.

Explant

For inducing organogenesis, different parts of the plant have been used: leaf disks, stems, roots, sepals, but, the optimal explant type is usually adjusted for each plant species.

Hippophae sp. are particularly hard to multiply *in vitro*, drawbacks being low proliferation rate, vitrification, medium browning, poor rooting and different response to *in vitro* multiplication protocols due to genotypic differences between different species/cultivars (SRISKANDARAJAH

& LUNDGUIST [20]). The success of *in vitro* micropropagation is determined by the quality of explants which, in turn, influences their response to subsequent treatments. Factors like physiological state of the tissue, time of the year when the explants are collected and cultured influence the proliferation rate and the success of subcultures and acclimatization (KALIA & al. [12]). Regarding the type of the explant, in the recent years different parts of the plants have been used in order to regenerate sea buckthorn via either direct or indirect organogenesis. For example, LEE & al. [21] used cotyledons and leaf segments for induction of adventitious buds, SAIKIA & HADIQUE [22] used cotyledonary node explants excised from aseptically germinated seedlings of *Hippophae salicifolia*, while CHAUHAN & al. [1] successfully regenerated and acclimatized *H. salicifolia* plants generated via *in vitro* direct organogenesis starting from nodal segments of mature shrubs. RUAN *et al.* [23], summarizes, in a 2007 review paper, all types of explants used, up to that date, for *in vitro* regeneration of sea buckthorn plants: apical and axillary meristems, stem segments, axillary buds, leaves.

For successful *in vitro* regeneration, the age of the explants should also be taken into consideration. For example, in a study conducted in 2009, SRISKANDARAJAH & LUNDGUIST [24] compared the performances of shoot formation of different age leaf explants and concluded that the segments collected from seedlings had a higher regeneration rate than those collected from mature shrubs.

Till now there are only a limited number of studies reporting successful micropropagation via embryogenesis (LIU & al. [25], SRISKANDARAJAH & LUNDGUIST [24]). LIU & al. [25] showed that the cotyledon and hypocotyl explants were not as responsive as leaf explants for somatic embryogenesis, but most of somatic embryos were able to germinate and develop into complete plantlets, with survival rates ranging from 30 to 55% after 2 months in a greenhouse. However, in the process of somatic embryogenesis abnormal embryos were also formed (jointed embryos, abnormal bud embryos, embryos with one or multiple cotyledons). SRISKANDARAJAH & LUNDGUIST [24] used as explants leaves from 3-4 months old juvenile seedlings and from adult plants and also cotyledons and hypocotyls collected from 5 days old seedlings. They reported that the somatic embryogenesis was induced from all types of explants, with the embryos forming directly on the explant, without going through the callus phase. However, the frequency of somatic embryogenesis was different between the explants, the highest percent of somatic embryos being obtained from juvenile and adult leaf explants (65% and, 78% respectively).

Sterilization methods

One of the most important steps in initiating an *in vitro* cell culture is the sterilization of the explants. When using explants from seedling germinated in control lab conditions, the contamination is not an issue, but plant tissue from natural or greenhouses may be contaminated by various microarthropods (mites, trips, and their vectors), microorganisms (filamentous fungi, yeasts, bacteria), viruses, and viroids (ALTAN & al. [26], DA SILVA & al. [27], HESAMI & al. [28]) so appropriate and suitable treatments are required before the initiation of *in vitro* culture (MIHALJEVIĆ & al. [29]). There are numerous factors that can influence the performance of the sterilization process: type, age and size of the explant, the conditions of cultivation and physiological state of the stock plant and the types of disinfectant, their concentration and time of treatment (DA SILVA & al. [27]). In plant *in vitro* culture technologies, different types of disinfectants have been used, starting from calcium hypochlorite or sodium hypochlorite, mercury chloride, hydrogen peroxide, silver nitrate up to fungicides and antibiotics (MIHALJEVIĆ & al. [29], NONGALLEIMA & al. [30]). Some research (NONGALLEIMA & al. [30], DA SILVA & al. [27], HESAMI & al. [31]) indicate that using a longer time of treatment along with a more concentrated disinfectant the greater the efficiency of the sterilization process will be. However, the same researches point out that there is a negative correlation between the high concentration of the disinfectant and the explant viability, and also the survival and regeneration potential of plant tissues that will be used to initiate the *in vitro* culture. For example, when 2-3 cm shoot tips explants of *H. rhamnoides* were sterilized with a NaClO solution with 4-5% active Cl for 10 minutes, the survival rate was only between 16,5% - 21% (depending on the media used), with 15-25% of the cultures dying out of fungous and bacterial contamination and the rest 46.7-64.6% dying of browning. The researchers concluded that the high rate of mortality at the initiation stage was probably due to the high concentration of NaClO, because when a 2-3% active Cl solution and an 8 minutes sterilization time was used, the survival rates were much higher (between 27% and 95%, depending on the media used) (YAO [32]). Therefore, in order to obtain the best results of asepsis, the concentration of disinfectant solutions as well as the treatment time of the plant material must be adapted to the type, age, cultivation conditions and to the species from which the explant comes.

In *Hippophae sp.* micropropagation, different types of sterilization methods, solutions, concentrations and exposure times have been used. CHAUHON & al. [1] applied different pretreatments to the explants (consisting of nodal parts excised from twigs of *H. salicifolia*): liquid detergent (Teepol, 5-10 drops/100 ml.) followed by washing with Tween-20 (2

drops/100 ml solution) in gentle agitating conditions for about 5 minutes, and again washed under running tap water followed by fungicide treatment [0.1% Bavistin (50% carbendazim WP)] for 10 minutes. The surface sterilization was performed either with mercuric chloride solution or sodium hypochlorite (4% available chlorine) in various concentrations for different time duration. The best results (80% uninfected green explants) were obtained when explants were treated with HgCl₂ solution (0.10% w/v) for 7 minutes. SRISKANDARAJAH

& LUNDQUIST [24] sterilized on the surface their nodal stems and leaves from juvenile seedlings and adult tree explants with 1,5% (v/v) NaOCl and 0,03% (v/v) Tween 20 for 20 minutes, followed by 1 minute rinsing with 70% ethanol and their highest percentages of organogenesis was 85% (for juvenile leaf explants) and 75% (for adult explants). A summary of the different types of sterilization methods, solutions, concentrations and exposure times which have been used in various researches is presented in Table 1.

Table 1. Sterilization of *Hippophae sp.* explants

Species used	Type of explant	Initial washing/pretreatment	Surface sterilization	References
<i>H. rhamnoides</i>	shoot tips from 2-3 years old culture plant	70% ethanol - 1min	- NaClO solution with 4-5% active Cl – 10 min	YAO, 1995 [32]
<i>H. rhamnoides</i> variants Sinensis and Indian Summer	stem segments	DW – 30 sec	- 10% javex solution (5,25% NaOCl + 0,1% Tween 20) – 12 min	LUMMERDING, 2001 [33]
<i>H. rhamnoides</i>	seeds	W+5 drops of Tween-20	- 70 % ethanol - 5 min - 30 % NaOCl e plus two drops of Tween-20 per 100 cm ³ solution – 1 h	LIU & al., 2007 [25]
<i>H. rhamnoides</i>	nodal stem cuttings	-	- 1.5% (v/v) NaOCl and 0.03% (v/v) Tween 20 - 20 min, - rinsed with 70% ethanol - 1 min,	SRISKANDARAJAH & LUNDQUIST, 2009 [24]
<i>H. rhamnoides ssp turkestanika</i>	active bud		- 0.1% detergent (2 Hours), - Tetracycline (2 Hours), 70% EtOH (4 Min) and 0.1 % HgCl ₂ (6 Min)	SINGH & GUPTA, 2014 [34]
	dormant bud		- 0.1% detergent (5 Hours), -Tetracycline (over night), 70% EtOH (15 Min) and 0.1 % HgCl ₂ (18 Min).	
<i>H. salicifolia</i>	nodal segments	-wash in liquid detergent (Teepol, 5–10 drops /100 ml.) - washing with Tween-20 (2 drops/100 ml solution) in gentle agitating conditions - 5 min. - fungicide treatment [0.1% Bavistin (50% carbendazim WP) - 10 min.	- HgCl ₂ solution (0.10% w/v) - 7 min.	CHAUHON & al., 2019 [1]
<i>H. salicifolia</i>	Buds, leaves, and soft stem parts	-1.500 mg L ⁻¹ ascorbic acid and citric acid (each) solution – 1 h - DDW 3 to 4 times – 30 min	- 0.1% (v/v) Tween® 20 + 5.0% (v/v) sodium hypochlorite solution (4.5% total active chlorine - 20 min. - 4% (w/v) Bavistin solution dissolved in autoclaved DDW – 1h - 70% (v/v) ethanol – 70 s. - 0.01% (w/v) HgCl ₂ , – 3 min	TRIVEDI & al, 2020 [35]
<i>H. rhamnoides</i>	seeds	- 70% ethanol - 30 s	- 50% NaOCl solution – 30 min - methanol surface heating treatment	LEE & al., 2021 [21]

W = water, DW = deionized water, DDW = double distilled water

Plant growth media and regulators

It is well known that direct organogenesis is promoted if high concentrations of either auxins (which favors the formation of roots) or cytokinin (which favors the formation of shoots) are used (HUSAINI & al. [36]). A balance of both auxin and cytokinin leads to the development of mass of undifferentiated cells known as callus, whereas media with no or reduced auxin content promotes the development of somatic embryos. Auxins are also responsible for establishing cell polarity in the embryo (apical and basal axis) (MAFTEI & NICUTA [37]). In the case of somatic embryogenesis, it has been suggested that cytokinin thidiazuron-TDZ is more effective than other cytokinins for somatic embryogenesis (MAFTEI & NICUTA [37]), but recent studies (SRISKANDARAJAH & LUNDQUIST [24], LIU & al. [25]) have shown that other phytohormones, like Kin, IAA, NAA and BA can induce direct embryogenesis.

Media

For *in vitro* regeneration via direct or indirect organogenesis of sea buckthorn, the most used media for callus induction or direct organogenesis is MS (MURASHIGE & SKOOG [38]) (Table 2) but in the recent years other media have been used, like WPM (Woody Plant Media) (LIU & al. [25], LEE & al. [21], LLOYD & MCCOWN [39]), SH media (LIU & al. [25], SCHENK & HILDEBRANDT [40]), or other combinations, with different degrees of success. TRIVEDI & al., 2020 [35]; first inoculated the buds on plain agar medium (water agar medium without micromineral and macromineral nutrients), which consisted of 1.2% (w/v) agar-agar type 1 supplemented with 0.01% (w/v) myo-inositol and 3% (w/v) sucrose) and incubated them for 12-14 days before being transferred to MS medium or WPM containing 3% (w/v) sucrose, 0.01% (w/v) polyvinylpyrrolidone (PVP) and 0.8% (w/v) agar-agar type. LEE & al., 2021 [21], used WPM mixed with 2.5% glucose and 0.5% sucrose to induce root formation with cotyledons and leaf explants.

Initiation media PGRs (Plant Growth Regulators)

One of the most important activities of the initiation stage of every *in vitro* culture is the control of the phenolic compounds released into the medium and their oxidation, which may cause medium browning. This is a defensive reaction of wounded plant tissues and is induced by plant age, the cutting of the tissue segment, the application of chemicals, or even from over rigorous washing with water and detergents (GARCIA-GONZALES & al. [10]). Another physiological problem that may arise in *in vitro* cultures is hyperhydricity of tissues (formerly called "vitrification", term currently used to characterize cryopreserved tissues)

(KEVERS & al. [41]). Hyperhydric plants have curled leaves with deformed, glassy, and brittle shoots containing excess amount of water. The accumulation of excessive amounts of water causes severe problems during *in vitro* propagation, organogenesis, germplasm maintenance, cryopreservation, and acclimatization (SUNDARARAJAN & al. [20])

The initiation phase of an *in vitro* culture is finalized, i.e. the explant is "introduced and established", when the explant shows a morphogenic response characterized by multiplication and/or differentiation of the plant tissues such as: shoots, roots, leaves or production of calli (CHRISTENSEN & al. [42]).

In organ culture of sea buckthorn, different initiation media have been used, most of them being a combination of an auxin and a cytokinin (usually BA = 6-benzyladenine), but high levels of PGRs such as BA, kinetin and 2, 4-D (2,4-dichlorophenoxy acetic acid) has been shown to induce hypertrophy and mortality (RUAN & al. [23], KALIA & al. [12]), SUN [43], GUO & XU [44], XU & LIANG [45] reported that the best initiation media for meristematic explants contained auxins (NAA = α -naphthaleneacetic acid or IBA = indole-3-butyric acid) at much lower concentration (0,003 – 0,01mg/L), then cytokinin BA (0,3 mg/L), while KANG & al. [46] and ZHOU & al. [47] used a balanced combination of IAA/NAA and BA (0,5 mg/L). CHAUHON & al. [1] used a BA (1.0 mg L⁻¹) + NAA (0.5 mg L⁻¹) + Adenine Sulphate (50.0 mg L⁻¹) combination to initiate an *in vitro* culture of *H. salicifolia* starting from nodal segments. There are also reports of initiation media containing only one type of phytohormone, either BA (LIU & al. [25]) either IBA (ZHAO & al. [47]). SRISKANDARAJAH & LUNDQUIST [24] showed that other growth regulators, including GA₃ (Gibberellic acid), growth-enhancing medium additives such as carbon sources and CPPU [N-(2-chloro-4-pyridyl) N-phenylurea] also enhanced the shoot production, since preculturing in WPM resulted in a tenfold higher production of shoots per root system.

Multiplication and regeneration media PGRs

Sea buckthorn is one of the most recalcitrant plants regarding *in vitro* propagation, explants having very specific requirements for PGR and nutrient composition of the culture media. (GUPTA & SIGH [48]). The optimal PGR type and concentrations of media for direct organogenesis of *Hippophae sp.* explants vary considerably between scientific reports. For example, SUN [43], ZHOU & al. [49], ZHOU & al. [47], obtained the best results for rooting when using a combination of auxins (either NAA or IBA) and cytokinin (either KT or BA) (Table 2), SRISKANDARAJAH & LUNDQUIST [24] used a combination of BAP and TDZ (Thidi-

Table 2. Plant growth media and regulators for tissue and organ culture in *Hippophae sp.*

Species/varieties	Explant	Optimal initiation media	Optimal multiplication media	References
Organogenesis				
<i>H. rhamnoides</i>	Nodal segments, apical meristems		full MS with 7.6 mM sucrose + 1 μ M BA	MONTPETIT & LALONDE, 1988 [13]
<i>H. rhamnoides ssp. sinensis</i>	Stem segments, lateral bud	$\frac{1}{2}$ B5 + IBA 0.4 mg/L + sucrose 1.5 % + agar 0.46 %	$\frac{1}{2}$ B5 + IBA 0.2 mg/L + IAA 0.2 mg/L	ZHAO & al., 1989 [5]
<i>H. rhamnoides ssp. mongolica</i>	Meristem	MS + IBA 0.01 mg/L + BA 0.2 mg/L		GUO & XU, 2000 [43]
<i>H. rhamnoides ssp. sinensis</i>	Cotyledon, hypocotyl, and meristem of aseptic seedling	$\frac{1}{4}$ MS + 6-BA 0.30 mg/L + NAA 0.002 mg/L	$\frac{1}{4}$ MS + NAA 0.05 mg/L + IBA 0.2 mg/L	XU & LIANG, 2001 [45]
<i>H. rhamnoides ssp. sinensis</i>	Nodal segments		MS + 1mg/ml TDZ	LUMMERDING, 2001 [33]
<i>H. rhamnoides ssp. sinensis</i> and <i>H. rhamnoides ssp. mongolica</i>	Stem segments	$\frac{1}{2}$ B5 + 6-BA 0.5 mg/L + IAA 0.5 mg/L	$\frac{1}{2}$ B5 + IAA (0.3-0.5 mg/L)	YANG & al., 2004 [14]
<i>H. rhamnoides ssp. mongolica</i>	Apical meristem	MS + NAA 0.03 mg/L ~0.05 mg/L + KT 0.3 mg/L ~0.5 mg/L	MS + NAA 0.002 mg/L + KT 1.0 mg/L	SUN, 2005 [43]
<i>H. rhamnoides ssp. mongolica</i>	Bud	B5 + 6-BA 0.5 mg/L + NAA 0.5 ~ 1.0 mg/L	$\frac{1}{2}$ B5 + 6-BA 0.1 mg/L + NAA 1.0 mg/L	ZHOU & al., 2005 [46]
<i>H. rhamnoides ssp. mongolica</i>	Meristem	$\frac{1}{2}$ MS + 6-BA 1.0 mg/L + IAA 0.5 mg/L		
<i>H. rhamnoides ssp. mongolica</i>	Hydroponic leaves	$\frac{1}{2}$ MS + 6-BA 0.5 mg/L + KT 0.2 mg/L + NAA 0.02 mg/L	$\frac{1}{2}$ B5 + 6-BA 0.3 mg/L + IBA 0.4 mg/L	ZHOU & al., 2006 [49]
<i>H. rhamnoides L</i>	Nodal segments, leaves, cotyledons, hypocotyls	WPM + 11 μ M BA + 5,811 μ M GA ₃ + 2,65 11 μ M NAA	MS + 4,5 11 μ M TDZ + 2,2 11 μ M BA + 0,53 11 μ M NAA	SRISKANDARAJAH & LUNDQUIST, 2009 [24]
<i>H. rhamnoides ssp. turkestanica</i>	Nodal segments with active and dormant buds Gupta and Singh	MS + 1ppM IBA	WPM with 3% sucrose + 1 ppm BAP + 0,5 ppm IAA	SINGH & GUPTA, 2014 [34]
<i>H. salicifolia</i>	Nodal segments	MS + 1,0 mg/L BA + 0,5 mg/l NAA + 50 mg/L ADS	$\frac{1}{2}$ MS + 1,0 mg/L IBA	CHAUCHAN & al, 2019 [1]
<i>H. salicifolia</i>	dormant and active buds	1.2% (w/v) agar supplemented with 0.01% (w/v) myo-inositol and 3% (w/v) sucrose	MS + 10 mg/L BA, 3 mg/L IAA + 2 mg/L GA ₃ WPM + 10 mg/L KN + 3 mg/L IAA + 2 mg/L GA ₃	TRIVEDI & al., 2019 [35]
<i>H. rhamnoides L</i>	Cotyledons, leaf segments	WPM + 1,0mg/l BA + 1,0 mg/L KN + 5 mg/l IAA	WPM + 1,0mg/l BA + 1,0 mg/L KN + 5 mg/l IAA	LEE & al., 2021 [21]
Embryogenesis				
<i>H. rhamnoides L</i>	cotyledons, hypocotyle, leaves	WPM + 0,5 mg/L BA	SH + 1,0 mg/L KN + 0,5mg/L IAA	LIU & al., 2007 [25]
<i>H. rhamnoides L. NAA</i>	Leaves		MS + 2 μ M CPPU + 0,53 μ M NAA + 2,2 μ M/13,2 μ M BA	SRISKANDARAJAH & LUNDQUIST, 2009 [24]

Media: MS = Murashige and Skoog (1962); B5 = B5 basic media (Gamborg, 1968, [50]), WPM = Woody Plant medium (Lloyd and McCown, 1980, [39]), SH = Schenk and Hildebrandt medium, (1972) [40]

Plant growth regulators: BA = 6-benzyladenine; IAA = indole-3-acetic acid; IBA = indole-3-butyric acid; KT = kinetin; NAA = α -naphthaleneacetic acid, TZD = Thidiazuron, ADS = adenin sulfat, GB₃ = Gibberellic acid, CPPU = N-(2-chloro-4-pyridyl) N-phenylurea,

azuron) or GA₃, BA and IAA to induce shoot organogenesis from either leaf explants or roots of intact seedlings, while SINGH & GUPTA [34] used a combination of BAP and IAA. SUN [43] indicated that the best rooting media was 0.002mg/L NAA + 1.0mg/L KN. Other researchers obtained the best results when using only BAP or TDZ (KALIA & al. [12]), while CHAUHON & al. [1] showed that, out of the 3 auxins tried for rooting of *in vitro* grown shoots (IBA 0.5–1.5 mg L⁻¹, IAA 0.5–1.5 mg L⁻¹, NAA 0.5–1.5 mg L⁻¹), the IBA (1.0 mg L⁻¹) gave maximum (60 ± 1.30%) rooting, with an average of 3.60 ± 0.09 roots per shoot after 8 weeks.

There are only a few reports of *in vitro* embryogenesis for *Hippophae* species. LIU & al., [25] successfully obtained somatic embryos after 40 days, using WPM medium supplemented with 0.5 mg dm⁻³ BA in absence of IBA. The first globular somatic embryos were formed after 20 days at the edges of cotyledon and leaf sections and over the surface of hypocotyls without callus formation and they proliferated and produced secondary embryos or embryo masses when transferred onto fresh media by the 45th day of culture.

SRISKANDARAJAH & LUNDQUIST [24] induced the formation of somatic embryos in MS-based medium supplemented with 2.0 IM CPPU, 0.53 IM NAA and varying concentrations of BA. They also observed a correlation between MS salt strength, BA concentration and age of the explant; the most effective media for juvenile explants was the combination of half strength MS salts and 2.2 I M BA, while for the adult explants the most effective was the combination full-strength MS salts and 13.2 I M BA.

Plant regeneration and acclimatization

From the numerous studies presenting organ and embryo cultures of *Hippophae sp.*, only few reported successful plant regeneration and, moreover, in the majority of cases, the regeneration rate was lower, even less than 10%. RUAN & al. [23], YAO [32] constructed a micropropagation system using WPM supplemented with BAP (0.125-0.25 mg/L for initiation and 0.4-1.0 mg/L for multiplication) and reported that after a period of 45 days growth in propagators the plants were transplanted to pots in a greenhouse and after more 40 days some plants were more than 30 cm high. At that time were planted in the field where grew normally. LUMMERDING [33] successfully micropropagated *H. rhamnoides ssp. sinensis* using chokecherry media (SBM) with 50% macroelements of MS basic media, but only 11 of the 427 rooted plants could survive transplanting. SRISKANDARAJAH & LUNDQUIST [24], successfully acclimatized plantlets in sand-vermiculite-perlite medium after rooting the shoots treated with IBA in medium supplemented with 6.15 IM IBA. LEE & al., [2] reported that shoots that have been im-

mersed for a 3 to 5 seconds in 100 ppm and 1,000 ppm of IBA and NAA solution, and then cultured in a sterilized soil, supplemented with ½ WPM (pH 5.7) formed roots. Plantlets with tiny roots were transplanted using mixed soil in outside condition and covered with a transparent acrylic plate which was removed after 3 weeks. The author doesn't present if any of these plantlets have survived. LIU & al., [25] reported that the survival rate of plantlets developed from somatic embryos induced from leaves, cotyledons and hypocotyls ranged from 30 to 55 % after growing in the greenhouse for 2 months. CHAUHON & al. [1] successfully transferred in the field regenerated plants of Himalayan *H. salicifolia* after the plantlets were first transferred to ¼ MS medium with 2% sucrose. After that, they were cultivated for 2-3 weeks in trays containing vermiculite in a mist chamber at temperature 30 ± 20°C and watered with 1/5 MS medium.

Conclusion and future perspectives

The development from the last few years in the field of *in vitro* micropropagation of *Hippophae sp* is spectacular, but the vast majority of researchers agree that much remains to be done. First of all, it is necessary to develop protocols that will generate comparable results when applied in different laboratories. However, in order to achieve this, it is essential to establish correlations between the genotype of the donor plant and the micropropagation protocol. This is not an easy task, because the genus *Hippophae* comprises 7 species and numerous subspecies, only *H. rhamnoides* including 8 subspecies. Therefore, for the realization of any correlations between the genotypic particularities and the specific requirements for PGR and nutrient composition of the culture media it is essential to perform complex genetic analyzes of the genomes of the species of interest, such as complete genomes sequencing and extensive characterization of genetic diversity and genetic relationships among and between different cultivars or species.

This comprehensive genetic analysis, along with efficient regeneration protocols are indispensable for obtaining genetic modified plants with improved traits regarding yield and harvesting and that can exceed the various types of pests, pathogens and climatic constraints that *Hippophae* species are vulnerable.

References

1. M.S. CHAUHAN, P. BISHT, M.S. BHANDARI. *In vitro* Propagation of Himalyan *Hippophae salicifolia* Through Nodal Segments. Acta Sci. Agric., 3(4), 314, 318 (2019).
2. E. SMALL, P.M. CATLING, T.S.C. LI, Blossoming Treasures of Biodiversity: 5. Sea Buckthorn (*Hippo-*

- phaë rhamnoides) - an ancient crop with modern virtues. *Biodivers. J.*, 3, 25, 27 (2002).
3. G. CHEN, Y. WANG, C. ZHAO, H. KORPELAINEN, C. LI, Genetic Diversity of *Hippophae rhamnoides* Population at Varying Altitudes in the Wolong Natural Reserve Reserve of China as Revealed by ISSR Markers, *Silvae Genet.*, 57 (1), 29, 36 (2008).
 4. B.R. YANG, H.P. KALLIO, Composition and physiological effects of sea buckthorn (*Hippophae rhamnoides*) lipids. *Trends Food Sci, Technol.*, 13, 160, 167 (2002).
 5. A. ZEB, Important Therapeutic Uses of Sea buckthorn (*Hippophaë*); a Review. *J. Biol. Sci.* 4, 687, 693 (2004).
 6. F. CSERNATONI, R. M. POP, F. ROMACIUC, F. FETEA, O. POP, C. SOCACIU, Sea buckthorn juice, tomato juice and pumpkin oil microcapsules/ microspheres with health benefit on prostate disease – obtaining process, characterization and testing properties. *Rom. Biotechnol. Lett.*, 23 (1), 13214, 13224 (2018).
 7. C. RĂCHIERIU, F. GRAUR, E. MOIS, C. SOCACIU, D.T. ENIU, N. AL HAJJAR, Metabolomic profile of colorectal cancer patients and its clinical implications. *Rom. Biotechnol. Lett.* 25(6), 2045, 2054 (2020).
 8. B. BARL, L. AKHOV, D. DUNLOP, S. JANA, W.R. SCHROEDER, Flavonoid content and composition in leaves and berries of sea buckthorn (*Hippophaë* spp.) of different origin. *Acta Hort. (ISHS)*, 626, 397, 405 (2003).
 9. T.S.C. LI, D. WARDLE, Effect of harvest period on the protein content in sea buckthorn leaves. *Can. J. Plant Sci.*, 83(2), 409, 410 (2002).
 10. R. GARCIA-GONZALES, K. QUIROZ, B. CARRASCO, P. CALIGARI, Plant tissue culture: Current status, opportunities and challenges. *Cienc. Inv. Agr. [online]*, 37(3), 5, 30 (2010).
 11. O.N. TOLKACHEV, O.P. SHEICHENKO, Flavonoids of seabuckthorn (*Hippophaë rhamnoides* L.): Chemistry and Pharmacology, In: *Seabuckthorn*, II, V. SINGH ed., Daya Publishing House, New Delhi, India, 2006, p. 159- 167.
 12. R.K. KALIA, R. SINGH, M.K. RAI, G.P. MISHRA, S.R. SINGH, A.K. DHAWAN, Biotechnological interventions in sea buckthorn (*Hippophae* L.): current status and future prospects. *Trees*, 25, 559, 575 (2011).
 13. D. MONTPETIT, M. LALONDE, *In vitro* propagation and subsequent nodulation of the actinorhizal *Hippophae rhamnoides* L. *Plant Cell Tissue Organ Cult.*, 15, 189, 200 (1988).
 14. L.P. YANG, H.L. ZHANG, X.M. ZHAO, Rapid propagation of sea buckthorn (*Hippophae rhamnoides* L.). *The Globe Sea Buckthorn Research and Development*, 2, 12, 16 (2004).
 15. S. BHATIA, T. BERA, Somatic Embryogenesis and Organogenesis. In: *Modern Applications of Plant Biotechnology in Pharmaceutical Sciences*, S. BHATIA, R. DAHIYA, K. SHARMA, T. BERA, eds., Academic Press, Elsevier inc, Amsterdam, 2015, p. 209-230.
 16. M.B. MUGUERZA, T. GONDO, G. ISHIGAKI, Y. SHIMAMOTO, N. UMAMI, P. NITTHAISONG, M.M. RAHMAN, R. AKASHI, Tissue Culture and Somatic Embryogenesis in Warm-Season Grasses—Current Status and Its Applications: A Review. *Plants*, 11, 1263 (2022).
 17. G. FRUGIS, *Plant Development and Organogenesis: From Basic Principles to Applied Research*. *Plants*, 8(9), 299 (2019).
 18. S. ARNOLD, I. SABALA, P. BOZHKOVA, J. DYACHOK, L. FILONOVA, Developmental pathways of somatic embryogenesis. *Plant Cell Tissue Organ Cult.*, 69, 233, 249 (2002).
 19. S. HUANG, M. MIRA, C. STASOLLA, *In Vitro Embryogenesis in Higher Plants*, *Methods in molecular biology*, Humana Press, ISSN 1064-3745 ISSN 1940-6029 (electronic) ISBN 978-1-4939-3060-9 ISBN 978-1-4939-3061-6 (eBook) DOI 10.1007/978-1-4939-3061-6 (1),
 20. P. SOUNDARARAJAN, A. MANIVANNAN, Y.S. CHO, B.R. JEONG, Exogenous supplementation of silicon improved the recovery of hyperhydric shoots in *Dianthus caryophyllus* L. by stabilizing the physiology and protein expression. *Front. Plant Sci.*, (2017) | <https://doi.org/10.3389/fpls.2017.00738>
 21. S. LEE, W. CHO, H. JANG, R. CHANDRA, S. LEE, H. KANG, Effect of Plant Growth Regulators in *In Vitro* Culture of *Hippophae rhamnoides*. *J. For. Environ. Sci. [online]*, 37(2), 148, 153 (2021).
 22. M. SAIKIA, P.J. HADIQUE, *In vitro* propagation and assessment of genetic fidelity of seabuckthorn (*Hippophae salicifolia* d. don) using RAPD markers and evaluation of their antibacterial efficacy: pharmaceutically important medicinal plant. *World J. Pharm Pharm Sci.*, 3(9), 1542, 1559 (2014).
 23. C.J. RUAN, J.A. TEIXEIRA DA SILVA, H. HUA JIN, H. LI, D.Q. LI, Research and biotechnology in sea buckthorn (*Hippophae* spp.) *Medicinal and Aromatic Plant Science and Biotechnology* 1(1), 47, 60 (2007).
 24. S. SRISKANDARAJAH, P.O. LUNDGUIST, High frequency shoot organogenesis and somatic embryogenesis in juvenile and adult tissues of seabuckthorn (*Hippophae rhamnoides* L...). *Plant Cell Tissue Organ Cult.*, 99(3), 259, 268 (2009).
 25. C.Q. LIU, X.L. XIA, W.L. YIN, J.H. ZHOU, H.R. TANG, Direct somatic embryogenesis from leaves, cotyledons and hypocotyls of *Hippophae rhamnoides*. *Biol. Plant.*, 51(4), 635, 640 (2007).

26. F. ALTAN, B. BÜRÜN, N. SAHIN, Fungal contaminants observed during micropropagation of *Lilium candidum* L. and the effect of chemotherapeutic substances applied after sterilization. *Afr. J. Biotechnol.*, 9, 991, 995 (2010).
27. J.A.T. DA SILVA, B. WINARTO, J., DOBRÁNSZKI, J.C. CARDOSO, S. ZENG, Tissue disinfection for preparation of *Dendrobium* in vitro culture. *Folia Horticult.*, 28, 57, 75 (2016b).
28. M. HESAMI, R. NADERI, M. YOOSEFZADEH-NAJAFABADI, Optimizing sterilization conditions and growth regulator effects on in vitro shoot regeneration through direct organogenesis in *Chenopodium quinua*. *Bio Technologia*, 99, 49, 57 (2018c).
29. I. MIHALJEVIĆ, K. DUGALIĆ, V. TOMAŠ, M. VILJEVAC, A. PRANJIĆ, Z. CMELIK, *In vitro* sterilization procedures for micropropagation of 'Oblačinska' sour cherry. *J. Agric. Sci.* 58, 117, 126 (2013).
30. K. NONGALLEIMA, T. DIKASH SINGH, D. AMITABHA, L. DEB, H. SUNITIBALA DEVI, Optimization of surface sterilization protocol, induction of axillary shoots regeneration in *Zingiber zerumbet* (L.) Sm. as affected by season. *Biol. Rhythm Res.*, 45, 317, 324 (2014).
31. M. HESAMI, N. ROOHANGIZ, T. MASOUD, Modeling and Optimizing *in vitro* Sterilization of Chrysanthemum via Multilayer Perceptron-Non-dominated Sorting Genetic Algorithm-II (MLP-NSGAI). *Front. Plant Sci.*, 10, 282 (2019).
32. Y. YAO, Micropropagation of sea buckthorn (*Hippophae rhamnoides* L), *Agricultural Science in Finland*, 4:503-512, (1995)
33. P. LUMMERDING, Micropropagation protocol development for sea buckthorn (*Hippophae rhamnoides*) selection for commercial orchard production, Agri-Food Innovation Fund Project # 19980162 Final Report, October (2001).
34. V. SINGH, R. GUPTA, Micropropagation of seabuckthorn (*Hippophae rhamnoides* ssp. *turkestanica*), *Int. J. Med. Aromat. Plants*, 4, 131, 139 (2014).
35. V.L. TRIVEDI, M.C. NAUTIYAL, J. SATI, D.C. ATTRI, *In vitro* propagation of male and female *Hippophae salicifolia* D. Don. *In Vitro Cell. Dev. Biol. Plant*, 56, 98, 110 (2020).
36. A. M. HUSAINI, J. MERCADO, J. TEIXEIRA DA SILVA, J. SCHAART, Review of Factors affecting organogenesis, somatic embryogenesis and *Agrobacterium tumefaciens* mediated transformation of strawberry. *Genes, Genomes and Genomics*, 5 (1), 1, 11 (2011).
37. D.E. MAFTEI, D. NICUȚĂ, *Biotehnologii vegetale: Ghid pentru lucrări practice*. Ed. Alma Mater, Bacău, 2013, p.182.
38. T. MURASHIGE, F. SKOOG, A revised medium for rapid growth and bioassays with tobacco tissue cultures. *Physiol. Plant.*, 15, 473, 497 (1962).
39. G. LLOYD, B. McCOWN, Commercially feasible micropropagation of mountain laurel (*Kalmia latifolia*) by shoot tip culture. *Proceedings of the International Plant Propagation Society*, 30, 421, 427 (1981).
40. R.U. SCHENK, A.C. HILDEBRANDT, Medium and techniques for induction and growth of monocotyledonous and dicotyledonous plant cultures. *Can. J. Bot.*, 50, 199, 204 (1972).
41. C. KEVERS, T. FRANCK, R.J. STRASSER, J. DOMMESAND, T. GASPAS, Hyperhydricity of micropropagated shoots: a typically stress-induced change of physiological state. *Plant Cell Tissue Organ Cult.*, 77 (2), 181, 191 (2004).
42. B. CHRISTENSEN, S. SRISKANDARAJAH, M. SEREK, R. MULLER, *In vitro* culture of *Hibiscus rosasinensis* L.: Influence of iron, calcium and BAP on establishment and multiplication. *Plant Cell Tissue Organ Cult.*, 93(2), 151, 161 (2008).
43. L.Y. SUN, A study on sea buckthorn tissue culture and plant regeneration. *The Globe Sea Buckthorn Research and Development*, 3, 28, 30 (2005).
44. C.H. GUO, Y.X. XU, Tissue culture of stem apex of superior lines of sea buckthorn. *Hippophae*, 13, 26, 27 (2000).
45. H. XU, Z.S. LIANG, Studies of tissue culture techniques of *Hippophae* L. *Acta Bot. Boreali-Occid. Sin.* 21, 267, 272 (2001).
46. B. KANG, G.J. ZHANG, Y.L. LU, W.H. LI, X.H. ZHANG, J.X. ZHANG, J.J. CAO, Studies on tissue culture of fine variety of *Hippophae rhamnoides* L. from Russia. *J. Northwest Sci. Tech. Univ. Agric. Forest.*, 30, 162, 166 (2002).
47. G.L. ZHAO, J.L. LIU, B. ZHU, Tissue culture and plantlet regeneration of *Hippophae rhamnoides*. *Plant Physiol. Commun.*, 25, 42 (1989).
48. R.K. GUPTA, V. SINGH, Studies on micropropagation in sea buckthorn (*Hippophae rhamnoides* L.), In: *Sea buckthorn (Hippophae L.): a multipurpose wonder plant*, vol 1. V. Singh, ed., Indus Publishing, New Delhi, 2003, p. 338-344.
49. S.K. ZHOU, X.D. SONG, Z.Q. ZHANG, Q.R. ZHAI, Y. ZHANG, F.L. ZHOU. A study on tissue culture of fine variety "Shiyou 1" of *Hippophae rhamnoides*. *J. Northwest For. Univ.*, 21(3), 67, 71 (2006).
50. O.L. GAMBORG, R.A. MILLER, K. OJIMA, Nutrient requirement of suspension culture of soybean root cells. *Exp. Cell Res.*, 9, 195, 198 (1968).



Received for publication: December, 09, 2021
Accepted: May, 26, 2022

Original paper

Influence of using low voltage electrostatic field during freezing and thawing processes on beef quality

**ATEF MOHAMED ELSBAAY^{1*}, NABIHAH H. ABOUELHANA¹,
ESSAM MOHAMED ELSEBAIE², AND MAHMOUD ABDELHAKIEM
MANSOUR BASUONY¹**

¹Agricultural Engineering Department, Faculty of Agric. Kafrelsheikh University, 33516 Egypt.

²Food Technology Department, Faculty of Agric. Kafrelsheikh University, Egypt.

Abstract

This study examined the effects of LVEF-assisted freezing-thawing on beef loin (*Longissimus dorsi*) quality and texture. In this work, the quality of beef specimens at 15, 30, and 45 cm from the LVEF plate (test group) and without LVEF treatment (control group) was examined during freezing-thawing. LVEF aided freezing (LVEFF) sped up beef freezing and thawing by 32.46% and 32.60% at 30 cm layer spacing (LVEF-30). LVEF30 created the smallest, most homogeneous ice crystals and less injured muscle fibre tissue. SEM indicated that LVEF30 preserved muscle fibre and perimysium structure, and muscle fibre gaps did not expand. Z-line and M-line were generally intact, while A-band and I-band were distinct and readable, indicating that LVEF30 preserved myofibrillar structure efficiently. LVEF30's L*, a*, and C values were substantially higher than the control group (P0.05) and fresh meat (P0.05). LVEF-30 reduced thawing loss, cooking loss, and drip protein content by 52.10%, 31.313%, and 15.97%. In conclusion, LVEF can improve the quality of thawed beef by reducing quality loss during freezing-thawing, and 30 cm is the best distance from the electrostatic field generation plate.

Keywords

beef, freezing-thawing, low voltage electrostatic field, texture and electric field

To cite this article: ELSBAAY AM, ABOUELHANA NH, ELSEBAIE EM, BASUONY MAM. Influence of using low voltage electrostatic field during freezing and thawing processes on beef quality. *Rom Biotechnol Lett.* 2022; 27(2): 3443-3452 DOI: 10.25083/rbl/27.2/3443.3452

✉ *Corresponding author: atef.ahmed@agr.kfs.edu.eg

Introduction

Beef is an important animal food resource, which can supply with high-quality protein and essential nutrients such as essential amino acids, unsaturated fatty acids, minerals, and vitamins [1, 2]. Freezing is a well-acknowledged method for long-term preservation of meat by slowing microbial growth rates and loss of meat quality [3]. Currently, airblast freezing (ABF) has been mentioned to be the principal freezing method for meat industry. However, huge ice crystals could be formed in meat owing to slow freezing rate of ABF, resulting in the deterioration in meat quality including protein denaturation, texture damage and flavour loss [4]. During freezing process, the migration of the intracellular water to intermolecular water will occur, resulting in the production of massive ice crystals and subsequent mechanical damage to muscle fibers, which may cause the texture degradation [5]. On the other side, muscle cells become unable to re-absorb the water that migrates outside of the cell in the process of thawing because of the breakdown of the cell membrane and tissues construction, leading to fluid loss [6]. These unanticipated alterations may significantly impair the quality of prepared beef products and are thus undesirable to customers. Therefore, great efforts should be made on the prevention of formation and growth of huge ice crystals throughout freezing storage. The quality of frozen products consists on the quantity of ice crystals as well as their size and distribution inside the material [7]. Therefore, there have been numerous studies performed to determine the best method for increasing the number of ice crystals or reducing their size. These can be achieved either by increasing the freezing rate or applying new emerging technologies, e.g. high-pressure-assisted freezing, power ultrasound-assisted immersion freezing and magnetic fields assisted freezing [8]. Compared with the above methods, the electrostatic field assisted-freezing technology has the advantages of high efficiency, low equipment cost, and simple operation [9]. The decrease of free energy owing to the reorientation of water molecules and the development of a more ordered cluster structure might be the possible mechanism of electric field-assisted freezing [10]. Among these methods, the use of static electric fields (SEF) has been considered because to its significant influence on nucleation, ease of operation, and low energy consumption. It can also simply be incorporated with available commercially freezers [10]. Recently some investigations have been done on the impact of the electro-freezing on real food system (pork meat and lamb meat) [11, 12], but these studies emphasize on the possibility of improving quality characteristics of food materials under electro-freezing. Currently, electrostatic field applying for food preservation has been receiving considerable attention. The use of a high

voltage electrostatic field is a significant non-thermal processing technique which has been used in the advancement of meat freezing and thawing [13]. However, certain limitations in the application of HVEF still exist, such as high energy consumption and security concern. In this regard, the use of low voltage electrostatic field (the output voltage does not exceed 2 500 V, and the current does not exceed 0.2 mA) is more energy-saving, safe, and widely applicable. Qian *et al* [14] investigated LVEF's influence on the rates of thawing and thawed beef quality, indicating that thawing with LVEF may reduce thawing time and maintain the muscular microstructure efficiently. Low-voltage electrostatic field, as a new type of non-thermal technology, has attracted widespread attention and provides new ideas for the technical innovation of meat freezing and thawing. However, the application of low-voltage electrostatic fields in food storage and preservation is still in the initial stage, and its application in meat freeze-thaw technology is rarely reported. In this study, low voltage electrostatic field at different distances from the electrostatic generating plate was utilized in beef freezing thawing process. The freezing and thawing characteristics, colour properties, textural profile, microstructure and ice crystals morphology in muscle fiber tissue of LVEF-assisted freezing (LVEFF) samples and AF samples were detected to evaluate the quality promotion of LVEF-assisted freezing-thawing process. This study provides experimental and theoretical basis for the application of low-voltage electrostatic field technology to assist meat freezing and thawing process.

Materials and methods

Beef samples preparation

Sixteen beef loins (*Longissimus dorsi*) pieces (5 cm × 4 cm × 4 cm, the average weight of 85.0 ± 2.0 g per each one) were purchased from a local butchery in Kafr El-shiekh governorate, Egypt. These pieces were taken from the steer carcass (Holstein × Baladi cross breed, age of 18 months) and were kept for 24 h after slaughter at chilling temperature (5°C) and rapidly transported to the laboratory in an ice box in order to minimize the changes.

LVEF experimental apparatus

The electrostatic field device used in this experiment is composed of an electrostatic field generator (AC220V, 50/60Hz) and a plate electrode (14 cm × 12 cm). The output voltage of the electrostatic field generator is 2 500 V and the current is 0.2 mA, which is a low voltage electrostatic field (LVEF). To perform freezing treatment under LVEF, the prepared beef cubes were placed on a copper plate (14 cm × 12 cm) which is fixed on a chamber. The layer spacing was set at 15 cm, 30 cm, and 45 cm respectively. The treat-

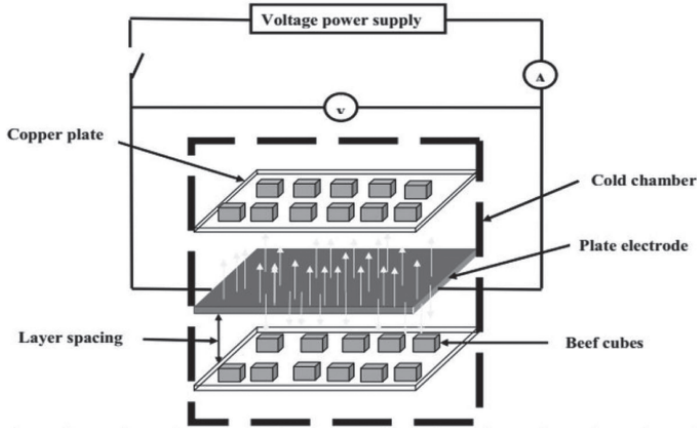


Figure 1. Schematic diagram of the LVEFF equipment.

ment chamber was placed in a cold incubator (YC-520L, MELNG, China) at -18°C or freezing process and 4°C for thawing process. The schematic diagram of the LVEFF-T system is shown in Fig. 1.

Beef samples freezing and thawing process

Sixteen meat samples were randomly divided into 4 groups. The beef that was naturally frozen and thawed (no electrostatic field was applied) was the control group, and the beef that was frozen and thawed under low voltage electrostatic field was the test group. The beef in the test group was divided into 3 groups depending on the distance away from the electrostatic field generating plate. The distances are 15, 30, and 45 cm, respectively. After packaging with transparent polyethylene film, the freezing test was carried out in a quick-freezer at -18°C . When the core temperature of the meat samples dropped to -18°C , the meat samples are considered to be completely frozen. After freezing process, the meat sample was placed in a 4°C refrigerator for thawing test. When the center temperature of the meat sample reaches to 4°C , the meat sample is considered to be completely thawed.

Temperature monitoring

Before freezing, a fiber optic thermocouple (Digi-Sense® Traceable® Kangaroo) was inserted into the center of each sample. The temperature was recorded at the interval of 1 min during freezing and thawing process and LOGGER 1.8.2 software was used to obtain the data.

Determination of color difference

Hunter Lab Colorimeter (MiniScan XE Plus, Reston, VA) has been directly used to measure the brightness value L^* , redness value a^* , and yellowness value b^* of the sample surface. The colorimeter is calibrated with a white board be-

fore use. Each sample was tested in parallel 5 times (select the four corners of the square meat sample and the geometric center of the meat sample) and calculate the chroma value C^* . The formula for calculating C^* value is as follows:

$$C = \sqrt{a^{*2} + b^{*2}}$$

Drip measurement

Drip loss was determined by weighing the samples before and after thawing, and calculated as the difference between initial and final weight, and expressed in percentage, according to a modification of the method of Zhang and Ding [15]. Total protein content of the drip was determined using the biuret procedure described by Ngapo et al [16].

Cooking loss

The cooking loss was calculated using the method of Hu et al [13]. Meat specimens were separately placed in polyethylene sachets and cooked at 80°C by immersion in water till its internal temperature reached 75°C . Cooked specimens were cooled with running water until they reached room temperature, then wiped dry with filter paper and weighed. The cooking loss (%) is calculated as follows:

$$\text{Cooking loss (\%)} = \frac{\text{Raw weight} - \text{Cooking weight}}{\text{Raw weight}} \times 100$$

Texture properties measurement

For meat samples textural analysis, cubes ($1\text{cm} \times 1\text{cm} \times 1\text{cm}$) were cut along the direction of the fiber at the geometric center of the thawed meat sample. Texture profile analyses (TPA) were done via a texture analyzer (Cometech B, Taiwan), and each processed sample is measured 3 times in parallel, and the result is the average of the 3 measurements. The selected 4 analysis indicators are elasticity, hardness, cohesiveness and

springiness. Measurement parameters: probe P35; lateral front velocity 2.0 mm/s; center measurement velocity 1.0 mm/s; post-measurement velocity 5.0 mm/s; compression ratio 40%; the interval between two probe measurements 5.00 s; trigger type is automatic.

Shear force measurement

The pre-treatment of the samples in shear force analysis was the same as that in the textural analysis. The sample was cut parallel to the fiber direction and sheared with a Warner-Bratzler shear force (WBSF) device attached to a universal testing machine (Cometech, B type, Taiwan) with a 55 Kg tension/compression load cell and the crosshead speed was set at 200 mm/min [17]. Each processed sample was measured 5 times in parallel, and the average value of the 5 measurements was taken.

Ice crystal morphology in muscle tissue observation

The ice crystal morphology was observed by light microscopy followed the indirect method called isothermal freezing substitution technique reported by Dalvi-Isfahan *et al* [11]. For each freezing treatment, cut 3 small rectangular cubes (5 mm × 4 mm × 4 mm), fix them with Carnoy solution, and let them stand at 4°C for 20 h. The samples were then dehydrated at 4°C with ethanol solutions of gradient concentrations (70%–100%, v/v). Then, the dehydrated sample was immersed in n-butanol and let to stand for 30 min (repeated 3 times). The samples were soaked in wax to ensure fixation of the meat tissue. The samples were then embedded in paraffin, and let it stand for 1 h (repeated 3 times) to facilitate slicing. Slices were obtained using a microtome and were subjected to 0.4% brilliant blue water solution for 3 min, followed by microscopic analysis.

Scanning electron microscopy (SEM)

SEM analysis was performed as described by Zhang and Ding [15] with slight modification. The samples were cut into blocks (2 mm × 2 mm × 5 mm) from the central part with a scalpel. The blocks were fixed in 2.5% glutaraldehyde

in 0.1 M phosphate buffer (pH 7.3) for 48 h. After washing with 0.1 M phosphate buffer (pH 7.3), the blocks were fixed in 1% osmium tetroxide in 0.1 M phosphate buffer (pH 7.3) for 1 h. The blocks were then washed with distilled water before being dehydrated with a succession of ethanol solutions, dried, and coated by gold. A scanning electron microscope (LEO 440i, UK) was used to examine and photograph cross sections of myofibers from the specimens at a magnification of ×500.

Transmission electron microscopy (TEM)

The samples were cut into blocks (4 mm × 4 mm × 2 mm) from the central part with a scalpel. The blocks were fixed, rinsed, and dehydrated as described in Section 2.11. After drying, the longitudinal sections were prepared on ultra-thin microtome, stained with uranyl acetate and lead citrate, and observed with a transmission electron microscope (H-7500, Hitachi, Japan) at a magnification of × 40,000.

Statistical analysis

The measurements were determined as the results of 3 parallel determinations, expressed as the mean ± standard deviation. ANOVA were performed using the general linear regression model of SPSS (Ver.16.0, 2007) analysis software ($P \leq 0.05$).

Results and discussion

Freezing and thawing processes temperature monitoring

The temperatures used for freezing and thawing of meat samples are -18°C and 4°C respectively. In order to study the influence of the low-voltage electrostatic field on the freezing-thawing process of beef, the temperature changes in the thermal center of different processed meat samples were compared. Time spent of different freezing stages and thawing process of the control group and the test groups were presented in Table 1.

Table 1. Time consumed at various freezing phases and thawing process of beef under various freezing techniques

Treatments	Precooling stage (min)	Phase transition stage (min)	Deep cooling stage (min)	Total freezing time (min)	Total thawing time (min)
LVEF-15	162.73 ± 6.32Bd	86.83 ± 5.93Ce	289.16 ± 5.69Cb	538.72 ± 7.81Ca	236.13 ± 3.42Cc
LVEF-30	138.41 ± 8.61Dd	75.29 ± 4.35De	282.79 ± 5.28Db	496.49 ± 7.06Da	210.32 ± 2.91Dc
LVEF-45	151.92 ± 7.84Cd	99.37 ± 6.70Be	343.07 ± 8.09Bb	594.36 ± 6.88Ba	267.69 ± 3.16Bc
AbF	186.59 ± 9.27Ad	112.16 ± 9.60Ae	436.45 ± 8.57Ab	735.20 ± 8.75Aa	312.08 ± 2.07Ac

Data are presented as mean ± SD (n = 3).

AbF: air-blast freezing; LVEF: low voltage electric-field assisted freezing at different discharge gaps (15 cm, 30 cm and 45 cm).

Means with different superscripts (A-D) uppercase letters in a column are significantly different at $P \leq 0.05$.

Means with different superscripts (a-e) lowercase letters in a row are significantly different at $P \leq 0.05$.

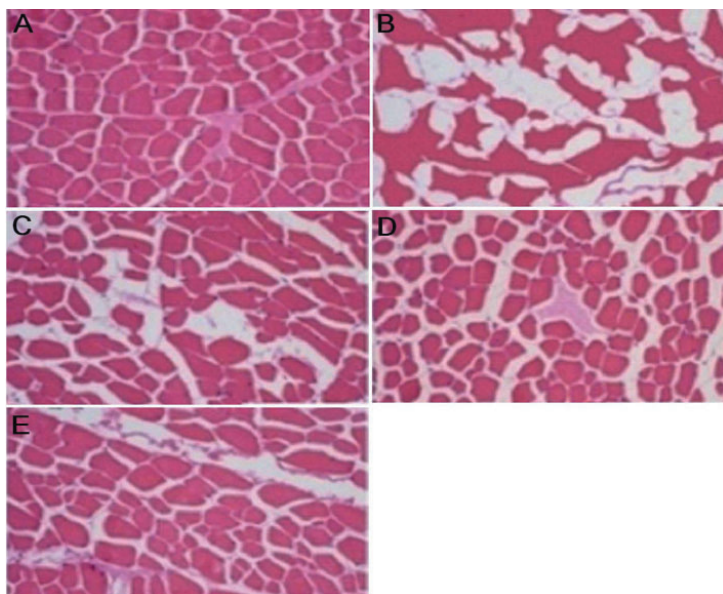


Figure 2. Micrograph of beef muscle fibers and ice crystals formed after different freezing treatments (200×)

A = Fresh sample, B = samples freeze and thawed in air blast freezer (AbF), C = LVEF-15, D = LVEF-30, and E = LVEF-45.

The freezing process was divided into three distinct stages, namely, the pre-cooling phase (in which the meat is cooled from its initial temperature to the freezing point), the phase transition ($-1^{\circ}\text{C} \sim -5^{\circ}\text{C}$) (which represents the crystallization process of the water in muscle), and the deep freezing stage (in which the temperature decreased to the final temperature) [18].

Treatments under layer spacing of 15 cm (LVEF-15), 30 cm (LVEF-30) and 45 cm (LVEF-45) passed the maximum ice crystal formation stage lasted 86.83 ± 5.93 , 75.29 ± 4.35 and 99.37 ± 6.70 min respectively, while the control group (AbF) passed the maximum ice crystal formation stage for 112.16 ± 9.60 min. It can be seen that the three groups of processed samples shorten the time taken to pass the maximum ice crystal formation stage when the meat is frozen to various degrees, indicating that the electrostatic field affects the water phase change process during meat freezing. Among them, LVEF-30 lasted the shortest time, which was 59.3% shorter than the control (AbF). The entire freezing process begins to cool down from 5°C , and ends when the sample center temperature reaches -18°C . The freezing time required for the treatment group LVEF15, LVEF30, and LVEF45 were 538.72 ± 7.81 , 496.49 ± 7.06 and 594.36 ± 6.88 min, while the freezing time required for the control group was 735.20 ± 8.75 min. The freezing time required for the samples under the electrostatic field was significantly lower than that of the control group where LVEFF-30 reduced freezing time the

most (47.1%). In this experiment, the meat sample is considered to be completely thawed when the center temperature of the meat sample reaches 1°C . As can be seen from Table 1, the thawing time required for the test group LVEF15, LVEF30, and LVEF45 are 236.13 ± 3.42 , 210.32 ± 2.91 and 267.69 ± 3.16 min, while the thawing time required for the control group was 312.08 ± 2.07 min. Moreover, thawing process under the electrostatic field significantly ($P \leq 0.05$) reduced the thawing time of the frozen meat, and LVEFF-30 was the most efficient one, where the thawing process was accelerated by 32.69%. These results suggested that, under the low-voltage electrostatic field, the meat freezes fast, and the ice crystals grown are small in size. When thawed, transitioning to the water molecules state is easy.

In addition, some studies stated that meat thawing in the same way, in an electrostatic field environment, can accelerate the breaking of hydrogen bonds in the ice structure, and the thawing speed will increase [14]. The electric field strength at a distance of 30 cm from the discharge plate can effectively improve the freezing-thawing efficiency of meat.

Morphology of ice crystals in frozen beef tissues

Fig. 2 shows the ice crystal morphology after freezing under different LVEFF and AbF conditions. It can be seen from Fig. 2 that the muscle fiber tissue structure of fresh beef is uniform and dense, with very small gaps between muscle

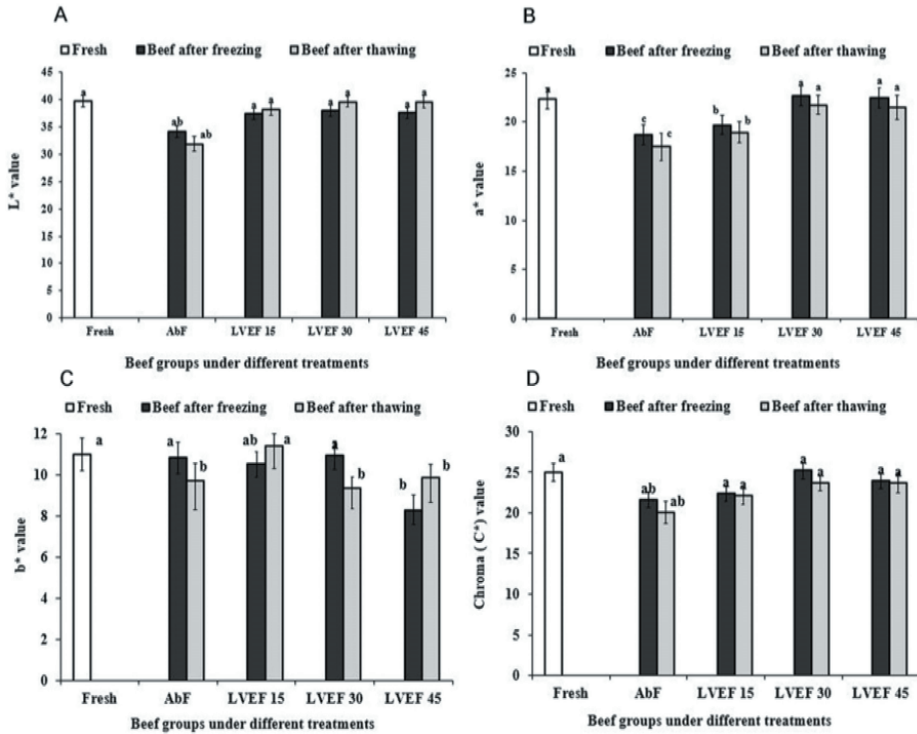


Figure 3. Changes in beef color after different freezing and thawing treatments.

Data are presented as mean±SD.

Means with different lowercase letters are significantly different at $P \leq 0.05$.

fibers. During the freezing process of muscles, water crystallizes in the tissues and increases in volume. The growth of ice crystals leads to the destruction of muscle tissues. The ice crystals formed in the control group (AbF) were large in size and small in number, and distributed chaotically in the muscle tissue.

However, the ice crystals produced in the test group were small in shape, large in number and evenly distributed. Control group and test group muscle fiber tissue was damaged by ice crystals to different degrees: the beef muscle fibers of the control group were obviously damaged and suffered severe mechanical damage while, the test group beef muscle fiber tissue structure was maintained well and was less affected by ice crystals. Among all groups, the LVEF30 treatment maintained muscle fiber tissue structure well and caused a relatively small degree of damage to the muscle fiber by ice crystals. This is due to the fact that the meat sample is frozen at a distance of 30 cm from the discharge plate and had ice crystals small in volume and uniformly distributed. Our results are consistent with those in the study of Kiani *et al* [19] and Dalvi-Isfahan *et al* [11] where they reported that in

the perspective of the thermodynamic law, electric-field can modify and lower the free energy barrier for ice nucleation, leading to the enhancement of the nucleation rate and the number of ice nuclei, and consequently, the size of the resulted ice crystals is relatively smaller.

Beef color parameters

Changes in beef color within the normal range will not have much impact on its nutritional value and flavor. However, as an important indicator of meat sensory quality, the color and luster largely affect consumers' preferences. The L^* value and a^* value of the flesh color represents the brightness value and the redness value of the flesh sample. The higher L^* value means the better meat gloss, and the higher a^* value refers to better meat color and fresher meat. The higher C (chroma) value indicates better meat brightness [20]. It can be seen from Fig. 3 that, the L^* value, a^* value and C value of the frozen meat sample have decreased to various degrees compared with fresh meat samples. The L^* value, a^* value and C value of the control group (AbF) after freezing were 34.12, 18.72 and 21.63, which were sig-

nificantly lower than 39.71, 22.40 and 24.96 registered for the fresh meat sample ($P \leq 0.05$). However, the test group frozen under low-voltage electrostatic field conditions maintained the better color of the meat sample, and the LVEF30 test group had the most obvious effect. The L^* , a^* and C values of the LVEF30 group after freezing were 37.95, 22.68 and 25.19, which were significantly higher than those of the control group ($P \leq 0.05$), and there was no significant difference compared with fresh meat samples ($P \leq 0.05$). The meat sample loses too much water after thawing and the L^* value is significantly lower than that of the fresh meat sample. In addition, if the meat sample has been in contact with air for too long, the increase in the oxidation rate of myoglobin reduces the a^* and C values [19]. Hence, the beef in the test group after thawing has a higher color and freshness compared with the control. The L^* , a^* and C values of the LVEF30 in the test group after thawing are of 39.56, 21.75 and 23.68 which were significantly higher than 31.87, 17.52 and 20.03 in the control group ($P \leq 0.05$).

Thawing loss, drip protein content and cooking loss

After the muscle is frozen, the water crystal volume increases, causing the muscle cell membrane break-cracking, drip loss occurs when thawing, and a large amount of soluble protein is lost with the drip, resulting in a serious decline in the meat nutritional value [21]. As shown in Fig. 4A, the thawing loss of frozen beef cubes specimens exposed to LVEF15, LVEF30 and LVEF45 were $5.48 \pm 0.52\%$, $4.10 \pm 0.31\%$, and $4.20 \pm 0.44\%$, respectively, which were significantly lower ($P \leq 0.05$) than that of AbF specimens ($8.56 \pm 0.47\%$). In the four treatment groups, the LVEF30 specimen showed the lowest rate of thawing loss, while the thawing loss rate of the LVEF45 specimen was somewhat less than that of LVEF15. According to Leygonie et al [3], ice melting in cell exo-spaces could lead to water flow into endo-spaces and their eventual re-absorption via dehydrated fibers and denatured proteins.

According to Qian et al [14], the electrostatic field can enhance the renaturation of freezing-induced denatured myofibrillar proteins and preserve the bonding capability amongst protein and water throughout the thawing step. This might account for the lower thawing loss of frozen beef cubes when treated with LVEF. Data presented in Fig. 4B indicated that the drip protein content of LVEF15, LVEF30 and LVEF45 in the test group were $10.84 \pm 0.19\%$, $9.31 \pm 0.25\%$ and $9.72 \pm 0.13\%$, which were significantly lower ($P \leq 0.05$) than the control group ($11.08 \pm 0.16\%$). Fig. 4C revealed that the LVEF30 specimen had the lowest cooking loss ($19.98 \pm 1.16\%$), which was significantly lower ($P \leq 0.05$) than that of

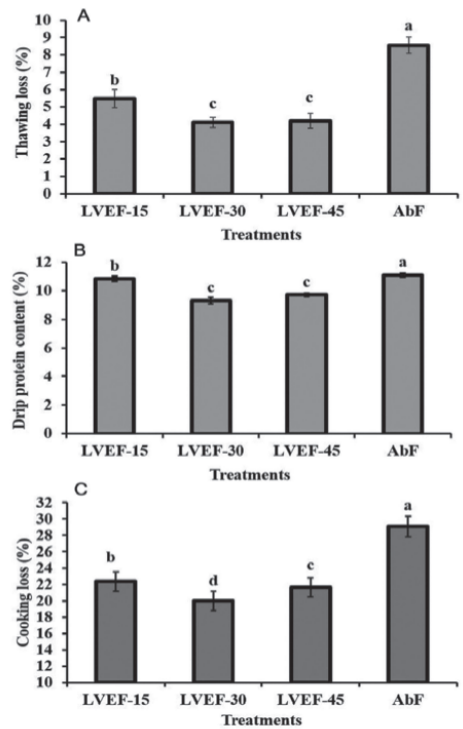


Figure 4. Effects of different freezing and thawing treatments on thawing loss (A), Drip protein content (B) and cooking loss (C).

Data are presented as mean±SD.

Means with different lowercase letters are significantly different at $P \leq 0.05$.

AbF ($29.09 \pm 1.25\%$), LVEF15 ($22.35 \pm 1.20\%$) and LVEF45 ($21.62 \pm 1.13\%$). The obtained results showed that the electrostatic field-assisted freeze-thaw process can effectively improve the water retention of beef and significantly reduce the nutrient loss of beef after thawing. Among all investigated groups, the LVEF30 treatment group presented a reduced thawing loss rate, cooking loss rate, and drip protein content by 4.46%, 9.11%, and 1.77% compared with the control group (AbF). Generally, water retention of meat samples was the best in all meat samples treated with LVEF. Also, results in Figure 4 (A, B and C) show that meat muscle fibers treated with LVEF30 are minimally damaged by ice crystals during freezing, and that drip loss is better suppressed during thawing. Same results were reported by Qian et al [14], where applying LVEF in the thawing process of raw beef could significantly decrease the thawing loss of the thawed beef compared with air thawing.

Table 2. Effects of different freezing and thawing treatments on texture of beef

Treatments	Elasticity/ N	Hardness/ N	Cohesiveness	Springiness /N	Shear force/N
Fresh	783.42±56.37a	423.89±20.12d	0.56±0.02a	0.98±0.01a	2.33±0.07c
LVEF-15	641.65±38.09b	457.92±17.27b	0.52±0.04a	0.95±0.03a	2.26±0.04c
LVEF-30	613.57±33.18b	439.76±21.50cd	0.56±0.03a	0.97±0.02a	2.01±0.09d
LVEF-45	594.10±56.53c	448.30±22.29c	0.53±0.02a	0.96±0.01a	2.58±0.07b
AbF	479.81±41.29d	512.73±18.32a	0.46±0.05b	0.81±0.03b	3.96±0.05a

Data are presented as mean±SD (n = 5).

AbF: air-blast freezing; LVEF: low voltage electric-field assisted freezing at different discharge gaps (15 cm, 30 cm and 45 cm).

Means with different superscripts (a-d) lowercase letters in a column are significantly different at $P \leq 0.05$.

Beef texture characteristics and shear force

Textural parameters are also an essential quality indicator for meat products, which may be assessed by hardness, chewiness and cohesiveness of the meat [22]. In this experiment, the texture characteristics and shear force of fresh meat samples and freeze-thaw beef under different conditions were analyzed (Table 2). The results indicated that the elasticity of LVEF15, LVEF30 and LVEF45 beef in the experimental group were 641.65±38.09N, 613.57±33.18N and 594.10±56.53N, which were significantly greater ($P \leq 0.05$) than the control group (479.81±41.29N). Notably, the hardness of the experimental group LVEF30 and LVEF45 was 439.76±21.50N and 448.30±22.29N, which was significantly lower ($P \leq 0.05$) than the control group (512.73±18.32N). This could be due to the dry and matte surface of meat caused by the thawing loss. However, the cohesiveness of the LVEF groups was not significantly different from that of the fresh specimen ($P \leq 0.05$).

LVEFF had a significant enhancement on parameter ($P \leq 0.05$). After the freezing procedure the springiness of the beef cubes diminished. None significant variation ($P \leq 0.05$) was found in the springiness values among LVEF-15, LVEF-30, LVEF-45 and the fresh beef specimen. Frozen beef tends to have more strength and lower softness than fresh meat owing to muscle fibers deteriorating and muscle drip loss after thawing stage [3]. The water is released from the myofibrils, and muscle fibers are less water-hydrated throughout the thawing process. The decreased hardness and increased springiness may potentially be due to muscular cell physical disruption (which will be shown later in Fig. 5A). Further, the shear force values of LVEFF samples were significantly lower than that of control (AbF) sample. As shear force reflects the muscle tenderness, and better tenderness is associated with lower shear force value [23]. Thus, electrostatic field assisted freeze-thaw can significantly improve the texture characteristics and maintain better tenderness of thawed beef. Additionally, the textural characteristics of the sample frozen with LVEFF-30 were the best among all samples. Our results were consistent with Dalvi-Isfahan *et al* [11].

Microstructure of beef Myofibril

Scanning electron microscope

Fresh and frozen-thawed beef under different conditions were observed by scanning electron microscopy to analyze the integrity of muscle fiber bundles and perimysial membranes, as well as the gaps between muscle fiber bundles. The results are shown in Figure 5A (photographed at $\times 500$). It can be seen from Figure 5A, that the muscle fiber bundles and perimysial membrane structure of fresh beef are complete, the muscle fiber bundles are tightly arranged, and the gaps in the muscle bundles are small. After thawing, the integrity of beef muscle fibers is lost, the arrangement of muscle fiber bundles is loose, the space between muscle bundles is large, and the structure of the myofibril cells membrane is broken. The beef muscle fibers of the control group were severely deformed, and some areas were even hollow. Compared with the control group, the muscle microstructure of the test group is relatively complete, the muscle fiber bundles are arranged tightly and the gaps are smaller, and the degree of damage to the fascia is less. Among all investigated groups, the LVEF15 and LVEF30 meat samples in the test group effectively maintained the structure of muscle fiber bundles and perineurium after thawing, and the gaps between muscle fiber bundles did not expand significantly. The perimysium in muscle is elastic and can maintain the integrity of muscle tissue and the dense arrangement of muscle fiber bundles. The destruction of the perimysium will cause the gaps between the muscle fiber bundles to increase, and the water will leak out more easily, the water retention of the muscles will decrease, and serious drip loss will occur.

Transmission electron microscope

Muscle fiber bundle longitudinal sections of fresh and frozen-thawed beef under different conditions were observed by transmission electron microscope and the results are shown in Fig. 5 (magnification $40000\times$). Fig. 5B shows that the fresh meat myofibril structure is completed, the muscle fiber bundles are tightly arranged, the A-band and the I-band are clearly distinguishable, and the Z-line and M-line

are obvious and complete. In the control group after thawing, the Z-line of the meat sample was broken, the M-line was blurred, and the A and I zones were severely damaged. Thawing meat samples under LVEFF15 or LVEFF30 kept Z-line and M-line relatively compelled, and the A and I belts are still clearly identifiable. This shows that the low electrostatic field assisted freezing and thawing can effectively maintain the structural integrity of beef muscle fiber tissue. Feng et al [24] found a significant correlation between the integrity of myofibrils and the water retention characteristics of muscles by studying the relationship between muscle tissue changes and water retention.

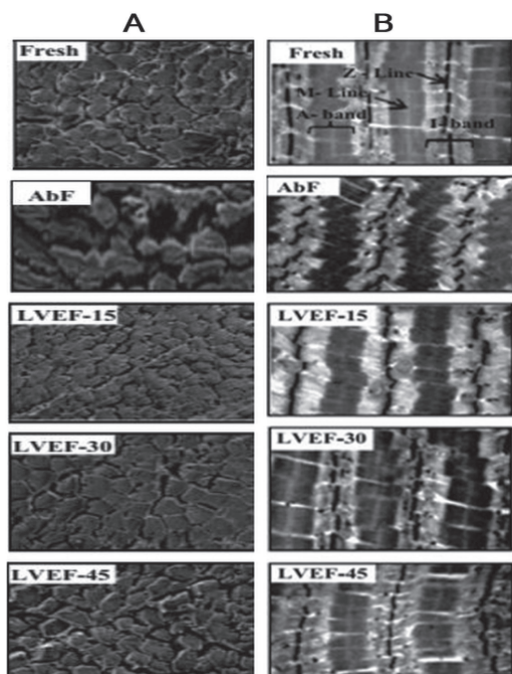


Figure 5. Scanning electron microscopy (SEM) images ($\times 500$) (A) and transmission electron microscopy (TEM) images ($\times 40000$) (B) of beef after different freezing and thawing treatments.

At the same time, the destruction of the complete and dense tissue structure of the muscle fiber bundles will lead to the reduction of the elasticity and chewiness of the meat. Low electrostatic field assisted freeze-thaw process maintained the structure of fleshy muscle fiber bundles being more complete and dense, which also verifies its low drip loss rate and better maintenance of texture properties.

Conclusion

The quality of beef has deteriorated after freezing and thawing, and different freezing and thawing methods will

affect the quality of beef to various degrees. In this study, the use of an electrostatic field to assist the freeze-thaw process of beef, compared with natural freeze-thaw, can effectively slow down the quality deterioration of beef during the freeze-thaw process and improve the quality of thawed beef as follows:

1) The freezing-thawing efficiency of beef under low-voltage electrostatic field has been significantly improved ($P \leq 0.05$). The ice crystals grown during the freezing process are small in size and evenly distributed in the muscle tissue. The damage to the muscle tissue is light, and the muscle fiber bundle structure is more complete and dense.

2) After thawing, the water holding capacity of beef is improved and the nutrient loss is reduced. Among them, the freeze-thaw at a distance of 30 cm from the electrostatic plate, the drip loss rate, cooking loss rate and the drip protein content are reduced by 4.46, 9.11, and 1.77 percentage points respectively compared with the natural freeze-thaw, the difference being significant ($P \leq 0.05$).

3) The color and texture characteristics of thawed beef are effectively maintained. The L^* value, a^* value and C value of the frozen-thawed meat sample at a distance of 30 cm from the electrostatic plate were significantly higher ($P \leq 0.05$) than the natural freeze-thaw (AbF); Elasticity, hardness, cohesiveness and springiness were significantly higher than those of natural frozen-thawed meat ($P \leq 0.05$).

4) Compared with the other test groups, the frozen-thawed meat sample at a distance of 30 cm from the electrostatic plate has a brighter color, better texture and water retention performance.

Conflict of interest

The authors have declared no conflicts of interest for this article.

References

1. Cabrera, M. and A.J.M.s. Saadoun, *An overview of the nutritional value of beef and lamb meat from South America*. 2014. **98**(3): p. 435-444.
2. Oh, M., et al., *Chemical compositions, free amino acid contents and antioxidant activities of Hanwoo (Bos taurus coreanae) beef by cut*. 2016. **119**: p. 16-21.
3. Leygonie, C., T.J. Britz, and L.C.J.M.s. Hoffman, *Impact of freezing and thawing on the quality of meat*. 2012. **91**(2): p. 93-98.
4. Hou, Q., et al., *Quality changes of pork during frozen storage: Comparison of immersion solution freezing and air blast freezing*. 2020. **55**(1): p. 109-118.

5. Jiang, Q., et al., *Changes in quality properties and tissue histology of lightly salted tuna meat subjected to multiple freeze-thaw cycles*. 2019. **293**: p. 178-186.
6. Pietrasik, Z. and J.J.F.R.I. Janz, *Utilization of pea flour, starch-rich and fiber-rich fractions in low fat bologna*. 2010. **43**(2): p. 602-608.
7. Zhu, Z., et al., *Measuring and controlling ice crystallization in frozen foods: A review of recent developments*. 2019. **90**: p. 13-25.
8. Cheng, X., et al., *The principles of ultrasound and its application in freezing related processes of food materials: A review*. 2015. **27**: p. 576-585.
9. Le-Bail, A., et al., *Electrostatic field assisted food freezing*. 2011. **2**: p. 685-692.
10. Dalvi-Isfahan, M., et al., *Review on the control of ice nucleation by ultrasound waves, electric and magnetic fields*. 2017. **195**: p. 222-234.
11. Dalvi-Isfahan, M., et al., *Effect of freezing under electrostatic field on the quality of lamb meat*. 2016. **37**: p. 68-73.
12. Jia, N., et al., *Changes in the structural and gel properties of pork myofibrillar protein induced by catechin modification*. 2017. **127**: p. 45-50.
13. Hu, F., et al., *Combined impacts of low voltage electrostatic field and high humidity assisted-thawing on quality of pork steaks*. 2021: p. 111987.
14. Qian, S., et al., *Effects of low voltage electrostatic field thawing on the changes in physicochemical properties of myofibrillar proteins of bovine Longissimus dorsi muscle*. 2019. **261**: p. 140-149.
15. Zhang, Y. and C.J.I.A. Ding, *The Study of Thawing Characteristics and Mechanism of Frozen Beef in High Voltage Electric Field*. 2020. **8**: p. 134630-134639.
16. Ngapo, T., et al., *Freezing and thawing rate effects on drip loss from samples of pork*. 1999. **53**(3): p. 149-158.
17. Shackelford, S., T. Wheeler, and M.J.J.o.a.s. Koohmaraie, *Evaluation of sampling, cookery, and shear force protocols for objective evaluation of lamb longissimus tenderness*. 2004. **82**(3): p. 802-807.
18. Castro-Giráldez, M., et al., *Thermodynamic approach of meat freezing process*. 2014. **23**: p. 138-145.
19. Kim, Y., et al., *Evaluation of antioxidant capacity and colour stability of calcium lactate enhancement on fresh beef under highly oxidising conditions*. 2009. **115**(1): p. 272-278.
20. Sales, L.A., et al., *Effect of freezing/irradiation/thawing processes and subsequent aging on tenderness, color, and oxidative properties of beef*. 2020. **163**: p. 108078.
21. Xia, X., et al., *Physicochemical change and protein oxidation in porcine longissimus dorsi as influenced by different freeze-thaw cycles*. 2009. **83**(2): p. 239-245.
22. Martinez, O., et al., *Texture profile analysis of meat products treated with commercial liquid smoke flavourings*. 2004. **15**(6): p. 457-461.
23. Zhang, M., et al., *Changes in microstructure, quality and water distribution of porcine longissimus muscles subjected to ultrasound-assisted immersion freezing during frozen storage*. 2019. **151**: p. 24-32.
24. Feng, Q., et al., *Effect of different cooking methods on sensory quality assessment and in vitro digestibility of sturgeon steak*. 2020. **8**(4): p. 1957-1967.